Ice dynamics and glacial history from remote sensing of the Seno Skyring-Seno Otway-Strait of Magellan region, southernmost Patagonia

LOVELL, HAROLD

Ice dynamics and glacial history from remote sensing of the Seno Skyring-Seno Otway-Strait of Magellan region, southernmost Patagonia

Photograph by Hauke Steinberg

Harold Lovell

M.Sc. (by research)

Department of Geography

Durham University

January 2011

Declaration of Copyright

Harold Lovell

Department of Geography

Durham University

January 2011

Abstract

The glacial geomorphology of southernmost Patagonia records the advance and retreat of the Patagonian ice sheet over a number of glacial cycles. The well-preserved landform assemblages and sediments that have been left behind comprise one of the longest and most complete records of Quaternary glaciations in the world. Despite this, little is known about the pre-Last Glacial Maximum (LGM) ice sheet dynamics in a number of areas, particularly around the Strait of Magellan. This study has mapped in detail the glacial geomorphology of the Seno Skyring-Seno Otway-Strait of Magellan region from a combination of Landsat and ASTER satellite imagery and oblique and aerial photographs for the purposes of reconstructing the ice sheet dynamics.

A wide variety of glacial landforms have been mapped, including glacial lineations, moraine ridges, meltwater channels, outwash plains and palaeo-shorelines. The most distinct features within the study area are highly elongate streamlined glacial lineations on the western side of the Strait of Magellan. A landsystems approach has been employed in order to decipher this group of lineations and three potentially plausible landsystems are evaluated: a palaeo-ice stream, a surging glacier, and an ice-marginal terrestrial landsystem. Based on the characteristic shape, dimensions and abrupt lateral margin of the flow-set, the lateral variation in lineation length and elongation ratios, and the presence of a potentially-deformable bed, these lineations are interpreted as being diagnostic of a terrestrial palaeo-ice stream. It is suggested that the initiation of ice streaming was caused by calving into one of two ice-dammed proglacial lakes. The lakes were located within the former Seno Skyring and Seno Otway ice lobes, which are well-defined by arcuate sequences of moraine ridges. The westernmost of the lakes, proglacial Lake Skyring, is delimited by a series of palaeo-shorelines surrounding the present-day lake Laguna Blanca. The size and orientation of meltwater channels and an outwash plain suggests that proglacial Lake Skyring drained eastwards towards the Strait of Magellan in an abrupt event.

The ice sheet has been reconstructed at 12 time-steps, documenting stages of both advance and retreat. An attempt has been made to place this reconstruction within the framework of the wider glacial chronology of the region. From this, it is suggested that ice stream activity contributed to the rapid deglaciation of this sector of the ice sheet during the penultimate glaciation. Future work should focus on applying fieldwork to help validate the interpretations of this study. This should include dating of the landforms and sediments that have been mapped in order to improve the pre-LGM glacial chronology of this region, which is currently poorly-constrained.

Contents

List of Figures

List of Tables

Acknowledgements

I would like to thank Chris Stokes and Mike Bentley for their expert supervision during all aspects of this project. Both were of great help throughout the year, and were also a lot of fun to work with. The Department of Geography at Durham University is thanked for financial support in the form of a Durham Academic Scholarship. I would also like to thank my fellow inhabitants of the GIS lab for their various helpful comments and advice at different stages during the project, but mainly for their good company. Finally, I would like to thank Ustinov College A.F.C. for an enjoyable, if not overly successful year of football.

Chapter 1 - Introduction and Rationale

Continental ice sheets can be highly dynamic and play a significant role in the global climate system (Boulton *et al.*, 1985; Clark, 1992). Their response to and triggering of climate changes can sometimes occur abruptly, over decadal to millennial timescales (e.g. Alley and Whillans, 1984; Boulton and Clark, 1990; Hughes, 1992; Tarasov and Peltier, 2005; Bamber *et al.*, 2007; Truffer and Fahnestock, 2007). Understanding the long-term behaviour and stability of contemporary ice sheets and their interactions with the ocean-atmosphere system is therefore of considerable importance (Alley and Bindschadler, 2001; Rignot and Thomas, 2002).

One way in which the future stability of ice sheets and their influence on the climate system can be predicted is through studying the dynamics of former ice sheets (MacAyeal, 1993; Hughes, 1992; Clark *et al.*, 2000). It has been recognised that the stability of Pleistocene ice sheets had an impact on global sea level and climate (Boulton *et al.*, 1985; Hughes, 1992). If a relationship can be found between former ice sheets and palaeoclimatic records then it may be possible to predict the response of contemporary ice sheets to future climate oscillations (Hughes, 1992; Benn and Evans, 1998; Stokes and Clark, 2001). The reconstruction of former ice sheets and their evolution through time is possible by piecing together the range of often fragmentary and discontinuous geomorphological evidence they leave behind (Kleman and Börgstrom, 1996; Clark, 1997, 1999; Stokes and Clark, 2002a).

The use of remote sensing enables mapping of glacial geomorphology on large spatial scales (Clark, 1997). Satellite imagery, in particular, has revolutionised the mapping of former ice sheets and has improved our knowledge of their dynamics (Stokes, 2002). The use of satellite imagery has allowed the detection of new landforms and patterns, such as mega-scale glacial lineations (MSGL; Clark, 1994), making it possible for a single user to map large areas at a much greater speed than from aerial photographs and fieldwork (Clark, 1997). Once the glacial geomorphology of an area has been mapped, the next step is to reconstruct the past ice sheet dynamics. This can be achieved by using a glacial geomorphological inversion model, which effectively involves the interpretation of ice sheet properties from the glacial geomorphology (Kleman and Börgstrom, 1996; Kleman *et al.*, 2006). The combined use of remote sensing and the inversion method has allowed the reconstruction of former ice sheet dynamics, including the identification of ice streams from the geomorphological record (e.g. Stokes *et al.*, 2009).

Ice streams are arguably the most dynamic feature within contemporary ice sheets and so have a central role to play in ice sheet stability (Binschadler *et al.*, 1998; Stokes and Clark, 1999, 2001; Bennett, 2003; Ó Cofaigh *et al.*, 2003, 2008; De Angelis and Kleman, 2005, 2007; Larter *et al.*, 2009). Described as fast-flowing arteries of ice within an ice sheet (Bentley, 1987; Bennett, 2003), it is thought that ice streams may have been responsible for forcing high-frequency millennial or sub-millennial climate change (Bond *et al.*, 1992; Broecker, 1994). In addition, contemporary ice streams respond to atmospheric and oceanic changes (Oppenheimer, 1998; Rignot and Kanagaratnam, 2006; Holland *et al.*, 2008). Understanding the processes which govern the location of ice streams and the mechanisms by which they flow is crucial for predicting the future stability of contemporary ice sheets in response to any climate perturbations (Stokes and Clark, 1999, 2001; Bennett, 2003). Therefore, identifying the location of palaeo-ice streams is important for the accurate reconstruction of former ice sheet histories and dynamics and the associated climate and environmental changes (Stokes and Clark, 2001; De Angelis and Kleman, 2005, 2007; Everest *et al.*, 2005).

Palaeo-ice stream beds also present the best opportunity to study the basal environment of ice streams because it is difficult and expensive to access contemporary ice stream beds (Stokes and Clark, 1999, 2001; Ó Cofaigh *et al.*, 2005; Hindmarsh and Stokes, 2008; Larter *et al.*, 2009). The detailed study of palaeo-ice stream beds can provide information about the basal conditions and processes which constrain their location and facilitate fast flow (Stokes and Clark, 2001, 2003). As a result, study of palaeo-ice streams contributes to advancing our understanding of ice stream behaviour in both former and contemporary ice sheets (Stokes and Clark, 1999, 2001; De Angelis and Kleman, 2005; Ó Cofaigh *et al.*, 2008).

Palaeo-ice streams have been identified within many former ice sheets, including the Laurentide (e.g. Dyke and Morris, 1988; Patterson, 1997, 1998; Clark and Stokes, 2001; De Angelis and Kleman, 2005), Fennoscandian (e.g. Punkari, 1997; Payne and Baldwin, 1999) and British (e.g. Knight *et al.*, 1999; Bradwell *et al.*, 2008) ice sheets, as well as at the margins of the Antarctic (e.g. Canals *et al.*, 2000; Ó Cofaigh *et al.*, 2005, 2008) and Greenland ice sheets (Roberts and Long, 2005). However, no ice streams have ever been explicitly described within the former Patagonian ice sheet, the next largest former mid-latitude ice mass after the Laurentide and Fennoscandian and the largest in the southern hemisphere (Glasser *et al.*, 2008). Clapperton (1989) and Benn and Clapperton (2000a)

hypothesised the presence of a palaeo-ice stream in the Strait of Magellan region, and this study intends to test this hypothesis.

The glacial history of southernmost South America has received a lot of research attention, from the pioneering mapping work of Nordenskjöld (1899) and Caldenius (1932), to more recent attempts to create a chronology of glacial advances through the use of modern dating techniques such as cosmogenic nuclide measurements (Kaplan *et al*. 2004, 2005, 2007; McCulloch *et al*., 2005a; Hein *et al*., 2009). Key glacial periods that have been identified include the greatest extent of ice in Patagonia, known as the Greatest Patagonian Glaciation (GPG), and the local Last Glacial Maximum (LGM). Most studies have focused on the LGM (Hulton *et al*., 1994, 2002; Clapperton *et al*., 1995; McCulloch and Bentley, 1998; Benn and Clapperton, 2000a, b; Bentley *et al*., 2005; Glasser and Jansson, 2005; McCulloch *et al*., 2005a; Douglass *et al*., 2006; Kaplan *et al*., 2008b) and a number of authors have investigated earlier glaciations, including the GPG (Mercer, 1976, 1983; Rabassa and Clapperton, 1990; Rabassa *et al*., 2000; Coronato *et al*., 2004a, b; Singer *et al*., 2004a; Glasser *et al*., 2008; Kaplan *et al*., 2009). The record of glacier fluctuations in southern Patagonia is of great importance because of its global location, as it presents a terrestrial record of glaciations in the southern hemisphere and spans the area of the Southern Westerlies (McCulloch and Davies, 2001; Douglass *et al*., 2005; Sugden *et al*., 2005). This location is therefore also ideal for testing alternative hypotheses about the mechanisms of climate change based on hemispheric synchrony or asynchrony (Sugden *et al*., 2005).

1.1 Aim and objectives

The main aim of this project is to reconstruct the ice sheet dynamics and glacial history of the Seno Skyring-Seno Otway-Strait of Magellan region in southernmost Patagonia.

To achieve this aim a number of objectives have been identified. These are:

(i) to accurately map the glacial geomorphology of the study area from remote sensing.

(ii) to evaluate whether the mapped glacial geomorphology presents evidence for a palaeo-ice stream in this region - as hypothesised by Clapperton (1989) and Benn and Clapperton (2000a) - by comparing to published criteria for the presence of palaeo-ice streams (Stokes and Clark, 1999).

(iii) to reconstruct the wider glacial dynamics from the geomorphological evidence and to attempt to place this reconstruction within the chronological framework of Patagonian ice sheet history.

1.2 Thesis structure

The glacial history of southernmost Patagonia is reviewed in Chapter 2, from the earliest recorded evidence for ice through to the Holocene. Particular attention is paid to the Strait of Magellan region because it is the focus of this study. In Chapter 3 ice streams and palaeo-ice streams are reviewed. This chapter discusses the dynamics of contemporary ice streams and the key geomorphological evidence which can be used to identify palaeo-ice streams. The characteristics of surging glacier and terrestrial ice margin landsystems are also discussed because these share a number of criteria with the palaeo-ice stream landsystem. Chapter 4 reviews the value of remote sensing to aid geomorphological mapping and the subsequent use of a glacial geomorphological model in order to reconstruct ice sheet processes. The way in which these have been implemented in this study is then outlined in Chapter 5 (Methods), along with brief descriptions of the types of geomorphology that are expected to be present.

The results of the study are contained in Chapter 6. This includes a copy of the full glacial geomorphological map (Figure 6.1; inside back cover), as well as detailed descriptions of the geomorphology found within the study area. An interpretation and discussion of the mapped geomorphology can be found in Chapter 7. This includes a reconstruction of the ice sheet position and dynamics over a number of time-steps. An attempt is then made to place the reconstruction within the chronological framework of the region. The main conclusions of this study are outlined in Chapter 8.

Chapter 2 - The Glacial History of Southernmost Patagonia

2.1 Introduction

The landscape of southernmost South America bears a distinct glacial imprint (Coronato *et al*., 2004b). During a succession of glaciations, an extended ice sheet formed along the southern Andes, known as the Patagonian Ice Sheet (Glasser *et al*., 2008). During the most extensive of these glaciations, valley and piedmont glaciers extended eastwards up to several hundred kilometres from the ice sheet (Rabassa, 2008). Deposits from these advances are thought to record an extensive glacial history stretching from the Late Tertiary through to the Holocene (Mercer, 1976; Rabassa and Clapperton, 1990; Clapperton, 1993). According to Rabassa and Clapperton (1990) and Rabassa and Coronato (2009), the glacial history of the southern Andes is one of the most complete in the world, and Kaplan *et al*. (2007) suggested that, outside of Antarctica, southern South America has the longest and most complete record of Quaternary glaciations. The advance and retreat of fluctuating outlet glaciers are recorded by well-preserved landform assemblages and sediments throughout the southern Andes, stretching from ca. 36°S to ca. 56°S (see Figure 2.1; Clapperton, 1993; Benn and Clapperton, 2000a, b; Glasser *et al*., 2008; Hein *et al*., 2009).

The glacial imprint of southern Patagonia presents a terrestrial record of glaciations in the southern hemisphere and spans the area of the Southern Westerlies (McCulloch and Davies, 2001; Douglass *et al*., 2005; Sugden *et al*., 2005). This makes it an important global location because one of the main questions that will help to determine global climate dynamics is whether the fluctuations of southern hemisphere glaciers respond in synchrony with northern hemisphere ice sheets and mountain glaciers (McCulloch *et al.*, 2000; Kaplan *et al.*, 2004; Singer *et al.*, 2004a; Sugden *et al*., 2005). The establishment of leads and lags between the hemispheres and between mid-latitudes and Antarctica allows for an insight into the mechanisms and resilience of global climate (Denton *et al.*, 1999; Sugden *et al.*, 2005). If ice sheet fluctuations on millennial and sub-millennial scales are in phase in both hemispheres then a dominance of atmospheric mechanisms of climate change is suggested, with insolation changes in the northern hemisphere driving changes in the southern hemisphere (McCulloch *et al.*, 2005a; Sugden *et al.*, 2005). If fluctuations are out of phase, with one hemisphere leading the other, then switches in the oceanic thermohaline circulation could well be dominant (Benn and Clapperton, 2000a; Kaplan *et al.*, 2004; McCulloch *et al.*, 2005a; Sugden *et al.*, 2005).

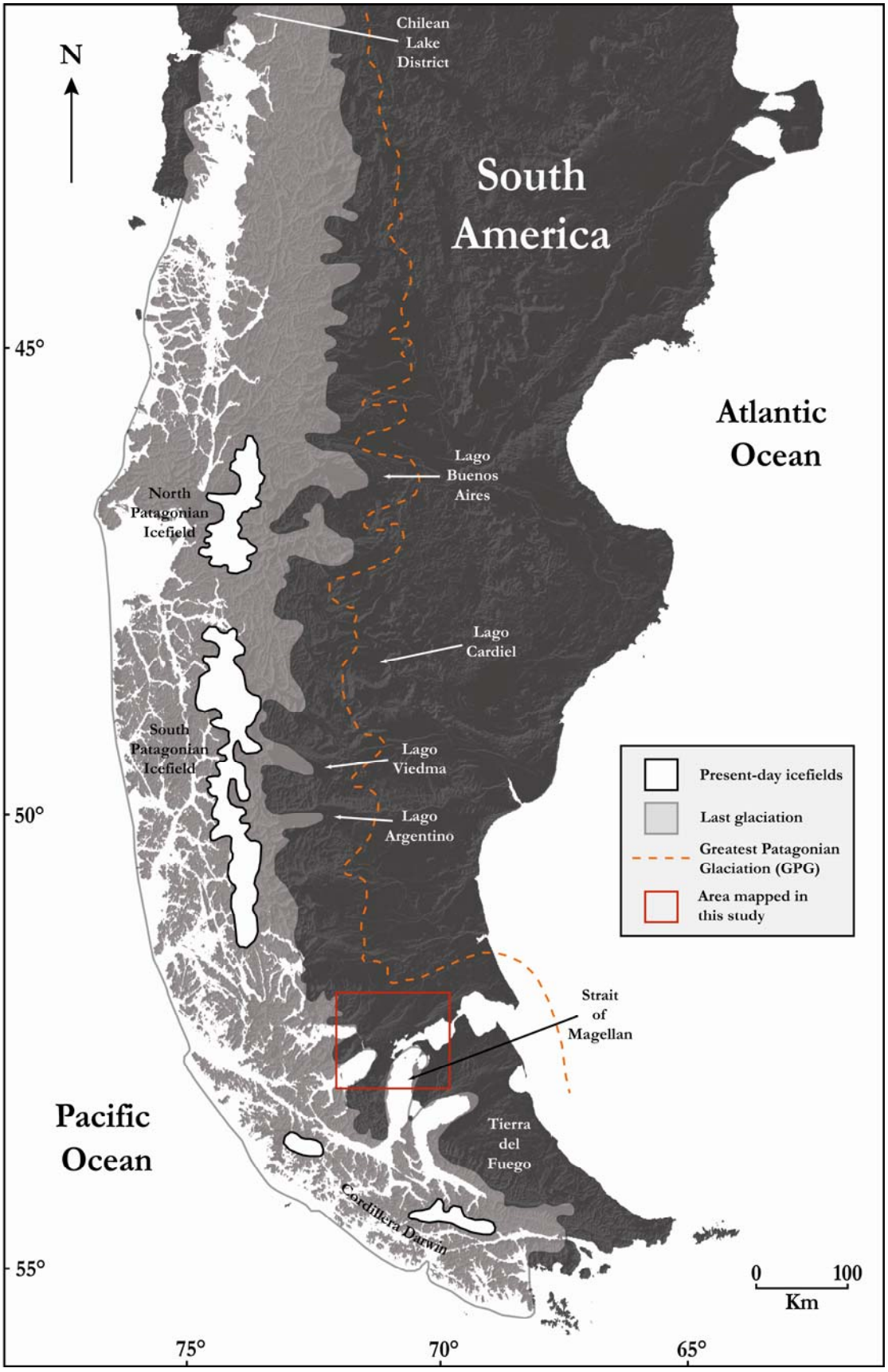

Figure 2.1 - Map of southernmost South America showing present-day icefields, former glacial limits and locations referred to in this study. Adapted from Sugden *et al.* (2005); after Caldenius (1932), Clapperton (1993), McCulloch *et al.* (2000) and Hollin and Schilling (1981).

High-resolution mapping and dating of terrestrial glacial records in the southern hemisphere, such as in South America, can help to unravel the processes that drive glacial climates (Kaplan *et al.,* 2004) and the mechanisms of climate change (McCulloch *et al.,* 2005a). In particular this may help us to distinguish between local and global patterns of environmental change, which will improve understanding as to how the ocean-atmosphere systems of the two hemispheres interact (Clapperton *et al.,* 1995; Denton *et al.*, 1999; Fogwill and Kubik, 2005). This highlights the importance of the terrestrial glacial record in South America because it is in an ideal location for testing alternative hypotheses about the mechanisms of climate change based on hemispheric synchrony or asynchrony (Sugden *et al.,* 2005).

This chapter aims to review the literature on the glaciations of southernmost South America, with a particular focus on the Strait of Magellan region (see Figure 2.1), in order to compile a chronology of the glacial history of the area from the Late Tertiary through to the present day. The moraine systems in southernmost Patagonia occur at a greater distance from the Andes (up to ca. 300 km) than those around the contemporary North and South Patagonian Ice Sheets (Glasser *et al*., 2008). According to Clapperton (1990), glaciers in the Patagonian Andes advanced in the Late Miocene and fluctuated several times during the Pliocene.

2.2 Late Miocene-Earliest Pliocene to Earliest Pleistocene Glaciation

Meteorological conditions suitable for the growth of glaciers in the Patagonian Andes are thought to have existed for at least the last 14 Ma (Clapperton, 1993). The presence of Late Miocene glacial deposits in Patagonia at Lago Cardiel (49°S) with ages as old as 10.5 Ma has been suggested by Wenzens (2006), with nine advances between 10.5 and 5.4 Ma. These ages are based on the dating of basaltic lava which partly covers Patagonian gravels (Wenzens, 2006). Rabassa (2008) agreed that the possibility of very early Late Miocene glaciations was interesting, but that further study was needed to confirm this interpretation. The oldest dated glacial deposits in South America can be found at Meseta del Lago Buenos Aires (see Figure 2.1), a basaltic plateau centred at 47°S and situated more than 100 km from the nearest Andean cordillera glaciers (Mercer and Sutter, 1982; Clapperton, 1993). The radiometric (K-Ar) dating of early and pre-Quaternary deposits was carried out by Mercer (1969, 1976, 1983) and Mercer and Sutter (1982), and was made possible by the fortuitous preservation of glacial sediments interbedded with basaltic lava flows (Clapperton, 1990, 1993). The basaltic lava flows at Meseta del Lago Buenos Aires have

average ages of 7.03 ± 0.11 Ma and 4.63 ± 0.07 Ma (Mercer, 1983), constraining the deposition of the till to between ca. 7 and 4.6 Ma (Mercer and Sutter, 1982; see Table 2.1). From this work, Coronato *et al*. (2004b) suggested the till deposits on the southern margin of Lago Buenos Aires (LBA) represent the oldest Cenozoic glaciation in South America, between 7.03 Ma and 6.75 Ma. The late Tertiary glacier that deposited this till was at least 30 km long according to Mercer and Sutter (1983), as demonstrated by the provenance of some erratics (Clapperton, 1993). Rabassa and Clapperton (1990) stated that the oldest glacial deposits were found at Lago Viedma (49°S), whereas all other studies refer to LBA as the site for the oldest till (Mercer and Sutter, 1982; Mercer, 1983; Clapperton, 1993; Coronato *et al*., 2004a, b). Late Miocene-Earliest Pliocene glaciation could perhaps have also affected the mountainous areas of Tierra del Fuego and the Cordillera Darwin at the southernmost tip of Patagonia (Coronato *et al*., 2004a). These Late Cenozoic glacial events in Patagonia indicate that outlet glaciers were extending more than 30 km east of the isolated ice caps in the Patagonian Andes (Rabassa, 2008). Furthermore, these outlet glaciers are inferred to have advanced as low-gradient, wide piedmont lobes over a low relief eastward-sloping surface (Rabassa, 2008). It is inferred that the local climate at this time must have been colder than today's (Mercer and Sutter, 1982). The Late Miocene deposits of Patagonia are important in a global context as chronological control on Tertiary glacial drifts is extremely poor outside of South America (Clapperton, 1990).

Rabassa *et al*. (2005) suggested that a minimum of eight glaciations occurred in the Middle-Late Pliocene. The next oldest dated deposits can be found at Lago Viedma (Clapperton, 1993). A 20m cliff exposure at this site displays four tills, which were interpreted as representing four glacial advances separated by long intervals of non-glacial conditions (Clapperton, 1993). The stratigraphically oldest till at this site lies between two lava flows and has been dated to 3.6 Ma by Mercer (1976; see Table 2.1). This is thought to represent the onset of severe and extensive glacial conditions in southern Patagonia (Mercer, 1976, 1983; Mercer and Sutter, 1982). At this site, the tills at Meseta Desocupada have been dated to 3.4 Ma and the tills at Meseta Chica have been dated to 3.68 - 3.55 Ma (Mercer, 1976). Both of these sites are located slightly further north of Lago Viedma. Mercer (1969) dated deposits at Cerro del Fraile (50°S) in the vicinity of Lago Argentino by using K-Ar analysis on overlying lava flows. This produced an age of 3.2 ± 1 Ma for the oldest lava flow, suggesting that glaciation in southern Argentina had begun before 2 Ma (Mercer, 1969). The dating carried out by Mercer (1976, 1983) and Mercer and Sutter (1982) at Meseta del Lago Buenos Aires show that there is evidence for a much earlier

glaciation in Patagonia than that suggested by the Cerro del Fraile deposit. This evidence from Lago Viedma and Lago Argentino indicates that several glacier advances occurred between the Middle and Late Pliocene at these sites, the first at ca. 3.5 Ma (Rabassa, 2008).

Mercer (1976) argued that little is known about glacial events in southern South America in the period from 3.3 Ma to 2.4 Ma. This period corresponds with the Gauss palaeomagnetic epoch and Mercer (1976) suggested that some of the tills north of Lago Viedma could have formed during this time. All that is known is that they are younger than 3.5 Ma (Mercer, 1976). This seems to contradict Rabassa and Clapperton (1990), who claimed that Mercer (1976) assumed the Lago Viedma area had remained unaffected by glaciation during the Gauss epoch. To the north and east of Lago Viedma, Wenzens (2000) obtained limiting ages of glacigenic deposits of 3.0 and 2.25 Ma. These ages are based on K-Ar dating of two basalts, one of which lies beneath glaciofluvial sediments (the older date) that merges into a river terrace upon which the second (younger) basalt sits (Wenzens, 2000). Basalt covering coarse outwash gravel at Cóndor Cliff in the Río Santa Cruz Valley, to the east of Lago Argentino, was dated at 2.79 ± 0.15 Ma (Mercer, 1976; Clapperton, 1993). This was used to imply that glaciation had begun in the mountains to the west at this time. Rabassa (2008) suggested that in some areas of southernmost Patagonia outlet glaciers extended from the mountain ice caps to points close to the GPG limits as early as the Middle Pliocene. At LBA the Chipanque Moraines (Malagnino, 1995) are suggested in one interpretation to be younger than 3.5 Ma but older than 2.3 Ma (Malagnino, 1995; Rabassa, 2008), following the chronology based on K-Ar dating of interbedded lava flows of Mercer (1976). Mercer (1983) suggested that the first glaciations in South America were rare events separated by long non-glacial periods.

Several glaciations occurred between ca. 2 Ma and ca. 1 Ma (Mercer and Sutter, 1982). Six tills interbedded with lava flows have been studied south of Lago Argentino at Cerro del Fraile (50°S) by Mercer (1976, 1983). This entire sequence was deposited between > 2.11 Ma and 1.51 - 1.05 Ma (Mercer, 1976). The maximum age of the oldest till at > 2.11 Ma is not known and the five successive tills are dated at 2.12 - 2.11 Ma, 2.11 - 1.91 Ma, 1.91 - 1.71 Ma (two of the tills) and 1.51 - 1.05 Ma respectively (Mercer, 1976, 1983). Till lies between lava flows dated at between 2.02 ± 0.09 Ma and 2.01 ± 0.1 Ma at a site 25 km to the east of Lago Argentino (Mercer, 1976, 1983). If the 2.73 Ma old deposit at Cóndor Cliff (2.79 ± 0.15 Ma old as dated by Mercer, 1976) is included, Clapperton (1993) suggested that at least seven glacial advances occurred in a 1.68 Ma interval. The more

recent study by Singer *et al*. (2004b) has re-dated the Cerro del Fraile sequence; a minimum of seven glaciations have been recognised between 2.16 and 1.43 Ma. On Tierra del Fuego, east of the Strait of Magellan (see Figure 2.1), Meglioli (1992) estimated an age of between 2.05 and 1.86 Ma for the Río Grande drift based on K-Ar dating of basalts south of the Río Gallegos valley, implying a pre-GPG Late Pliocene-Early Pleistocene age. Rabassa and Coronato (2009) suggested that during the Ensenadan Stage (ca. 2.1 – 0.5 Ma) a well-defined alternating sequence of glacial and interglacial events occurred in Patagonia. There could have been up to 15 distinct glacial events during this time, including the GPG (Rabassa and Coronato, 2009).

The chronology of glacial advances in southern Patagonia from the Late Miocene to the Early Pleistocene reviewed here supports Mercer (1983), who stated that glaciations occurred in South America between 7 and 4.6 Ma, at 3.6 Ma, and repeatedly after about 2 Ma. There is also evidence for glacial advances in the period between ca. 3.6 and ca. 2 Ma (Mercer 1976; Clapperton, 1993; Malagnino, 1995; Wenzens, 2000; Rabassa, 2008).

2.3 The Greatest Patagonian Glaciation

The Patagonian Ice Sheet reached the Atlantic Ocean in southernmost Patagonia at its maximum extent, named the Greatest Patagonian Glaciation (GPG) by Mercer (1976, 1983; see Figure 2.1 and Table 2.1). Outlet glaciers reached the Atlantic Ocean in the area south of the Rio Gallegos valley and north of the Strait of Magellan for the first time in the Cenozoic (Rabassa, 2008). Coronato *et al*. (2004b) and Rabassa (2008) suggested that these limits correspond to the 'Initioglacial Glaciation' as mapped by Caldenius (1932). These outermost GPG deposits are dated at ca. 1.1 Ma (Mercer, 1976; Rabassa and Clapperton, 1990; Rabassa *et al*., 2000; Singer *et al*., 2004a; Bentley *et al*., 2005; Kaplan *et al*., 2007) and are best represented in Patagonia by deposits from the former Magellan lobe (see Figure 2.2a), the former Rio Gallegos lobe and at LBA (see Figure 2.1). Clapperton (1990) claimed that the morainic landforms that mark the furthest eastward extent of ice may well be the oldest of any such features on the planet. According to Glasser *et al*. (2008), the GPG developed between 1.168 Ma and 1.016 Ma and represents the most extensive glacial event that has taken place in South America during the Early Pleistocene (Coronato *et al*., 2004a; Kaplan *et al*., 2009).

Table 2.1 – Chronology of selected Miocene, Pliocene and Pleistocene glaciations in Patagonia. All examples are from studies cited within this project. Ages marked by * are ^{14}C, all other ages are in calendar years.

Geologic Epoch	Age (Ma)	Glaciation Name (if any)	Strait of Magellan		LBA		CLD		Lago Viedma		Lago Argentino		Other	
			Drift Name	Age Constraint	Drift Name	Age Constraint	Drift Name	Age Constraint	Drift Name	Age Constraint	Drift Name	Age Constraint	Location	Age Constraint
PLEISTOCENE	0.01	LGM	E D C B	12.0-10.3ka* > 17.5 ka >21.7-20.4ka 25.3-23.1 ka	*Fenix* VI - I	23 - 15.6 ka	Llanquihue VI V IV III II I	14.9 ka* 21.0 ka* 23.1 ka* 26.9 ka* 29.6 ka* ≥ 33.5 ka*/ > 49.9 ka*						
	0.025		A	> 90 ka										
	0.05	GPG - 3	Primera Angostura	> 47-45 ka	*Moreno* III - I	760 - 109 ka								
	0.1	GPG - 2	Punta Delgado	> 47-45 ka	*Deseado* III - I									
	0.5	GPG - 1	Cabo Virgenes	1070 - 360 ka	*Telken* VI - I	1016 - 760 ka								
	1.0	GPG	Sierra de Los Frailes Bella Vista	> 450 ka 1168-1070 ka	*Telken* VII	> 1016 ka								
	1.5										Cerro Del Fraile	2.16 - 1.43 Ma		
PLIOCENE	2.0								Río Shehuen	3.0-2.25 Ma			Bahía Inútil - Rio Grande Drift	2.05 - 1.86 Ma
	3.0				*Chipanque* Moraines	3.5 - 2.3 Ma			Meseta Chica/ Desocupada	3.6 - 3.4 Ma	Cóndor Cliff	> 2.79 Ma		
	4.0													
MIOCENE	5.0													
	6.0													
	7.0				Meseta del LBA	7 - 4.6 Ma							Lago Cardiel ?	10.5 - 5.4 Ma ?
	10.5													

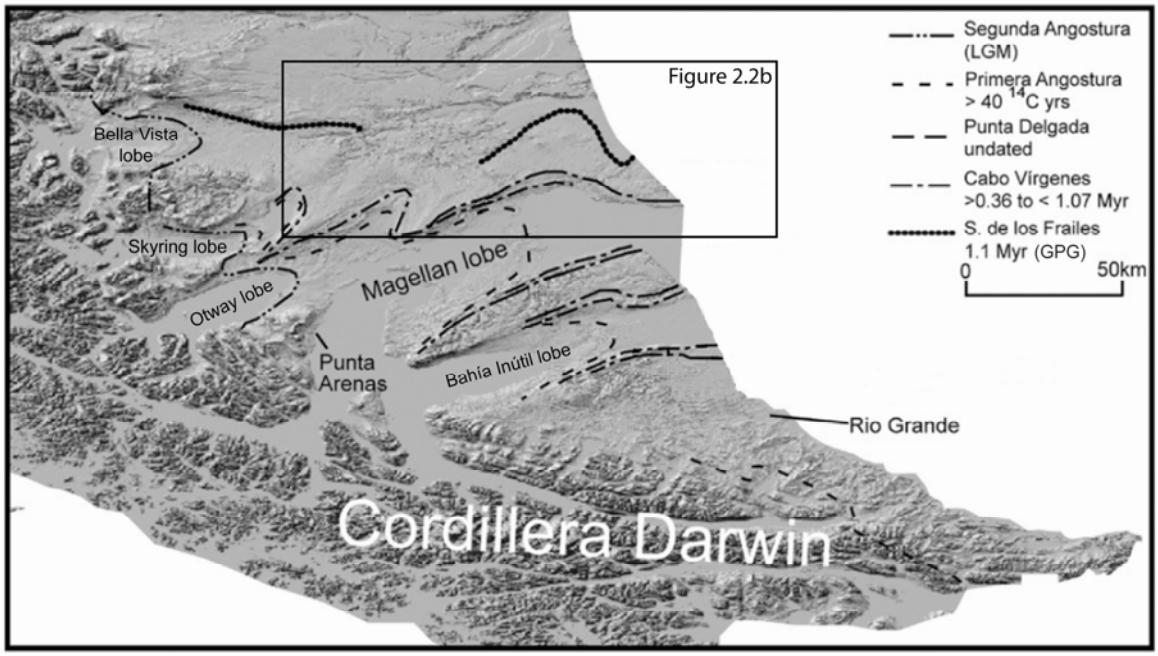

Figure 2.2a - Area of five former ice lobes and five major glacial limits correlated across southernmost Patagonia (Meglioli, 1992; Rabassa *et al.*, 2000; Bentley *et al.*, 2005). The names of the units are for the Magellan lobe. Adapted from Kaplan *et al.* (2007).

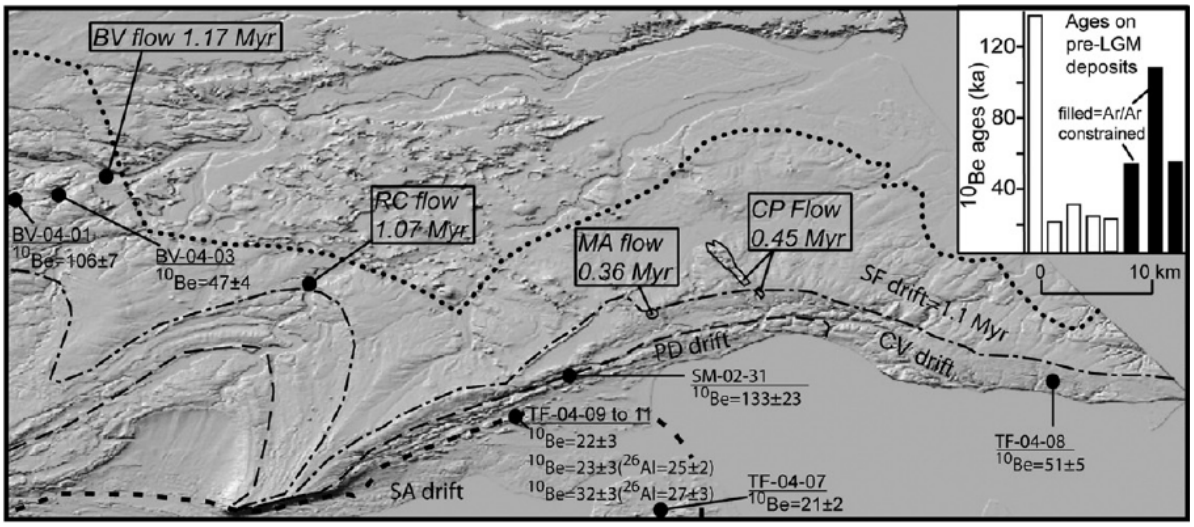

Figure 2.2b – Inset shown on Figure 2.2a. SF = Sierra de Los Frailes drift, BV = Bella Vista drift, CV = Cabo Virgenes drift, PD = Punta Delgado drift, SA = Segunda Angostura drift. All ages are from Kaplan *et al.* (2007).

The Strait of Magellan lobe was the largest and most impressive glacier in southernmost Patagonia, and indeed the southern hemisphere outside of Antarctica (Coronato *et al.*, 1999; Rabassa *et al.*, 2000). The GPG limit for the Magellan lobe is known as the Sierra de Los Frailes drift (Kaplan *et al.*, 2007; Rabassa, 2008; see Figures 2.2a and 2.2b). Three basalt flows that overlie this drift produced dates of 320 ± 20, 310 ± 30, 360 ± 40 and 450 ± 100 ka (Meglioli, 1992; Kaplan *et al.*, 2007) and provide minimum ages for the Sierra de Los Frailes drift. Glacial landforms associated with this drift are not obvious according to

Rabassa *et al*. (2000), but the till can be seen along the marine cliffs. Coronato *et al*. (2004a) suggested that the Sierra de Los Frailes Glaciation in the Río Santa Cruz valley and Bahía Inútil-Bahía San Sebastián depression is represented by till deposits that form extensive plains with very subdued topography, and Rabassa *et al*. (2000) stated that the drift occurs as till remnants of glacial landforms that are hard to pick-out from the superficial morphology. A piedmont-type glaciation is inferred during the GPG in this area (Rabassa *et al*., 2000; Coronato *et al*., 2004a) with large lobes of reduced thickness but great extension (Rabassa, 2008). The GPG date for the Magellan lobe was constrained to be between ca. 1.0 Ma and 1.2 Ma from the use of K-Ar techniques on basaltic lavas to the north of the Strait of Magellan (Mercer, 1976). Approximately 60 km to the north of the Strait, the Rio Gallegos lobe deposited the Bella Vista drift during the GPG (Singer *et al*., 2004a; Bentley *et al*., 2005; Kaplan *et al*., 2007; see Figures 2.2a and 2.2b). Basalts above and below the Bella Vista drift have been $^{40}Ar/^{39}Ar$ dated to 1,168 ± 14 and 1,070 ± 20 ka, providing maximum and minimum ages for the greatest extent of ice (Singer *et al*., 2004a).

The GPG is also well dated at LBA, ca. 1000 km to the north (Kaplan *et al*., 2007, 2009; see Figure 2.3). Here, the glacial record comprises one of the most complete and well-preserved sequences of Quaternary moraines in the world (Clapperton, 1993; Singer *et al*., 2004a; Douglass *et al*., 2006). From the $^{40}Ar/^{39}Ar$ and K-Ar dating carried out by Singer *et al*. (2004a) on three lava flows a chronology of the LBA moraine system has been produced. Using the informal names of Kaplan *et al*. (2004, 2005; see Figure 2.3), at least six *Telken* moraines were deposited between 1016 and 760 ka, five *Deseado/Moreno* moraines were deposited between 760 and 109 ka and six *Fenix* moraines after 109 ka (Kaplan *et al*., 2009). The GPG at LBA is represented by the oldest glacial deposit (*Telken* VII) which underlies the Arroyo Telken lava flow (Singer *et al*., 2004a; Kaplan *et al*., 2004, 2005, 2009). The Arroyo Telken flow has been dated to 1016 ± 10 ka, resulting in a GPG age at LBA of > 1016 ka (Singer *et al*., 2004a). This provides an additional minimum age for the GPG in southern Patagonia (Kaplan *et al*., 2007).

The Pleistocene moraines and till representing the greatest extent eastwards of the Patagonian Ice Sheet were correlated from Lago Epuyén (41°S) to the Strait of Magellan (52°S) by Singer *et al*. (2004a). Combined with the basalt flow dates from Bella Vista and Arroyo Telken, Singer *et al*. (2004a) suggested this provided strong evidence that the mapping by Caldenius (1932) was valid and that the GPG occurred between 1168 ± 14 ka and 1016 ± 10 ka. This provides a more precise lower limit for the GPG than that of

Mercer (1976), and also explains the origin of the dates suggested by Glasser *et al.* (2008) for the development of the GPG.

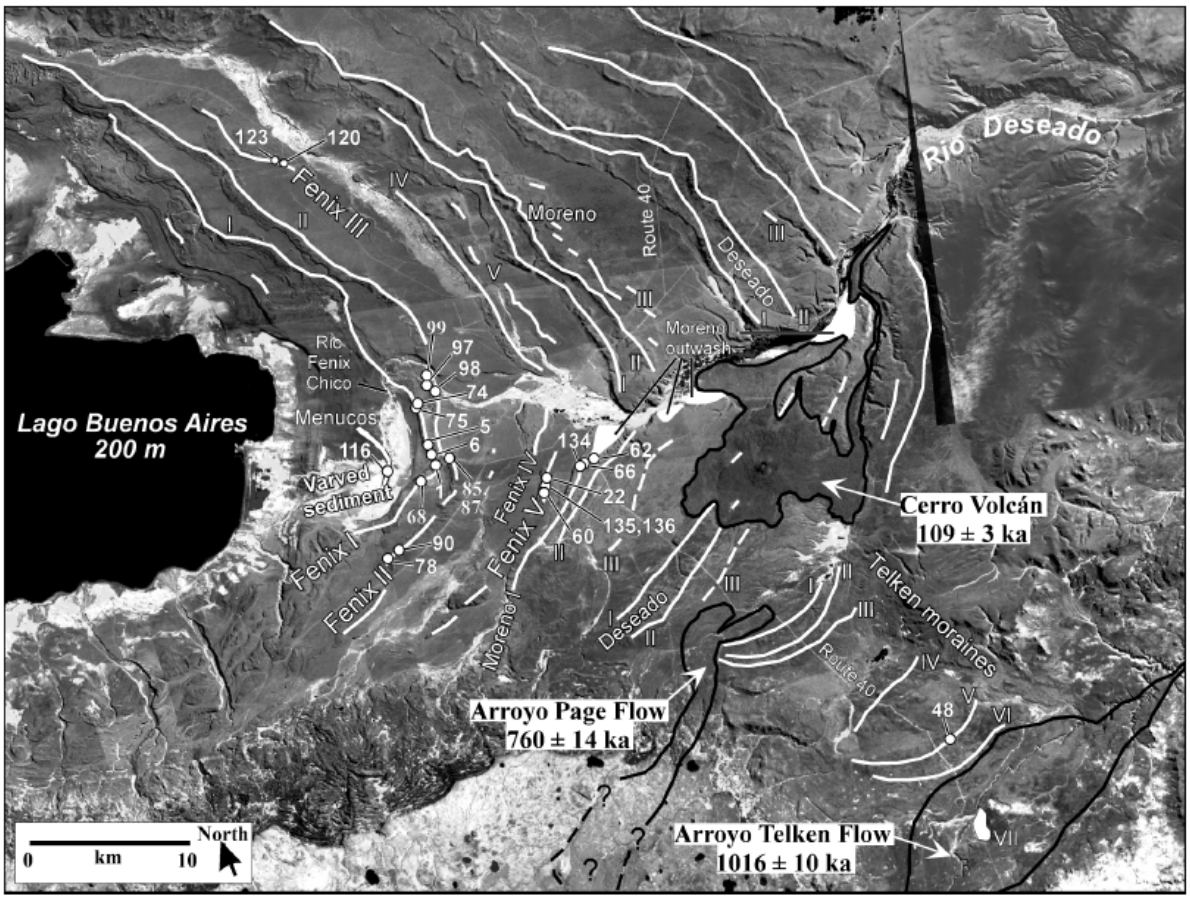

Figure 2.3 - Landsat image showing the moraine system around the eastern edge of Lago Buenos Aires, with dated lava flows. From Singer *et al.* (2004a).

During the GPG, the areal extent of ice in southern Patagonia was estimated by Kaplan *et al*. (2009) to be ca. 558,000 - 542,000 km^2, compared to ca. 422,000 km^2 during the LGM. These figures were achieved by digitising the GPG limit mapping and entering the data into a geographic information system (Kaplan *et al*., 2009). The resulting areas differ markedly from those proposed by Clapperton (1990), in which it was suggested the GPG areal ice extent was 300,000 km^2 and the LGM areal ice extent was 100,000 km^2. The reason for this large discrepancy is hard to pinpoint because Clapperton (1990) makes no mention of how these figures were calculated. This suggests that the difference in estimates could be because of the inclusion by Kaplan *et al*. (2009) of more recent mapped limits for both the GPG and LGM, which in particular appear to show a greater extent of ice to the west of the Andes and off the eastern coast of Tierra del Fuego (compare Figure 2.4 from Kaplan *et al*., 2009 and Figure 2.5 from Singer *et al.*, 2004a). Ice appears to have formed a continuous ice sheet along the southern Andes during the GPG, from which

outlet lobes overran a landscape of piedmont gravels to the east (Rabassa and Clapperton, 1990; Singer *et al*., 2004b; Kaplan *et al*., 2009). These lobes include the Rio Gallegos and Magellan lobes in southernmost Patagonia. Singer *et al*. (2004a) inferred that an ice sheet capable of feeding the large outlet glaciers that produced the GPG limits grew at ca. 1.2 - 1.1 Ma.

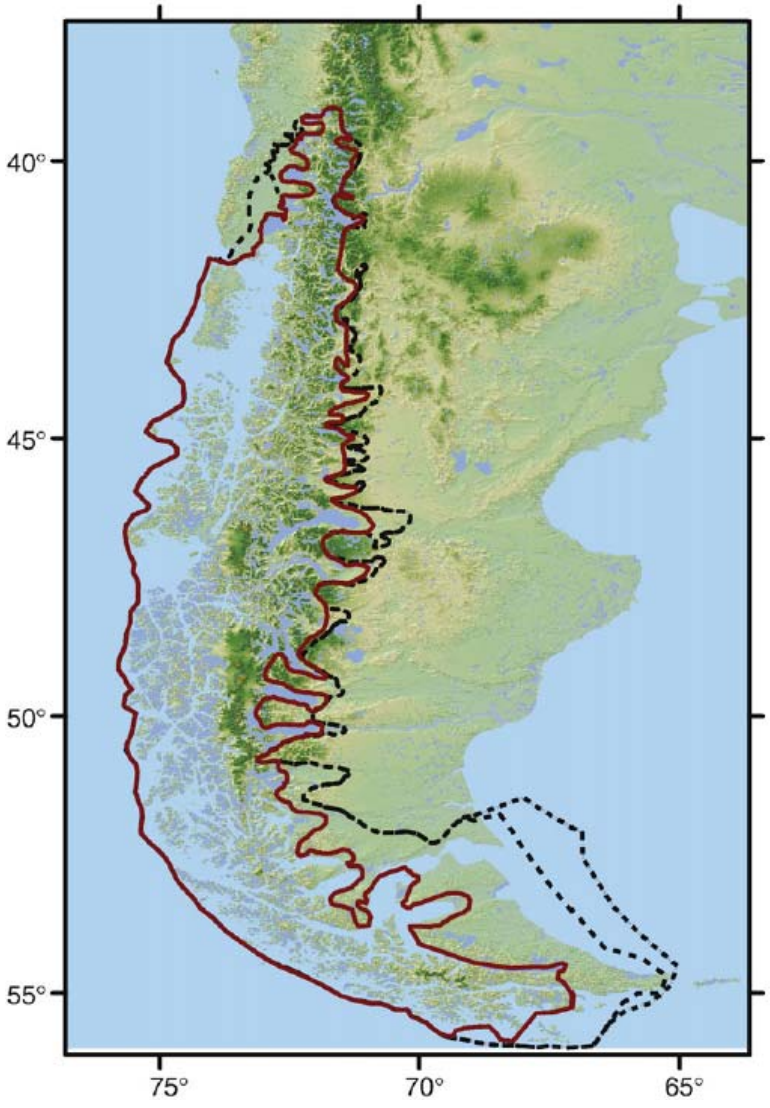

Figure 2.4 – Ice limits in southern Patagonia during the GPG (in black) and LGM (in red). From Kaplan *et al.* (2009).

Following the greatest extent of Patagonian ice of the GPG, successive glaciations have been less extensive (Clapperton, 1993; Kaplan *et al*., 2009). Climatic changes such as a rise in temperature or decreasing precipitation could help to explain the long-term trend of decreasing ice. However, available studies suggested that the GPG was not fundamentally cooler than glacial maxima during the last several glacial cycles (Hodell *et al*., 2002; Carter and Gammon, 2004). In addition, no data exist for palaeoprecipitation rates, which makes it difficult to gauge the importance of rainfall to the trend of decreasing ice extent

(Kaplan *et al.*, 2009). It is claimed that no evidence exists for increasing palaeotemperatures that would cause a decrease in the areal ice extent over the last 1 Ma (Kaplan *et al*., 2009). Kaplan *et al*. (2009) suggested that the decrease in ice extent following the GPG is a result of non-climatic effects, principally glacial erosion of mass-accumulation areas and modification of low areas at and below the Equilibrium Line Altitude (ELA). It is thought that this glacial erosion over time could foster low-gradient fast ice in low-lying areas (Kaplan *et al*., 2009). It is notable that the maximum extent of ice in the northern hemisphere occurred after 800 ka, > 200 ka later than the GPG (Kaplan *et al*., 2009).

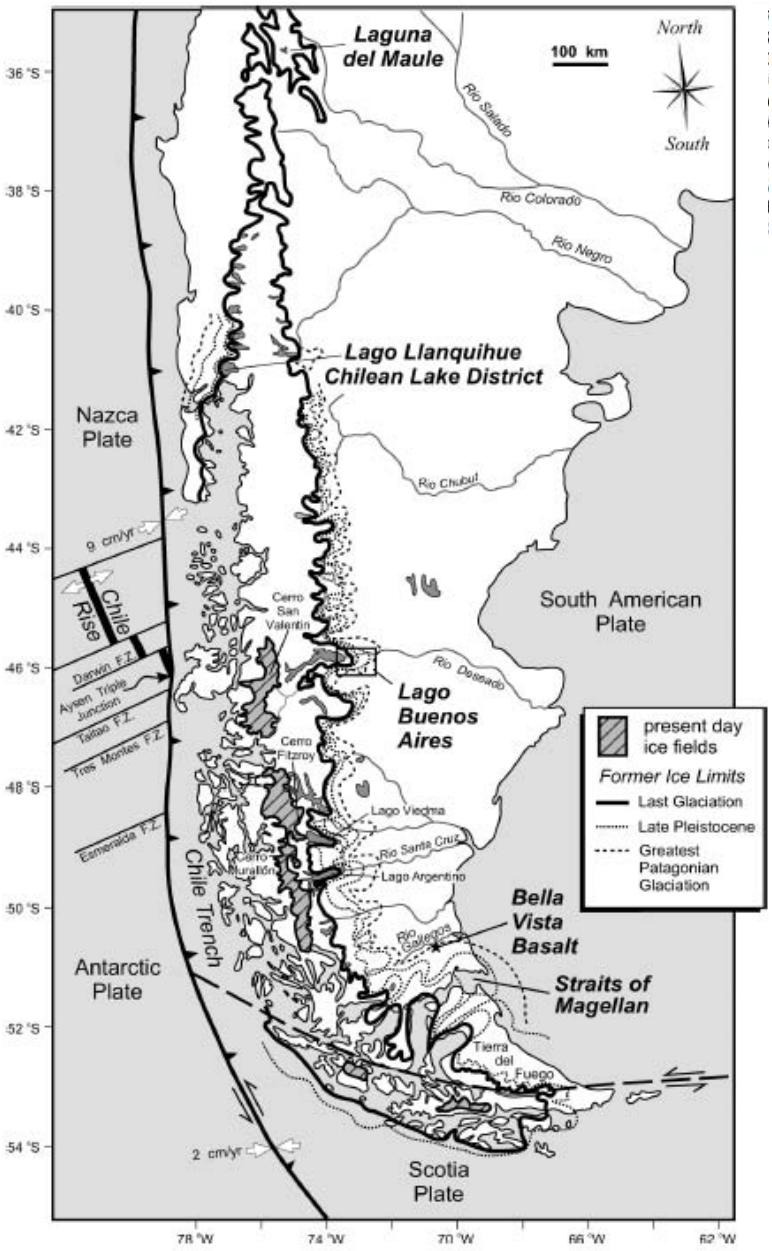

Figure 2.5 – Glacial deposits of South America after Caldenius (1932) and Clapperton (1993; and references therein). From Singer *et al.* (2004a).

2.4 Middle to Late Quaternary Glaciation: After the GPG

After the GPG, 14 to 16 glacial and stadial events alternated with corresponding interglacial/interstadial equivalents (Rabassa *et al*., 2005). At least four of these are thought to have been full glacials (Coronato *et al.*, 2004a). The glaciations show a trend of decreasing ice extent since ca. 1.1 Ma (Clapperton, 1993; Kaplan *et al*., 2009). In southernmost Patagonia, the Rio Gallegos, Magellan and Bahía Inútil-San Sebastián ice lobes deposited five distinct glacigenic limits (Kaplan *et al*., 2007). The outermost of these deposits, known as the Serro de los Frailes Glaciation, records the extent of ice in southernmost Patagonia during the GPG (Coronato *et al*., 2004a; Kaplan *et al*., 2007). The four inner drift limits represent post-GPG glaciations of decreasing extent, during which ice lobes repeatedly occupied the low-lying topographic depressions to the east of the Andes (Glasser *et al*., 2008). For the former Magellan lobe the drift limits closely correspond with the mapping of Caldenius (1932).

2.4.1 Magellan lobe

The first major drift unit of the Magellan lobe that is younger than the GPG is known as the Cabo Vírgenes drift (Rabassa *et al*., 2000; Coronato *et al*., 2004a; Kaplan *et al*., 2007; see Figures 2.2a and 2.2b), named Post-GPG 1 by Coronato *et al.* (2004b). This glacial advance is represented by well-defined morainic arcs (Rabassa *et al*., 2000; Rabassa, 2008). It is thought that this advance corresponds to the 'Daniglacial' event of Caldenius (1932). In southernmost Patagonia this drift was deposited by two ice lobes (Coronato *et al*., 2004a). A combined glacier that covered the region of Seno Skyring, Seno Otway and the Straits of Magellan was the northernmost of the two (Coronato *et al*., 2004a). Terminal moraines associated with this advance surround lakes near the heads of both Seno Skyring and Seno Otway and lateral moraines exist along both margins of the Strait (Coronato *et al*., 2004a). The terminal position of this lobe is not visible and Rabassa (2008) suggested that this is either because it is submerged in the eastern entrance of the Strait or that it was eroded by the meltwater streams of later glaciations.

The second lobe occupied the Bahía Inútil- Bahía San Sebastián depression (Coronato *et al*., 2004a). The age of this drift has been estimated at between > 0.36 and < 1.07 Ma by Meglioli (1992), placing it in the latest Early Pleistocene (Rabassa, 2008). The minimum age is constrained by $^{40}Ar/^{39}Ar$ dating of the Monte Aymond and Cerro la Pirca lava flows north of the Strait of Magellan, with results of 450 ± 100 and 360 ± 40 ka respectively (Meglioli, 1992). Dating of pre-LGM deposits is often more difficult than that of LGM

deposits because they mostly lie outside the ^{14}C dating limits according to Glasser *et al*. (2008). However, $^{40}Ar/^{39}Ar$ and K-Ar dating of interbedded lava flows (Mercer, 1976, 1983; Mercer and Sutter, 1982; Meglioli, 1992; Singer *et al.*, 2004a) and more recent cosmogenic nuclide surface exposure dating of morainic boulders and outwash gravels (Kaplan *et al.*, 2004, 2005, 2007; Douglass *et al.*, 2006; Hein *et al.*, 2009) have helped to provide pre-LGM ages throughout southern Patagonia.

Subsequent glaciations in the Strait of Magellan region are 'nested' within each other (Kaplan *et al*., 2007). The next youngest drift is called the Punta Delgado drift (Coronato *et al*., 2004a; Kaplan *et al*., 2007; Rabassa, 2008; see Figures 2.2a and 2.2b). This is the second drift that correlates to the 'Daniglacial' of Caldenius (1932) and represents a second, less-extensive advance of the confluent ice lobes (Coronato *et al*., 2004a; Rabassa, 2008). It is distinguished from the Cabo Vírgenes drift due to differences in morphology, soil development and periglacial features (Rabassa *et al*., 2000; Rabassa, 2008). The frontal position of the Skyring-Otway-Magellan lobe is represented at Bahía Posesíon and Punta Catalina by small, isolated moraines covered in outwash deposits and separated from younger moraines by extensive glaciofluvial plains (Coronato *et al*., 2004a). The Punta Delgado drift itself is undated, although two ^{14}C dates of 47 and 45 ^{14}C ka BP of shelly till north of Punta Arenas provide a minimum age (Kaplan *et al*., 2007).

The Primera Angostura drift (see Figures 2.2a and 2.2b) represents the next less-extensive advance in the Strait of Magellan region (Clapperton, 1993; Rabassa *et al*., 2000; Coronato *et al*., 2004a; Kaplan *et al*., 2007) and corresponds to the 'Gotiglacial' as defined by Caldenius (1932). The frontal morainic complex forms the first narrows of the Strait, the Primera Angostura (Coronato *et al*., 2004a), where isolated moraines of eroded summits are generally covered by fluvioglacial deposits (Rabassa *et al*., 2000). The glaciation relating to the moraines would have advanced as ice lobes, with the Seno Skyring lobe separated from the Otway-Magellan lobe (Coronato *et al*., 2004a). The minimum age of the Primera Angostura drift is limited to the ^{14}C ages of 47 and 45 ^{14}C ka BP from the Punta Arenas shelly till (Kaplan *et al*., 2007). An assumed age for Primera Angostura has been suggested by Kaplan *et al*. (2007) of 150 ka (Marine Isotope Stage 6 or MIS 6), based on relative weathering data, the topographic setting, and ^{14}C and AAR dating. The Punta Delgado drift is assumed to be at least one glacial cycle older by Kaplan *et al*. (2007). Both Rabassa and Clapperton (1990) and Clapperton (1993) suggested that the Primera Angostura moraines may have formed during the penultimate glaciation, ca. 140 ka. However, Clapperton (1993) also proposed that the Primera Angostura moraines consist

partly of drift laid down during earlier Quaternary glaciations, including the cold periods of the Middle Pleistocene between MIS 8 and MIS 16 (Rabassa, 2008). Thus it is clear that the ages of the Punta Delgado and Primera Angostura drifts are not yet well-constrained.

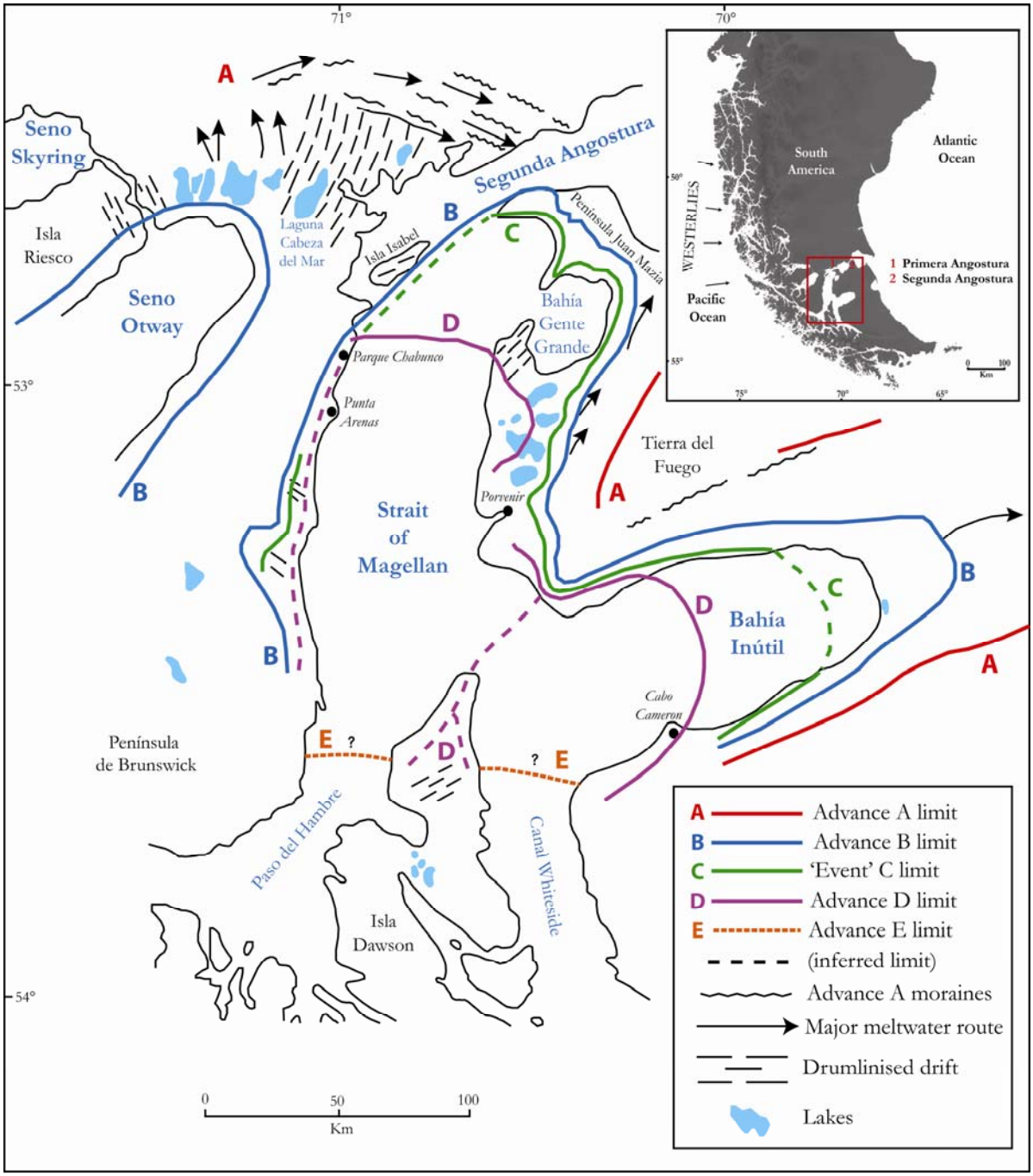

Figure 2.6 - Map showing the position of glacier advances A to E in the central Strait of Magellan and Seno Otway. Adapted from Clapperton *et al.* (1995).

There is evidence for a less extensive advance of a confluent Otway-Magellan lobe following the Primera Angostura Glaciation (Benn and Clapperton, 2000a). A prominent composite moraine belt is present on the western side of the Strait of Magellan, curving around the northeastern ends of Seno Otway and the Strait (Clapperton *et al.*, 1995; Benn

and Clapperton, 2000a). The moraine belt consists of up to four parallel ridges to the west of Segunda Angostura (see Figure 2.6) and throughout the area the moraines are associated with glaciofluvial landforms (Benn and Clapperton, 2000a). The innermost terminal moraine corresponds to Advance A of Clapperton *et al*. (1995; see Figure 2.6). As no matching moraine could be found on the eastern side of the Strait, Clapperton *et al*. (1995) suggested that it could have been destroyed by meltwater associated with the LGM advance up the Strait. The LGM glacier, Advance B of Clapperton *et al*. (1995), terminated at Segunda Angostura (Rabassa and Clapperton, 2000; Rabassa *et al*., 2000; Coronato *et al*., 2004a; Bentley *et al*., 2005; Kaplan *et al*., 2008; see Figure 2.6). According to Clapperton (1993), the composite Segunda Angostura belt which includes the Advance A deposits is made up of at least three separate tills, interbedded with glaciolacustrine and meltwater sediments. On the northern side of Segunda Angostura the uppermost of four glacial diamicts exposed at Punta Garcia was interpreted as being the basal till of Advance A (Clapperton *et al*., 1995), although the reasons for this interpretation are not made clear. It was concluded that the confluent Otway-Magellan lobe is likely to have terminated at Segunda Angostura (Clapperton, 1989, 1993).

There is limited dating evidence for Advance A (McCulloch *et al*., 2005a) and the composite nature of many of the Strait of Magellan landforms creates problems for developing a glacial chronology (Benn and Clapperton, 2000a). Advance A was considered to have occurred during an early part of the Last Glaciation (Clapperton *et al*., 1995). An age of between 90 ka and 55 ka was put forward by Sugden *et al*. (2009), based on radiocarbon dates, cosmogenic nuclide ages and amino acid analysis from McCulloch *et al*. (2005a) and Kaplan *et al*. (2007). On the western side of the Strait the Advance A moraine belt is clearly situated outside the LGM limit, which is now well-established (Clapperton *et al*., 1995; Rabassa *et al*., 2000; Coronato *et al*., 2004a; Bentley *et al*., 2005; Sugden *et al*., 2005; Glasser *et al*., 2008). This makes the age bracket of between 90 ka and 55 ka suggested by Sugden *et al*. (2009) hard to understand because it would appear to assign Advance A to the early Last Glacial. To add to the confusion, Kaplan *et al*. (2008b) presented an age of after ca. 31 ka for the beginning of the last glaciation. Amino acids dating of shells from Parque Chabunco, near Punta Arenas Airport (see Figure 2.6), suggest that Advance A may have occurred prior to ca. 90 ka (McCulloch *et al*., 2005a).

It seems most likely that the confluent Otway-Magellan lobe of Advance A occurred during the penultimate glaciation (Clapperton, 1993) and may have been contemporary with the *Moreno* complex of moraines at LBA. These are thought to have been deposited

sometime during MIS 6 based on cosmogenic exposure ages (Kaplan *et al*., 2005; McCulloch *et al*., 2005a; Rabassa, 2008), although the age of the Moreno complex has recently been questioned by Hein *et al*. (2009). Advance A, which reached Segunda Angostura, could represent a retreat stage associated with the Primera Angostura glaciation. However, the fact that the age of the Primera Angostura drift is poorly-constrained, as alluded to previously, means this link could well be inaccurate.

The area of most interest to this study is situated to the west of the Strait of Magellan, between the Advance A and Advance B - LGM limits. In particular, Clapperton (1989) described in great detail an area of drumlinised drift near Laguna Cabeza del Mar, 10 to 15 km northeast of Seno Otway (see Figures 2.6 and 2.7). The drumlins cover an area of 25 x 30 km and are situated 15 to 20 km inside the Advance A limit (Clapperton, 1989). A potentially deformable bed existed in this region, as evidenced by exposed stratigraphy along the east side of Laguna Cabeza del Mar (Clapperton, 1989). These exposures dissect an inter-drumlin hollow and show that thick sequences of glaciofluvial and glaciolacustrine sediments may underlie a large portion of the drumlin field (Clapperton, 1989). It was suggested by Clapperton (1993) that the drumlins were formed by a readvance over these earlier sediments, not necessarily separated by a long time interval. More precisely, Clapperton (1989) attributed the drumlins to the erosion and streamlining of pre-existing sediments in a subglacial deforming layer and concluded that they were formed by a confluent lobe that terminated at Segunda Angostura (Advance A, as outlined above; see Figure 2.6).

Benn and Clapperton (2000a) suggested that the streamlined features indicate a zone of rapid ice flow within the combined Otway-Magellan lobe, based on the work of Clark (1994) who suggested drumlin elongation was a function of increased ice velocity. Clapperton (1989) proposed a Last Glacial (LG) age for the features. However, because they are situated outside of the LGM limit and within the Advance A moraines, a pre-Last Glacial age seems equally possible. A series of meltwater channels traverse the drumlinised zone, and these are thought to post-date the streamlining phase (Benn and Clapperton, 2000a). A high magnitude drainage event of a pro-glacial lake to the west was hypothesised (Benn and Clapperton, 2000a). This is supported by Caldenius (1932), who suggested that a glacial lake formed in front of the Seno Skyring glacier before draining eastwards to the Strait of Magellan. As well as the elongate streamlined features and the extensive meltwater channels, Benn and Clapperton (2000a) reported on the presence of a

zone of unmodified thrust moraines and a number of radial excavational basins located up-ice of the streamlined zone.

A number of studies have mapped this interesting area between the Advance A and B limits (Clapperton, 1989; Benn and Clapperton, 2000a; Glasser *et al*., 2008), but little attempt at detailed interpretation of the 'glacial landsystem' (Evans, 2003, 2006) has been made. Alongside other criteria, including the presence of deformable till and lateral shear moraines, highly-attenuated bedforms are thought to be characteristic of palaeo-ice stream beds (Stokes and Clark, 1999). Evidence exists for at least two of these criteria in the zone between Advances A and B to the west of the Strait of Magellan (Clapperton, 1989, 1993; Benn and Clapperton, 2000a). The importance of identifying palaeo-ice stream beds is dealt with in greater detail in Chapter 3.

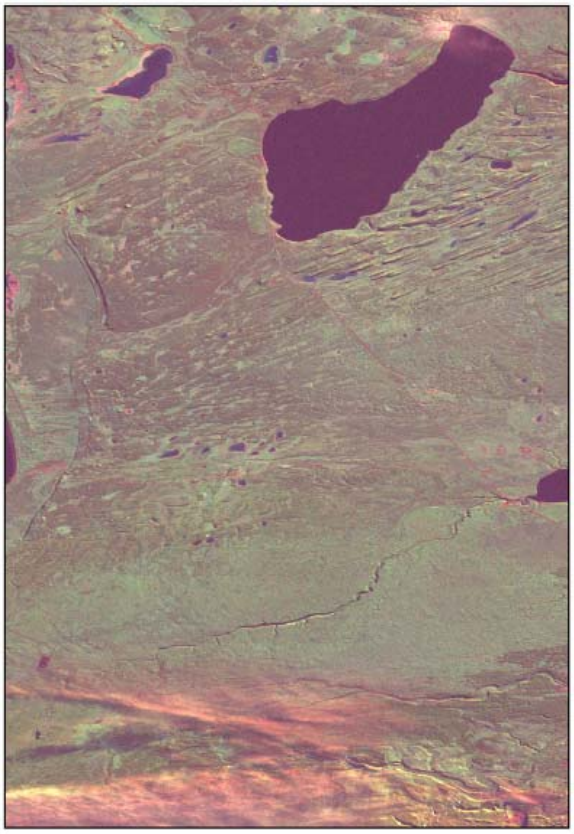

Figure 2.7 - Landsat sub-scene of area northeast of Seno Otway. Laguna Cabeza del Mar is situated at the top of the image and the streamlined features can clearly be seen immediately to the southeast of the lake. From Glasser *et al*. (2008).

2.4.2 Lago Buenos Aires lobe

The Lago Buenos Aires (LBA) moraine system provides dateable evidence of post-GPG advances (Singer *et al*., 2004a; Kaplan *et al*., 2005; Douglass *et al*., 2006). During the last ca. 1.2 Ma, at least 19 terminal moraines were deposited at LBA (Singer *et al*., 2004a; see

Figure 2.3). As previously discussed, the outermost *Telken* VII moraine is thought to represent the GPG (Singer *et al*, 2004a; Kaplan *et al*., 2004, 2005, 2009). The moraines *Telken* I-VI were deposited between 1016 ± 10 ka and 760 ± 15 ka, as bracketed by the dated Arroyo Telken and Arroyo Page lava flows (Singer *et al*., 2004a). Each of the large *Telken* moraine complexes deposited in this ca. 256 ka period is assumed to represent a major glaciation (Singer *et al*., 2004a).

The six *Deseado* and *Moreno* moraines were deposited during a ca. 651 ka period as delimited by the Arroyo Page and Cerro Volcán lava flows (Singer *et al*., 2004a; Kaplan *et al*., 2005). The ages of the flows are 760 ± 15 ka and 109 ± 3 ka respectively (Singer *et al*., 2004a). Cosmogenic surface exposure ages of boulders on the *Moreno* I moraine range between 172 ± 18 and 115 ± 11 ka (Kaplan *et al*., 2004), although Hein *et al*. (2009) warned that exposure ages from moraine boulders can underestimate the age of deposition by ca. 100 ka and Kaplan *et al*. (2007) indicated that cosmogenic exposure dating of pre-LGM glacial deposits cannot be used reliably. Singer *et al*. (2004a) suggested that the six *Deseado* and *Moreno* moraines could perhaps represent multiple advances within only one major glaciation. This conclusion was reached due to the consistency of the *Deseado/Moreno* moraine complexes with the six dated *Fenix* moraines (Kaplan *et al*., 2004), which record multiple advances during the LGM (Singer *et al.,* 2004a). As the six *Fenix* moraines were deposited during only one glaciation, the same was suggested for the *Deseado/Moreno* complex, although it was acknowledged that further cosmogenic surface exposure dating is required to test this hypothesis (Singer *et al.,* 2004a).

The exposure ages from the *Moreno* I boulders are consistent with deposition during the penultimate glaciation between ca. 130 and 190 ka (Singer *et al*., 2004a), with a best estimate for maximum ice expansion of between 150 and 140 ka during MIS 6 (Kaplan *et al*., 2004, 2005; Douglass *et al*., 2006). This would appear to correlate the *Moreno* I moraine with the Primera Angostura moraines around the Strait of Magellan (Rabassa and Clapperton, 1990; Clapperton, 1993; Kaplan *et al*., 2007) and the Advance A moraines north of Seno Otway (Clapperton *et al*., 1995; McCulloch *et al*., 2005a; Rabassa, 2008). At LBA, the exposure age chronology of Kaplan *et al*. (2005) provides evidence for ice expansion eastwards from the Andean Cordillera on to the Patagonian plains at least once between 760 and 200 ka, and that the next glaciation occurred between ca. 190 and 109 ka. It should be mentioned that the recent work of Hein *et al*. (2009) has raised questions concerning cosmogenic nuclide dating of moraine boulders, as alluded to previously. It

was found that ^{10}Be concentrations in outwash cobbles at Lago Pueyrredón, located in close proximity to LBA, revealed a major ca. 260 ka (MIS 8) glacial advance (Hein *et al*., 2009). This raises questions about the MIS 6 age given for the *Moreno* I and II moraines at LBA which occupy a similar stratigraphic position relative to the LGM limits (Hein *et al*., 2009).

2.5 Last Interglacial and Early Parts of Last Glacial Cycle

Following the penultimate glaciation of MIS 6, thought to be represented by the Primera Angostura drift and Advance A in the Strait of Magellan (Clapperton, 1993; McCulloch *et al*., 2005a) and possibly the Moreno morainic complex at LBA (Singer *et al*., 2004a; Kaplan *et al*., 2005; McCulloch *et al*., 2005a), it is suggested that the last interglacial occurred during MIS 5e (Clapperton, 1993; Coronato *et al*., 1999). This is thought to have been a relatively short interval of ca. 15,000 years, between 125,000 and 110,000 years BP, based on the marine isotope record (Clapperton, 1993). It is suggested that the environment at this time was similar to that of the early Holocene (Clapperton, 1993).

The Last Glacial followed this interglacial and it is estimated that the Patagonian Ice Sheet took at least 30,000 years to re-form (Rabassa, 2008). This ice expansion is presumed to have taken place during an advance stage of MIS 4 (Rabassa, 2008), although it is not clear how extensive Andean glaciers were at this time (Clapperton, 1993). There is limited knowledge about glacial advances during MIS 4 in southern Patagonia (similar to other regions around the world) due to poor or a lack of preservation of deposits (Kaplan *et al*., 2008a). There is no conclusive evidence for an early Last Glacial advance of ca. 70,000 years (MIS 4) age in Patagonia according to Clapperton (1993), although Mercer (1983) loosely suggested an age of ca. 73,000 for the deposition of the Llanquihue I moraine in the Chilean Lake District (CLD, ca. 41°S; see Figure 2.1) on the western side of the Andes, based on oxygen isotope data from deep sea cores (Clapperton, 1993). More recently Lowell *et al*. (1995) put forward an age of > 49, 892 ^{14}C yr BP for the outermost Llanquihue moraine on Isla Grande de Chiloé, this minimum age comes from ^{14}C dating of basal organic material from a mire. Kaplan *et al*. (2008a) suggested that ice may have been more extensive in the CLD during MIS 4 than in MIS 2, in contrast to LBA and the Strait of Magellan region. A major MIS 4 glacial advance at LBA was inferred by Kaplan *et al*. (2005) from correlation with ice core data, although any evidence of it would have been destroyed by the more extensive LGM advance.

In the Strait of Magellan, Sugden *et al*. (2009) have suggested an age of between 90 ka and 55 ka for Advance A, and so potentially of MIS 4 age. However, McCulloch *et al*. (2005a) suggested that Advance A is older than 90 ka and Clapperton (1993) attributed it to the penultimate glaciation. The position of Advance A outside of the LGM limits seems to support Clapperton (1993). Therefore, there is no robust evidence of MIS 4 deposits in the Strait of Magellan region. This again highlights the problems associated with producing a glacial chronology for the Strait (Benn and Clapperton, 2000a), particularly pre-LGM.

Reworked shell fragments on the western shore of the Strait of Magellan and the eastern shore of Isla Dawson have been ^{14}C dated, with dates ranging from > 40,000 to 27,690 ^{14}C yr BP (44,760 ± 460 to 31,250 ± 670 cal yr), by McCulloch *et al*. (2005b). These ages reflect a pre-LGM period during which the Strait of Magellan was open to the sea (Clapperton *et al*. 1995; McCulloch *et al*., 2005b). At Llanquihue in the CLD, a glacier advanced to within 2 km of the Llanquihue I moraine prior to 36,960 to 34,775 ^{14}C yr BP, based on the ages for a basal organic silt (Lowell *et al*., 1995). This suggests a regional asynchrony of glacial expansion in southern Patagonia at this time. In the Strait of Magellan it is suggested that the growth of the LGM ice sheet began after ca. 31 ka , following a relatively long ice-free period (Kaplan *et al*., 2008b).

2.6 The Local Last Glacial Maximum

The LGM is the most recent major expansion of the last glaciation (Clapperton, 1989), the 'Finiglacial' of Caldenius (1932). At this time the Patagonian Ice Sheet stretched for over 1,800 km along the crest of the Andes (Hulton *et al*., 2002; Sugden *et al*., 2002). In the Strait of Magellan there is general agreement that during the LGM ice reached Segunda Angostura and formed a moraine complex on Península Juan Mazia (Clapperton, 1989; Porter *et al*., 1992; Clapperton, 1993; Clapperton *et al*., 1995; Rabassa and Clapperton, 2000; Rabassa *et al*., 2000; Coronato *et al*., 2004a; Bentley *et al*., 2005; McCulloch *et al*., 2005a; Sugden *et al*., 2005; Kaplan *et al*., 2007, 2008b; Glasser *et al*., 2008; see Figure 2.6). Labelled Advance B by Clapperton *et al*. (1995), the LGM limit is marked by prominent morainic belts on both sides of the Strait (Benn and Clapperton, 2000a). Glaciers flowed as independent ice lobes along Seno Skyring, Seno Otway and the Strait of Magellan (Coronato *et al*., 2004a; see Figure 2.8).

The LGM limit for the Seno Otway lobe is situated between the inlet and Laguna Cabeza de Mar (Porter *et al*., 1992; Clapperton *et al*., 1995; Coronato *et al*., 2004a; see Figure 2.6),

suggesting the glacier just filled its basin. Meltwater from the Otway lobe deposited a delta into a glacial lake that had formed against the northwest side of the Magellan Glacier (Bentley *et al.*, 2005; McCulloch *et al*., 2005a). Clapperton *et al*. (1995) described a much smaller amount of ice than that associated with Advance A, and the independent Otway and Magellan lobes diverged around the Península Brunswick which remained ice-free at this time. Benn and Clapperton (2000a) suggested a reconstructed basal shear stress for the Magellan Glacier of 8.8 kPa, comparative with that of some modern fast outlet glaciers and ice streams. This figure was calculated using the following basal shear stress formula: $\boldsymbol{\tau = pgh \sin \alpha}$ (where τ is the basal shear stress; p is the ice density of ca. 900 kg m^{-3}; g is the gravitational acceleration of 9.81 m s^{-2}; h is the ice thickness; and α is the surface slope angle; Benn and Clapperton, 2000a). The ice thickness used in this calculation appears to be based on the reconstructed surface contours of the Magellan lobe (Figure 16 in Benn and Clapperton, 2000a). It was concluded from this that the Magellan lobe moved over a subglacial deforming layer and underwent fast ice flow (Benn and Clapperton, 2000a). This is supported by Glasser and Jansson (2005), who suggested that the Patagonian Ice Sheet at the LGM was strongly controlled by fast-flowing outlet glaciers and ice streams. Clapperton (1989) and Benn and Clapperton (2000b) both inferred that the Magellan lobe was largely wet-based and underlain by a weak deforming layer.

The total Patagonian Ice Sheet volume at the LGM was modelled at ca. 500,000 km^3, the equivalent to ca. 1.2 m of global sea level (Hulton *et al*., 2002). This figure was based on an icesheet/climate model that displayed a good match with the empirical record according to Hulton *et al.* (2002). The areal ice extent was ca. 422,000 km^2 according to Kaplan *et al*. (2009), and Kaplan *et al*. (2008b) estimate the distance from the LGM ice divide to ice margin to be in the region of between 350 and 400 km. According to Porter *et al*. (1984), the Magellan lobe had a maximum ice thickness of over 700 m during the LGM. McCulloch *et al*. (2005a) used both ^{10}Be and ^{14}C dating of moraine boulders and shell samples associated with Advance B. From this it was concluded that the Strait of Magellan lobe culminated at ca. 25,300 to 23,100 yrs during the LGM (McCulloch *et al*., 2005a). Sugden *et al*. (2009) suggested a similar time constraint of between 25.6 and 23.1 ka, based on radiocarbon dates, cosmogenic exposure ages and amino acid analysis. Kaplan *et al*. (2008b) carried out ^{10}Be exposure dating of boulders and recorded an average age of 24.6 ± 0.9 ka for the maximum ice margin position during the Last Glacial in the Strait of Magellan.

These ages show similarities to LGM dates at LBA, where the outermost Fenix moraine is dated to ca. 23 ka (Kaplan *et al*., 2004, 2008a; Sugden *et al*., 2005; Douglass *et al*., 2006). In most areas in southern Patagonia Andean outlet glaciers reached their greatest ice extent of the last glaciation between 27 ka and 22 ka (Kaplan *et al*., 2004; Sugden *et al*., 2005). It is concluded that glaciers in the Strait of Magellan and LBA reached a maximum at around 25 - 23 ka, with the LGM advance in the CLD occurring at around 26 ^{14}C ka BP based on radiocarbon dating (Denton *et al*., 1999; Sugden *et al*., 2005). At orbital scales it is suggested that the LGM Patagonian glacier fluctuations are in phase with those in the northern hemisphere (Sugden *et al*., 2005). Atmospheric cooling during the LGM was approximately synchronous and of a similar magnitude in both hemispheres (Denton *et al*., 1999).

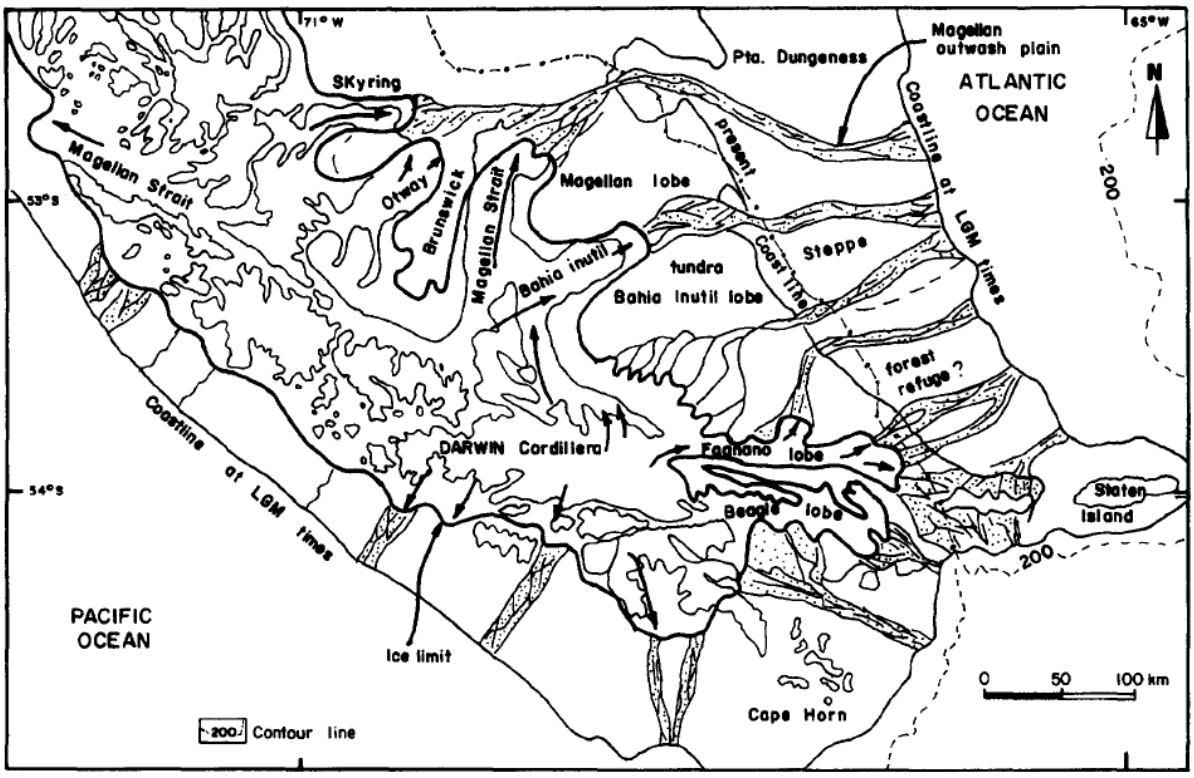

Figure 2.8 - Extent and position of the mountain ice sheet of southernmost Patagonia during the LGM. From Coronato *et al.* (1999).

Following the LGM advance in the Strait of Magellan there was a separate glacial readvance (Advance C of Clapperton *et al.*, 1995) to just within the Advance B limit (Clapperton *et al*., 1995; Bentley *et al*., 2005; McCulloch *et al*., 2005a). Advance C reflects a phase following the LGM during which the ice lobe reached a position close to the maximum extent (Clapperton *et al*., 1995; Benn and Clapperton, 2000a; Bentley *et al*., 2005; see Figure 2.6). Meltwater channels that dissect the outer Advance B moraine show

that the inner limit represents a younger advance (Bentley *et al*., 2005). Surface exposure ages and ^{14}C dating show that the Advance C ice lobe was in retreat by ca. 21,700 to 20,400 yrs (McCulloch *et al*., 2005a). During Advances A to C in the Strait of Magellan glaciers discharged directly onto outwash plains because the Strait was above sea level at this point (Sugden *et al*., 2009). There is evidence for advances following the LGM at both LBA, where the five Fenix advances occurred between ca. 23 and 16 ka (Kaplan *et al*., 2004) and in the CLD, where advances into the outer Llanquihue moraine belt have been recognised at 23,060 and 21,000 ^{14}C yrs BP (Lowell *et al*., 1995).

2.7 Late-Glacial to the Holocene

The Late-Glacial is defined as a period between ca. 16 and 10 ^{14}C ka BP (Coronato *et al*., 1999). Moraine ridges on both sides of the Strait of Magellan provide evidence for a less extensive advance following B and C (Clapperton *et al*., 1995; Benn and Clapperton, 2000a; Bentley *et al*., 2005). It was labelled Advance D by Clapperton *et al*. (1995; see Figure 2.6) and is thought to have extended ca. 150 km from the current ice limits (McCulloch *et al*., 2005b). On the western side of the Strait of Magellan the limit is marked by a large continuous meltwater channel that runs through the suburbs of Punta Arenas (Bentley *et al*., 2005). A multichannel seismic survey of the bed of the Strait showed a mounded ridge which is thought to represent the limit of this advance (Bartole *et al*., 2008). The lack of shell fragments in the till associated with Advance D led Clapperton *et al*. (1995) to infer that there was no marine incursion following the retreat of ice from the Advance C limits, but it is not known how extensive retreat was (McCulloch *et al*., 2005a). Benn and Clapperton (2000b) suggested that Advance D was a major late-glacial readvance of the Magellan lobe.

Evidence for lake shorelines and glaciolacustrine sediments supports the presence of a pro-glacial lake at this time (Clapperton *et al*., 1995; McCulloch and Bentley, 1998; McCulloch *et al*., 2005b). During the LGM the Strait of Magellan was separated from the Atlantic Ocean by a dry land barrier to the north and northeast of Segunda Angostura (McCulloch *et al*., 2005b). Advance D is thought to have dammed a large proglacial lake between the ice front and the Segunda Angostura (Clapperton *et al*., 1995; McCulloch and Bentley, 1998; Anderson and Archer, 1999). The outermost limit of Advance D has not been directly dated, but ^{10}Be exposure ages for boulders within this limit suggest the advance occurred sometime before ca. 17,500 yrs (McCulloch *et al*., 2005a). Along the southern shore of Bahía Inútil, minimum ^{14}C ages of 13,980 and 13,614 ^{14}C yrs BP (ca.

17,580 – 16,620 cal. yrs) date ice retreat from Advance D limits (McCulloch *et al*., 2005a). These dates suggest that Advance D was possibly coeval with the youngest Llanquihue advance in the CLD (Lowell *et al*., 1995; Denton *et al*., 1999; McCulloch *et al*., 2005b). During Advances A to D it is inferred that the mean annual temperature was around 7-8 °C lower than today's (Benn and Clapperton, 2000a).

A pattern of major and extensive ice retreat in the Strait of Magellan followed Advance D (McCulloch *et al*., 2005b). Widespread deglaciation throughout southern Patagonia, from the CLD to the Strait of Magellan, was initiated synchronously between ca. 14,550 and 14,260 ^{14}C yrs BP (Ashworth and Hoganson, 1993; Lowell *et al.*, 1995; Denton *et al.*, 1999; Heusser, 1999; Heusser *et al*., 2000; McCulloch *et al*., 2000, 2005b), based on the dating of advance limits at these locations (Clapperton *et al.*, 1995; McCulloch and Bentley, 1998; Denton *et al.*, 1999). A minimum age for deglaciation of Seno Otway at 12,460 ± 190 ^{14}C yrs BP was suggested by Mercer (1976), based on ^{14}C dating of basal peat which rests on cobbles associated with the lowest meltwater channel that drained an ice-dammed proglacial lake.

The main phase of deglaciation in South America is thought to have started at approximately the same time as deglaciation in the northern hemisphere (Lowell *et al.*, 1995; Denton *et al.*, 1999; McCulloch *et al.*, 2005b). This has been identified from glacier records, pollen records and ocean cores around the world (Lowell *et al.*, 1995; Denton *et al.*, 1999). Moreno *et al.* (2001) suggested that this supports the idea that interhemispheric linkage through the atmosphere was the primary control on climate during the last deglaciation, and that local oceanic influences may have influenced regions where climate events were out of phase with those in the northern hemisphere.

Following initial deglaciation, the southern end of the Strait was open to the Pacific Ocean for ca. 400 – 700 ^{14}C years, before a late-glacial readvance that re-formed the ice dam and created a new proglacial lake (McCulloch *et al*., 2005b). This readvance was labelled Advance E by Clapperton *et al*. (1995; see Figure 2.6) and extended up to 80 km from the present ice margins in the Cordillera Darwin (McCulloch and Bentley, 1998; McCulloch *et al*., 2000; Bentley *et al*., 2005). The culmination of this advance is constrained to between 12,010 and 10,300 ^{14}C yrs BP, due to the association of glaciolacustrine sediments with a Volcan Reclús tephra layer that has been dated at 12,010 ^{14}C yrs BP (McCulloch *et al*., 2000). An anomaly in the stratigraphic record for the Late-Glacial period in the Strait of Magellan was addressed by Bentley and McCulloch (2005). It concerned the lack of

glaciolacustrine sediments at Puerto del Hambre (see Figure 2.6), a site that should have been inundated by the proglacial lake formed during Advance E. It was concluded that the Puerto del Hambre section was affected by postglacial neotectonics and had been substantially downfaulted during the early Holocene (Bentley and McCulloch, 2005). This implies that during the existence of the proglacial lake, Puerto del Hambre was at a higher position above the maximum lake level (Bentley and McCulloch, 2005). The problematic ^{14}C ages for the moraine limit at Parque Chabunco (see Figure 2.6) which implied an anomalously early age of deglaciation in the Strait are thought to be because of lignite contamination (McCulloch *et al.,* 2005a). The retreat of ice into the Cordillera Darwin and the collapse of the ice-dam and subsequent draining of the proglacial lake is constrained to a minimum age of 10,315 ^{14}C yrs BP (McCulloch and Davies, 2001; McCulloch *et al*., 2005b). This coincides with palaeoecological records in the region that suggest a warming to Holocene conditions at ca. 10,300 ^{14}C yrs BP (Heusser *et al*., 2000; McCulloch and Davies, 2001).

The significant glacial expansion of Advance E was restricted to the Strait of Magellan (McCulloch *et al*., 2000). One of the main points of contention in the literature concerns this advance. Several authors argue that the Late-Glacial cooling associated with Advance E in the Strait of Magellan corresponds to the Younger Dryas (YD) chron of between ca. 11,000 and 10,000 yrs (Heusser and Rabassa, 1987; Heusser, 1993; Marden, 1997; Wenzens, 1999; Heusser *et al*., 2000). Moreno *et al*. (2001) inferred that southern and northern hemisphere climate changed in unison between ca. 13 and 10 ^{14}C yrs BP. Others suggested that the reversal in the warming trend occurred around 550 years before the YD (Anderson and Archer, 1999; Hajdas *et al*., 2003) and ended during this period (Fogwill and Kubik, 2005). Markgraf (1993) argued that the environmental changes in Tierra del Fuego that were interpreted as coeval cooling with the YD by Heusser and Rabassa (1987) were in fact due to local and regional disturbance by fires. A further line of thought is that Late-Glacial cooling is in phase with the Antarctic Cold Reversal (ACR) at ca. 15,300 cal. yrs (Blunier *et al*., 1998; Bennett *et al*., 2000; McCulloch *et al*., 2000; McCulloch *et al*., 2005b; Sugden *et al.*, 2005). The best-dated Late-Glacial records in the Strait of Magellan appear to support this view. Clearly this is a topic that requires further investigation, particularly as it would provide key evidence for or against synchrony of climate change between the hemispheres.

Holocene and present-day glaciation in southern Patagonia is restricted to three main regions – the North and South Patagonian Icefields and the Cordillera Darwin in the south

(Rabassa and Clapperton, 1990; see Figure 2.1). The North Patagonian Icefield covers an area of ca. 4,500 km^2 and outlet glaciers descend to the Pacific Ocean (Rabassa and Clapperton, 1990). The South Patagonian Icefield is the largest of the three, stretching for 360 km with an average width of 40 km (Rabassa and Clapperton, 1990). The Cordillera Darwin, from which the Magellan and Otway lobes extended throughout the Quaternary, has a number of outlet glaciers that descend to the Pacific Ocean (Rabassa and Clapperton, 1990). There have been many studies of Holocene glacier chronologies in the region but these are beyond the scope of this project and so are not discussed further here.

2.8 Summary

There is evidence for glaciation in southern Patagonia between 7 and 4.6 Ma, at 3.6 Ma, and several times between 2 Ma and 1 Ma (Mercer, 1983). The greatest extent of ice in Patagonia, the GPG, has been dated to between 1.168 Ma and 1.016 Ma (Singer *et al*., 2004a; Kaplan *et al*., 2007; Glasser *et al*., 2008). Following the GPG, glaciations in the Strait of Magellan region have been successively less extensive (Kaplan *et al*., 2009). Four main glacial limits have been identified, with the innermost representing the LGM (Rabassa *et al*., 2000; Coronato *et al*., 2004a; Kaplan *et al*., 2007). A morainic belt outside of the LGM limits on the western side of the Strait, labelled Advance A by Clapperton *et al*. (1995), is a poorly-dated area that requires further study (McCulloch *et al*., 2005a). Of particular interest is an area of streamlined features to the northeast of Seno Otway in the vicinity of Cabeza de Mar, which lies between Advance A and the LGM limits (Clapperton, 1989; Clapperton *et al*., 1995; Benn and Clapperton, 2000a; Glasser *et al*., 2008). This area is of importance because it appears to display characteristics of a palaeo-ice stream landsystem (Stokes and Clark, 1999). Palaeo-ice streams have been hypothesised within the former Patagonian ice sheet (Clapperton, 1989; Benn and Clapperton, 2000a; Glasser and Jansson, 2005) but have never been explicitly described.

Clapperton *et al*. (1995) labelled four advances from the LGM to the Late-Glacial. Advance B represents the LGM limit in the Strait of Magellan, Advance C is a readvance to similar limits and Advance D dammed a proglacial lake (Clapperton *et al*., 1995; McCulloch and Bentley, 1998; Benn and Clapperton, 2000a, b; McCulloch *et al*, 2000; Bentley *et al*., 2005; McCulloch *et al*., 2005a, b). Advance E was a Late-Glacial readvance that re-formed a new, lower proglacial lake (McCulloch and Bentley, 1998; Bentley and McCulloch, 2005). There is ongoing discussion as to whether climate change was coeval between the hemispheres, or whether one led the other (Sugden *et al*., 2005).

The terrestrial glacial record in South America presents an opportunity to test these alternative hypotheses (Sugden *et al.*, 2005).

Chapter 3 - Ice Streams and Palaeo-ice Streams

3.1 Introduction

The importance of ice streams in contemporary and former ice sheet dynamics was introduced in Chapter 1. The following chapter will discuss the different types of ice streams; the mechanisms that facilitate fast ice flow; and the controls on their location, initiation and stoppage. Palaeo-ice streams will then be reviewed, including their importance for former ice sheet reconstructions; the characteristic criteria used to identify them in the geomorphological record; and the landsystems these criteria produce. The landsystems of a surging glacier and a terrestrial ice margin are also discussed because they share a number of criteria with the palaeo-ice stream landsystem.

3.2 Ice streams

An early definition of ice streams was put forward by Swithinbank (1954), who suggested they were "part of an inland ice sheet in which the ice flows more rapidly than, and not necessarily in the same direction as, the surrounding ice". In more recent reviews they are commonly described as corridors or arteries of fast ice flow within an ice sheet (Stokes and Clark, 2001; Bennett, 2003; Truffer and Echelmeyer, 2003). The actual velocities of ice streams exhibit a large amount of variety. Stokes and Clark (2001) suggested that they flowed at least an order of magnitude faster than the surrounding ice. Whillans *et al.* (1987) found that the ice streams draining the West Antarctic Ice Sheet generally had speeds in the order of 500 m a^{-1}. The same ice streams were suggested to move at speeds of up to 800 m a^{-1} by Kamb (1991), in contrast to speeds of 10 m a^{-1} for the surrounding ice (Bentley, 1987). In a comprehensive review of ice streams, Bennett (2003) also suggested that they flowed in the order of 800 m a^{-1}. However, it has since been established that ice streams can flow at considerably faster velocities. Jakobshavn Isbræ was found to be flowing at 12,600 m a^{-1} in the spring of 2003 (Joughin *et al.*, 2004). Observations at Jakobshavn Isbræ have recognised an ice velocity increase of over 30% between 1997 and 2003 (Joughin *et al.*, 2004; Thomas, 2004). The mechanisms that are thought to facilitate these fast velocities will be discussed in more detail in Section 3.2.2.

Ice streams dominate ice-sheet discharge and thus have a major influence on ice-sheet configuration and regulation (Oppenheimer, 1998; Clark and Stokes, 1999, 2001). Their ability to rapidly drain large areas means ice streams also have an important role to play in ice sheet stability and mass balance (Bamber *et al.*, 2000; Stokes and Clark, 2001; Bennett,

2003; Joughin *et al.*, 2004; Ó Cofaigh *et al.*, 2007, 2008). This instability is created as the rate of flow and discharge of ice sheets through ice streams can exceed accumulation (Bindschadler *et al.*, 1998). The large amounts of ice they can drain into an ocean basin provides a link between the cryosphere and the ocean, and episodes of ice streaming are thought to have been responsible for forcing abrupt high-frequency millennial or sub-millennial climate change (Broecker, 1994; Stokes and Clark, 2001; Bennett, 2003). For example, large iceberg discharge events through ice streaming from the eastern margin of the Laurentide Ice Sheet between 60,000 and 10,000 years BP are postulated to have had a considerable impact on ocean circulation and the climate of the northern hemisphere (Bond *et al.*, 1992; Broecker, 1994). Three of the five most recent iceberg rafting Heinrich events (H-4, H-2 and H-1) have been specifically linked to ice streaming in the Hudson Strait through the association of carbonate detritus to sedimentary rocks eroded by the ice stream (Andrews and Tedesco, 1992; Andrews and Maclean, 2003). Ice streams are also thought to respond to atmospheric and oceanic changes (Oppenheimer, 1998; Holland *et al.*, 2008). The possible instability of the Antarctic and Greenland ice sheets in a warming climate is the focus of a lot of current research (Howat *et al.*, 2007; Shepherd and Wingham, 2007). Specifically, this research is concerned with monitoring ice streams that drain the ice sheets and improving understanding of any future response to climate change (Howat *et al.*, 2007).

3.2.1 Ice stream types: pure to topographic

Stokes and Clark (1999) first suggested that most contemporary ice streams could be broadly classified as either ‘pure’ ice streams or ‘topographic’ ice streams. The ice streams of the Siple Coast in West Antarctica are highlighted as examples of pure ice streams because they do not appear to lie in bedrock troughs (Stokes and Clark, 1999). In contrast, a good example of a topographic ice stream is Jakobshavn Isbræ in Greenland, where its location is largely governed by the underlying bedrock topography (Stokes and Clark, 1999). The classification of ice stream types was expanded upon by Truffer and Echelmeyer (2003). The pure and topographic terms of Stokes and Clark (1999) were replaced with ‘ice-stream’ and ‘isbræ’ types (Truffer and Echelmeyer, 2003). The Siple Coast ice streams were still used as examples of archetypal shallow and soft-bedded ‘ice streams’ and Jakobshavn Isbræ was suggested as an example of a typical ‘isbræ’ (Truffer and Echelmeyer, 2003). Because this mixture of four different terms could create confusion, this study will refer to *pure* ice streams and *topographic* ice streams.

An important point made by Truffer and Echelmeyer (2003) is that the two types should be viewed as opposite ends of a continuum, rather than two distinct entities (see Figure 3.1). This is supported by a number of examples of both types of flow in the same ice stream, such as Rutford Ice Stream and Pine Island Glacier in West Antarctica (Truffer and Echelmeyer, 2003) and Lambert Glacier in East Antarctica (Hambrey and Dowdeswell, 1994). Even the 'pure' Siple Coast ice streams have topographically-controlled tributaries further up-ice (Joughin *et al.*, 1999). The type of ice stream appears to also have an influence on the velocity of ice flow, as the Siple Coast ice streams move at ca. 0.8 km per year (Shabtaie *et al.*, 1987; Whillans *et al.*, 1987) compared to a velocity of 12.6 km per year at Jakobshavn Isbræ (Joughin *et al.*, 2004). Ice streams can also be classified as marine or terrestrial depending on the environment in which they terminate (Stokes and Clark, 1999). All contemporary ice streams are marine-terminating (Stokes and Clark, 1999).

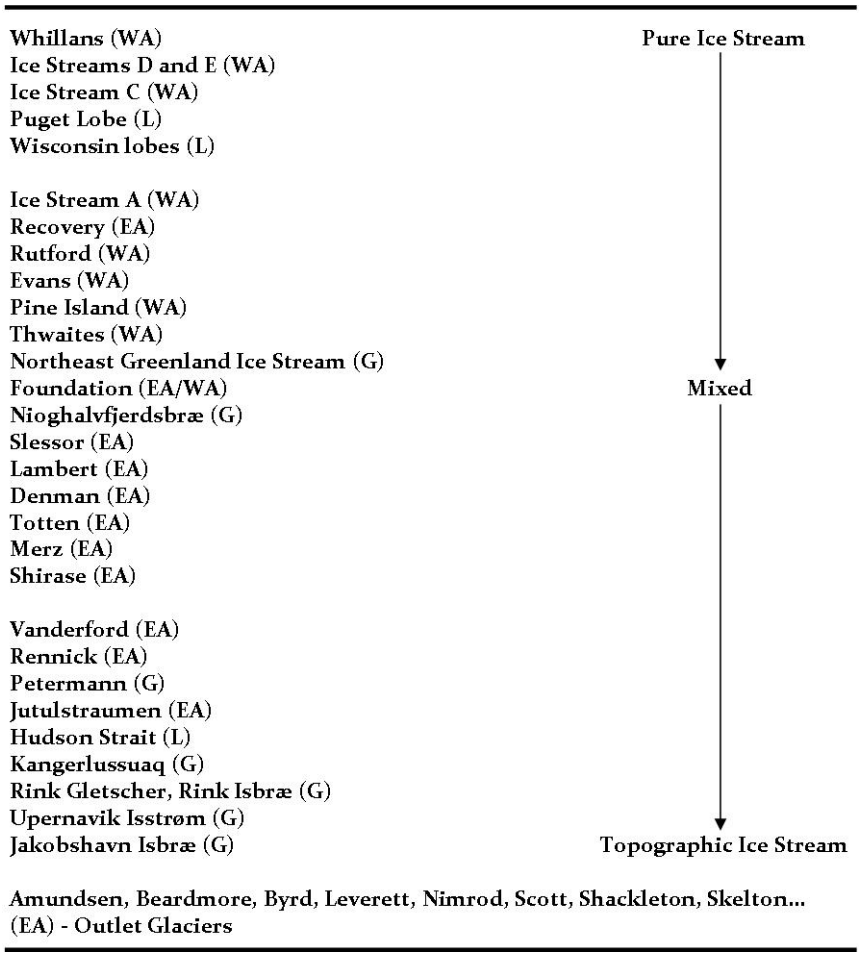

Figure 3.1 – Continuum of ice stream types from Truffer and Echelmeyer (2003). The arrow going down represents the transition from 'pure' ice streams to 'topographic' ice streams. The data are from a variety of sources, including McIntyre (1985), Bentley (1987) and Swithinbank (1988). WA = West Antarctica, EA = East Antarctica, G = Greenland and L = Laurentide/Cordilleran palaeo-ice sheet.

3.2.2 Mechanisms of flow

The continuum of ice stream types is strongly linked to the three main mechanisms for fast ice flow that have been identified (Truffer and Echelmeyer, 2003). The first mechanism that was suggested involved elevated basal water pressure leading to enhanced basal sliding (Rose, 1979). A lubricating layer of water at the ice sheet bed can reduce the basal stress between the ice and the underlying substrate, allowing for an increase in speed through sliding (Engelhardt *et al.*, 1990; Kohler, 2007; Bell, 2008). The vertical weight of the ice above the bed is countered by the high basal water pressures, decreasing the friction and facilitating rapid basal motion (Bennett, 2003). Secondly, the internal mechanics of ice deformation and superplasticity were suggested by Hughes (1977) as being responsible for fast ice movement. This idea focused on enhanced basal and marginal-ice shear due to stress-induced recrystalisation within the ice (Hughes, 1977). It was concluded by Lüthi *et al.* (2002) from borehole investigations that internal ice deformation in the lower half of Jakobshavn Isbræ accounted for most of the ice stream motion. This supported the suggestion of previous studies that high ice deformation rates rather than basal motion contributed most to the rapid ice flow of Jakobshavn Isbræ (Iken *et al.*, 1993; Funk *et al.*, 1994).

A third mechanism for fast flow within an ice stream was developed following the discovery of a 6 m thick layer of soft sediment beneath the Whillans Ice Stream (formerly Ice Stream B) on the Siple Coast, West Antarctica, using seismic reflection techniques (Blankenship *et al.*, 1986). This mechanism is based on the Boulton and Jones (1979) deformable bed theory, in which saturated soft sediments at the base of an ice sheet deform at a lower shear stress than ice. This sediment deformation is thought to contribute up to 90% of the forward movement of a glacier (Boulton and Hindmarsh, 1987; Boulton *et al.*, 2001a). The layer of soft sediment at the base of the Whillans Ice Stream was confirmed following the recovery of samples from drilled boreholes (Engelhardt *et al.*, 1990). The subglacial deformation mechanism is further supported by the work of Anandakrishnan *et al.* (1998), Bell *et al.* (1998) and Studinger *et al.* (2001), who found that ice streaming in West Antarctica coincided with the presence of sedimentary basins.

The principal mechanism for fast ice flow appears to vary according to the ice stream. For example, 80% to 90% of the forward movement of Ice Stream D on the Siple Coast has been attributed to subglacial deformation, compared to only 25% of the motion of the Whillans Ice Stream (Kamb, 2001; Bennett, 2003). The Whillans Ice Stream was found to

be melting at its base, allowing for a combination of basal sliding and subglacial deformation to operate (Engelhardt *et al.*, 1990). This shows how basal hydrology plays a key role in both basal sliding and subglacial deformation (Bennett, 2003) and the spatial and temporal variation of these two forms of flow within an ice stream (Alley, 1989a, b; Iverson *et al.*, 1998; Boulton *et al.*, 2001a). The uncertainty regarding the relative division of these ice stream flow mechanisms was exemplified by Engelhardt *et al.* (1990), who were unable to determine the proportions of motion of the Whillans Ice Stream due to basal sliding, subglacial deformation and enhanced creep.

The proposed mechanisms for rapid flow in ice streams can be linked to the continuum of ice stream types as suggested by Stokes and Clark (1999) and Truffer and Echelmeyer (2003). Pure ice streams, such as those of the Siple Coast, have thinner ice, lower surface slopes, low driving stresses, and forward motion is mainly thought to be through basal sliding and subglacial deformation (Engelhardt *et al.*, 1990; Bennett, 2003). Topographic ice streams are thought to have thicker ice, steeper surface slopes, higher driving stresses and significant internal ice deformation (Iken *et al.*, 1993; Funk *et al.*, 1994; Lüthi *et al.*, 2002; Truffer and Echelmeyer, 2003). Bennett (2003) suggested that there is a tendency for ice to accelerate within topographically constrained corridors. It is possible for basal sliding to occur within topographically controlled ice streams, as at Jakobshavn Isbræ (Truffer and Echelmeyer, 2003; Roberts and Long, 2005), and for ice streams to change down-ice from pure to topographically constrained (e.g. Lambert Glacier, East Antarctica; Hambrey and Dowdeswell, 1994) and *vice-versa* (e.g. the Siple Coast ice streams; Joughin *et al*., 1999). In addition, Stokes and Clark (2003) found that the Dubawnt Lake palaeo-ice stream was located on the hard bedrock of the Canadian Shield, challenging the view that ice streams can only flow in bedrock troughs or across basins of thick deposits of soft sediments. Similarly, ice stream assemblages have been identified in Finland, where deformable sediment and bedrock troughs are largely absent (Payne and Baldwin, 1999). This highlights the importance of viewing ice stream types as a continuum (Truffer and Echelmeyer, 2003) and the importance of studying palaeo-ice streams.

3.2.3 Ice stream onsets

The transition zones between ice sheet and ice stream flow are called onsets (Bamber *et al.*, 2000; De Angelis and Kleman, 2008). These have been readily identified in Antarctica from satellite imagery (Hodge and Doppelhammer, 1996) and synthetic aperture radar measurements over time (Bamber *et al.*, 2000), and are characterised by a large

convergence zone where slower moving ice is incorporated into the main ice stream channel (Hodge and Doppelhammer, 1996). Understanding the factors that control the switching-on of streaming flow is crucial when evaluating the potential for ice sheet collapse (Hodge and Doppelhammer, 1996). A number of possible controls on the location of onsets have been identified. The occurrences of sedimentary basins (Anandakrishnan *et al.*, 1998; Bell *et al.*, 1998; Studinger *et al.*, 2001) and steep topographic beds and valleys (Joughin *et al.*, 2002; De Angelis and Kleman, 2008) have previously been suggested as geological constraints on ice stream location. In addition, discontinuities in basal topography may also control onset location (McIntyre, 1985). Changes in the thermal state of the bed, from frozen to melted, produces meltwater to allow basal sliding and subglacial deformation, and so may occur at onsets (De Angelis and Kleman, 2008).

Recent studies in East Antarctica using interferometric synthetic aperture radar have revealed the presence of four large subglacial lakes (Bell *et al.*, 2007; Kohler, 2007). The significance of this discovery is that they are located within the onset region of the Recovery Ice Stream (Bell *et al.*, 2007). The way in which these lakes could initiate ice streaming is through the reduction of friction as ice flows over the lake surface and the freezing of lake water on to the underside of the ice sheet (Bell *et al.*, 2007; Kohler, 2007). The freezing of lake water adds thermal energy to the basal ice, preventing the ice from freezing to the substrate when it encounters bedrock again, and allows faster flow as warm ice is softer than cold ice (Bell *et al.*, 2007; Kohler, 2007). Byrd Glacier in East Antarctica was observed to have increased in velocity by about 10% of its original speed between December 2005 and February 2007 by Stearns *et al.* (2008). This onset of acceleration coincided with the discharge of about 1.7 km^3 of water from two large subglacial lakes located 200 km up-ice from the ice stream grounding line, and deceleration coincided with the end of the flood (Stearns *et al.*, 2008). This evidence highlights the possible importance of subglacial hydrology to the initiation of ice streaming (Bell *et al.*, 2007).

A further possible trigger for the initiation of ice streaming was suggested by Stokes and Clark (2004) following the identification of the Dubawnt Lake palaeo-ice stream on the northwestern Canadian Shield. It was argued that a deep proglacial lake at the ice sheet margin initiated rapid motion through the removal of ice by calving (Stokes and Clark, 2004). It is thought that the onset of streaming at any one location may be due to a combination of these controls (De Angelis and Kleman, 2008).

3.2.4 Ice stream shutdown

It has been recognised that the lower parts of Ice Stream C on the Siple Coast have little or no surface velocity (Whillans *et al.*, 1987) and that shutdown occurred around 150 years ago (Bennett, 2003). A number of theories have been proposed to explain ice stream shutdown, with particular reference to Ice Stream C (Anandakrishnan *et al.*, 2001; Bennett, 2003). The loss of a lubricating basal sediment layer through basal erosion within the ice stream was initially suggested by Retzlaff and Bentley (1993). This was supported by Tulaczyk *et al.* (2000), who stated that ice streams may cease to flow rapidly if the lubricating conditions are removed. The exhaustion of till is one of the four primary causes of localised patches of basal friction known as 'sticky spots' (Stokes *et al.*, 2007). An increase in the exposure of till-free areas in an ice stream that operates mainly through subglacial deformation could lead to ice stream shutdown through sediment exhaustion (Stokes *et al.*, 2007). A second possible cause of ice stream shutdown is through the reduction of available subglacial water that had previously lubricated the bed (Bennett, 2003). This removal of available water could occur due to two main reasons. Firstly, it could be captured by another ice stream. It was suggested by Anandakrishnan and Alley (1997), for example, that the subglacial water that had previously lubricated Ice Stream C was captured by the neighbouring Whillans Ice Stream. This would cause the till beneath Ice Stream C to consolidate and cease to deform in a ductile manner (Anandakrishnan and Alley, 1997). Secondly, the collapse of the high pressure distributed drainage network at the bed of an ice stream into a more efficient channelised system could reduce basal water pressure and rapid basal movement (Retzlaff and Bentley, 1993; Stokes *et al.*, 2007). Both of these would reduce the amount of free water at the ice-till interface and cause the withdrawal of pore water from underlying subglacial sediments, which could trigger ice stream stoppage (Christoffersen and Tulaczyk, 2003b). Dewatering of the subglacial till layer could produce patches of well-drained stronger till, thought to be another major cause of sticky spots (Stokes *et al.*, 2007, 2008).

In the same way that water could be captured by another ice stream, it was proposed by Payne and Dongelmans (1997) that the accumulation area of ice could also be captured. As an individual ice stream continually increases the area it drains it could affect the accumulation areas of neighbouring ice streams (Payne and Dongelmans, 1997). Only the Siple Coast ice streams are thought to have displayed such switching behaviour, and it has also been observed in numerical models (Payne and Dongelmans, 1997). The final possible cause of ice stream shutdown is through a change in thermal processes (Bennett,

2003). This is mainly through a switch from basal melting to basal freezing (Christoffersen and Tulaczyk, 2003b). Rapid ice flow in an ice stream will ultimately cause ice thinning (Bennett, 2003). This in turn will cause the advection of cold ice closer to the bed, leading to a shutdown in rapid basal motion (Bennett, 2003). A switch from basal melting to freezing could cause basal freeze-on to take place, whereby subglacial water and debris are accreted onto the ice base (Alley *et al.*, 1997). Basal freeze-on beneath mid-latitude palaeo-ice streams was hypothesised by Christoffersen and Tulaczyk (2003a) to be most likely triggered by fast horizontal advection of cold ice from upstream. Thermal "freeze-on" sticky spots could in theory result from this (Anandakrishnan and Alley, 1997; Stokes and Clark, 2007). It has been suggested that the advection of cold ice from upstream leading to basal freeze-on could have a significant influence on ice stream dynamics and stoppage (Christoffersen and Tulaczyk, 2003a). It should be noted that basal freeze-on does not necessarily result in ice stream stoppage (Kamb, 2001), and Stokes and Clark (2003) were unable to determine whether it was the cause or a result of shutdown of the Dubawnt Lake palaeo-ice stream.

It is clear from this review of ice streams that the nature of the bed is of particular interest because it facilitates fast ice flow and also appears to exert a control on ice stream location, onsets and shutdown (Stokes and Clark, 2001).

3.3 Palaeo-ice streams

Ice streams are thought to have played an important role in the dynamics and stability of former ice sheets (Stokes and Clark, 1999; Bennett, 2003; De Angelis and Kleman, 2005, 2007; Ó Cofaigh *et al.*, 2008). Identifying the beds of palaeo-ice streams is of great importance for a number of reasons. In order to accurately reconstruct former ice sheets dynamics and histories we need to know where and when ice streams operated (Stokes and Clark, 2001, 2003; De Angelis and Kleman, 2007). This was first recognised by Denton and Hughes (1981), who predicted the location of ice streams in their reconstruction of the former northern hemisphere ice sheets (see Figure 3.2).

Assessing the interactions of palaeo-ice streams with climate is of importance when reconstructing past climates and predicting ice sheet response to future climate changes (Stokes and Clark, 1999). The control that the bed has on the location, dynamics and flow of ice streams has been discussed in the previous section. However, studying the beds of contemporary ice streams is extremely difficult due to their inaccessibility (Payne and

Baldwin, 1999; Stokes and Clark, 1999; Ó Cofaigh *et al.*, 2005) and has been confined to limited boreholes (Engelhardt *et al.*, 1990), seismic studies (Blankenship *et al.*, 1986; Anandakrishnan *et al.*, 1998) and more recent radar data (Bell *et al.*, 2007; King *et al.*, 2009). The beds of palaeo-ice streams, therefore, present an excellent opportunity to investigate the processes that occur beneath ice streams (Stokes and Clark, 1999; Stokes, 2002; Ó Cofaigh *et al.*, 2005). In addition, as all contemporary ice streams are marine-terminating, palaeo-ice streams provide a unique chance to also study terrestrially-terminating ice streams (Stokes and Clark, 1999).

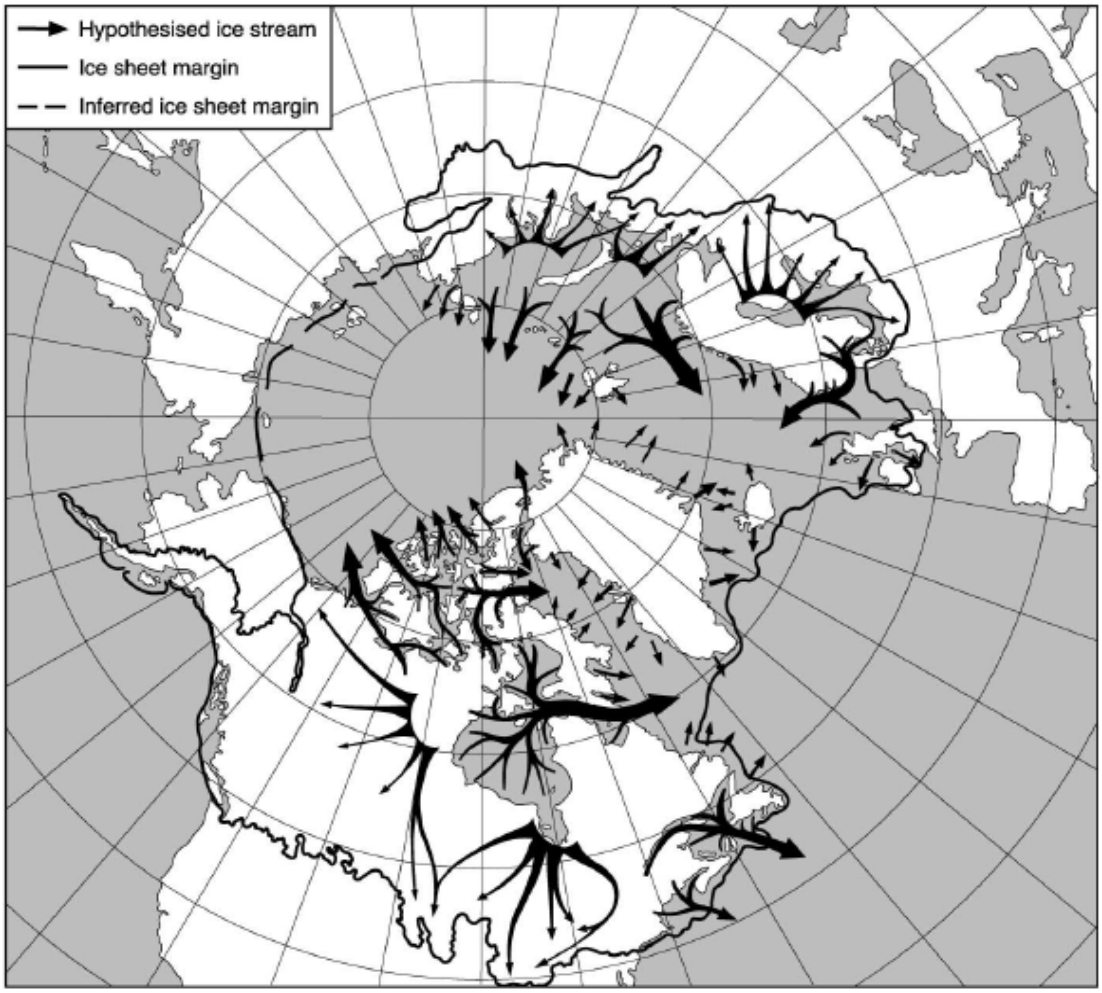

Figure 3.2 - Locations of palaeo-ice streams (black arrows) in the former northern hemisphere ice sheets as hypothesised by Denton and Hughes (1981).

3.3.1 Terrestrial ice streams

It is thought that former ice sheets are likely to have been drained by terrestrial ice streams, as well as marine-based ice streams (Patterson, 1997; Clark and Stokes, 2003). The best examples of terrestrially-terminating ice streams are found at the southern margin of the former Laurentide Ice Sheet, which are thought to have terminated as lobes (e.g. Clark,

1992; Patterson, 1997, 1998; Jennings, 2006; Evans *et al.*, 2008). Terrestrial ice records have also been reported from the southern sector of the former Fennoscandian Ice Sheet (Boulton *et al.,* 2001b). There are no modern analogues for land-based ice streams (Patterson, 1997; Boulton *et al.*, 2001b). Consequently, it has been suggested that both modern fast moving or surging glaciers (Patterson, 1997) and the piedmont lobes of the southern Alaskan glaciers (Boulton *et al.*, 2001b) may present the best contemporary models.

The main consideration for both marine-based and terrestrial ice streams is the way in which ice is removed from the margins (Clark and Stokes, 2003). For marine-based ice streams this is achieved through calving directly into the ocean or via a floating ice shelf (Patterson, 1997; Clark and Stokes, 2003; see Figure 3.3, c and d). A floating margin is not necessary for ice streaming but is an effective way to remove discharged ice (Patterson, 1997). Terrestrial ice streams are also thought to ablate large ice fluxes in two main ways: either through calving into a large proglacial lake or through a large splayed lobe at the terminus that extends beyond the ice sheet margin (Patterson, 1997, 1998; Stokes and Clark, 2004; Clark and Stokes, 2003; Jennings, 2006; see Figure 3.3, a and b). The large surface area presented by the splayed lobe and its location below the equilibrium line altitude would allow it to facilitate efficient surface melting and mass loss (Clark and Stokes, 2003). Clark and Stokes (2003) regard this as the only way in which sufficiently high ablation losses and the high ice flux delivered to the margin could be balanced, other than through calving into a proglacial lake. Evidence for a splayed lobe in the geomorphological record is thought to include a strongly divergent terminus following the main streamlined trunk (Boulton *et al.*, 2001b; see Figure 3.3, a), substantial zones of hummocky topography associated with ice stagnation, and considerable volumes of exported sediment (Patterson, 1997; Stokes and Clark, 2003; Jennings, 2006). Evans *et al.* (2008) acknowledged that ice streams terminating as lobate snouts would produce many of the landform-sediment assemblages characteristic of smaller-scale modern outlet glaciers. The Dubawnt Lake palaeo-ice stream in Canada is an example of a terrestrial ice stream, and during its lifespan it is thought to have terminated both as a splayed lobe and, as the margin retreated inland, in a proglacial lake (Stokes and Clark, 2003).

3.3.2 Geomorphological evidence of palaeo-ice streaming

Palaeo-ice streams have been identified from a variety of geomorphological evidence (Stokes and Clark, 1999), a few of these examples will now be outlined. On Prince of

Wales Island, in the Canadian Arctic, Dyke and Morris (1988) suggested that large ice streams comparable in size to Hudson Strait had existed. The geomorphological evidence to support this included: a large drumlin field with a highly convergent flow pattern, with the longest drumlins situated in the central part of the field where ice was presumed to flow fastest; a lateral shear moraine marking a shear zone at the edge of the ice stream; and a Boothia-type dispersal train (see Figure 3.4; Dyke and Morris, 1988).

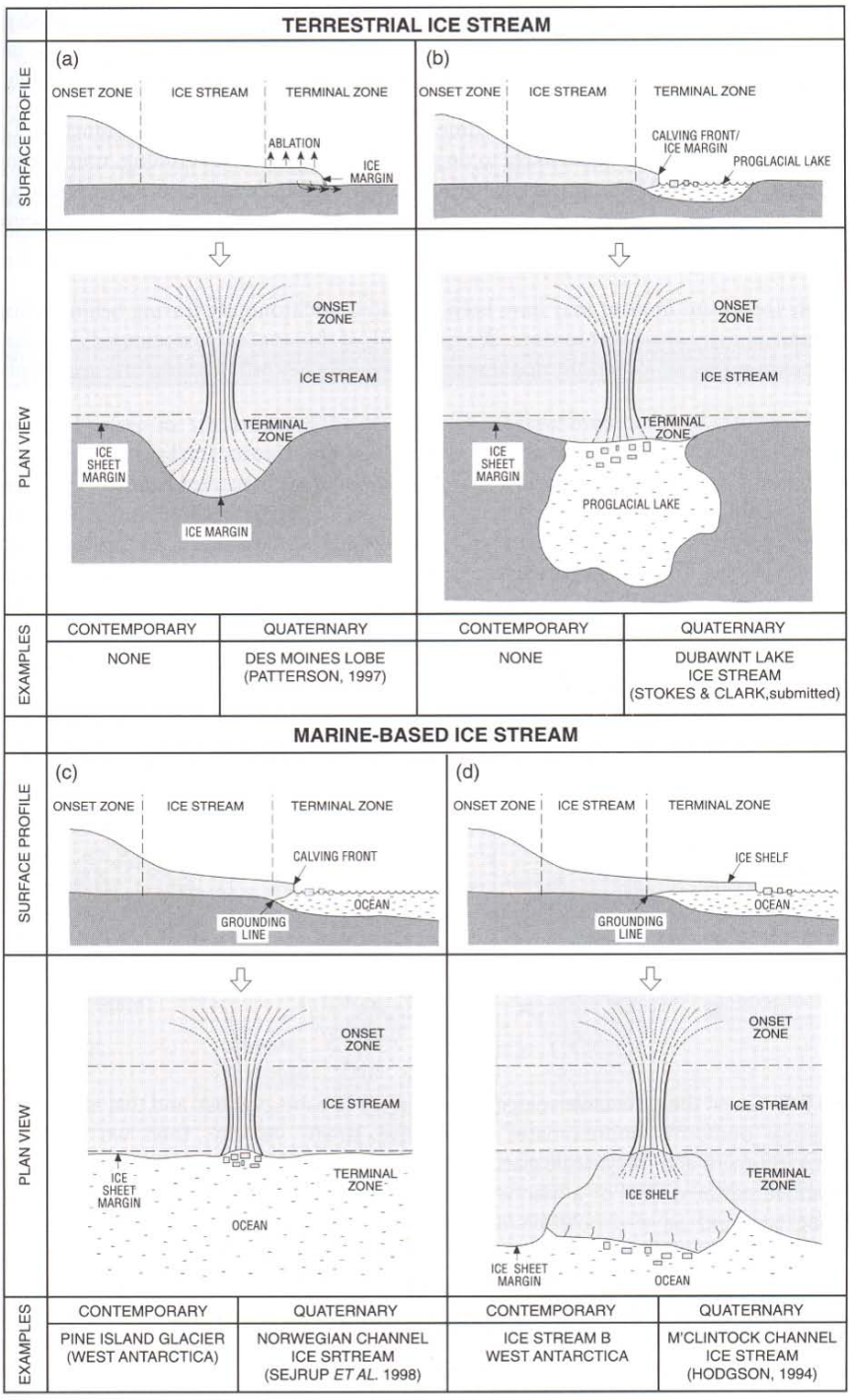

Figure 3.3 - Simplified configurations of terrestrial and marine-based ice streams, from Clark and Stokes (2003). Contemporary and palaeo examples of each are included.

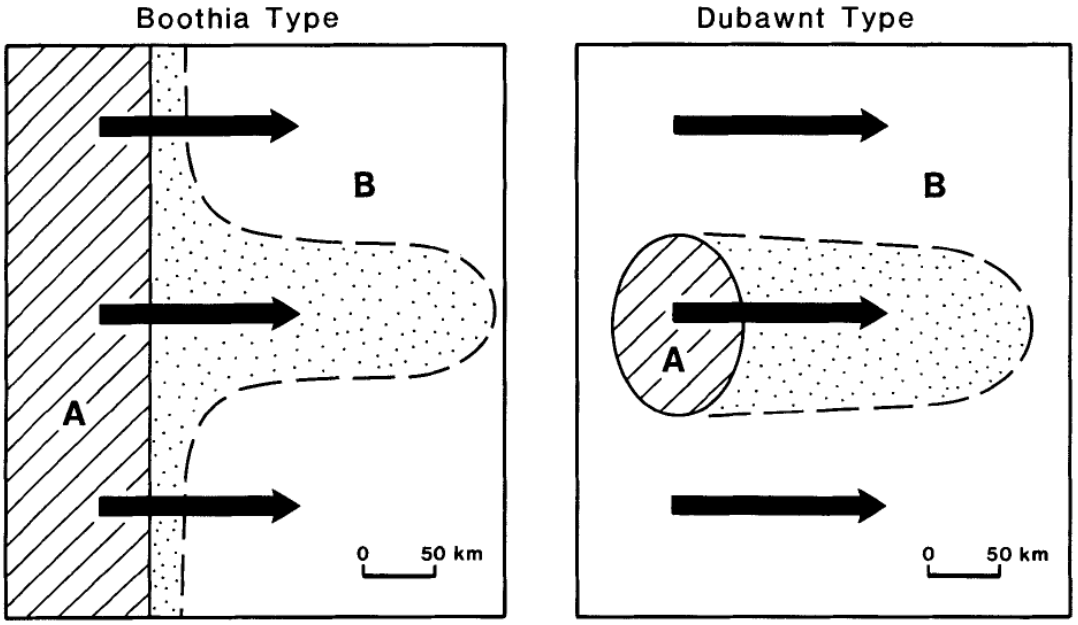

Figure 3.4 - Diagram of Boothia- and Dubawnt-type dispersal trains. The Boothia-type is indicative of ice streaming and the Dubawnt-type is formed by normal but sustained regional ice. A and B are two distinctly different rock types; arrows indicate ice flow direction; dots represent glacial dispersal of rock type A. From Dyke and Morris (1988).

An 80 km-wide, 200 km-long ice stream was identified on Victoria Island in the Canadian Arctic by Hodgson (1994). This was based on evidence of: highly attenuated bedforms within a large drumlin field, thought to be indicative of fast-ice flow; an abrupt margin to the drumlin field; and extended ridges interpreted as lateral shear moraines (Hodgson, 1994). At the southern margin of the Laurentide Ice Sheet, Patterson (1997) suggested that the suite of landforms developed by the Des Moines Lobe, Minnesota, was indicative of ice streaming. Evidence for this included: highly convergent topography in the onset zone; broad zones of stagnation landforms such as hummocky topography in the outer 20 to 50 km; and radiocarbon chronology indicating rapid ice advance (Patterson, 1997). Analysis of satellite imagery of the former Fennoscandian Ice Sheet allowed for the identification of 11 ice streams (Punkari, 1997). Fan-shaped flow patterns, abundant flow-parallel features and eskers, and indications of effective glacial erosion were the main forms of geomorphological evidence this was based on (Punkari, 1997). A comprehensive review of early examples of identified palaeo-ice streams and the evidence these were based on can be found in Stokes and Clark (2001).

The identification of palaeo-ice streams in these studies was based on a variety of often subjective evidence which escaped detailed scrutiny according to Stokes and Clark (1999), which they attributed to a poor understanding of the evidence for ice stream activity. In a

few cases this may have resulted in ice streams being hypothesised where meaningful evidence for their existence was lacking (Stokes and Clark, 1999).

3.3.3 Geomorphological criteria for identifying palaeo-ice streams

The need to establish a set of criteria by which ice streams could be identified in formerly glaciated terrain was noted by Stokes and Clark (1999). This combination of evidence can then be used to create a conceptual landsystem of geomorphological evidence left behind by ice streams, which can then be applied and tested on hypothesised palaeo-ice streams tracks (Stokes and Clark, 1999). Identifying the geomorphological and geological signatures of ice streams allows the overall landsystem 'fingerprint' (Everest *et al.*, 2005; Golledge and Stoker, 2006), or perhaps 'footprint', to be compared with formerly glaciated landscapes around the world (Hart, 1999; Stokes and Clark, 2001). The Stokes and Clark (1999) criteria are logically based on the fundamental characteristics of contemporary ice streams and fast ice flow. It should be noted that individual criteria may not be exclusive to ice stream activity, but that the collective landsystem can be thought to be characteristic of palaeo-ice streaming (Stokes and Clark, 1999). The geomorphological criteria for palaeo-ice streaming proposed by Stokes and Clark (1999) are summarised in Table 3.1, alongside the fundamental characteristics of contemporary ice streams that each geomorphological signature relates to.

Table 3.1 – Geomorphological criteria for identifying former ice streams as proposed by Stokes and Clark (1999).

Contemporary ice stream characteristic	Proposed geomorphological signature
A. *Characteristic shape and dimensions*	1. Characteristic shape and dimensions 2. Highly convergent flow patterns
B. *Rapid velocity*	3. Highly attenuated bedforms (length-to-width > 10:1) 4. Boothia-type erratic dispersal trains
C. *Sharply delineated shear margin*	5. Abrupt lateral margins 6. Lateral shear moraine
D. *Deformable bed conditions*	7. Glaciotectonic and geotechnical evidence of pervasively deformed till 8. Submarine till delta or sediment fan

3.3.3.1 Characteristic shape and dimensions

Perhaps the most obvious characteristic of a palaeo-ice stream is its overall shape and dimensions (Stokes and Clark, 1999). Figure 3.5 shows a simplified ice stream shape, with

converging flowlines in the onset zone feeding into the main channel of streaming ice. For terrestrially-terminating ice streams, flowlines could be expected to diverge again towards the terminus (Stokes and Clark, 2003). They are generally thought to be greater than 20 km wide and 150 km in length (Stokes and Clark, 1999, 2003; Stokes, 2002). The Siple Coast ice streams that drain West Antarctica are between 30 and 50 km wide and 300 to 500 km long (Whillans *et al.*, 1987; Engelhardt *et al.*, 1990; Bennett, 2003). The M'Clintock Channel palaeo-ice stream in northwest Canada was reconstructed as 140 km wide and 740 km long (Clark and Stokes, 2001) and palaeo-ice streams up to 1000 km long have been identified in the submarine record off the coast of West Antarctica (Mosola and Anderson, 2006). At the other end of the scale, Knight *et al.* (1999) reported the presence of two palaeo-ice streams in eastern Ireland with widths of 5 km and 10 km and lengths of 46 km and 18 km, and De Angelis and Kleman (2008) identified three palaeo-ice streams in northeast Canada less than 70 km long. This shows the potential variety in ice stream dimensions, particularly if the overall shape remains consistent with that of contemporary ice streams (Stokes and Clark, 1999).

3.3.3.2 Highly convergent flow patterns

As seen in Figure 3.5, a strongly convergent pattern of former ice flow is a key characteristic of palaeo-ice streams (Stokes and Clark, 1999). The onsets of contemporary ice streams are characterised by a large convergence zone, where surrounding slower moving ice is incorporated into the main ice stream channel (Hodge and Doppelhammer, 1996). According to De Angelis and Kleman (2008), all documented palaeo-ice stream onsets comprise a highly convergent zone of lineations leading into the main channel. This is supported by a number of examples of highly convergent flow patterns at the head of palaeo-ice stream beds, including the Dubawnt Lake palaeo-ice stream in the Keewatin Sector of the Laurentide Ice Sheet (Stokes and Clark, 2003); the Tweed palaeo-ice stream in Berwickshire (Everest *et al.*, 2005); the Strathmore Ice Stream in western Scotland (Golledge and Stoker, 2006); and a palaeo-ice stream in Marguerite Bay, offshore of the Antarctic Peninsula (Anderson and Oakes Fretwell, 2008).

3.3.3.3 Highly attenuated bedforms

Linear subglacial bedforms aligned parallel to former ice-flow directions are common in areas of formerly glaciated terrain (Clark, 1993, 1994). Flutes, drumlins, megaflutes and megadrumlins comprise an assemblage of these features that are thought to be related in terms of form and scale (Clark, 1994). Large-scale streamlined lineations were first

detected by Clark (1993) from Landsat satellite images of the former Laurentide Ice Sheet. These features were much larger in scale than previously documented lineations and ranged in length from 8 km to 70 km (Clark, 1993). Termed mega-scale glacial lineations (MSGL; Clark, 1993, 1994), they are highly attenuated bedforms that have a high length-to-width ratio. This ratio is usually of the order of > 10:1 and Clark (1994) suggested they could be formed by either fast ice flow over a short duration or slower moving ice over a longer duration. It is now generally accepted that MSGL and other highly-attenuated streamlined bedform lineations are indicative of fast ice flow (Clark, 1999; Stokes and Clark, 1999, 2002a, Stokes, 2002; Evans *et al.*, 2008; King *et al.*, 2009).

It follows that the presence of such elongated features may well record fast ice flow within an ice stream (Clark, 1993, 1999; Stokes and Clark, 1999). They have been found on the Antarctic continental margin, distal to positions of active ice streams (Canals *et al.*, 2000). This is further supported by a recent study by King *et al.* (2009), in which MSGL were detected beneath the active Rutford Ice Stream in West Antarctica using radar. The longest of these features extended for > 18 km and had elongation ratios of between 15:1 and 35:1. These were found to be indistinguishable from features identified from palaeo-ice stream beds in both marine and terrestrial settings, providing indisputable evidence for the association of MSGL with fast-flowing ice (King *et al.*, 2009). The presence of MSGL and other streamlined bedforms have been invoked as evidence for a number of palaeo-ice streams (Hodgson, 1994; Clark and Stokes, 2001; Jansson *et al.*, 2003; De Angelis and Kleman, 2005, 2007; Everest *et al.*, 2005; Ó Cofaigh *et al.*, 2005, 2008; Stokes *et al.*, 2005, 2006, 2009; Golledge and Stoker, 2006; Evans *et al.*, 2008; Ottesen *et al.*, 2008a).

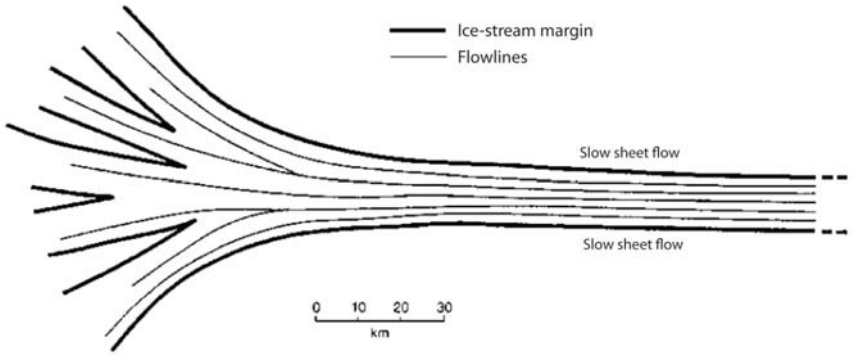

Figure 3.5 - Simplified theoretical shape of an ice stream, with ice flow from left to right. Note the convergent flowlines in the onset zone feeding the main ice stream channel. From Stokes and Clark (1999).

A spatial variation in elongation ratios of streamlined bedforms within palaeo-ice streams has been recognised. Hart (1999) compared elongation ratios from the New York drumlin field with the lateral velocity patterns of the Whillans Ice Stream and Jakobshavn Isbræ and found that the velocity changes were similar in all three examples. The occurrence of longer and more elongate bedforms towards the central axis of flow of former ice streams, where ice velocities are presumed to have been higher, is well documented (Dyke and Morris, 1988; Stokes and Clark, 2002, 2003; Ó Cofaigh *et al.*, 2005). A down-ice increase in bedform elongation has also been detected within the Oneida Sublobe of the New York Drumlin Field (Hess and Briner, 2009) and the Marguerite Trough palaeo-ice stream that drained the Antarctic Peninsula Ice Sheet (Ó Cofaigh *et al.*, 2002). This pattern was attributed to a progressive down ice increase in ice stream velocity (Ó Cofaigh *et al.*, 2002). No such observations could be made for the M'Clintock palaeo-ice stream, where lineation length exhibited no clear pattern laterally and length and elongation were found to decrease slightly in the down ice direction (Clark and Stokes, 2001). A downstream increase in density of drumlins and MSGL was hypothesised to be the geomorphological product of the mechanism of ice stream shutdown (Clark and Stokes, 2001).

The genesis of streamlined bedforms and MSGL in particular is not well understood and is the subject of conflicting hypotheses (Clark, 1993; Clark *et al.*, 2003; Shaw *et al.*, 2008). It was suggested by Shaw *et al.* (2008) that MSGL on the Antarctic continental shelf could have been formed through erosion by turbulent meltwater floods. The subglacial megaflood theory of drumlin and attenuated lineation formation has not been widely accepted and has been criticised by, among others, Benn and Evans (2006), who argued that it is incompatible with a large body of mainstream research on contemporary and past ice sheet beds. The discovery of MSGL beneath the Rutford Ice Stream by King *et al.* (2009) was presented by Ó Cofaigh *et al.* (2010a) as further evidence to discredit the Shaw *et al.* (2008) claim that MSGL have not been observed beneath modern ice streams.

A second theory of MSGL formation is the groove-ploughing hypothesis suggested by Clark *et al.* (2003), following work by Tulaczyk *et al.* (2001). This theory argued that MSGL are grooves in a soft sediment layer, rather than ridges of sediment (Clark *et al.*, 2003). It is envisaged that large bumps are created in the ice base as it passes over uneven hard bedrock upstream, and that these "keels" maintain their shape and plough through soft sediments down ice (Clark *et al.*, 2003). Elongate grooves are carved and sediment is squeezed up into intervening ridges (Clark *et al.*, 2003). Initial modelling suggested that ice keels could survive downstream propagation, and it was noted that exposed bedrock

exists immediately upstream of all known examples of MSGL (Clark *et al.*, 2003). This evidence is used to support the groove-ploughing theory (Clark *et al.*, 2003), but it is clear that this hypothesis, as with all hypotheses of MSGL formation, requires further testing.

3.3.3.4 Boothia-type erratic dispersal trains

The down ice transport of a narrow belt of glacial debris from a source area is known as a dispersal train (Dyke and Morris, 1988). Two types were recognised by Dyke and Morris (1988): a Boothia-type and a Dubawnt-type (see Figure 3.4). As the Dubawnt-type can be formed by slow ice sheet flow, only Boothia-type dispersal trains are indicative of ice streaming (Dyke and Morris, 1988). The reason for this is that ice streams have the ability to transport and disperse sediment in a very distinctive fashion (Stokes and Clark, 1999). In Boothia-type dispersal trains, debris is dispersed down ice from a small part of a relatively large source area, and this greater transport of material within a narrow belt is taken to indicate a zone of ice streaming (Dyke and Morris, 1988). The presence of two palaeo-ice streams on Melville Peninsula in the northeastern Canadian Arctic was determined from evidence including carbonate dispersal trains (Dredge, 2000). The dimensions of the dispersal trains, between 50-125 km wide and 100-300 km long, were found to be similar to those of contemporary Antarctic ice streams (Dredge, 2000).

3.3.3.5 Abrupt lateral margins

Ice streams are bordered by slower-moving ice (Stokes and Clark, 2001) and so former ice streams can be expected to have a sharp zonation at their lateral margins between evidence for fast ice flow and non-streamlined terrain (Stokes and Clark, 1999; Everest *et al.*, 2005). Such a well-defined margin requires a distinct discontinuity in the overlying ice, either through a contrast in the basal thermal conditions or ice velocities (Clark and Stokes, 2001). Both of these are characteristic of ice stream margins (Clark and Stokes, 2001). Echelmeyer *et al.* (1994) showed that the abrupt change in velocity at ice stream margins created a heavily crevassed zone, about one-tenth of the entire ice stream width. Palaeo-ice streams can be expected to exhibit a similarly proportioned abrupt marginal area (Stokes and Clark, 1999). Examples of identified palaeo-ice streams with abrupt lateral margins include the M'Clintock Channel ice stream (Clark and Stokes, 2001) and Ungava Bay ice streams (Jansson *et al.*, 2003) in Canada; and the Tweed (Everest *et al.*, 2005) and Strathmore palaeo-ice streams (Golledge and Stoker, 2006) in Scotland.

3.3.3.6 Lateral shear moraine

Large subglacial ridges up to several kilometres long and tens of metres high and wide have been identified at the margins of palaeo-ice streams (Dyke and Morris, 1988; Hodgson, 1994; Stokes and Clark, 2002b). These features have been interpreted as lateral shear moraines and are thought to mark a shear zone at the margins of an ice stream separating fast and slower ice (Dyke and Morris, 1988). The mechanism of formation of these features is unknown and observations of them on palaeo-ice stream beds are limited (Hindmarsh and Stokes, 2008). A number of possible mechanisms for their formation have been suggested by Stokes and Clark (2002b). These included: meltwater processes depositing sediment in englacial and subglacial streams; melt-out and deposition of entrained englacial debris; downstream sediment recycling; differential erosion; and lateral advection of sediment towards the margin (Stokes and Clark, 2002b).

Hindmarsh and Stokes (2008) favoured the differential erosion hypothesis, in which their formation is explained by the lateral variations in the erosional power of ice streams. This theory may also help to explain the relative scarcity of lateral shear moraines in the geomorphological record, as it is suggested that they are rarely formed (Hindmarsh and Stokes, 2008). This is attributed to the unique glaciological setting required for their formation, specifically a metres-thick layer of unconsolidated sediment, an abrupt lateral transition in ice velocity, and relatively high ablation rates (Hindmarsh and Stokes, 2008). The presence of lateral shear moraines has formed part of the evidence for identifying a number of palaeo-ice streams, including the M'Clintock Channel ice stream in Canada (Clark and Stokes, 2001); the Strathmore ice stream in Scotland (Golledge and Stoker, 2006); and the Vestfjorden-Trænadjupet, Norwegian Channel and Bear Island Trough palaeo-ice streams (Ottesen *et al.*, 2005a, b).

3.3.3.7 Evidence of pervasively deformed till

The importance of a layer of deformable sediment at the ice base for fast ice flow has been discussed in detail in a previous section. Anandakrishnan *et al.* (1998), Bell *et al.* (1998) and Studinger *et al.* (2001) suggested that ice stream position may well be dependent on subglacial geology and, in particular, the presence of a soft sedimentary basin. This suggests that areas of pervasively deformed till may well predispose a section of an ice sheet to fast ice flow (Stokes and Clark, 1999). In addition, the discovery of deformed till at the bed of a palaeo-ice stream provides some clues as to the mechanism for fast ice flow (Ó Cofaigh *et al.*, 2005, 2007). In Antarctica, the presence of deformation till was found in

association with MSGL on the bed of the Marguerite Trough palaeo-ice stream (Ó Cofaigh *et al.*, 2005) and in troughs situated in the Ross Sea that were occupied by ice streams (Mosola and Anderson, 2006), and also on palaeo-ice stream beds in the southwest Laurentide Ice Sheet (Evans *et al.*, 2008).

3.3.3.8 Submarine till delta or sediment fan

The presence of substantial amounts of sediment on a continental shelf may also be indicative of ice stream activity (Stokes and Clark, 1999). Known as trough mouth fans, they are described as fan-shaped, diamict-dominated sediment accumulations (Ó Cofaigh *et al.*, 2003). Large volumes of sediment are delivered to the shelf edge by marine-terminating ice streams that advanced across continental shelves underlain by a sedimentary substrate (Ó Cofaigh *et al.*, 2003). This sediment is then remobilised and redeposited down the continental slope (Ó Cofaigh *et al.*, 2003). Trough mouth fans have been identified in the Polar North Atlantic and on the Antarctic continental margin (Kuvaas and Kristoffersen, 1991; Vorren and Laberg, 1997; Ó Cofaigh *et al.*, 2003).

3.3.3.9 Additional evidence for palaeo-ice streaming

There are some features that have been associated with palaeo-ice stream activity that do not feature in the Stokes and Clark (1999) criteria. Widespread hummocky topography has been reported from areas of former ice streaming at the southern margin of the Laurentide Ice Sheet (Patterson, 1997; Jennings, 2006; Evans *et al*., 2008). The outer 20 to 50 km of many of the margins of the Des Moines Lobe are composed of such terrain, indicating that at least the outer reaches of the lobe underwent periodical stagnation (Patterson, 1997; Jennings, 2006). Evans *et al*. (2008) suggested that hummocky terrain in southern Alberta was constructed by the lobate margins of neighbouring ice streams as they advanced. Thrust block moraines have also been reported from the southern margin of the Laurentide Ice Sheet (Jennings, 2006; Evans *et al*., 2008). In southern Alberta, Evans *et al.* (2008) suggested that large thrust block moraines were formed by the retreating lobate margins of palaeo-ice streams. This additional geomorphological evidence appears to be unique to terrestrially-terminating ice streams.

3.3.3.10 Summary

The Stokes and Clark (1999) criteria for the identification of palaeo-ice streams in the geomorphological record are: characteristic shape and dimensions; highly convergent flow patterns; highly attenuated bedforms; Boothia-type dispersal trains; abrupt lateral margins;

lateral shear moraine; evidence of pervasively deformed till; and trough mouth fans (see Table 3.1). Stokes and Clark (1999) highlighted the fact that the occurrence in one location of all eight of the aforementioned criteria for palaeo-ice streaming is unlikely. However, the existence of a number of these can imply the presence of a palaeo-ice stream, and the combination of all eight should be viewed as an idealised example of a palaeo-ice stream landsystem (Stokes and Clark, 1999). The M'Clintock Channel ice stream identified by Clark and Stokes (2001) fulfils four of the Stokes and Clark (1999) criteria: appropriate shape and dimensions; the presence of MSGLs; abrupt lateral margins; and lateral shear moraines. The Strathmore palaeo-ice stream in Scotland was found to exhibit six of the eight criteria, with only a Boothia-type dispersal train and an offshore fan lacking (Golledge and Stoker, 2006). Additional evidence for ice streaming, not included in the Stokes and Clark (1999) criteria and perhaps unique to terrestrially-terminating ice streams, includes substantial zones of stagnation landforms such as hummocky terrain, and thrust moraines (Patterson, 1997; Stokes and Clark, 2003; Jennings, 2006).

3.3.4 Palaeo-ice stream landsystems

The geomorphological signature of a palaeo-ice stream, based on the criteria of Stokes and Clark (1999), is shown in Figure 3.6. Ice streams can terminate in either marine or terrestrial settings and the differences between the two will be reflected in the geomorphological record (Stokes and Clark, 1999). For example, terrestrial-terminating ice streams can be characterised by hummocky topography and thrust block moraine complexes around their lobate margins (Patterson, 1997, 1998; Jennings, 2006; Evans *et al.*, 2008) and would not produce trough mouth fans. In addition, the geomorphological record of palaeo-ice streams can be broadly classified as either *isochronous* or *time-transgressive* (Clark, 1999). An isochronous or 'rubber-stamped' record may be produced when an ice stream switches off and a largely intact record of ice stream activity is preserved (Stokes and Clark, 1999, 2001; Jansson *et al.*, 2003). A synchronous record implies that the landforms record true flow patterns (Kleman and Borgström, 1996; Clark *et al.*, 2000). Ice streams may also operate throughout various stages of advance and retreat, during which younger ice flow patterns may be superimposed on the older record (Stokes and Clark, 1999, 2001; De Angelis and Kleman, 2005). This would produce a more complex time-transgressive or 'smudged' record as it is continuously reorganised over time (Kleman and Borgström, 1996; Stokes and Clark, 1999, 2001; Greenwood and Clark, 2009).

The four types of landsystem signature produced by palaeo-ice streams according to Stokes and Clark (1999) are shown in Figure 3.6: marine-terminating and isochronous (a); marine-terminating and time-transgressive (b); terrestrial-terminating and isochronous (c); and terrestrial-terminating and time-transgressive (d). Figure 3.7 focuses on terrestrial-terminating ice streams, (a) shows the isochronous record; (b) shows the time-transgressive record; and (c) shows how the time-transgressive record produces a number of bedform populations which may have similar orientations or cross-cutting relationships (Clark, 1999). Terrestrial-terminating ice streams can also terminate in large proglacial lakes (e.g. Stokes and Clark, 2004).

A number of subsequent studies that have identified palaeo-ice streams in both terrestrial and marine settings have reported similar geomorphological records to the Stokes and Clark (1999) landsystems (e.g. De Anglis and Kleman, 2005; Golledge and Stoker, 2006; Ottesen *et al.*, 2008; Ó Cofaigh *et al.*, 2010b). However, it is clear that a simplified conceptual landsystem is insufficient to encapsulate the full range of geomorphological evidence that may be produced by ice streams. This is particularly true for the lobate margins of terrestrial ice streams reported from the southern Laurentide Ice Sheet, which are characterised by evidence for thrusting and ice stagnation more akin to a surging landsystem (Patterson, 1997, 1998; Evans and Rea, 1999; Jennings, 2006; Evans *et al.*, 2008). This demonstrates the broad range of geomorphology produced by palaeo-ice streams. Despite this, the Stokes and Clark (1999) idealised model provides a useful template by which palaeo-ice streams can be better interpreted.

3.3.5 Similar glacial landsystems

The geomorphological criteria for identifying a palaeo-ice stream, and the landsystem these produce, exhibits a degree of overlap with other types of glacial landsystem. This is as can be expected, as it has already been shown that individual criteria are not necessarily exclusive to ice-stream activity (Stokes and Clark, 1999). It is important that these alternative landsystems are considered in order to allow for a more accurate interpretation of the geomorphological record.

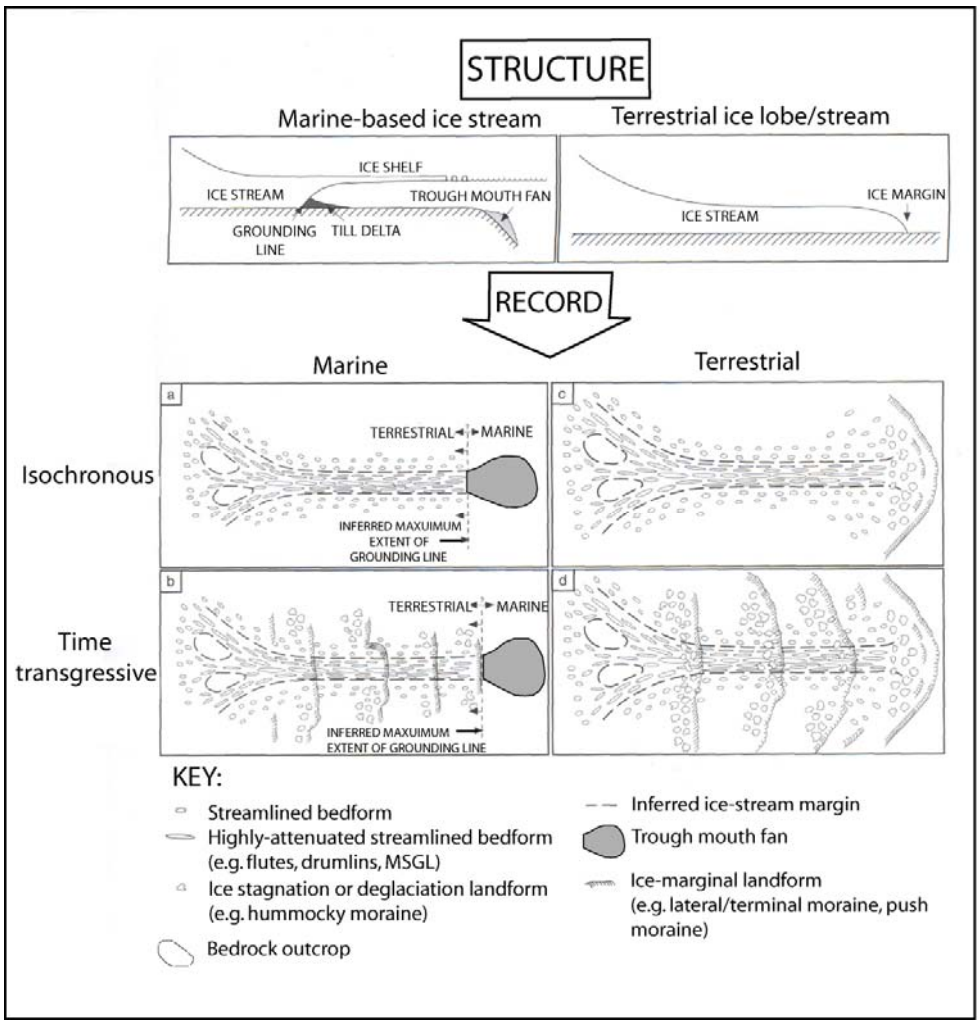

Figure 3.6 - Four types of landsystem signature produced by palaeo-ice streams, from Stokes and Clark (1999). Ice streams can be either marine or terrestrial, depending on the environment in which they terminate. The recorded geomorphological signature may also be loosely classified as *isochronous* or *time-transgressive*.

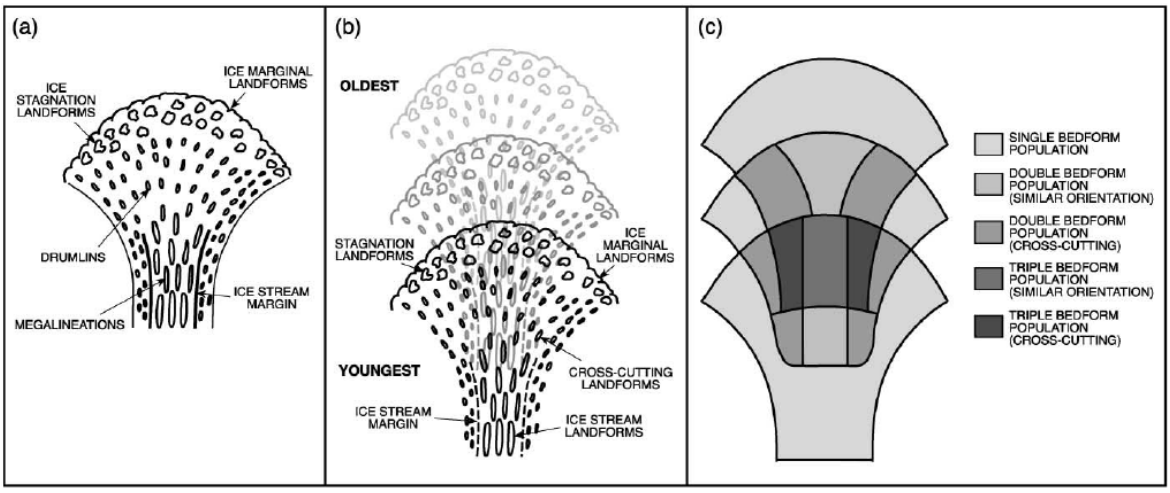

Figure 3.7 – Conceptual landsystems of a terrestrial-terminating ice stream from Stokes and Clark (2001). (a) shows the isochronous or 'rubber stamped' record; (b) shows the time-transgressive or 'smudged' record; and (c) shows how the time-transgressive record can leave behind a complicated assemblage, in which each area can contain a number of bedform populations.

3.3.5.1 Surging glacier landsystem

Glacier surges are highly dynamic events that represent a flow instability triggered from within the glacier system and are largely independent from climate forcing (Evans and Rea, 1999, 2003; Christoffersen *et al.*, 2005). During glacier surges ice-flow velocity increases abruptly by up to several orders of magnitude (Christoffersen *et al.*, 2005). It is therefore not too surprising that some of the landforms produced during a glacier surge are similar to those thought to be indicative of ice streaming, particularly for terrestrial ice streams that terminate as lobes (Evans *et al*., 2008). According to the Evans and Rea (1999, 2003) surging glacier landsystem (see Figure 3.8), which was based on observations from contemporary surging glacier margins, evidence includes: thrust-block moraines and push moraines; concertina eskers; crevasse-squeeze ridges; flutings; zones of thrusting and squeezing; hummocky moraine; ice-cored outwash and glaciolacustrine sediments; and complex till stratigraphies. Evans and Rea (1999, 2003) provide comprehensive details on these landform-sediment assemblages. It is noted that these criteria cannot be used independently to identify a surging glacier (Evans and Rea, 2003), as with the Stokes and Clark (1999) criteria for palaeo-ice streams.

A number of the criteria for surging glaciers highlighted in the Evans and Rea (1999, 2003) landsystem are similar to that for ice streams. Fluting length is thought to provide evidence for rapid advances over substantial distances in a surging glacier landscape (Evans and Rea, 2003). Elongated subglacial bedforms, particularly MSGL, are also a key indicator of ice streaming (Stokes and Clark, 1999). Submarine MSGL have been identified within the limits of known tidewater glacier surges in Van Keulenfjorden and Rindersbukta, Svalbard (Ottesen *et al.*, 2008b; see Figure 3.9 for a surging tidewater glacier landsystem). The main difference between the presence of elongated bedforms in both landsystems is that flutings are often associated with crevasse-squeeze ridges in a surging environment (Evans and Rea, 2003). The length of the bedforms also appears to display some distinction; the longest bedforms recorded by Ottesen *et al.* (2008b) were up to 3.5 km in length, whereas MSGL associated with ice streaming are thought to be much longer than drumlins and megaflutes, typically ranging from 6 to 100 km (Clark, 1994; Clark and Stokes, 2003).

The presence of pervasively deformed sediment is thought to be indicative of ice streaming (Stokes and Clark, 1999), and the complex till stratigraphies associated with surging glaciers include the thickening of deformation till (Evans and Rea, 1999, 2003). This is

thought to be produced by the advance of surging glacier snouts into areas of softer sediments (Evans and Rea, 2003). It appears that the presence of deformation till represents another possible overlap between the landsystems.

Hummocky moraine and thrust/push moraines are both included in the Evans and Rea (1999, 2003) surging glacier landsystem. Although not present in the Stokes and Clark (1999) palaeo-ice stream criteria, both have been associated with ice streams and feature in the landsystem (Stokes and Clark, 1999; see Figure 3.6). Terrestrial ice streams that terminated in a splayed lobe are thought to be characterised by evidence of stagnation, such as hummocky topography (Patterson, 1997; Stokes and Clark, 2003; Jennings, 2006). This stagnation is suggested to be caused by rapid subglacial drainage terminating the advance of the ice lobe, and could also produce thrust moraines (Jennings, 2006).

To add to the possible confusion surrounding these similarities, it has been suggested that ice streams can also behave in a dynamic, possibly surging, manner (Evans and Ó Cofaigh, 2003). Evidence from the former Irish Sea ice stream to support this included thrust-block moraines and deformation tills (Evans and Ó Cofaigh, 2003). It is clear that there is a degree of overlap between the idealised landsystems for both ice streams and surging glaciers and this will need to be taken into account when interpreting the geomorphological record of any area displaying these characteristics.

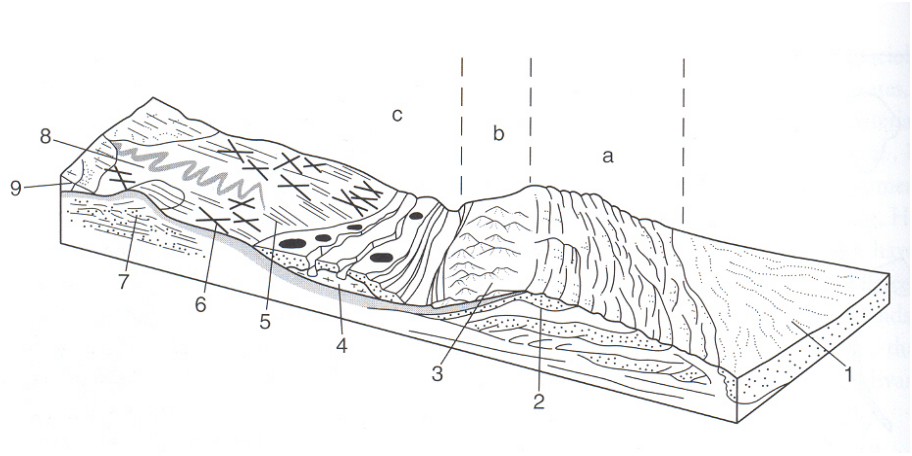

Figure 3.8 - Surging glacier landsystem from Evans and Rea (1999, 2003): a = outer zone of proglacially thrust pre-surge sediment which may grade into small push moraines in areas of thin sediment cover, b = zone of weakly developed chaotic hummocky moraine, c = zone of flutings, crevasse-squeeze ridges and concertina eskers; 1 = proglacial outwash fan, 2 = thrust-block moraine, 3 = hummocky moraine, 4 = stagnating surge snout, 5 = flutings, 6 = crevasse-squeeze ridge, 7 = overridden and fluted thrust-block moraine, 8 = concertina esker, 9 = glacier with crevasse-squeeze ridges emerging at surface (Evans and Rea, 2003).

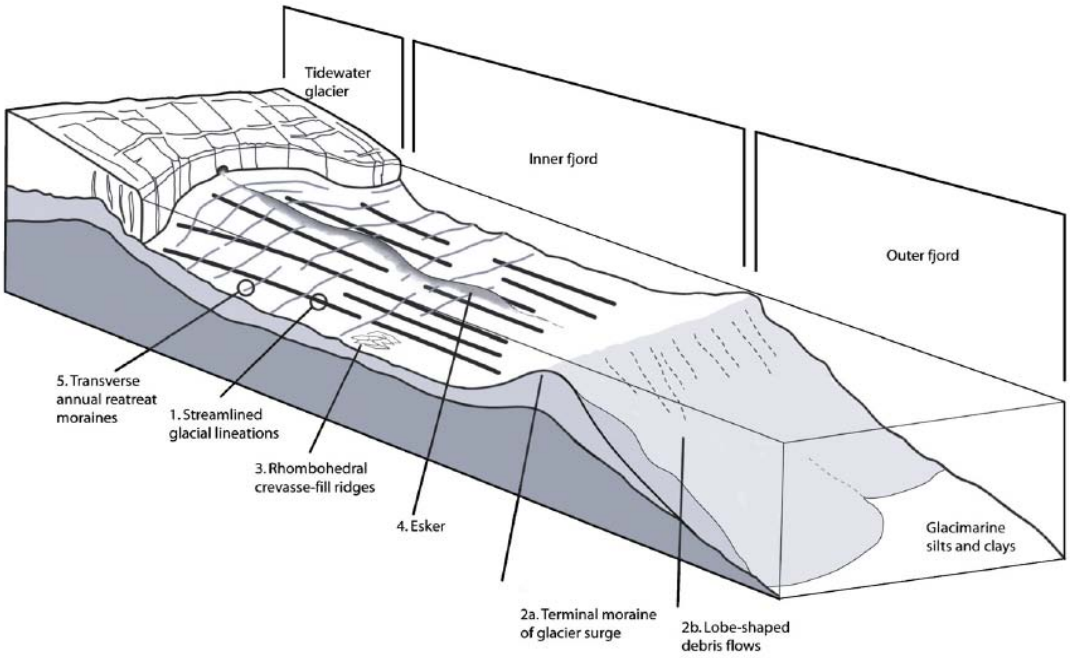

Figure 3.9 - Tidewater surging glacier landsystem from Ottesen *et al.* (2008b).

3.3.5.2 Ice-marginal terrestrial landsystem

One of the landsystems developed by Colgan *et al.* (2003, see Figure 3.10) for the southern margin of the Laurentide Ice Sheet contains a number of similarities to both the palaeo-ice stream (Stokes and Clark, 1999) and surging glacier (Evans and Rea, 1999, 2003) landsystems. Labelled landsystem B, it is characterised by drumlins and high-relief hummocky end moraines and is mainly found in North Dakota, Minnesota, Wisconsin, northern Michigan, Pennsylvania, New York and New England (Colgan *et al.*, 2003). Most of the surface in the subglacial zone has been streamlined by ice flow, with drumlins reaching lengths of up to 6 km in the former Green Bay lobe, Wisconsin (Colgan and Mickelson, 1997). Features of this length are comparable to the MSGL that characterise palaeo-ice streams (Stokes and Clark, 1999). Hummocky moraine and push moraines are both present in this ice-marginal landsystem (Colgan *et al.*, 2003), as in the surging glacier landsystem (Evans and Rea, 1999, 2003), and they have also been associated with palaeo-ice streams (Patterson, 1997; Stokes and Clark, 2003; Jennings, 2006).

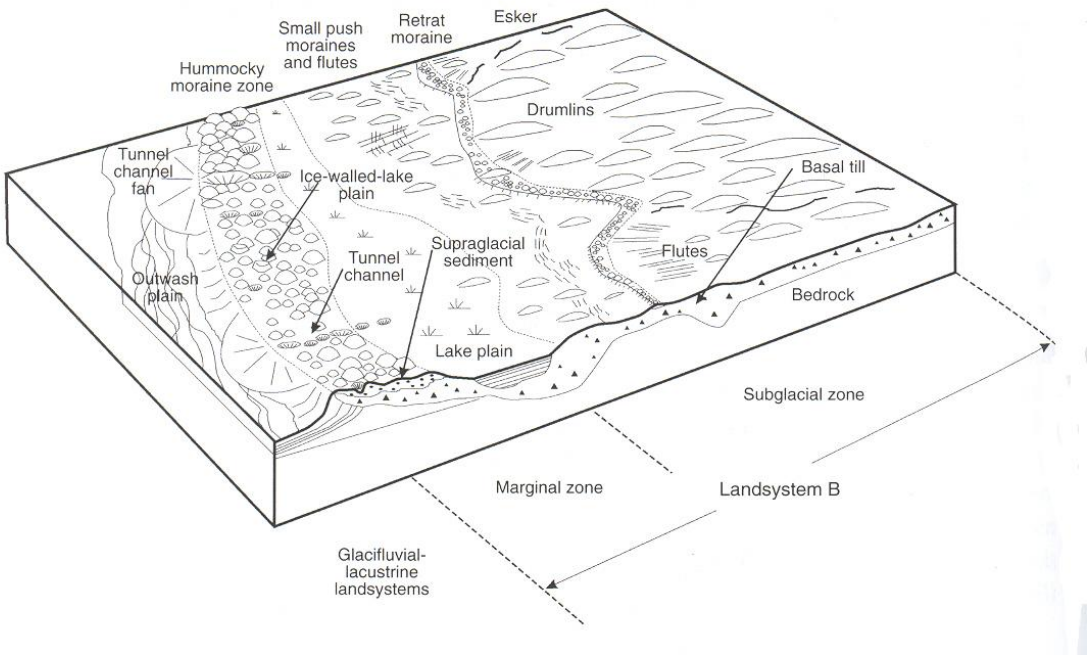

Figure 3.10 - Ice-marginal terrestrial landsystem of the southern Laurentide Ice Sheet, from Colgan *et al.* (2003).

This landsystem is interpreted by Colgan *et al.* (2003) as representing: (i) subglacial sediment transport and extensive subglacial erosion and deformation in the drumlin zone; (ii) extensive accumulation of debris on the ice surface in a narrow marginal zone (2 to 20 km wide); (iii) ice motion dominated by a combination of sliding and subglacial deformation; and (iv) an initial advance over a frozen subglacial bed followed by progressively retreating ice during deglaciation. This suggests that the presence of deformable sediment may well also overlap with the palaeo-ice stream criteria (Stokes and Clark, 1999).

It is interesting that some areas at the southern margin of the Laurentide Ice Sheet, which bear a resemblance to that of the Colgan *et al.* (2003) landsystem outlined here, have been interpreted as palaeo-ice streams. These include the Des Moines Lobe in Minnesota (Patterson, 1997; 1998) and the New York Drumlin Field (Hess and Briner, 2009). This perhaps best highlights the potential overlap between different landsystems and the care that needs to be taken when interpreting any mapped evidence of glaciated terrain.

3.3.6 Evidence from Patagonia

Palaeo-ice streams have been identified in the geomorphological record of most major former ice sheets (Laurentide and Cordilleran, Fennoscandian, British), as well as at the

margins of both the Antarctic and Greenland contemporary ice sheets (Canals *et al.*, 2000; Stokes and Clark, 2001; Long and Roberts, 2003). An obvious omission from this list is the Patagonian ice sheet, which at its greatest areal extent reached ca. 550,000 km^2 (Kaplan *et al.*, 2009). As they are present in most other major former ice sheets, it seems plausible that ice streams were also active in the Patagonian Ice Sheet. This has been suggested by a number of studies (Glasser and Jansson, 2005; Clapperton, 1989; Benn and Clapperton, 2000a) and yet none have ever been explicitly identified. In addition, it is possible that ice streaming eastwards from the former Patagonian Ice Sheet following the GPG would have terminated in a terrestrial environment (see Figure 2.1). The lack of contemporary analogues of terrestrial ice streams highlights the importance of their identification within former ice sheets (Patterson, 1997; Stokes and Clark, 1999, 2001).

In Section 2.4.1 of this study, an area of streamlined features to the northeast of Seno Otway in southern Patagonia was highlighted. This zone covers an area of 25 x 30 km and coincides with what was thought to be a deformable bed (Clapperton, 1989). There appears to be an abrupt margin to the main streamlined zone (see Figure 2.7). Benn and Clapperton (2000a) also described the presence of unmodified thrust-moraines, located up-ice from the drumlinised area. Elongated bedforms, abrupt margins and the presence of deformable till are all featured in the Stokes and Clark (1999) criteria for palaeo-ice stream identification, and thrust moraines have been associated with areas of terrestrial ice streaming (Jennings, 2006). As previously discussed, many of these features are also present in other glacial landsystems. This area to the northeast of Seno Otway has been suggested to be indicative of a zone of ice streaming (Clapperton. 1989; Benn and Clapperton, 2000a), but a palaeo-ice stream has never been explicitly identified. Thus, it provides an ideal opportunity to investigate the potential presence of a terrestrial ice stream within the former Patagonian Ice Sheet.

3.4 Summary

Ice streams are fast-flowing corridors of ice which have a key role to play in ice sheet stability (Stokes and Clark, 1999, 2001; Bentley, 2003). The relative inaccessibility of contemporary ice stream beds means that locating palaeo-ice stream tracks is of great importance for improving understanding of the basal processes in operation (Stokes and Clark, 1999, 2001; Ó Cofaigh *et al.*, 2005). Stokes and Clark (1999) outlined eight geomorphological criteria for identifying palaeo-ice streams within former ice sheets. These criteria are summarised in Table 3.1, and the idealised landsystem records of

isochronous and time-transgressive palaeo-ice streams are displayed in Figures 3.6 and 3.7. These criteria and landsystem models were developed with the aim of improving the identification and interpretation of palaeo-ice streams (Stokes and Clark, 1999). Other landsystems, particularly for surging glaciers (Evans and Rea, 1999, 2003), share individual characteristics with the palaeo-ice stream landsystem and so need to be considered when interpreting an area that appears to be indicative of ice streaming. Such an area exists to the northeast of Seno Otway in southernmost Patagonia, although no palaeo-ice stream has ever been explicitly identified.

Chapter 4 - Remote Sensing and the Glacial Inversion Model

4.1 Introduction

The use of remote sensing to aid the mapping of former ice sheets is a technique that has been implemented in a range of studies (Boulton and Clark, 1990; Clark, 1994, 1997; Kleman *et al.*, 1997; Clark and Stokes, 2001; Jansson *et al*., 2002; Stokes, 2002; Stokes and Clark, 2002a, 2003, 2004; De Angelis and Kleman, 2005, 2007, 2008; Stokes *et al*. 2005, 2006, 2008, 2009; Hess and Briner, 2009). A number of authors have used remote sensing to infer the presence of palaeo-ice streams, particularly within the former Laurentide Ice Sheet (Stokes, 2002; Stokes and Clark, 2002a, 2003, 2004; De Angelis and Kleman, 2005, 2007, 2008, Stokes *et al*. 2005, 2006, 2008, 2009; Evans *et al*. 2008). Clark (1997) highlighted the value of remote sensing as a key tool in glacial geomorphology and palaeoglaciology. The main forms of remote sensing are aerial photographs and satellite imagery (Jansson *et al*., 2003; Hubbard and Glasser, 2005; Smith *et al.*, 2006). Increasingly, digital elevation models (DEMs) are being utilised because they also allow a landscape to be visualised (Smith *et al*., 2006). These are often used in conjunction with fieldwork to reconstruct parts of former ice sheets, as by Evans *et al*. (2008) in Alberta, Canada; Clapperton *et al*. (1995) and Bentley *et al*. (2005) in the Strait of Magellan, southern South America; and Bradwell *et al.* (2008) in northwest Scotland.

Satellite imagery has revolutionised the mapping of former ice sheets according to Stokes (2002) and has improved our knowledge of the dynamics of former ice sheets. Clark (1997) identified the key advantages of satellite remote sensing over intensive fieldwork and aerial photographs. Firstly, large-scale landforms are easier to detect on satellite imagery than through fieldwork or the use of aerial photographs (Clark, 1997). In addition, the large-area view allows the discovery of new landforms and patterns. An example of this is the identification of MSGL and distinctive cross-cutting landforms (Clark, 1994, 1997). Satellite imagery also allows a user to work at a wide range of scales and at a much greater speed of mapping than from fieldwork or aerial photographs (Clark, 1997). Finally, and perhaps most importantly, satellite imagery allows a single researcher to reconstruct large areas of a former ice sheet (1997). This will be discussed further in Section 4.2.2 in relation to relevant studies.

Once the glacial landforms of a former ice sheet have been mapped the next important step is to reconstruct the ice sheet scale dynamics. This is not the same as simply deciphering

which glacial processes produced which landforms, although this has a key role to play (Kleman *et al*., 2006). The process of reconstructing past ice sheet dynamics from glacial landforms and landsystems is carried out by using a glacial geomorphological inversion model (Kleman and Borgström, 1996; Kleman *et al*., 2006). This effectively involves the interpretation of ice sheet properties from glacial geomorphology (Kleman and Borgström, 1996; Kleman *et al*., 2006). This model will be discussed in detail in Section 4.3.

The reconstruction of a former ice sheet involves the identification and mapping of glacial landforms followed by an interpretation of the processes and relative chronology of landform formation (Kleman *et al*., 2006; Stokes *et al*., 2009).

4.2 The use of remote sensing to map former ice sheets

4.2.1 Aerial Photography

Aerial photographs provide the highest available spatial resolution of all forms of remote sensing (Clark, 1997; Hubbard and Glasser, 2005; Smith *et al*., 2006); this allows the fine resolution mapping of landforms (Jansson, 2005; Evans *et al*., 2008). An example of the implementation of aerial photographs for this purpose can be seen in the study of the southwest Laurentide Ice Sheet by Evans *et al.* (2008). The regional scale geomorphology was mapped using a DEM and 1:63,360-scale aerial photograph mosaics were used to assess the finer details of some landform assemblages (Evans *et al*., 2008). The detailed mapping of glacial landforms in the Strait of Magellan carried out by Bentley *et al.* (2005) preferentially used aerial photographs over satellite imagery, which was only solely used in areas with no available aerial photography coverage. On a larger scale, the glacial geomorphology of the entire Laurentide Ice Sheet was mapped from aerial photographs by Prest *et al.* (1968). Clark (1997) noted that the mapping of entire ice sheets using aerial photography is possible, given sufficient dedication and time. Aerial photographs are normally recorded in visible light, so that landforms appear as they would to the naked eye (Hubbard and Glasser, 2005). However, the solar elevation at the time of capture has an impact on the quality of information that can be gleaned from aerial photographs (Clark, 1997).

4.2.2 Satellite Imagery

For mapping glacial landforms of a large area, such as an entire ice sheet, satellite imagery is a highly valuable tool (Clark, 1997; Hubbard and Glasser, 2005; Smith *et al*., 2006).

Single satellite images typically cover areas of over 100 x 100 km, allowing widespread mapping of landforms by a single researcher (Clark, 1997). In addition to the large areal coverage, satellite images are relatively cheap in comparison to aerial photography and fieldwork and allow rapid mapping of landforms (Punkari, 1982; Clark, 1997). One of the more important aspects of using satellite imagery is that large-scale landforms and patterns can be detected that may otherwise have been missed by fieldwork and aerial photography alone (Clark, 1994, 1997; Stokes, 2002). The best example of this can be seen in the pioneering work by Clark (1993, 1994), in which previously undetected large-scale streamlined lineations were identified from Landsat images of the former Laurentide Ice Sheet. These large subglacial bedforms, known as MSGL (Clark 1993, 1994), exceed the resolution of fieldwork and aerial photography (Clark, 1993; Stokes, 2002).

This helps to demonstrate the importance of satellite imagery to this study, as MSGL are a key characteristic of palaeo-ice streams (Stokes and Clark, 1999, 2001). Cross-cutting patterns on landforms are also easily identified on satellite imagery, allowing relative ages of flow to be determined (Clark, 1994, 1997). Other key advantages of satellite imagery include the wide range of scales it is possible to work at, the ease of identification of many landforms and the digitised nature of the images, which allows on-screen digitised mapping (Clark, 1997; Smith *et al*., 2006). Table 4.1 displays the main types of satellite imagery, with a summary of key characteristics and a selection of relevant studies that have used them.

Since 1972, the Landsat (see Table 4.1) series of satellites have provided complete coverage of previously glaciated terrain (Clark, 1997). The Multispectral Scanner (MSS) produced the most widely used data, before the introduction of the Thematic Mapper (TM) sensor on Landsats 4 and 5 (Clark, 1997). TM improved the resolution from 80 m to 30 m and used seven rather than four wavebands (Clark, 1997). Landsat 7 introduced the Enhanced Thematic Mapper Plus (ETM +) sensor which has a spatial resolution of 15 m in the panchromatic band eight (De Angelis and Kleman, 2007). The increased resolution of TM and ETM+ allows mapping in finer detail, including individual drumlins, eskers, outwash deltas, meltwater channels and moraines (Clark, 1997). Since March 2000, data has been collected from the ASTER sensor onboard the Terra satellite (Hirano *et al*., 2003). ASTER provides along-track stereo image data in the near-infrared wavelength region (Hirano *et al.*, 2003). Figure 4.1 shows examples of glacial lineations and lateral shear moraine as seen on Landsat TM and ETM+ and ASTER satellite imagery. The ERS-

1 satellite was launched in 1991 and uses microwaves to collect data about the Earth's surface (Clark, 1997). Known as Synthetic Aperture Radar (SAR), it provides imagery at a spatial resolution of 25 m (Clark, 1997). Clark (1997) suggested that SAR data requires a greater level of remote sensing expertise and resources than the available optical imagery (TM, ETM+ and MSS). SPOT (Satellite Pour l'Observation de la Terre) provides the best resolution (10 m) of any satellite imagery but has rarely been utilised for mapping glacial geomorphology, perhaps because of the greater cost per unit area compared with other forms of satellite imagery (Clark, 1997).

Table 4.1 - Detail on main types of satellite imagery used in geomorphological mapping. Adapted from Clark (1997, Table 1). ETM = Enhanced Thematic Mapper, TM = Thematic Mapper, MSS = Multispectral Scanner, ASTER = Advanced Spaceborne Thermal Emission and Reflection Radiometer, SAR = Synthetic Aperture Radar, SPOT = Satellite Pour l'Observation de la Terre.

Satellite	Sensor	Approximate Spatial Resolution (m)	Image Size (km)	Most detailed mapping scale	Relevant studies imagery is used in:
Landsat	ETM+	30 (15 for Band 8)	185 x 185	1:45,000 (1:20,000 for Band 8)	Clark *et al*., 2003; Stokes and Clark, 2003, 2004; De Angelis and Kleman, 2005, 2007, 2008; Glasser and Jansson, 2005; Glasser *et al*., 2005, 2008; Stokes *et al*., 2005, 2006, 2008, 2009; Storrar and Stokes, 2007
Landsat	TM	30	185 x 185	1:45,000	Boulton and Clark, 1990; Clark, 1993, 1994; Benn and Clapperton, 2000a; Clark and Stokes, 2001; Stokes, 2002; Bentley *et al*., 2005
Landsat	MSS	80	185 x 185	1:120,000	Sugden, 1978; Punkari, 1980, 1982; Boulton and Clark, 1990; Clark and Stokes, 2001; Stokes and Clark, 2002a, 2003; Jansson *et al*., 2003
Terra	ASTER	15	60 x 60	1:20,000	Glasser and Jansson, 2005; Glasser *et al*., 2005, 2008
ERS-1	SAR	25	100 x 100	1:40,000	Clark *et al*., 2000; Clark and Stokes, 2001
SPOT	XS	20	60 x 60	1:30,000	
SPOT	Pan	10	60 x 60	1:15,000	

The first example of the use of satellite remote sensing to map large areas of a former ice sheet was by Sugden (1978), who used 1:1,000,000 scale photomosaics of Landsat MSS images to map erosion by the former Laurentide Ice Sheet. Clark (1997) described this study as an innovative use of remote sensing to acquire evidence and to test an ice sheet model. The first use of satellite imagery to map glacial depositional features was carried out by Punkari (1980, 1982). This was achieved by mapping glacial landforms in Finland from photographic prints of Landsat MSS images and, from this work, the lobe dynamics of the Scandinavian Ice Sheet during ice retreat were reconstructed (Punkari, 1980). The large-area view provided by satellite imagery made it possible to view interlobate deposits alongside ice flow indicators (Punkari, 1980).

The use of Landsat satellite imagery to study the former Laurentide Ice Sheet allowed the identification of large-scale lineations and cross-cutting patterns, which had previously gone unrecognised (Boulton and Clark, 1990). Clark (1993, 1994) built on these initial observations, naming these features MSGL. It was tentatively concluded that MSGL could only be formed by rapid ice flow (Clark, 1994), a theory that is now generally accepted (Clark, 1999; Stokes and Clark, 1999, 2002a, Stokes, 2002; Evans *et al.*, 2008; King *et al.*, 2009). This demonstrates the great value of satellite imagery when determining the position of palaeo-ice streams (Stokes, 2002) because highly attenuated bedforms are one of the key criteria suggested by Stokes and Clark (1999) for the identification of former ice stream beds. The large-scale view that satellite imagery provides allows the identification of other key characteristics of palaeo-ice streams as suggested by Stokes and Clark (1999), such as abrupt lateral margins and lateral shear moraines (Stokes, 2002). This has resulted in satellite imagery (Landsat MSS, TM and ETM+; ASTER and ERS-1 SAR) being used in a number of studies, particularly of the former Laurentide Ice Sheet, in which palaeo-ice streams have been identified (Clark *et al.*, 2000, 2003; Clark and Stokes, 2001; Stokes and Clark, 2002a, 2003, 2004; Jansson *et al.*, 2003; De Angelis and Kleman, 2005, 2007, 2008; Stokes *et al.* 2005, 2006, 2008, 2009). This highlights the great importance of satellite imagery to this study.

Limitations associated with solely using satellite imagery to map glacial geomorphology have been noted, particularly in comparison to fieldwork and aerial photographs (Clark, 1997; Smith *et al.*, 2006). As alluded to previously, aerial photographs provide a higher level of detail than satellite images (Clark, 1997). The spatial resolution of satellite imagery ranges from 80 m (Landsat MSS) to 10 m (SPOT Pan), whereas aerial photographs typically have a spatial resolution of a few metres (Clark, 1997). This explains the preference some studies have given to aerial photographs over satellite imagery when analysing the finer details of particular landforms (Bentley *et al.*, 2005; Evans *et al.*, 2008). Smith *et al.* (2006) found that in a study of glacial landforms in south west Scotland that had been mapped in the field, no features could be identified from a Landsat TM image. It should be noted that aerial photographs also failed to identify any glacial landforms in this particular study (Smith *et al.*, 2006).

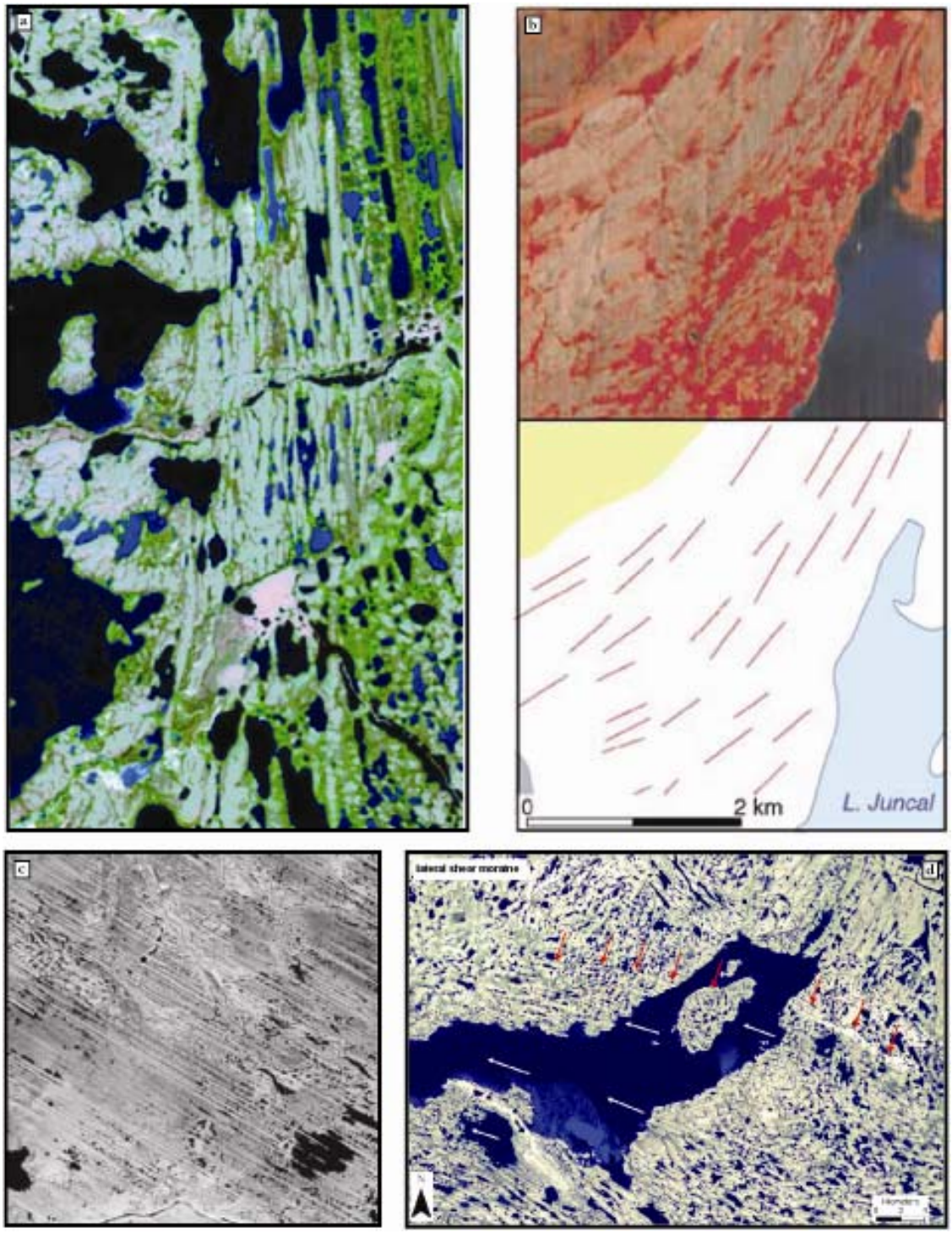

Figure 4.1 – Examples of glacial lineations as seen on: A – Landsat TM imagery (Stokes, 2002); B – ASTER imagery, with interpretation (Glasser *et al.* 2005); C – Landsat ETM+ imagery (Stokes and Clark, 2003). D shows lateral shear moraine on Landsat ETM+ imagery (Storrar and Stokes, 2007).

4.2.3 Digital Elevation Models

Digital elevation models (DEMs) are raster-based models of topography that record absolute elevation (Clark, 1997; Smith *et al.*, 2006). The main value of DEMs to mapping

glacial geomorphology is that they can be used to visualise landscapes and that they have a spatial resolution of 1 – 90 m (Smith *et al.*, 2006). They are derived from topographic maps, stereo aerial photography and satellite imagery (Clark, 1997; Hirano *et al.*, 2003; Smith *et al.*, 2006). DEMs have been produced from Shuttle Radar Topography Mission (SRTM) data and ASTER stereo images (Hirano *et al.*, 2003; Smith *et al.* 2006). Clark (1997) noted that DEMs are often superior to satellite imagery alone when mapping glacial geomorphology, but that they were not always available for formerly-glaciated areas. The near-global DEM produced from SRTM data suggests that this is no longer the case, although the resolution is not always appropriate (Hirano *et al.*, 2003; Smith *et al.* 2006).

A number of studies have implemented DEMs to aid the mapping of glacial geomorphology, particularly when identifying palaeo-ice streams of the former Laurentide Ice Sheet (Clark and Stokes, 2001; Stokes and Clark, 2003, 2004; Stokes *et al.*, 2006; De Angelis and Kleman, 2007, 2008; Evans *et al.*, 2008). Clark and Stokes (2001) used a 30 arcsec (ca. 0.5 km) DEM to visualise the topography and roughness of the M'Clintock Channel palaeo-ice stream, and Stokes *et al*. (2006) acquired a ca. 1 km resolution DEM in order to overlay mapped flow-sets on the regional topography for a palaeo-ice stream in the Amundsen Gulf, although the resolution was not high enough to allow for any detailed mapping.

Bradwell *et al.* (2008) used high-resolution digital surface models (DSM) to map large-scale lineations in northwest Scotland. Known as NEXTMap Britain, this DSM is most useful at scales of > 1:20,000 and can be used at a variety of resolutions (Bradwell *et al.*, 2008). NEXTMap DSMs and digital terrain models (DTM) have been used to record glacial landforms throughout northern England and Scotland, including to map landforms of the Tweed palaeo-ice stream (Everest *et al.*, 2005), to map areas of Rogen moraine in the vicinity of Loch Shin in northern Scotland (Finlayson and Bradwell, 2008) and to reconstruct the glacial history of Shetland (Golledge *et al.*, 2008). Hess and Briner (2009) also used digital elevation data to map 6,566 subglacial bedforms in the New York Drumlin Field, with the length, width and orientation of each bedform recorded in a geodatabase. DTMs are sometimes distinguished from DEMs by recognising that they include break lines and other topographic features, whereas DEMs do not (El-Sheimy *et al.*, 2005), although the terms are often used interchangeably (Pfeifer and Mandlburger, 2008). DSMs include surface features such as trees and buildings (Pfeifer and Mandlburger, 2008).

A combination of fieldwork, aerial photography, satellite imagery and DEMs would appear to provide the best means to reconstruct a former ice sheet at range of scales. Integrating these different forms of evidence could be achieved using a geographic information system (GIS; Clark, 1997). Satellite imagery is of great value for identifying and mapping palaeo-ice stream geomorphology (Stokes, 2002) and has often been used in conjunction with DEMs for this purpose (Clark and Stokes, 2001; Stokes and Clark, 2003, 2004; Stokes *et al.*, 2006; De Angelis and Kleman, 2007, 2008; Evans *et al.*, 2008).

4.3 The Glacial Geomorphological Inversion Model

Once a map of glacial geomorphology has been produced for an area of a former ice sheet, the next step is to reconstruct the glacial processes and relative chronology. The patchy and often incomplete nature of this evidence can complicate the interpretation of ice sheet properties (Kleman and Borgström, 1996). This process is known as glacial inversion, whereby glacial geomorphology and geology are used to reconstruct the properties of a former ice sheet (Kleman and Borgström, 1996; Kleman *et al.*, 2006; see Figure 4.2 for a schematic representation). This section will discuss early attempts at developing an inversion model, before outlining the glacial geomorphological inversion model presented by Kleman *et al.* (2006). It should be noted that all ice sheet reconstructions from geomorphological evidence will have used the inversion method to some degree (Stokes *et al*., 2009) and Kleman *et al*. (2006) have helped to formalise this procedure.

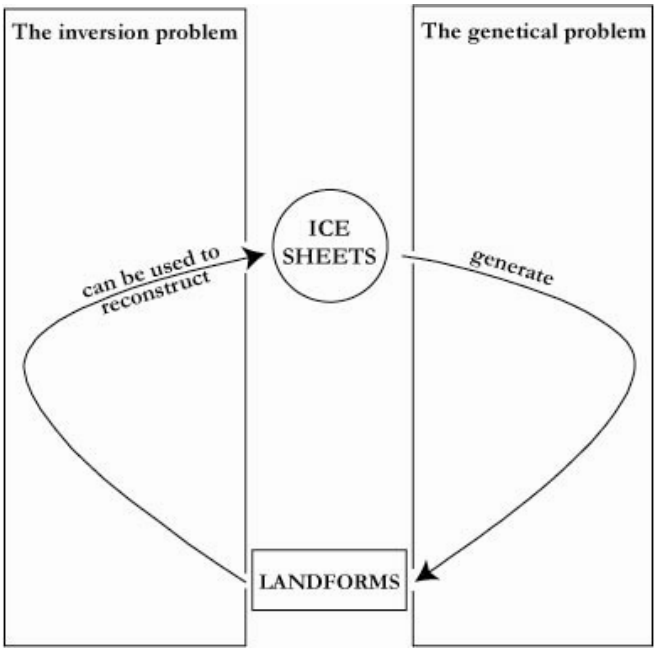

Figure 4.2 - The nature of the inversion problem. From Kleman and Borgström (1996).

The basic principle of glacial inversion involves the grouping of ice flow patterns into discrete landform assemblages based on their pattern and composition (Boulton and Clark, 1990; Kleman and Borgström, 1996; Kleman *et al.*, 1997; 2006; Clark, 1999; Stokes *et al.* 2009). One of the first examples of this was carried out by Boulton and Clark (1990) in their reconstruction of the Laurentide Ice Sheet. Glacial lineations were grouped into different *flow-sets*, which were then assigned relative ages through the examination of cross-cutting features (Boulton and Clark, 1990). From this, the evolution of the Laurentide Ice Sheet was reconstructed as a stack of events (Boulton and Clark, 1990). Kleman *et al.* (2006) noted that little attempt was made in this study to trace the deglaciation pattern and that meltwater features were not used in the reconstruction. In contrast, Kleman (1990) included meltwater landforms in what was principally an inversion model based on striation data for the Fennoscandian Ice Sheet.

Kleman *et al.* (1994) developed this in work in Quebec-Labrador, in which features were grouped into flow traces and meltwater traces. These landform *swarms*, or *fans*, were then sorted into a relative-age stack according to cross-cutting relationships, as in Boulton and Clark (1990). The three fan types identified by Kleman *et al*. (1994) were the *dry-bed deglaciation fan*, *wet-based deglaciation fan* and *"synchronous" fan*. This was a forerunner to the conceptual inversion model developed by Kleman and Borgström (1996), in which a *surge fan* was added. Kleman *et al.* (1997) implemented this inversion model to reconstruct the Fennoscandian Ice Sheet, essentially combining the approach of Boulton and Clark (1990) with a consideration for basal thermal zonation and the treatment of lineation and meltwater fans as separate entities (Kleman *et al.*, 2006). The need for refinement of their early iteration of an inversion model was noted by Kleman and Borgström (1996), but it did provide a suitable framework for a number of ice sheet reconstructions from geomorphology (Kleman *et al*., 1997; Jansson *et al*., 2002, 2003; De Angelis and Kleman, 2005).

The grouping of lineament patterns into flow-sets was discussed in detail by Clark (1997, 1999). This is of great importance because flow-sets represent the basic unit of ice sheet reconstruction (Clark, 1997; see Figure 4.3). A set of criteria for grouping landforms into flow-sets was put forward by Clark (1999) and Clark *et al.*, (2000), who suggested that they should have a similar orientation, be in close proximity and display similar morphometry. Once landforms have been assigned a flow-set according to these principles, the next step is to define whether they represent a time-transgressive or synchronous flow event (Clark, 1997, 1999). This is necessary to determine under what

portions of an ice sheet bedforms were formed and at what point during the glacial cycle (Clark, 1999). This technique was used by Clark and Stokes (2001) to reconstruct the extent and basal characteristics of the M'Clintock Channel palaeo-ice stream. Figure 4.4 shows the distribution of flow-sets on Victoria Island, Canada, as determined by Stokes *et al.* (2009) following the production of a glacial geomorphological map by Storrar and Stokes (2007).

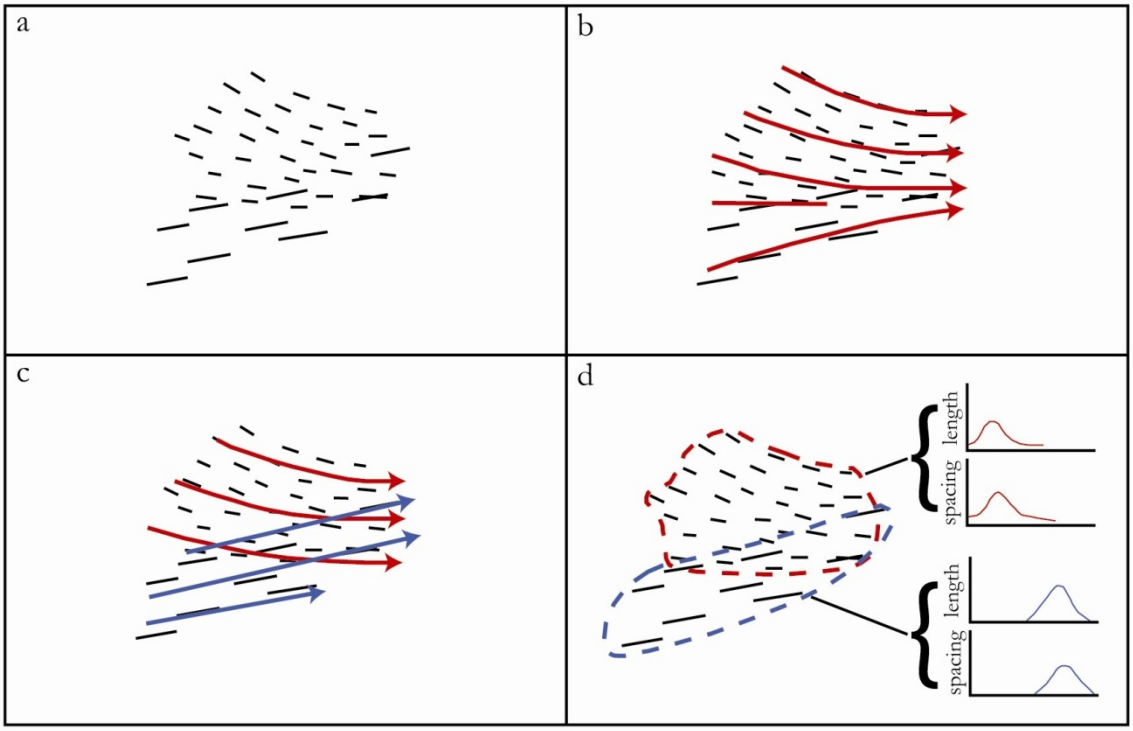

Figure 4.3 – The grouping of flow direction indicators into flow events. It is easy to make the mistake of grouping evidence into a single flow event when it may in fact represent information of different ages. (a) represents a hypothetical lineament pattern; (b) an interpretation that assumes all the flow evidence is of the same age; (c) an alternative that takes account of the cross-cutting lineaments and (d) shows how the spatial pattern and morphometry can assist in assigning different flow events. Adapted from Clark (1997).

The inversion model of Kleman *et al.* (2006) represents a revised form of the Kleman and Borgström (1996) model. The theoretical framework of the model is that landform creation, destruction and preservation is controlled by the thermal state of the bed (De Angelis and Kleman, 2005; Kleman *et al.*, 2006). The key component of the model is the grouping of landforms into coherent groups, as in Boulton and Clark (1990) and Clark (1997, 1999). These landform groups were termed *flow-sets* by Clark (1997, 1999) and are named *swarms* for the purposes of the Kleman *et al.* (2006) model. Kleman *et al.* (2006) noted that coherent swarms should also fit a glaciologically-plausible pattern. The four swarm or flow-set types recognised in the Kleman *et al.* (2006) inversion model are as follows: (i) *Warm-based deglaciation*: defined by ice flow indicators aligned with eskers

suggesting formation close to or during deglaciation; (ii) *Cold-based deglaciation*: a relict glacial or non-glacial surface superimposed by a pattern of meltwater features, presumably preserved by cold-based ice (marginal meltwater channels are dominant and eskers are small or lacking); (iii) *Event*: defined by landform systems with abundant ice flow indicators but without aligned eskers or moraines, thought to be generated prior to deglaciation; and (iv) *Ice stream*: defined by MSGL, convergent flow patterns, abrupt lateral margins and other criteria for palaeo-ice streams (see Stokes and Clark, 1999). Ice stream flow-sets can be subdivided as deglacial or event (Stokes *et al.* 2009). The use of these flow-set types can be seen in Figure 4.4. Whether flow-sets were formed isochronously or time-transgressively must also be determined (Clark, 1997, 1999; Kleman *et al.*, 2006).

Once landforms have been ordered into flow-sets the relative chronologies can be established by using cross-cutting relationships (Kleman *et al.*, 2006). Flow-sets are then sorted into relative-age stacks, to allow the reconstruction of a glaciologically-plausible pattern and chronology of ice sheet evolution (Kleman *et al.*, 2006). An example of this can be seen in Table 2 in Stokes *et al.* (2009), where flow-sets on Victoria Island were assigned relative age brackets based on cross-cutting landform relationships and available radiocarbon dates.

It should perhaps be noted that the Kleman *et al.* (2006) glacial inversion model provides a useful framework for reconstructing the dynamics of former ice sheets from geomorphological evidence, principally by combining the long-standing use of flow-sets (Boulton and Clark, 1990; Clark, 1997, 1999) with the development of previous techniques and models (Kleman, 1990; Kleman *et al.*, 1994; Kleman and Borgström, 1996). This systematic approach, which is based on current glaciological understanding of landform creation (Kleman *et al.* 2006), has been utilised in a number of ice sheet reconstructions, particularly to identify palaeo-ice streams (De Angelis and Kleman, 2007, 2008; Stokes *et al*., 2009). This highlights the value of some form of glacial geomorphological inversion to palaeo-ice stream identification in former ice sheets. Kleman *et al.* (2006) suggested that the full potential of glacial geomorphological inversion can only be realised when geomorphologists (three-dimensional space), dating experts (time) and ice-sheet modellers (glaciological processes) collaborate together.

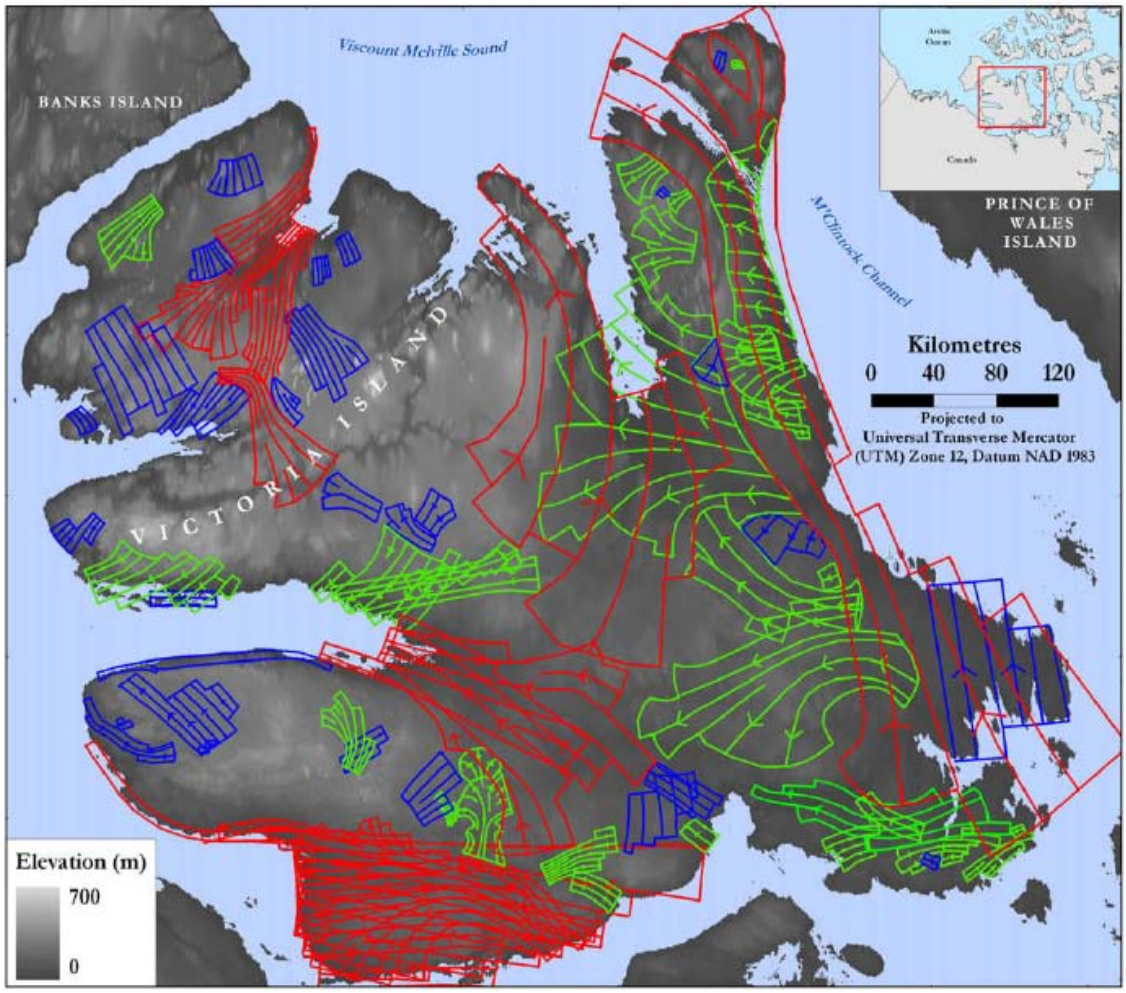

Figure 4.4 - The distribution of flow-sets on Victoria Island, Canada from Stokes *et al.* (2009). Following the Kleman *et al.* (2006) inversion model, the flow-sets are classified as 'ice stream' (red), 'event' (blue) or 'deglacial' (green).

4.4 Summary

Remote sensing is a very useful tool to aid the reconstruction of former ice sheets (Clark, 1997; Smith *et al.*, 2006). In particular, satellite imagery has been utilised in a number of studies for this purpose (Boulton and Clark, 1990; Clark, 1994, 1997; Clark and Stokes, 2001; Jansson *et al.*, 2002; Stokes, 2002; Stokes and Clark, 2002a, 2003, 2004; De Angelis and Kleman, 2005, 2007, 2008; Stokes *et al.*, 2005, 2006, 2008, 2009). The main advantages of satellite imagery are the large areas that can be covered by a single researcher, the rapid mapping that is possible in comparison to fieldwork and aerial photographs and the identification of large-scale landforms (e.g. MSGL) and cross-cutting features that would otherwise remain undetected (Clark, 1997). Several different types of satellite imagery have been used to map former ice sheets, including Landsat TM and ETM+ and ASTER (see Table 4.1 for details on the main types of satellite imagery). Satellite imagery has been used to identify the characteristic landform assemblage of

palaeo-ice streams, according to the criteria of Stokes and Clark (1999). DEMs are also of great value when reconstructing former ice sheets as they allow the topography to be visualised (Smith *et al.*, 2006).

Following the production of a glacial geomorphological map from remote sensing the glacial geomorphological inversion method can be used to reconstruct the dynamics of a former ice sheet (Kleman *et al.*, 2006; Stokes *et al.*, 2009). This involves grouping ice flow patterns into discrete landform assemblages and then assigning a relative chronology to each group or *flow-set* based on cross-cutting relationships (Boulton and Clark, 1990; Kleman and Borgström, 1996; Clark, 1999; Kleman *et al.*, 2006; Stokes *et al.*, 2009). Kleman *et al.* (2006) have helped to formalise this procedure, which has been implemented in a number of studies (De Angelis and Kleman, 2007, 2008; Stokes *et al.*, 2009). The successful reconstruction of former ice sheets combines accurate landform mapping from remote sensing with the interpretation of glacial processes and the relative chronology of landform formation (Kleman *et al.*, 2006; Stokes *et al.*, 2009).

Chapter 5 - Methods

5.1 Introduction

The methods used in this study to produce the glacial geomorphological map, and the subsequent reconstruction of glacial dynamics from this evidence, are based on a combined remote sensing and glacial inversion methodology (Clark, 1997, 1999; Kleman *et al.*, 1997, 2006). The value of this approach and its suitability for this purpose has been discussed in detail in Chapter 4. This chapter will outline the remotely sensed data sources used and the techniques and software implemented during mapping. The initial mapping of landforms was based on their morphological characteristics, followed by subsequent interpretation. Hubbard and Glasser (2005) highlighted the importance of ensuring that interpretation does not guide the mapping process, in order that the researcher remains as objective and unbiased as possible. However, a pre-existing knowledge of landform type and morphology, coupled with a familiarity with previous mapping of the study area, will inevitably guide some aspects of the mapping process.

Following the production of the map a regional-scale reconstruction of flow-sets was conducted, following the criteria of Clark (1999). These in turn allowed for the reconstruction of the glacial dynamics and chronology of the area, by closely following the glacial inversion model of Kleman *et al.* (2006). The geomorphological evidence recorded in the map also allowed for the deciphering of the glacial landsystem (cf. Evans *et al.*, 2003), particularly in the area northeast of Seno Otway. This highlights the suitability of this combination of methods for achieving the aim and objectives outlined in Section 1.1.

5.2 Imagery used during mapping

5.2.1 Satellite imagery

The regional-scale geomorphology of the study area, which covers over 16,000 km^2, was assessed and mapped from a variety of remotely sensed data. At the broadest scale four Landsat scenes were mosaiced together to provide complete coverage of the study area (see Figure 5.1). Each of these scenes covers an area of 185 x 185 km and the imagery has a spatial resolution of approximately 30 m (see Table 4.1). Three out of the four scenes were Enhanced Thematic Mapper Plus (ETM+) and the fourth scene was Thematic Mapper (TM; see Table 5.1). The digitised Landsat images were all downloaded from the Global Land Cover Facility (GLFC) website (http://glcf.umd.edu). Five ASTER scenes were

downloaded from the NASA Land Processes Distributed Active Archive Center website (https://LPDAAC.usgs.gov). ASTER scenes cover an area of 60 x 60 km and have a higher spatial resolution of approximately 15 m (see Table 4.1). All satellite imagery was imported into ERDAS Imagine 9.3 and the scenes and all subsequent mapping have been projected to the Universal Transverse Mercator (UTM), Zone 19, Datum WGS 84. It was necessary to geo-rectify three of the five ASTER images using the image geometric correction tool within ERDAS. In addition to the Landsat and ASTER imagery, QuickBird imagery from 2005 available on Google Earth© was used as a reference to guide mapping of a small section on the southern edge of Seno Skyring.

Table 5.1 – Details of the four Landsat scenes used, including sensor type, path and row, and acquisition date.

Sensor Type	Path	Row	Acquisition Date
ETM+	228	096	27/02/2001
ETM+	228	097	10/02/1986
ETM+	229	096	05/02/2002
TM	229	097	16/1/1986

5.2.2 Aerial photographs

Hard copies of 39 stereo-aerial photographs covering some of the southern section of the study area around Seno Otway were also available. The approximate flight lines are shown in Figure 5.1 and Table 5.2 contains a full list of photograph numbers. All photographs were black and white and had an approximate scale of 1:60,000. Along with oblique aerial photographs from a flight over the area, these were used to check the mapping of individual lineation features within the study area and to make detailed comparisons between different areas of lineations and their relationship to each other (e.g. any superimposition and cross-cutting relationships). The stereo-aerial photographs were captured by the Servicio Aerofotogrametrico de la Fuerza Aerea de Chile (SAF; Chilean Air Force Aerial Photogrammetric Service). 33 of the 39 photographs were taken in 1983, the remaining six were taken in 1985.

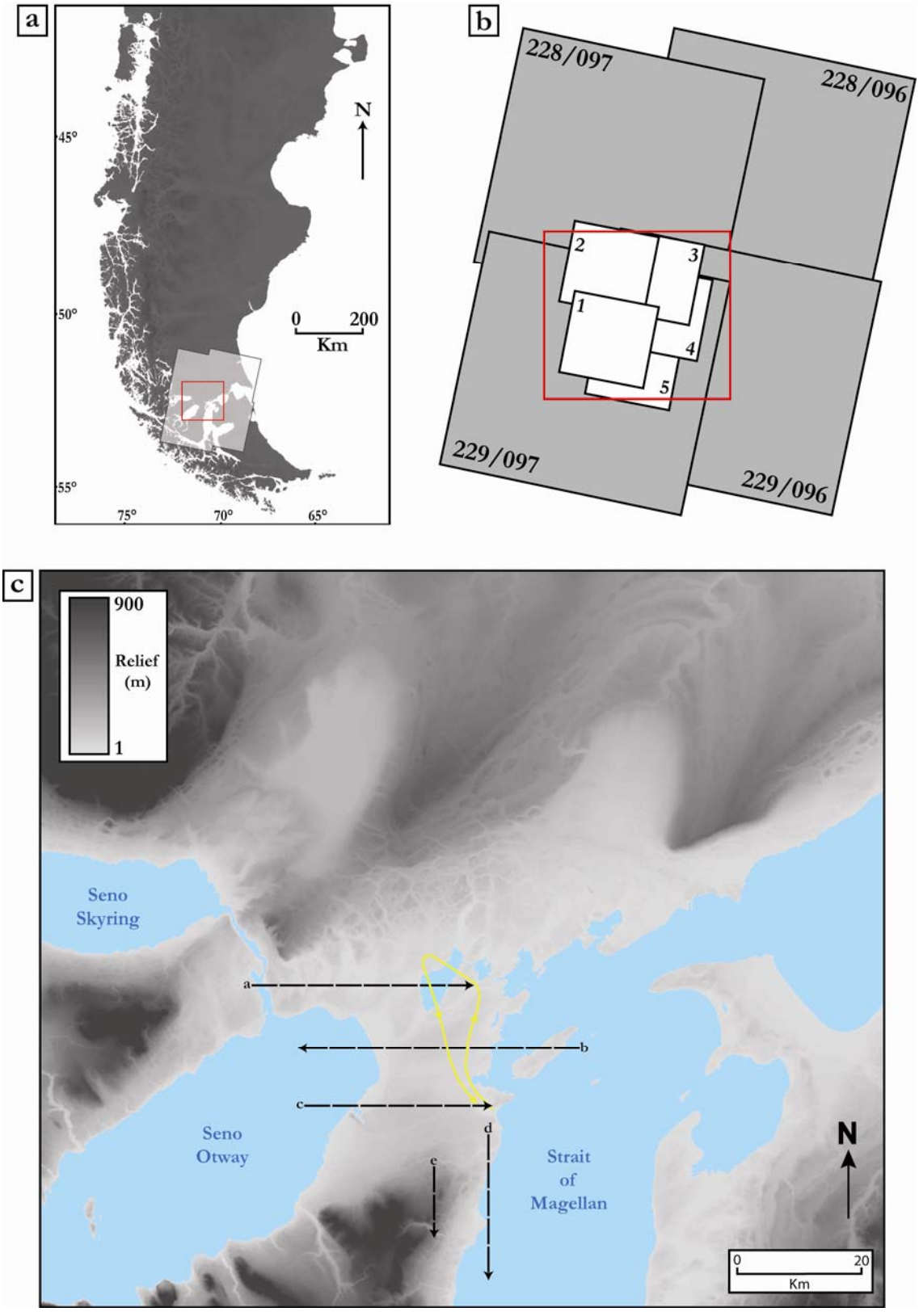

Figure 5.1 – Location of Landsat and ASTER satellite imagery scenes used in this study (a and b) and approximate flight lines for stereo-aerial (dashed black) and oblique (yellow) photographs (c). Red rectangle shows the location of the study area.

Table 5.2 - Aerial photograph numbers and their associated approximate flight lines (see Figure 5.1).

Approximate Flight Lines	Aerial Photograph Numbers
A	021738, 021739, 021740, 021741, 021742, 021743, 021744
B	021764, 021765, 021766, 021767, 021768, 021769, 021770, 021771, 021772, 021773, 021091, 021092
C	021774, 021775, 021776, 021777, 021778, 021090, 021800, 021801, 021802
D	026205, 026206, 026207, 026208, 026209, 026210
E	021799, 021808, 021809, 021810, 021811

5.2.3 Shuttle Radar Topography Mission

In addition to optical imagery, 3 arcsec Shuttle Radar Topography Mission (SRTM) data were acquired, from which a DEM could be built, to visualise topography and to provide a context to the mapping. The greyscale represents changes in topography, which ranges from sea level up to a high of approximately 900 m in the study area. The reason for inverting the greyscale, where lighter shades represent lower topography, is so that mapped features are easier to identify. This is particularly important in the main areas of streamlining. The DEM provided useful altitude data across the study area, as well as allowing the visualisation of topography. The Filled Finished-B SRTM topographic data (path 229, row 097) were downloaded from the GLFC website and were cropped to the size of the study area within ESRI ArcMap 9.3.

5.3 Mapping techniques

Mapping was conducted by on-screen digitisation of features within ERDAS Imagine 9.3. Features were mapped as either polygons or lines. Various band combinations of the Landsat images were used to detect landforms: a Red-Green-Blue rendition using bands 4, 3, 2 and 7, 5, 2 were found to be the most useful. For the ASTER scenes, band combinations of 1, 2, 3 and 3, 2, 1 were mainly used. The different features were digitised on separate vector layers after visual interpretation (e.g. Clark, 1997) and stored as shapefiles (.shp). Landforms were identified and mapped at a variety of different scales to avoid any scale-bias in their detection. The previous mapping work in the area by Clapperton (1989), Benn and Clapperton (2000a) and Glasser and Jansson (2008) provided a very useful cross-reference and check of our mapping in areas common to both.

All image processing and mapping was carried out using ERDAS Imagine 9.3. The final geomorphological map was produced using ESRI ArcMap version 9.3 and Adobe Illustrator CS4.

5.4 Glacial landforms

A variety of glacial geomorphology has been described in the Strait of Magellan region by previous studies, including Clapperton (1989); Clapperton *et al.* (1995); Benn and Clapperton (2000a); Bentley *et al.* (2005) and Glasser and Jansson (2008). This section briefly defines the key landforms that have been identified and mapped in this study.

5.4.1 Glacial lineations

Streamlined drumlin features, or glacial lineations, are "round, oval or elongated hills" (Embleton and King, 1975) with long axes orientated parallel to ice-flow direction (Benn and Evans, 1998). Clapperton (1989) described in detail four main areas of drumlinised drift in the Strait of Magellan region, the most distinct of which is located near Laguna Cabeza del Mar. The mapping of drumlins and glacial lineations helps to determine former ice-flow directions in an area (Benn and Evans, 1998). In addition, the plan form of the landforms has traditionally been seen as an important parameter for constraining drumlin formation theories (Spagnolo *et al.*, 2010), which are thought to be linked to ice velocity (Stokes and Clark, 2002a). This shows the importance of the accurate mapping of glacial lineations to this project, which aims to test the hypothesis of ice streaming on the western side of the Strait of Magellan.

5.4.2 Moraine ridges

The margins of former glacier and ice sheets are demarcated by a variety of depositional evidence, including composite moraine ridges (Benn and Evans, 1998). These can be identified as arcuate suites of sub-parallel ridges which conform to the shape of the ice margin that produced them (Benn and Evans, 1998). Prominent moraine belts have been identified on both sides of the Strait of Magellan (Clapperton *et al.*, 1995; Benn and Clapperton, 2000a; Bentley *et al.*, 2005; Glasser and Jansson, 2008) and these have been mapped in order to constrain ice limits in the study area.

5.4.3 Meltwater channels

Erosion by meltwater flow close to glacier and ice-sheet margins produces distinct channels, the distribution and characteristics of which can be used to reconstruct patterns

of glacial retreat (Greenwood *et al.*, 2007). A number of different meltwater channel types are recognised: lateral channels, which flow along the ice margin; proglacial channels, which drain in front of the ice margin; subglacial channels and supraglacial/englacial channels (see Table 5.3; Greenwood *et al.*, 2007).

Table 5.3 – Diagnostic criteria for classification of meltwater channels. From Greenwood *et al.* (2007).

Subglacial	Lateral		Proglacial	Supraglacial/englacial
	Marginal	Submarginal		
• Undulating long profile[1,2]	• Parallel with contemporary contours[4,7]		• Regular meander bends[10]	• Meander forms crescentic valley on face of hill[1]
• Descent downslope may be oblique[1,3]	• Forms 'series' of channels parallel to each other[1,8,9]		• Occasional bifurcation[10]	• Low gradient[7]
• Descent downslope may form steep chutes[1]	• Approximately straight[4]		• Flows direct downslope[7]	• Sinuous[7]
• Complex systems—bifurcating and anastomosing[3,4]	• Perched on valley sides[10]		• *Large dimensions — wide and deep*[10]	• *Approximately constant width*[7]
• High sinuosity[4]	• May terminate in downslope chutes[1,8]		• *Crater chains*[10]	
• *Abandoned loops*[4]	• Absence of networks[4]	• May form networks[1]		
• *Abrupt beginning and end*[1,2]	• Gentle gradient[1]	• Steeper gradient (oblique downslope)[1]		
• *Absence of alluvial fans*[1]	• Parallel for long distance[1]	• Sudden change in direction[1]		
• *Cavity systems and potholes*[3]	• *May terminate abruptly*[10]			
• *Ungraded confluences*[3]	• *May be found in isolation from all other glacial features*[6,9]			
• *Variety of size and form within the same connected system*[5]				
• *Association with eskers*[6]				

Sources: [1]Sissons (1961); [2]Glasser and Sambrook Smith (1999); [3]Sugden *et al.* (1991); [4]Clapperton (1968); [5]Sissons (1960); [6]Kleman and Borgström (1996); [7]Price (1960); [8]Schytt (1956); [9]Dyke (1993); [10]Benn and Evans (1998).

5.4.4 Eskers

Eskers are sinuous ridges of glaciofluvial sediment (Warren and Ashley, 1994; Hambrey, 1994) which are generally aligned sub-parallel to the direction of former ice flow (Benn and Evans, 1998). They are part of a spatially coherent but metachronous system of meltwater features created during regional deglaciation (Kleman *et al.*, 1997). Clapperton (1989) identified two large esker systems within the area of drumlinised drift near Laguna Cabeza del Mar.

5.4.5 Outwash plains

One of the more distinctive features of terrestrial proglacial environments is the zone of outwash accumulation (Maizals, 2002). Where outwash is unconfined and extends laterally for a considerable distance it is known as an outwash plain or sandur (Hambrey, 1994; Maizals, 2002). Outwash plains can be up to several kilometres wide and are generally gently sloping featureless surfaces (Benn and Evans, 1998) characterised by braided meltwater channels across their extent (Hambrey, 1994).

5.4.6 Former lake shorelines

Ice-dammed and proglacial lakes are subject to wide fluctuations and can therefore produce a series of former shorelines at different levels (Hambrey, 1994). Some of the shorelines associated with late-Pleistocene lakes have survived and can be identified in the geomorphological record (Hambrey, 1994; Stokes and Clark, 2004).

5.5 Glacial inversion method

Following the completion of the glacial geomorphological map by the methods outlined above, the next task is to interpret the landforms and landform signature in order to reconstruct the glacial dynamics and chronology of the area. The glacial inversion method describes the process by which the geomorphological record is inverted to reconstruct ice sheet dynamics (Kleman *et al.*, 1997, 2006; see Section 4.3). The first step is to group landforms into a series of flow-sets in order to reconstruct regional-scale ice flow directions. Adhering to the Clark (1999) criteria for flow-set reconstruction, a number of flow-sets have been identified in the Skyring-Otway-Magellan region. The criteria for grouping lineations into flow-sets are: parallel concordance (similar orientation), close proximity to neighbouring lineations and similar morphometry (Clark, 1999). Once patterns were recognised, flow-sets were mapped by drawing flowlines parallel to the orientation of lineations, and perceived diverging/converging patterns within individual flow-sets have been incorporated.

A conservative approach has been taken to the grouping of similarly-orientated lineations separated by large distances into one flow-set. As well as providing regional-scale ice flow directions, flow-sets have also been classified according to the Kleman *et al*. (2006) guidelines (see Section 4.3, this study). The isochronous/time-transgressive nature of each individual flow-set has been determined and an attempt has been made to order them chronologically (Kleman *et al.*, 2006). This is in order to provide a glaciologically-plausible reconstruction of ice-sheet history in this area. The reconstruction of ice-margin positions at various stages is based primarily on the geomorphological evidence, particularly moraine ridges and meltwater channels. Where evidence is lacking for ice-marginal positions they have been interpolated in a glaciologically-plausible manner.

5.6 Length, width and elongation ratio

The mapping of lineations as polygons in this study allows the plan form of individual features to be shown. The area and perimeter of each polygon is automatically calculated within ERDAS and can be compiled into an attribute table. From this the lengths, widths and elongation ratios (length/width) of each feature can be approximated. This has been done following the methods used by Clark *et al.* (2009) in their study of drumlin size and characteristics within Britain and Ireland. The plan form of drumlins and lineations can be reasonably approximated by an ellipse, and using the area and perimeter it is possible to mathematically-derive an estimate for length and width, and therefore the elongation ratio (Clark *et al.*, 2009). The formulae used by Clark *et al.* (2009) and in this study are

$$L = \frac{1}{\pi}\sqrt{P^2 + \sqrt{P^4 - 16\pi^2 A^2}}$$

$$W = \frac{1}{\pi}\sqrt{P^2 - \sqrt{P^4 - 16\pi^2 A^2}}$$

where L = length, W = width, P = perimeter and A = area. From this it is fairly simple to calculate the elongation ratio (E) by dividing the length (L) by the width (W).

Lengths calculated with the approximation and manually-measured lengths for 20 lineations across the elongation range produced a high correlation (r^2 = 0.999), although for lineations with the highest elongation ratios the approximation was found to underestimate the length by up to 9 %. Clark *et al.* (2009) experimented with a number of other approximations in case feature plan forms were not accurately captured by an ellipse. They found that for highly elongated lineations (ca. E > 15) an approximation based on a rectangle was more accurate. However, for greater consistency during analysis, Clark *et al.* (2009) used the ellipse approximation throughout. For the same reasoning only the ellipse approximation is used in this study.

5.7 Landsystems classification

A large part of the reconstruction of the ice-sheet history in this study involves the classification of the landsystem (cf. Evans *et al.*, 2003) as evidenced by the geomorphological record, as this can then be related to specific ice dynamics. The key criteria which characterise different landsystems have been discussed in detail in Section

3.3.4 of this study, particularly for an ice stream landsystem (Stokes and Clark, 1999; Clark and Stokes, 2003), a surging glacier landsystem (Evans and Rea, 1999, 2003) and an ice-marginal terrestrial landsystem (Colgan *et al.*, 2003). A number of criteria are shared by these three landsystems. In order to classify the landsystem that dominates this study area the mapped record has been critically compared to the characteristics of these different landsystems.

5.8 Summary

The methods used in this study to map and assess the glacial geomorphological record of the Skyring-Otway-Magellan region are well-established. The principal data sources used are the remotely-sensed Landsat and ASTER satellite imagery. Aerial photographs have also been used in some areas to aid mapping accuracy. All mapping was carried out digitally using ERDAS Imagine 9.3. The implementation of these methods has resulted in the creation of a regional glacial geomorphology map of the study area, whilst maintaining the accurate mapping of individual landforms. The geomorphological evidence recorded in the map has then been assessed following a glacial inversion method. This involved the grouping of lineation patterns into coherent flow-sets based on orientation and landform characteristics. These flow-sets have then been assigned a typology in accordance with the Kleman *et al.* (2006) model and an attempt has been made to order them chronologically. A landsystems approach (cf. Evans *at al.*, 2003) has also been undertaken in order to decipher the mapped geomorphological record. This combination of methods enables a detailed palaeoglaciological reconstruction of the ice sheet dynamics of this region from the geomorphological evidence.

Chapter 6 - Results

A variety of glacial geomorphology is present in the study area, which covers over 16,000 km^2. This chapter will outline the main landforms that have been mapped and will describe their morphology, distribution, orientation and relationship to other features. Seven main landform types have been identified; glacial lineations, moraines, meltwater channels, irregular dissected ridges, eskers, outwash plains and former lake shorelines. The full glacial geomorphological map (Figure 6.1; Lovell *et al.*, submitted) is included on a CD inside the back cover. Detailed insets from this map are presented in this section, along with examples of the different landforms on satellite imagery and oblique aerial photographs. The location of these figures is shown in Figure 6.2. Chapter 7 describes the interpretation of the different features and landform assemblages.

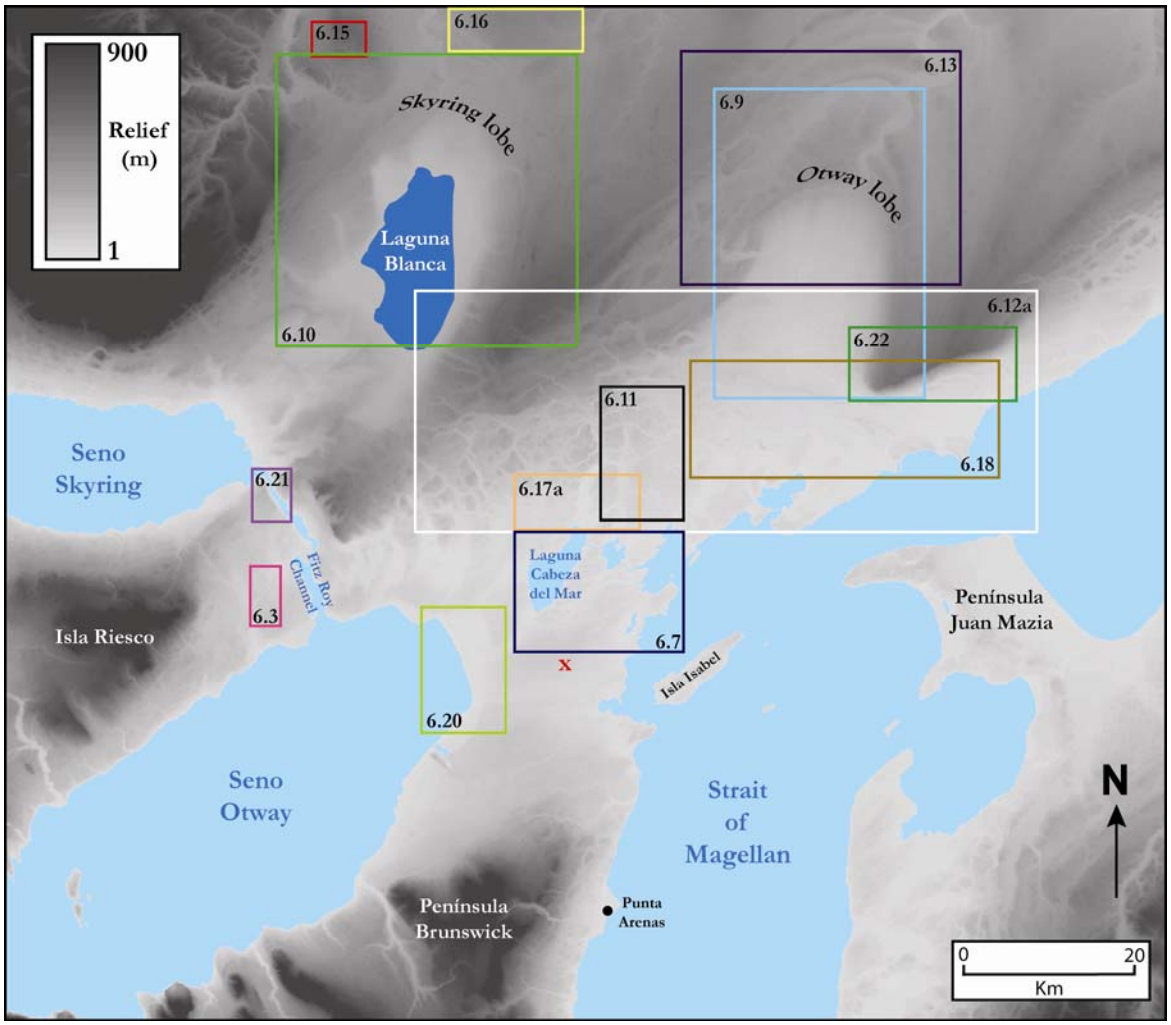

Figure 6.2 - SRTM showing extent of mapped area and location of figures in Chapter 6. Red X indicates approximate position from which the oblique aerial photographs in Figures 6.4, 6.6 and 6.8 were taken, looking northwards.

6.1 Glacial lineations

The most distinct landforms within the mapped area are streamlined drumlin features, or glacial lineations, and examples of these are shown in Figures 6.3 and 6.4. They occur over large parts of the study area. The main zone of these is located south east of Laguna Cabeza del Mar (Figure 6.4) and they splay out from this main trunk towards the moraine systems in the north (see Section 6.2). Lineations are also present on Península Brunswick, Isla Riesco (Figure 6.3), Isla Isabel and the eastern side of the Strait of Magellan. In total 1,349 lineations have been mapped across the entire study area. The length of individual lineations ranges from 0.1 km to 3 km and many are highly elongated (length to width ratios > 10:1). Figure 6.5 shows the varying morphology of these features, from the 'classic' drumlin form (cf. Clark et al., 2009; Spagnolo et al., in press), through to highly elongate glacial lineations (Clark, 1994). Where the outline of the glacial lineations are clearly visible they have been mapped as polygons, otherwise they have been mapped as line features (Figure 6.3); in total 1,064 have been mapped as polygons and 285 as lines.

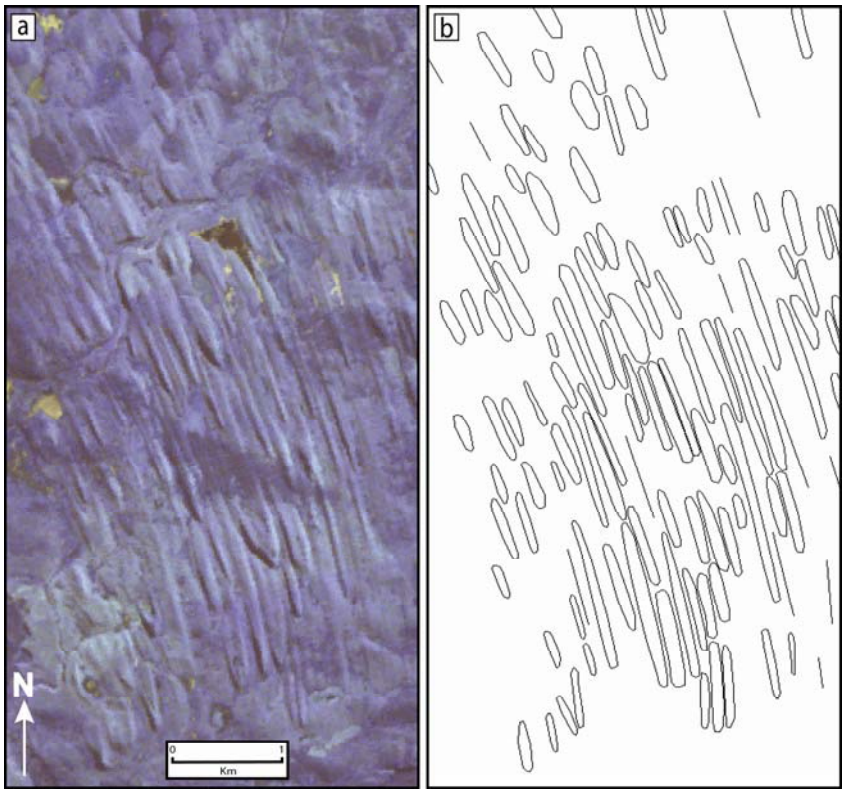

Figure 6.3 – Lineations on Isla Riesco, (a) viewed on ASTER satellite imagery (band combination 1, 2, 3) and (b) as they have been mapped as both polygons and lines. Location shown on Figure 6.2.

Figure 6.4 - Oblique aerial photograph, looking northwards, of glacial lineations to the east of Laguna Cabeza del Mar (just out of shot to the left of the photograph). Reproduced with the kind permission of Hauke Steinberg (www.haukesteinberg.com).

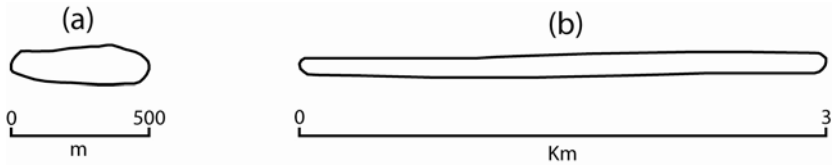

Figure 6.5 – Example of the range of glacial lineations mapped across the study area. (a) shows an example similar to 'classic' drumlin morphology (e.g. Clark *et al.*, 2009; Spagnolo *et al.*, in press); (b) shows a longer and more elongated example (e.g. Clark, 1994). The two examples are shown at different scales and are located near Laguna Cabeza del Mar.

Lineations are densely spaced in the main zone to the east of Laguna Cabeza del Mar, shown in Figures 6.4, 6.6 and 6.7, where some are less than 20 m apart. This is the same group that was described in great detail by Clapperton (1989) and appears in the mapping of Clapperton *et al.* (1995), Benn and Clapperton (2000a) and Glasser and Jansson (2008). There is a distinct north east orientation of the features in this area, with little evidence of either cross-cutting or convergence/divergence of feature direction. The longest lineation in this zone has a length of 2.9 km, which is the largest in the study area. The highest elongation ratio (length to width) of 35:1 is also present in this group. Over 10 other lineations in this area have lengths greater than 2 km and many more have elongation ratios over 10:1. Distinct sharp crest lines can be identified on the oblique aerial photographs of the lineations (Figures 6.4, 6.6 and 6.8), but were less obvious on both stereo-aerial photographs and satellite imagery. Many of the lineations in this area have clear asymmetric cross profiles (see Figure 6.4), with steeper south-east facing sides (Clapperton, 1989). Individual feature morphologies in this area range between the two examples shown in Figure 6.5, with the majority more similar to type (b). This is particularly noticeable in the central zone, approximately 6 km east of Laguna Cabeza del Mar. Meltwater channels and lakes occur in the spaces between lineations (Figures 6.4, 6.6, 6.7 and 6.8). These meltwater channels, some of which are still occupied by water, are orientated sub-parallel to lineation direction. This zone of lineations is located on an area of lower ground (< 30 m altitude).

Immediately to the west of Laguna Cabeza del Mar, lineations are orientated in the same direction as those to the east. In general, these are not as densely grouped or as long (mostly less than 1.5 km in length). To the north east of this main zone, lineation direction begins to diverge. Lineations are more dispersed, shorter, and exist on lower ground (< 50 m altitude). The diverging effect is created as lineations to the west and centre of this area begin to be orientated northwards, whilst those furthest east continue in a north easterly direction. A group of 21 lineations are located on Isla Isabel in the Strait of Magellan, these are orientated in a similar direction as lineations along the eastern shore of the strait.

There is a noticeable lack of lineations in the area to the north of Laguna Cabeza del Mar dominated by an extensive outwash plain running perpendicular to lineation direction (see Section 6.6).

Figure 6.6 - Oblique aerial photograph, looking north, of glacial lineations east of Laguna Cabeza del Mar (seen to the left). See Figure 6.2 for approximate position photograph was taken from. Photograph by M. J. Bentley.

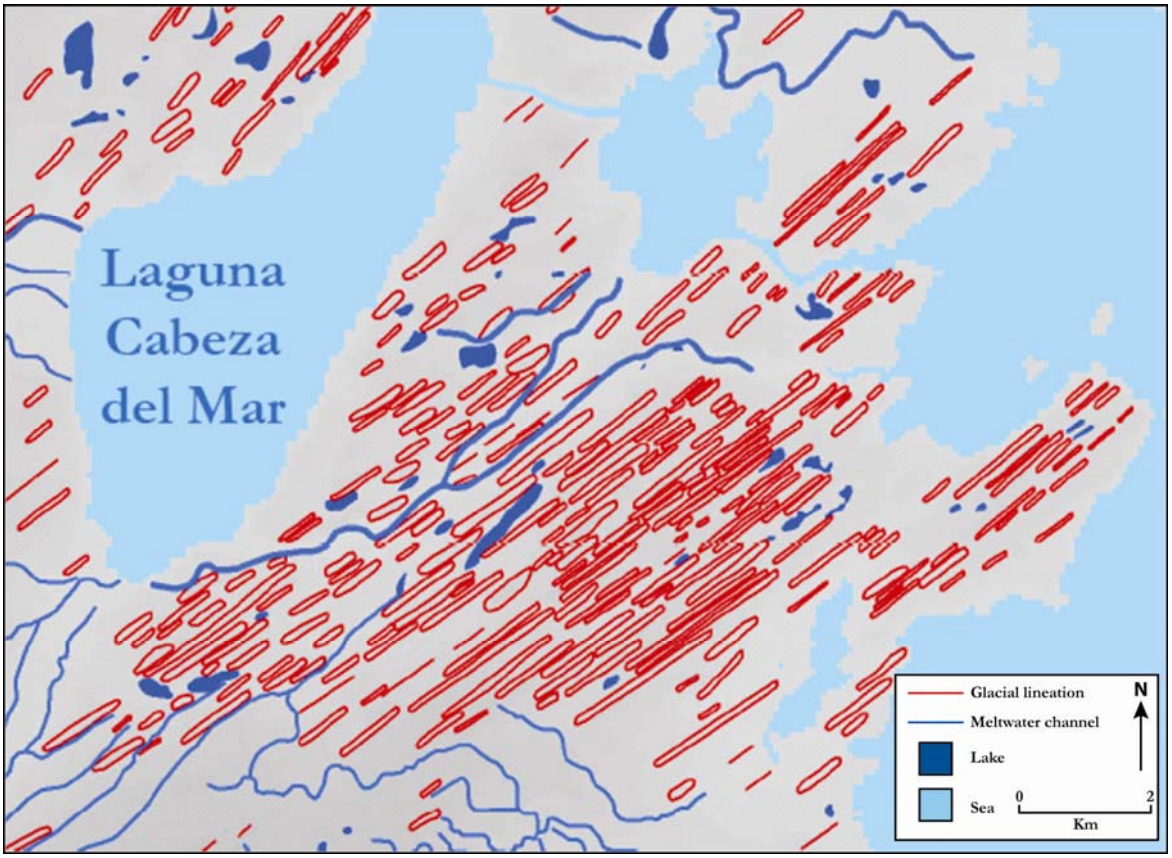

Figure 6.7 – Zone of densely spaced lineations to the east of Laguna Cabeza del Mar. See Figure 6.2 for location.

To the west of this main zone of diverging lineations located on the lower ground, a smaller group of lineations are orientated in a slightly north west direction. These are more dispersed and range from between 300 to 800 m in length. The majority are located on an area of higher ground of between 100 and 200 m altitude and are orientated at 45° to many of the lineations in the main zone to the east. 25 km south west of this group, a densely spaced collection of lineations can be found on the lower ground (< 60 m altitude) of Isla Riesco (Figure 6.3). This group is briefly described by Clapperton (1989) and appears in the map by Glasser and Jansson (2008). Located immediately to the west of the Fitz Roy Channel, general feature orientation is in a northern direction at the southern edge of the group, before curving to the north east as they move towards Seno Skyring. This trend can be seen all along the lower ground of the northern shore of Seno Otway. The longest lineation on Isla Riesco is over 2 km in length and very few are present on the higher ground at the centre of Isla Riesco (> 600 m altitude). A narrow band of lineations exists along the southern shore of Seno Skyring, these display a change in orientation (towards the north west) from east to west along the group. The majority of these are located on lower ground.

Two small groups of lineations are also located on areas of higher ground on Isla Riesco to the west of the study area. A group of 30 lineations aligned in a north eastern direction are located at a height of between 250 and 400 m altitude. The length of these features ranges from 0.3 to 2 km. Less than 10 km south of this area, a group of 12 lineations orientated in a north western direction are located at a height of between 350 and 390 m altitude A similar group of lineations are located on Península Brunswick, at the southern extent of the study area. Orientated in a south east-north west direction, these range from 0.2 to 2 km in length, are at a height of between 200 and 300 m altitude, and are closely associated with a number of small lakes that exist between individual features.

A large group of lineations, orientated to the north east, can be found on the eastern side of the Strait of Magellan. This group features in the mapping of Clapperton *et al.* (1995), Benn and Clapperton (2000a), Bentley *et al.* (2005) and Glasser and Jansson (2008). The largest of these lineations is 2.8 km long and a number are highly elongated. 10 km further south of this main group, five smaller features (< 800 m long) are orientated in the same direction. South east of Península Juan Mazia, a group of six small lineations (< 500 m long) are orientated in a south east to north west direction. These have been mapped as line features because their entire form could not be determined.

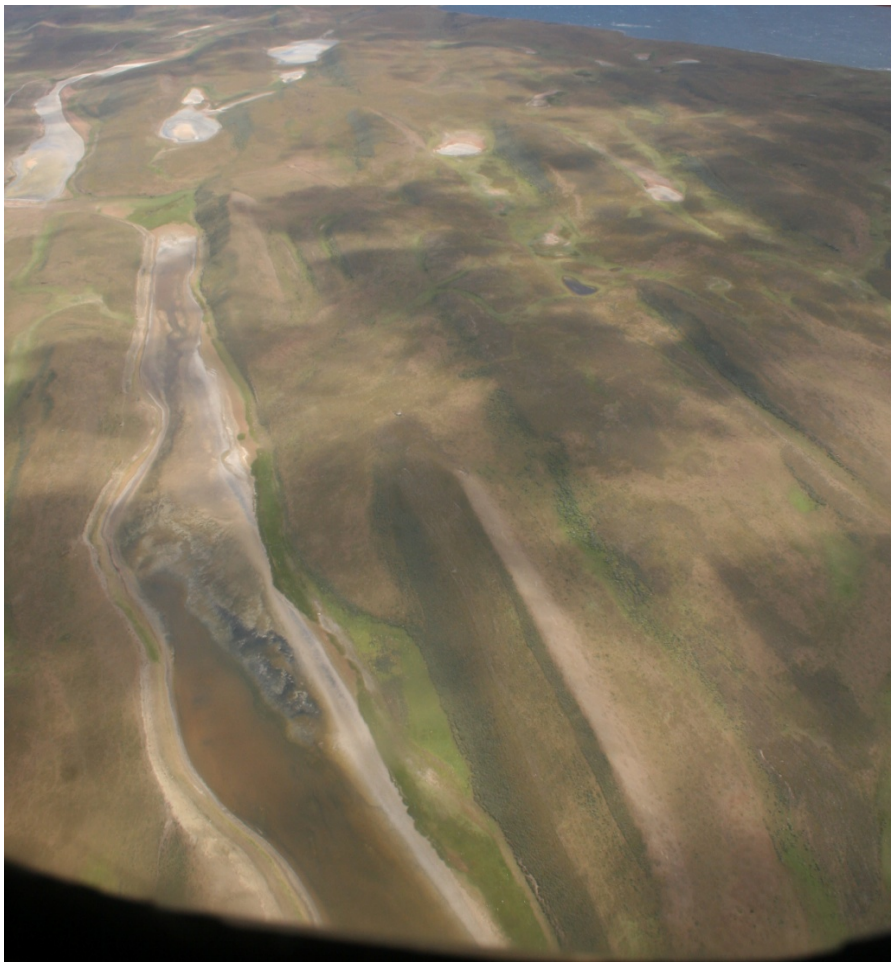

Figure 6.8 – Oblique aerial photograph of lineation to the east of Laguna Cabeza del Mar. Note the distinctive sharp crest and meltwater channels running alongside. See Figure 6.2 for approximate position photograph was taken from. Photograph by M. J. Bentley.

6.2 Moraine ridges

Two distinct former ice lobes are delimited by latero-terminal moraine systems in the north of the study area and have been recognised in a number of previous studies (Caldenius, 1932; Benn and Clapperton, 2000a; Kaplan *et al.*, 2007). These can be clearly identified on the satellite imagery as arcuate moraine ridges, forming the eastern/Seno Otway lobe and the western/Seno Skyring lobe, hereafter referred to as the Otway lobe (Figure 6.9) and Skyring lobe (Figure 6.10), respectively. A number of nested former lobe positions can be identified. These are generally separated by lateral meltwater channels. The outermost evidence for the Otway lobe reaches the northern extent of the study area, where the lobate form is created by a series of spaced ridges and their relationship with meltwater channels. A number of these ridges are up to 5 km long and, although there are large gaps between

ridges in places, the overall outer form of the lobe can still be clearly determined. A second series of ridges are situated approximately 5 km inside this outermost extent. At the northwestern extent of this group, four ridges less than 2 km long are nested within each other. Further north, this position of the lobe is clearly delimited by two longer (ca. 8 km) arcuate ridges. The innermost of these two ridges is accentuated by its close relationship with a large lateral meltwater channel that follows the lobate form (see Section 6.3). 6 km south of this ridge a series of closely-nested ridges delimits the northern extent of a third prominent lobate position. These ridges range in length from 0.5 to 9 km and are dissected by a meltwater channel which runs perpendicular to the moraines. The outermost and innermost nested ridges are 2 km apart. The discontinuous evidence for this position of the lobe can be traced to both the east and west, in both cases lateral meltwater channels occur between ridges. To the west, ridges extend all the way to the south east margin of the Skyring lobe.

A spectacular series of extensive nested moraine ridges delimits the innermost position of the Otway lobe. These arcuate ridges, the largest of which are over 20 km long, create a near-complete lobate form. In places, particularly at the western margin, meltwater channels dissect the ridges. The eastern extent of this lobe is delimited by three closely nested ridges that extend for 25 km. To the south west of the lobe, ridges can be traced all the way to the south east margin of the Skyring lobe, although this evidence is less complete.

There is a strong relationship between the moraine ridges and topography, with the innermost morainic evidence draped on the higher ground (c. 200 m altitude). This can be clearly seen on the greyscale SRTM data that provides the background to the map (Figure 6.1). To the east of the Otway lobe, beyond a prominent scarp that marks the southern edge of the higher ground, a series of moraine ridges extends in a north easterly direction towards the study area limits. These ridges run roughly parallel to the northern shore of the Strait of Magellan at this point and are situated on the edge of the higher ground. To the south of the Otway lobe, on lower ground (c. 40 m altitude), a series of small ridges extends from west to east. Surrounded by an extensive outwash plain (see Section 6.6), this group of ridges is aligned perpendicular to glacial lineation direction and parallel to the dominant orientation of ice-marginal meltwater channels in this area (see Section 6.3). The eastern extent of these ridges reaches the northern shore of Segunda Angostura and they feature in the mapping of Clapperton *et al.* (1995), Benn and Clapperton (2000a) and Glasser and Jansson (2008).

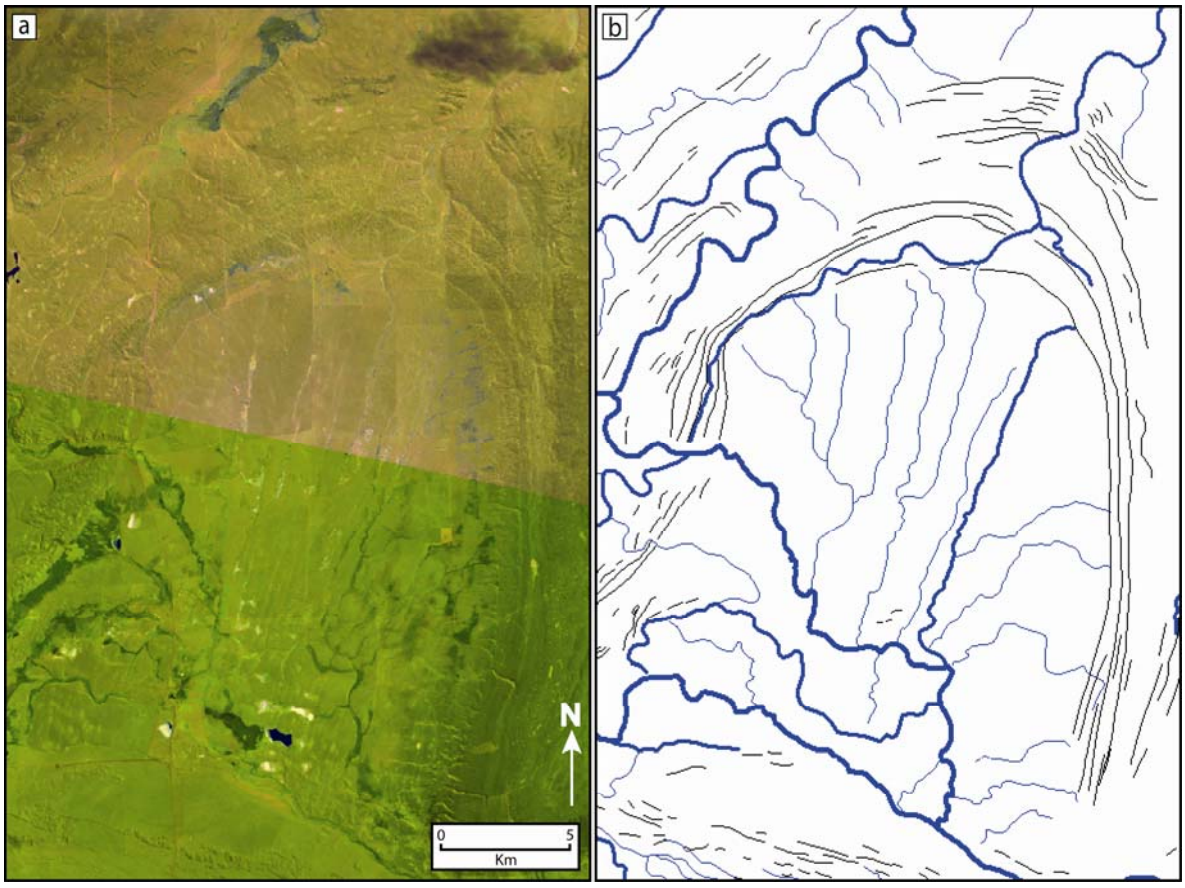

Figure 6.9 – Eastern/Otway lobe (a) as shown on Landsat TM and ETM+ satellite imagery (band combination 6, 5, 2) and (b) an example of how the moraine limits and meltwater channels have been mapped. Location shown on Figure 6.2.

Evidence associated with the Skyring lobe appears to be more fragmentary than that of the Otway lobe, with discontinuous moraine crests situated between the more continuous lateral meltwater channels that help delineate the lobate form (see Figure 6.10). The eastern margin of the lobe contains a series of densely-spaced ridges ranging from 0.5 to 5 km in length. Many of these ridges are nested within each other and a prominent network of lateral meltwater channels occurs between them. These ridges run parallel to a series of former lake shorelines of Laguna Blanca. Moraine ridges that delimit the western margin of the lobe border an extensive outwash plain, which appears to cut through them, and are closely associated with lateral meltwater channels. The largest ridge to the west of Laguna Blanca is 5 km long. As with the Otway lobe, the innermost ridges are draped on the edge of the higher ground (c. 250 m altitude). Meltwater channels are predominantly orientated parallel to the ridges, although in a number of places they are aligned perpendicular and cut through gaps in moraines. A series of five moraine ridges are located 10 km west of the southern end of Laguna Blanca. These arcuate ridges, separate from the other evidence for the Skyring lobe, extend for over 12 km. At the western end two ridges are nested within

the outer moraine, which is dissected by a small meltwater channel. These ridges were at first difficult to identify, as a prominent meltwater channel runs along the outer edge of them.

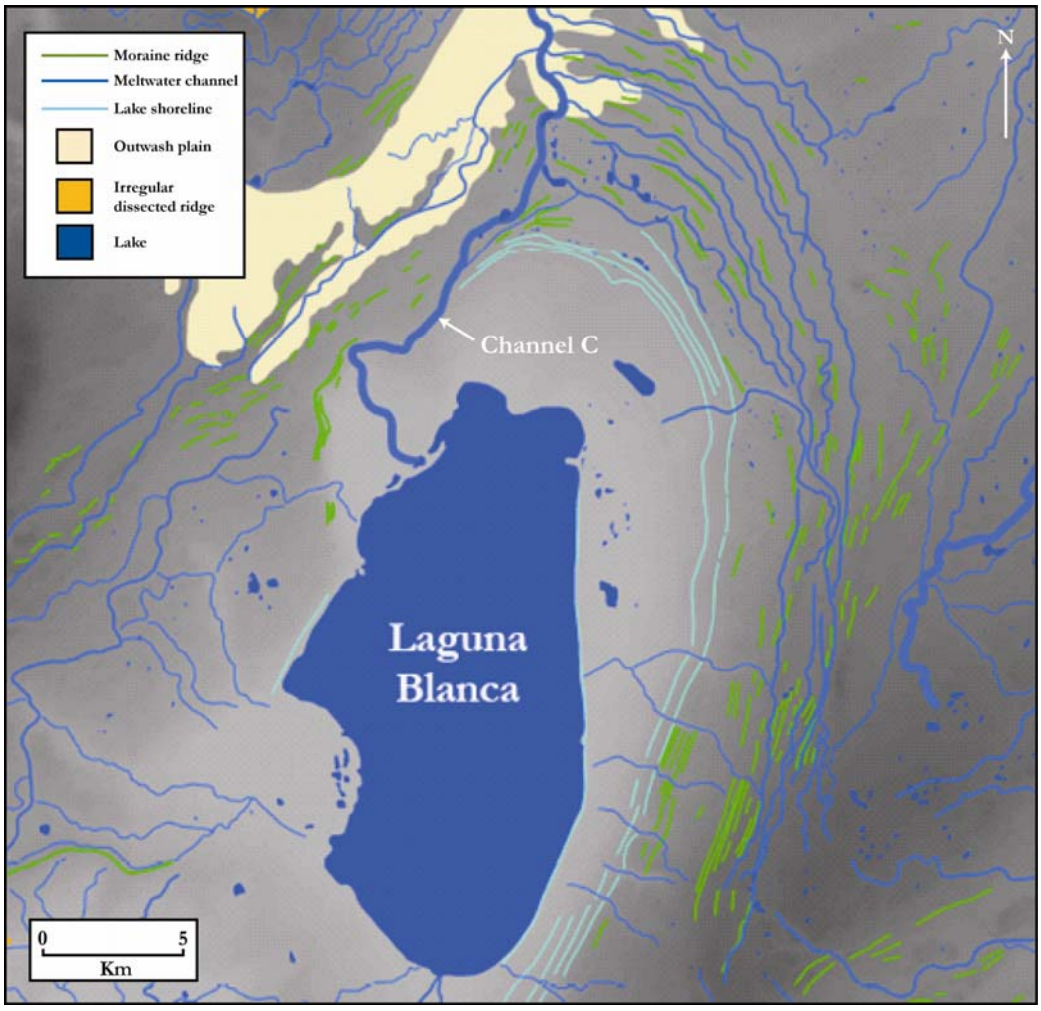

Figure 6.10 – Detail of the Skyring lobe. Note the prominent lateral meltwater channels that help to delimit the lobate form, with moraine ridges in between. See Figure 6.2 for location.

A number of moraine ridges are also located on Península Juan Mazia, on the eastern side of the Strait of Magellan. These ridges, which range from 0.5 to 5 km in length, extend from the northern shore of the peninsula at Segunda Angostura in a south easterly direction and have been mapped by Clapperton *et al.* (1995), Benn and Clapperton (2000a), Bentley *et al.* (2005) and Glasser and Jansson (2008). The eastern extent of these ridges borders the expansive outwash plain that dominates the peninsula (see Section 6.6).

6.3 Meltwater channels

A complex and extensive system of braided ice-marginal and proglacial meltwater channels exists across the study area. A hierarchy of channel sizes has been determined (approximate widths: small < 50 m; medium = 50 to 150 m; large > 150 m) and these are represented on the map by different line thicknesses (see Figure 6.1). Black arrow heads on Figure 6.1 show the inferred direction of former meltwater flow. Channels are located in all areas across the mapped region and in some cases create an extensive and interconnected network stretching for over 60 km. It is possible that some of the mapped channels are in fact sub-aerial rivers (active, seasonally active or dry), but it is difficult to conclusively differentiate between these on satellite imagery. The centre of the study area is dominated by a major ice-marginal drainage network, shown in Figures 6.11 and 6.12, and this extends from the south east margin of the Skyring lobe to the Strait of Magellan. This network has been mapped by Benn and Clapperton (2000a) and Glasser and Jansson (2008). One of the largest channels in this area (labelled Channel A in Figure 6.12a) is over 50 km long and up to 400 m wide, is highly sinuous, and runs approximately west to east following a natural gradient, from c. 200 m to < 10 m altitude (see Figure 6.12c).

Three other large channels cross this area of lower ground, all sinuous in nature and over 300 m wide in places. The northernmost of these channels (labelled Channel B in Figure 6.12a) runs along the southern margin of the Otway lobe and borders an extensive outwash plain (see Figure 6.12 and Section 6.6). Between these larger channels a series of medium and small channels create an interconnected network. Some of these smallest channels are no more than 50 m wide and are less than 5 km long. This network runs directly across the main zone of glacial lineations. The dominant orientation of the majority of the channels in this network is perpendicular to lineation direction. In places channels appear to cut across individual lineations, as well as meandering through gaps between denser groupings of lineations and moraine ridges.

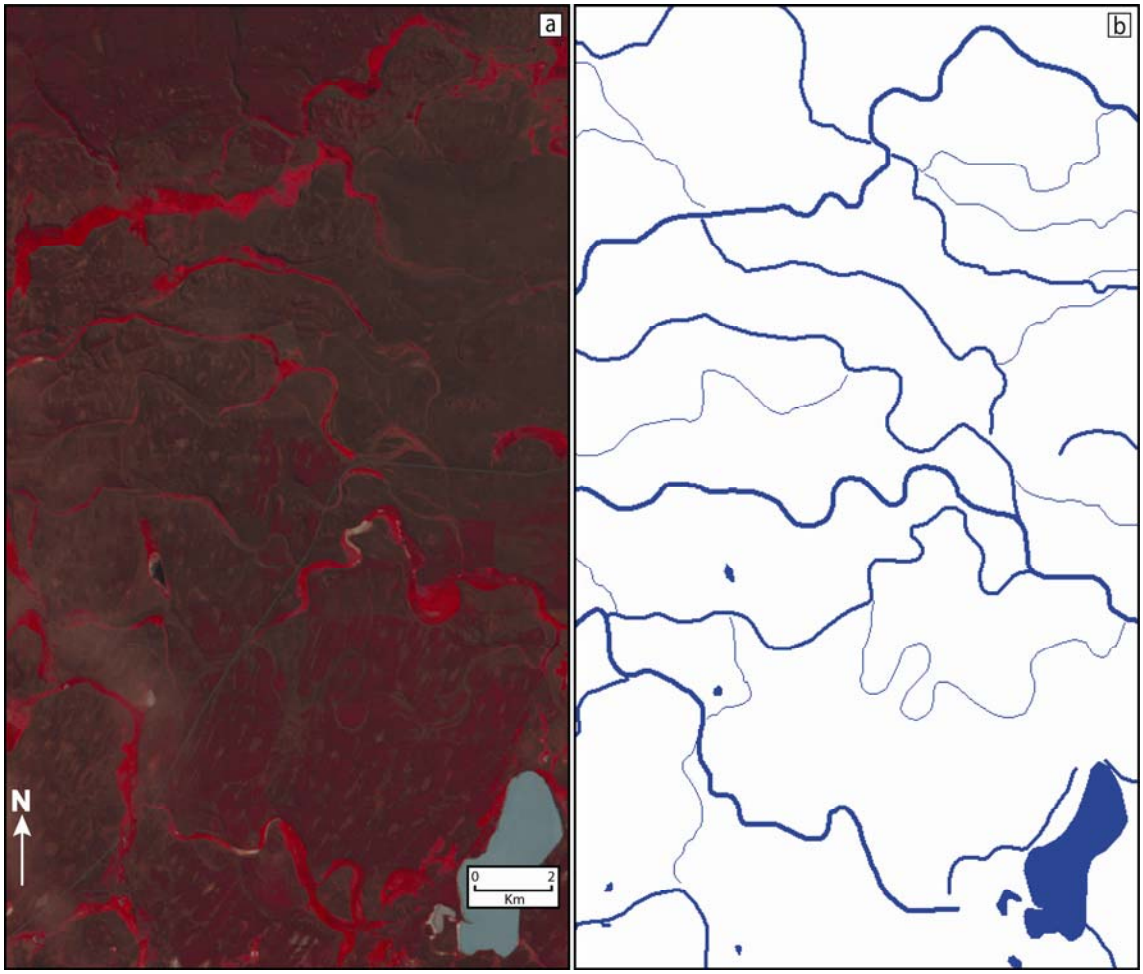

Figure 6.11 – Meltwater channels, (a) on Landsat TM satellite imagery (band combination 4, 3, 2) and (b) an example of how they have been mapped, in association with some lakes. Location shown on Figure 6.2.

In the north of the study area, three large proglacial meltwater channels that are closely associated with the Skyring and Otway lobes drain northwards. These have been mapped as sandar/terrace edges by Glasser and Jansson (2008). The furthest west of these (labelled Channel C in Figure 6.10), which is over 400 m wide in places, runs from Laguna Blanca, through a small gap in the morainic evidence that delimits the Skyring lobe and across an extensive outwash plain which extends in the same direction (see Section 6.6). A prominent sequence of lateral meltwater channels to the east of Laguna Blanca drain into this major channel. These channels, which are all ca. 100 m wide, occur either side of moraine ridges of the Skyring lobe, and help to create the eastern extent of the lobate form. A similar but more-extensive series of lateral channels to the west of Laguna Blanca also drain towards the larger channel. This interconnected network of channels is part of a larger system that runs along the northern shore of Seno Skyring, before heading in a north-easterly direction along the western margin of the Skyring lobe. As at the eastern margin of the lobe, moraine ridges occur between the channels. The channels then cross

the extensive outwash plain, which is orientated in the same direction, before joining the larger meltwater channel.

To the east of the Skyring lobe, a large lateral meltwater channel drains along the western margin of the Otway lobe. Labelled Channel D in Figure 6.13, this channel is highly-sinuous and is part of an interconnected network of channels that drain in a north-easterly direction from the south east margin of the Skyring lobe. This network of channels picks its way through the outermost moraine ridges of the Otway lobe. A medium-sized channel (c. 150 m wide) drains between the innermost series of nested moraine ridges, following the lobate form before running out into the larger channel through a gap between ridges at the top of the lobe (labelled Channel E in Figure 6.13). A smaller group of lateral meltwater channels also drains northwards along the eastern margin of the Otway lobe, before joining the larger channel. The third large channel in the north of the study area is situated between the Skyring and Otway lobes. This channel, which is up to 200 m wide in places, drains northwards and is closely associated with a series of smaller channels.

Meltwater channels are present within the dense areas of glacial lineations, specifically around Laguna Cabeza del Mar, on Isla Riesco and on the eastern side of the Strait of Magellan. In the main zone of glacial lineations east of Laguna Cabeza del Mar, four meltwater channels are orientated sub-parallel to lineation direction. These channels, the largest of which is up to 140 m wide, occupy the space between lineations and drain towards the Strait of Magellan (see Figures 6.6, 6.7 and 6.8). This larger channel is mapped by Benn and Clapperton (2000a). In this area there is little evidence of channels running perpendicular to lineation direction. Immediately to the west of Laguna Cabeza del Mar, meltwater channels also run sub-parallel to lineation direction and drain into the lake. A similar relationship between meltwater channels and lineations exists on both Isla Isabel and the eastern side of the Strait of Magellan. On Isla Riesco, a series of meltwater channels drain across the zone of lineations closest to the Fitz Roy Channel. These are orientated roughly perpendicular to lineation direction and in places they appear to cut across lineations. Some of these channels are connected by smaller channels running parallel to lineation direction. Along the southern shore of Seno Skyring a network of lateral meltwater channels runs through a group of lineations. The channels are orientated both sub-parallel and perpendicular to lineation direction. Extensive networks of lateral meltwater channels are also present east of the Otway lobe along the northern shore of the Strait of Magellan and on the eastern side of the strait.

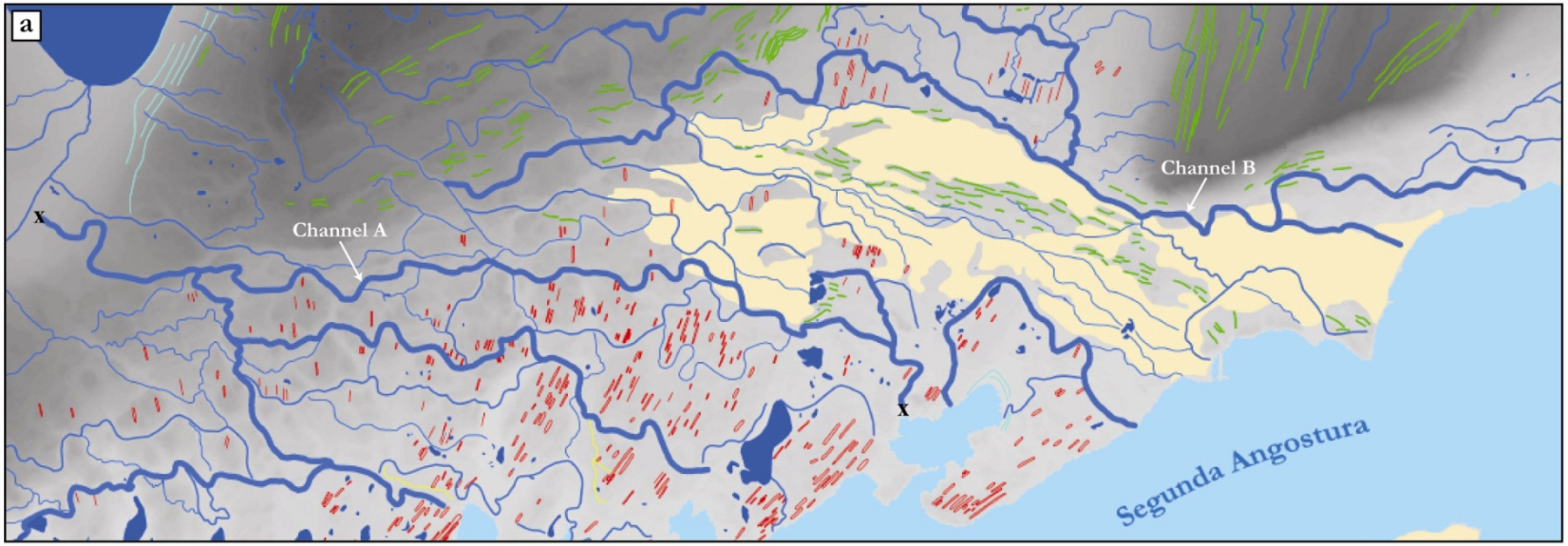

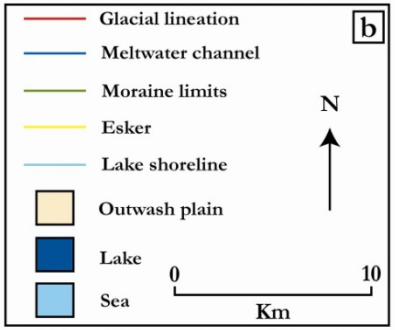

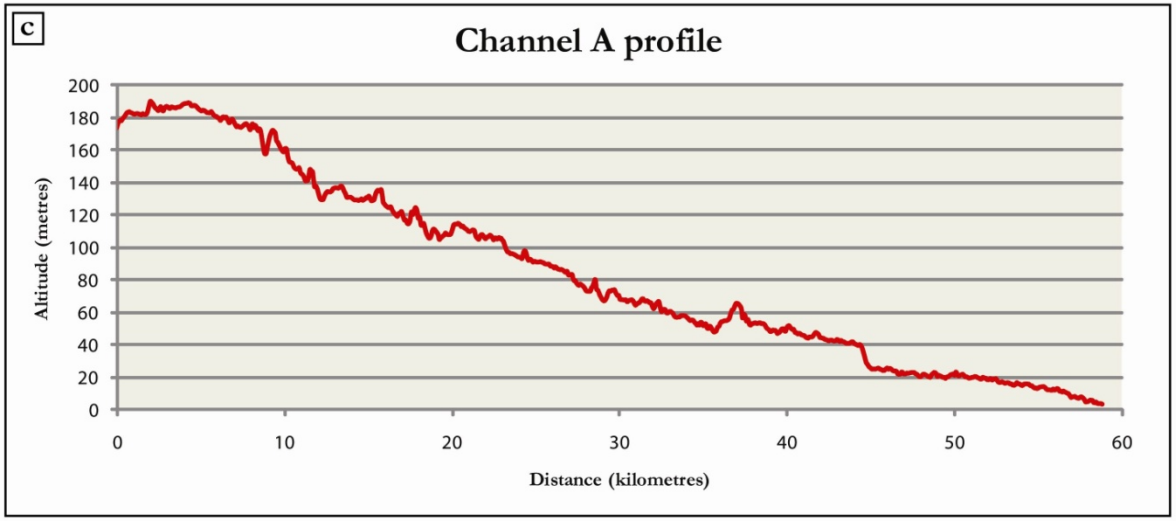

Figure 6.12 – (a) Major network of channels that runs from west to east across the centre of the study area. Note the orientation of the channels in relation to lineation direction, and the expansive outwash plain. Channels A and B are referred to in the text. (b) Shows the legend for (a). (c) Shows the profile of Channel A along its entire length from west to east. The beginning and end of the profile transect are marked by x on (a).

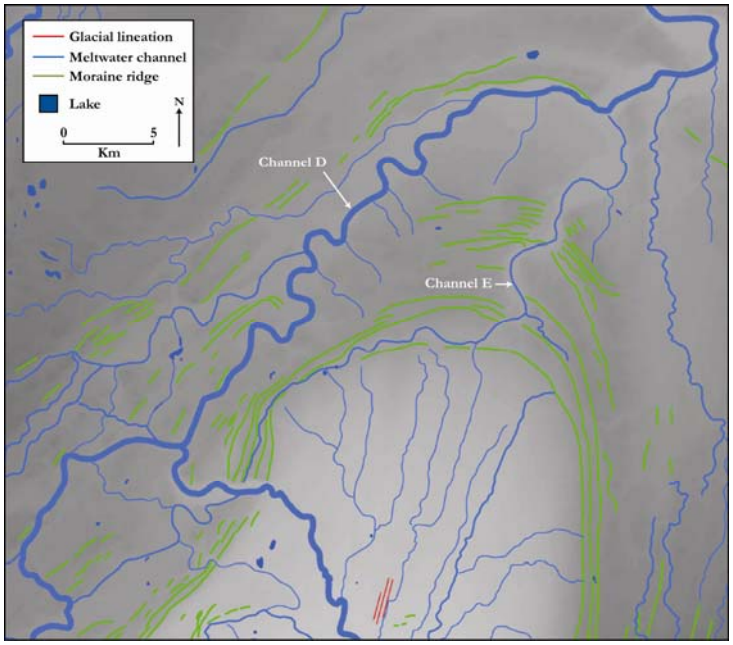

Figure 6.13 – Meltwater channels located around the Otway lobe. Channels D and E are referred to in the text.

Figure 6.14 - Small meltwater channels south of Laguna Cabeza del Mar. Note the sinuosity of individual channels. Photograph by M. J. Bentley.

Dense and complex networks of small interconnected meltwater channels are found in several places across the study area. An example of this can be seen in Figure 6.14, which is located south of Laguna Cabeza del Mar and the main zone of lineations. The majority of these channels are less than 50 m wide and drain towards the Strait of Magellan. In

other areas similar networks of small channels are closely associated with groups of irregular ridges (see Section 6.4).

6.4 Irregular dissected ridges

Groups of closely-spaced irregular ridges occur at four main locations in the study area. These ridges exhibit a variety of morphologies; some are long, thin and sinuous in nature, whilst others are more rounded. The orientation of the ridges also varies, both between the groups but also within an individual group. As well as irregularity of morphology, a shared characteristic of the groups of ridges is their close association with meltwater channels. In all cases a network of small meltwater channels dissects the ridges, helping to create their individual forms. The densest group containing 37 ridges is located 10 km north west of the Skyring lobe. These are shown in Figure 6.15, where it can be seen that the group contains both long, sinuous ridges and more-rounded examples. The largest of these ridges is up to 2 km long and 150 m wide and they often merge into neighbouring ridges. The orientation of the ridges varies in this area, but in general they are aligned approximately east-west. A larger area of similar ridges is located 10 km east of this first group; these are shown in Figure 6.16. This group contains a large number of long, sinuous ridges, the largest of which is 3 km long and 150 m wide. The orientation of these long ridges is more uniform than in the first group, with an approximate west-east direction. There are fewer rounded ridges and the group is dissected by a network of small meltwater channels trending in the same approximate west-east direction. Both of these groups are located beyond the northern limits of the Skyring lobe and have been mapped by Glasser and Jansson (2008) as linear moraine limits along their determined crest.

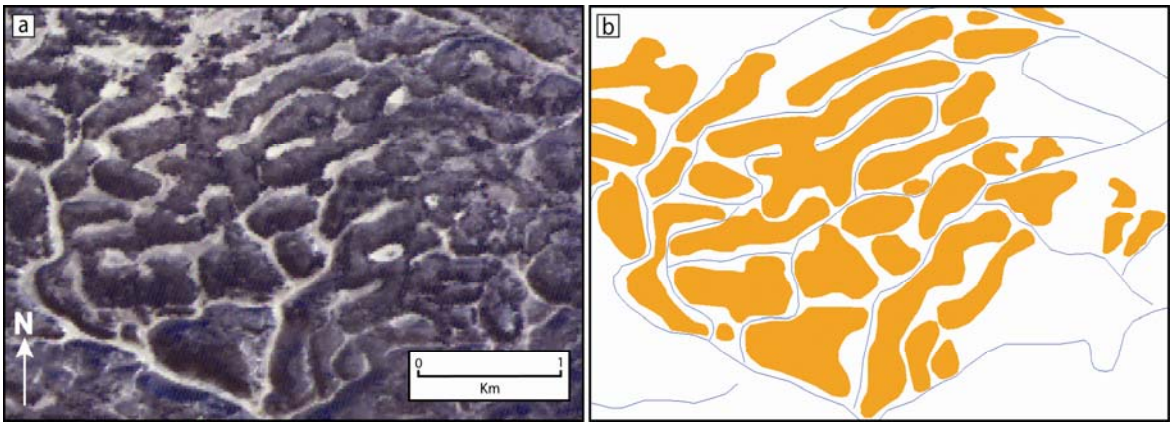

Figure 6.15 – Area mapped as irregular dissected ridges to the north west of Laguna Blanca, (a) ASTER satellite imagery (band combination 1, 2, 3) and (b) an example of mapped features. Location shown on Figure 6.2.

A third group of irregular ridges is found at the eastern end of Seno Skyring. This group contains 31 individual ridges, the majority of which are more rounded, but there are also examples of ridges with very irregular morphologies. No clear overriding orientation can be determined for this group, unlike the examples shown in Figures 6.15 and 6.16, and small meltwater channels can be seen between ridges. A further group of irregular ridges is located immediately east of the end of Seno Otway. This is a smaller group containing 19 individual ridges and they are closely associated with meltwater channels, glacial lineations and small lakes. A number of the ridges are orientated at 90° to lineation direction, particularly at the southern edge of the group, whilst others are aligned in a similar direction. Small meltwater channels dissect the group and the curvilinear appearance of many of the ridges is accentuated by the meltwater channels either side. These last two groups of ridges are both located on lower topography at the ends of Seno Skyring and Seno Otway (< 100 m altitude), whilst the first two groups described are located on higher ground (> 250 m altitude).

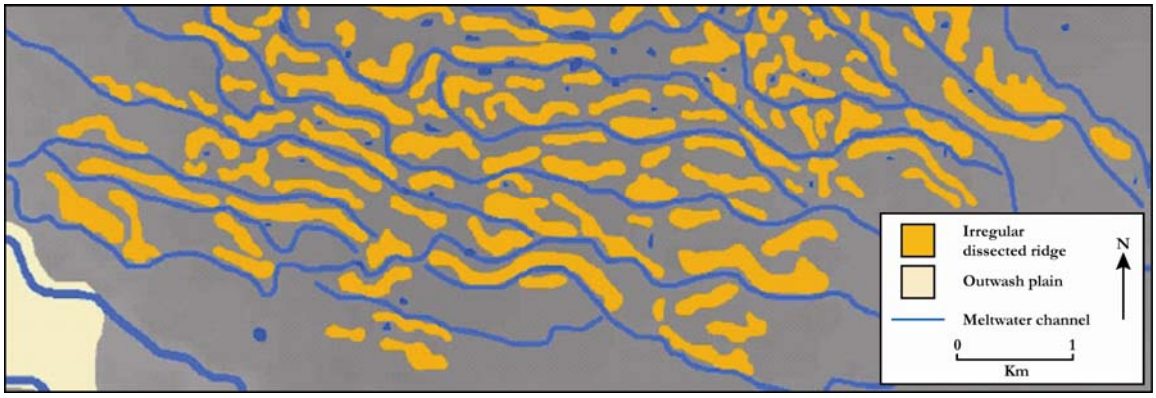

Figure 6.16 – Group of irregular ridges located 20 km north east of Laguna Blanca. See Figure 6.2 for location.

6.5 Eskers

Two small sinuous ridges, to the north east and north west of Laguna Cabeza del Mar, have been mapped as eskers on the basis of sinuous plan form, orientation and relationship to drumlins (sub-parallel) and moraines (transverse). Both ridges are approximately 5 km long and are less than 10 km apart and were mapped by Clapperton (1989), who described them as two large esker systems superimposed on the drumlins. Figure 6.17 shows that the further west of the two eskers has a small tributary joining it at an angle of approximately 45°. The eskers were difficult to pick out on satellite imagery due to their small size, but could be seen most clearly on the higher-resolution ASTER imagery (Figure 6.17). Larger meltwater channels can be seen trending in a similar direction to both eskers, which also

appear to overprint the edges of some lineations. The westernmost esker terminates at a large ice-marginal meltwater channel that runs approximately west to east towards the Strait of Magellan. Perhaps because of the difficulty involved with picking them out on satellite imagery (Evans *et al.*, 2008) no other eskers were identified in the study area. In addition, other than Clapperton (1989) they do not feature in previous mapping.

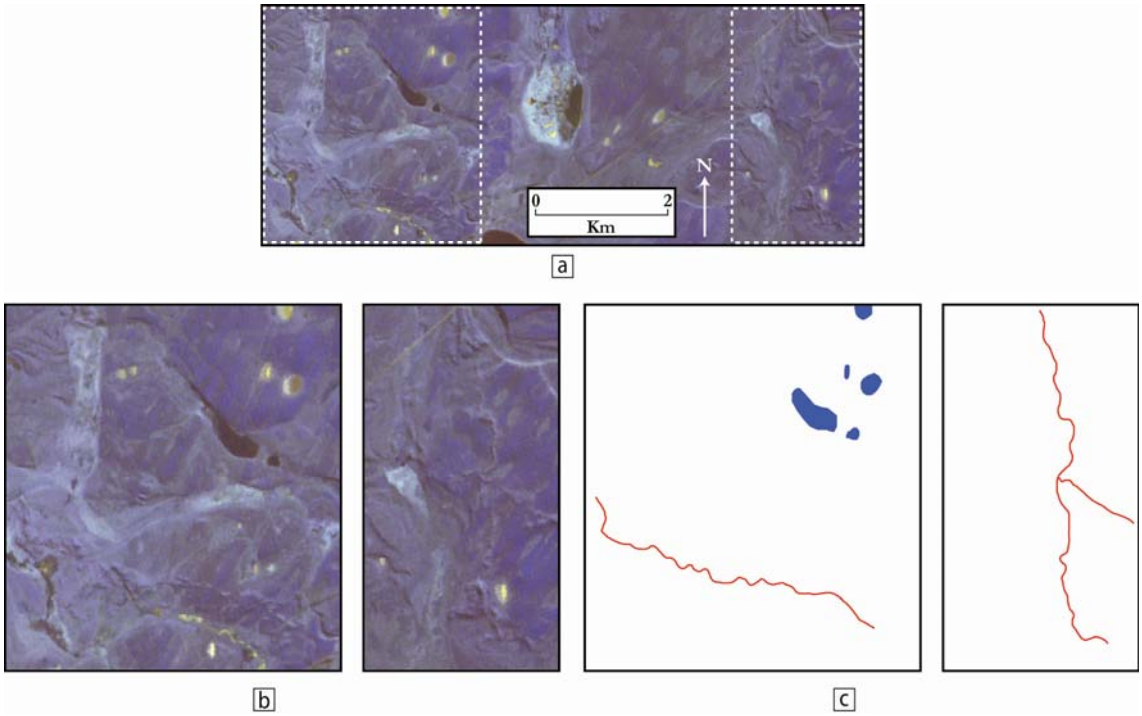

Figure 6.17 – (a) Sinuous ridges to the north west and north east of Laguna Cabeza del Mar (northern tip seen in the centre bottom) on ASTER satellite imagery (band combination 1, 2, 3); (b) detail of two boxes delimited by white dashes in (a); and (c) mapped eskers (in red). Location shown on Figure 6.2.

6.6 Outwash plains

Three large outwash plains are located within the mapped area. These are to the north west of the Skyring lobe, south of the Otway lobe, see Figure 6.18, and on Península Juan Mazia on the eastern side of the Strait of Magellan, and have been mapped in previous studies (Benn and Clapperton, 2000a; Bentley et al., 2005; Glasser and Jansson, 2008). They appear as extensive smooth surfaces on the satellite imagery and have been mapped as complete polygons where possible. Meltwater channels can be detected on their surfaces; these are generally orientated in the same direction as the outwash plains. This is particularly the case for the outwash plains to the west of the Skyring lobe and to the south of the Otway lobe. The large meltwater channel that drains the Skyring lobe runs across the surface of the outwash plain to the north west and several other smaller channels are

also present. These smaller channels are part of a system of lateral meltwater channels that help to delimit the lobate form (see Section 6.3 and Figure 6.10). The outwash plain south of the Otway lobe is bordered by two large ice-marginal meltwater channels that trend from west to east, from the Skyring lobe towards the Strait of Magellan (Figure 6.18). There is a noticeable lack of lineations and moraine ridges on the surface of the outwash plains, these instead exist either side of the plains, or in pockets within them. This is clearest south of the Otway lobe, where lineations are present either side of the outwash plain but rarely within, and moraine ridges can be identified in large pockets (Figure 6.18). The outwash plain on Península Juan Mazia is bordered at its proximal edge by a series of small moraine ridges. The outwash plains cover areas of approximately 120 km^2 (north west of Skyring lobe), 240 km^2 (south of Otway lobe) and 230 km^2 (on Península Juan Mazia).

6.7 Former lake shorelines

Distinct continuous or near-continuous linear features that closely parallel the current active shorelines of embayments and lakes have been mapped as former shorelines. These are mostly located around Seno Otway and Laguna Blanca, where they are often characterised by a series of shorelines closely nested within each other, and have been mapped by Glasser and Jansson (2008). The most distal of the shorelines to the north of Laguna Blanca is over 6 km from the active shoreline and is located at an altitude of up to 215 m, 105 m above the current lake level (Figure 6.19 shows a profile of the shorelines north of Laguna Blanca). These shorelines stretch for over 40 km, parallel with the eastern shore of Laguna Blanca for the most part before curving around the north of the lake. Small meltwater channels cut through the former shorelines at various points and both ends of this series of shorelines coincide with large channels. At the southern end, the large ice-marginal meltwater channel runs eastwards towards the Strait of Magellan, whereas the proglacial channel in close proximity to the northern extent of the shorelines extends north of Laguna Blanca.

Former shorelines are also particularly distinctive around Seno Otway, as shown in Figure 6.20. The most distal of these shorelines is located 5 km from the northern end of Seno Otway at an altitude of up to 35 m and is dissected by a meltwater channel that would have drained towards Laguna Cabeza del Mar. Former shorelines are also located on the flanks of Seno Otway, most notably on Península Brunswick. Here, a closely-spaced series of six shorelines are nested within each other, approximately 4 km from the active shoreline and

at an altitude of up to 40 m. These are part of the semi-continuous series of shorelines that stretches northwards around the end of Seno Otway. In several places, small meltwater channels cut through the shorelines. Former shorelines are also present on Isla Riesco and Península Juan Mazia.

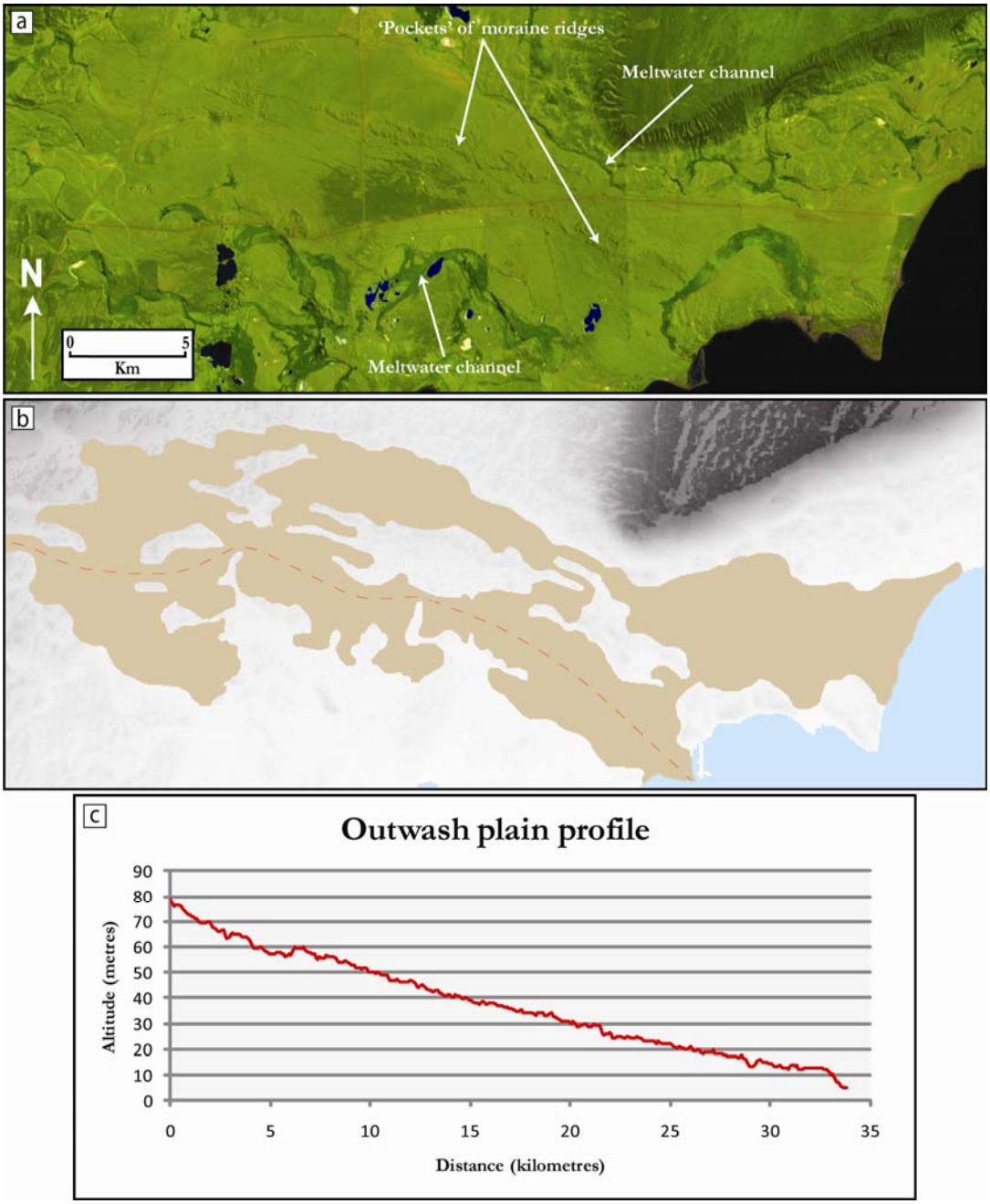

Figure 6.18 – Outwash plain south of the Otway lobe, (a) as seen on Landsat TM satellite imagery (band combination 6, 5, 2) and (b) as mapped (light brown colour). (c) Shows profile from west to east of transect shown in (b) as a red dashed line. Location shown on Figure 6.2.

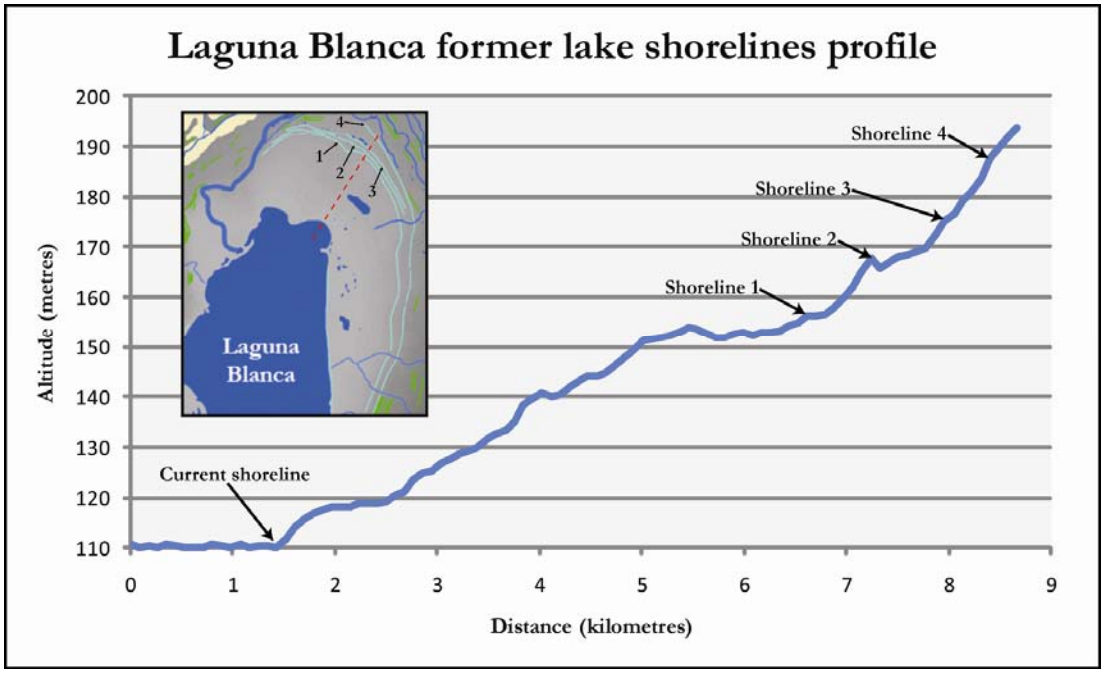

Figure 6.19 – Profile of lake shorelines around Laguna Blanca. Inset shows position of transect (red dashed line) and labelled shorelines.

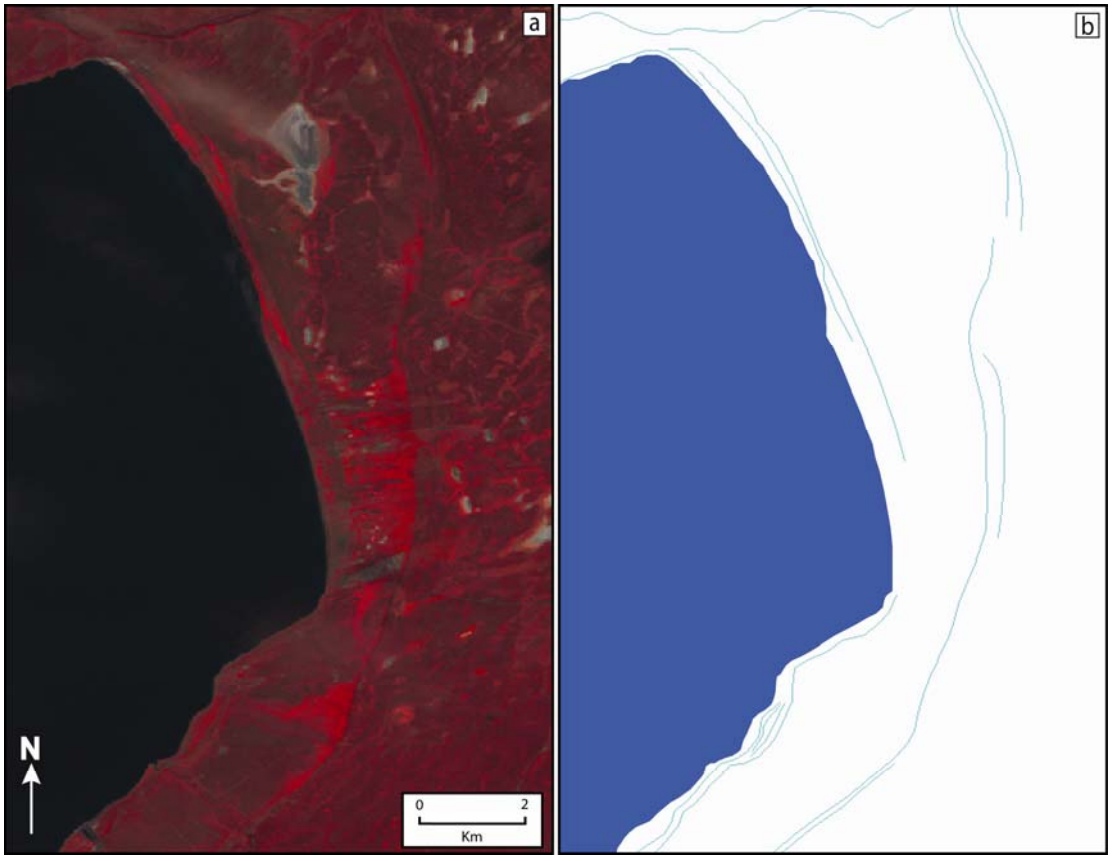

Figure 6.20 – Former lake shorelines at the north eastern end of Seno Otway, (a) Landsat TM satellite imagery (band combination 4, 3, 2) and (b) as mapped. Location shown on Figure 6.2.

6.8 Other features

A large number of lakes exist across the study area, ranging in size from less than 500 m^2 to over 160 km^2 (Laguna Blanca). Laguna Blanca is situated on the lower ground within the Skyring lobe and at its greatest extent is approximately 20 km long and 12 km wide. Other significant lakes (> 2 km^2) are mapped within the study area, most notably immediately north of Seno Otway and on the eastern side of the Strait of Magellan. A number of these larger lakes north of Seno Otway are aligned roughly in the same direction as the surrounding glacial lineations. A good example of this is a lake located 15 km north east of Laguna Cabeza del Mar, near the western shore of the Strait of Magellan. Other examples can be seen immediately to the west of Laguna Cabeza del Mar and on Isla Riesco. Throughout the study area smaller lakes exist within meltwater channels. The smallest lakes (< 1 km^2) are scattered across the region, including on both the lower ground around the northern end of Seno Otway and the higher ground between the two former lobes. A dense grouping of over 600 small lakes is located on the lower ground (< 70 m altitude) at the northern end of Península Brunswick, east of Seno Otway.

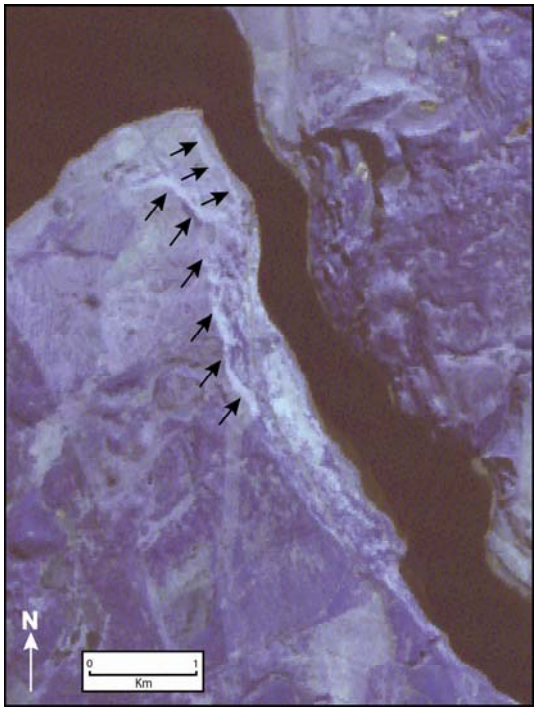

Figure 6.21 – Two of the distinct linear features located at the northern end of Fitz Roy Channel, on ASTER satellite imagery (band combination 1, 2, 3). Location shown on Figure 6.2.

A number of scarp lines have been mapped at either end of the Fitz Roy Channel. Figure 6.21 shows these distinct linear features running sub-parallel to the channel on both sides. Glasser and Jansson 2008) mapped these features as moraine ridges. A large and

prominent scarp is located east of the Otway lobe, this feature has a height of 350 m altitude, is over 20 km long and is heavily gullied (see Figure 6.22).

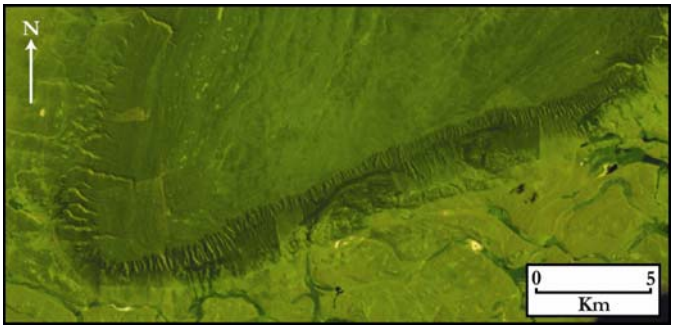

Figure 6.22 – Large scarp located to the east of the Otway lobe. Location shown on Figure 6.2.

6.9 Summary

A rich variety of glacial landforms and landform assemblages are distributed across the study area. The most notable of these are distinct zones of streamlined glacial lineations, mostly located on areas of lower ground on the western side of the Strait of Magellan. A combination of composite moraine ridges and lateral meltwater channels delineate two former ice lobes in the north of the study area. Throughout the mapped area a complex interconnected network of proglacial and ice-marginal meltwater channels exists, some of these channels are up to 500 m wide in places and stretch for over 60 km. At four locations, networks of small meltwater channels dissect closely-spaced groups of irregularly-shaped and chaotically-aligned ridges. Other mapped features include eskers, extensive outwash plains, former lake shorelines, lakes and scarps.

Chapter 7 - Interpretation and Discussion

7.1 Flow-set identification

Nine separate flow-sets have been identified in the study area from the glacial lineation record. The process by which flow-sets are determined is relatively straightforward once lineations have been mapped (Clark, 1999). Following the Clark (1999) criteria, lineations have been grouped into spatially coherent and distinctive patterns based on parallel concordance (similar orientations), close proximity and similar morphometry. In addition to these three criteria, flow-sets have also been defined according to a glaciologically plausible pattern (Clark, 1997; Kleman *et al.*, 1997, 2006; De Angelis and Kleman, 2005). This means that flow-set extent and orientation are also controlled by feasible ice sheet dynamics following the least complex possible solution (De Angelis and Kleman, 2005). The flow-sets have been labelled Fs-1 to 9 and their locations and extents are shown in Figure 7.1.

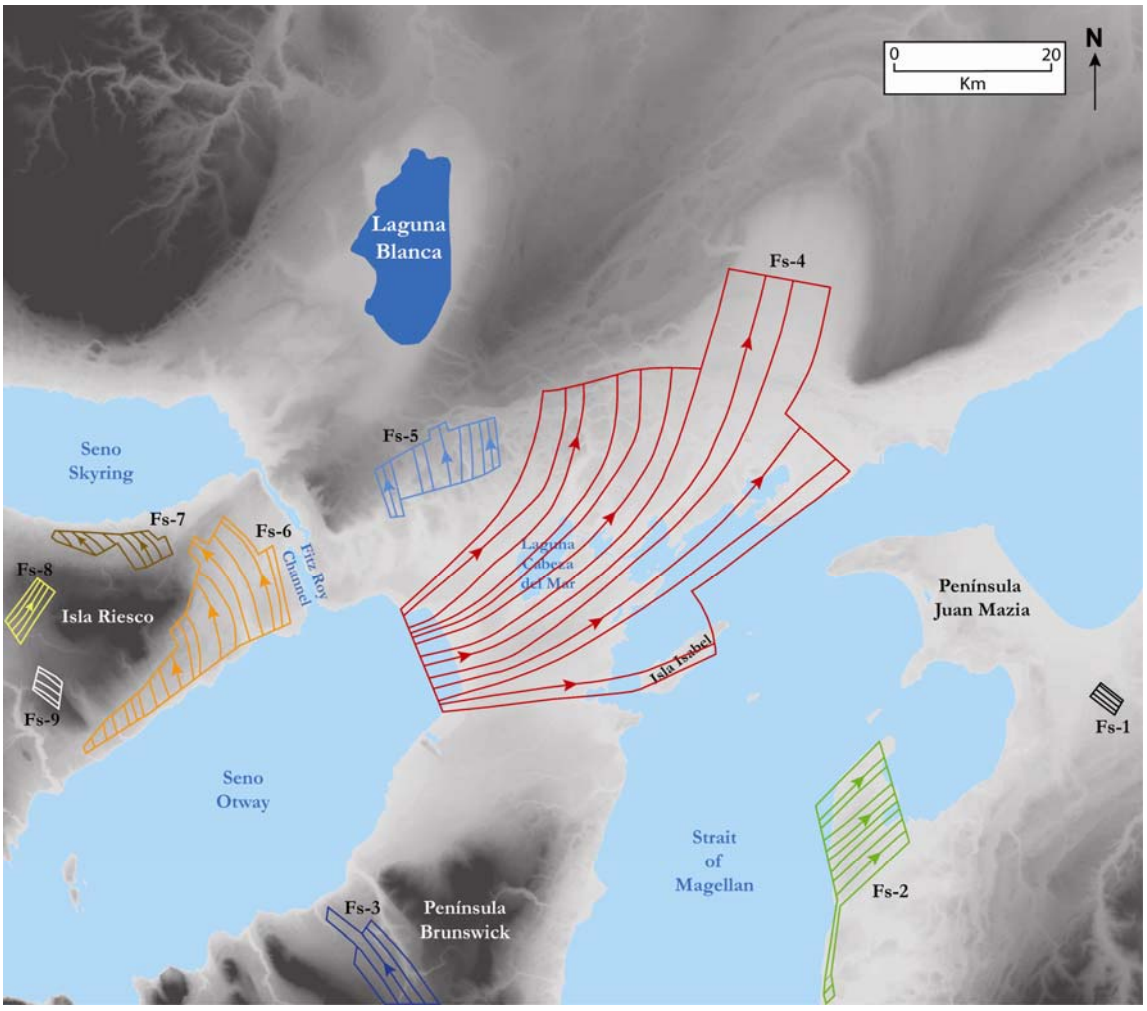

Figure 7.1 – Flow-sets identified in the study area from the geomorphological map (Figure 6.1). Table 7.1 contains further data on individual flow-sets.

Table 7.1 summarises key data of each individual flow-set, including total number of lineations; maximum, minimum and mean lengths; and maximum, minimum and mean elongation ratios. Fs-1 is a small group of six lineations (mean length = 462 m) to the south east of Península Juan Mazia. These have not been mapped as polygons so no elongation data are available. In this location, a number of small meltwater channels are aligned perpendicular to lineation direction, which is approximately north west-south east. Fs-2 is a medium-sized group of lineations (n = 115), containing a large proportion of elongate features (mean length = 892 m; maximum elongation ratio = 16:1). Located on the eastern side of the Strait of Magellan, the lineations have a close relationship with a series of small lateral meltwater channels which are orientated sub-parallel to lineation direction. A group of five small lineations (< 800 m long) located 15 km to the south of this main group have been included in the flow-set on the basis of similar orientations.

Table 7.1 – Lengths and elongation ratios of lineations within the different flow-sets. Elongation ratios are calculated solely from lineations mapped as polygons. Fs-1 and Fs-9 contain only lineations mapped as lines. See Figure 7.1 for location of flow-sets.

Flow-set	Number of Lineations	Maximum Length (m)	Minimum Length (m)	Mean Length (m)	Elongation Ratio (highest)	Elongation Ratio (lowest)	Elongation Ratio (mean)
Fs-1	6	580	362	462	-	-	-
Fs-2	115	2738	423	892	17	3	7
Fs-3	60	2154	265	631	15	3	5
Fs-4	663	2913	189	712	35	2	6
Fs-5	29	837	280	525	10	3	6
Fs-6	368	2041	196	590	17	3	5
Fs-7	69	658	121	355	6	3	4
Fs-8	27	2063	308	673	11	3	5
Fs-9	12	834	259	543	-	-	-
Entire Dataset	1,349	2913	121	665	35	2	6

Fs-3 is a medium-sized group (n = 60) located on Península Brunswick. The overall orientation of the group is from northwest to southeast. The majority of the lineations have elongation ratios less than 10:1 and are located in a narrow 5 km-wide band. A number of small meltwater channels orientated sub-parallel to lineation direction are closely associated with the flow-set.

The largest flow-set that has been identified is Fs-4. This group stretches for over 60 km and contains 663 lineations. Many of these lineations, particularly in the centre of the flow-set where features are densely-packed (Figure 6.7), are over 1 km long and exhibit elongation ratios over 10:1. The longest lineation in the flow-set is 2.9 km long and the highest elongation ratio of the entire study area dataset is also contained in this group

(35:1). The main orientation of the lineations is a uniform south west-north east alignment away from the marine embayment of Seno Otway, and further north the lineations diverge. The inclusion of the group of lineations on Isla Isabel in this flow-set reflects the eastern extent of this divergence. Glaciofluvial features are located within the extent of the flow-set. These include eskers orientated both sub-parallel and perpendicular to lineation direction and an extensive network of ice-marginal meltwater channels. The flow-set terminates at the large lobate moraine sequence in the north of the study area (Figure 6.9), and another sequence of moraine ridges, orientated perpendicular to lineation direction, is located within the northern extent of the flow-set. This moraine sequence is surrounded by an extensive outwash plain trending in the same direction (Figure 6.18).

Fs-5 (n = 29) has been defined as a separate flow-set to Fs-4 despite their close proximity and the similar orientations of some of the lineations within both groups. This is mainly because the orientations of many of the lineations within Fs-5 are aligned at more than 45° to the dominant direction of lineations within Fs-4. Considering the close proximity of the groups, it has been determined that they must belong to different flow-sets based on glaciological plausibility. This distinction becomes less clear-cut towards the border between flow-sets, as the lineations within Fs-4 diverge towards the terminus of the flow-set, resulting in similar orientations to those in Fs-5. The morphometry of the lineations also helped to determine the flow-sets because those in Fs-5 are in general shorter and less elongate than features in Fs-4.

Four flow-sets are located on Isla Riesco, in the east of the study area. The largest of these (Fs-6) contains 368 lineations, the main zone of which is located towards Fitz Roy Channel in the east of Isla Riesco (Figure 6.3). This flow-set extends westwards along the northern shore of Seno Otway. This eastern extent of the flow-set contains many lineations over 1 km in length and with elongation ratios up to 16:1. From south to north it displays a slight curve in lineation direction towards the north west. This flow-set is closely associated with meltwater channels orientated both perpendicular and sub-parallel to lineation direction. Fs-7 is located along the southern shore of Seno Skyring and contains 69 lineations aligned predominantly from south east to north west. All of the lineations in this flow-set are less than 700 m in length and the mean elongation ratio in the group is 4:1.

Fs-8 contains 27 lineations orientated in a south west to north east alignment and is approximately 7 km long and 3 km wide. The longest feature in the group is 2.1 km long and has an elongation ratio of 10:1. However, the vast majority are shorter than 800 m and

the mean elongation ratio is 4:1. The final flow-set, Fs-9, contains 12 lineations. These have been mapped as line features only and so it was not possible to calculate any elongation ratios. The lineations in this group have a mean length of 543 m.

7.2 Flow-set classification

Following the delineation of flow-sets, the next step is to classify these according to the four categories outlined in the glacial inversion method of Kleman *et al.* (2006), discussed in detail in Section 4.3. The isochronous or time-transgressive generation of each flow-set must also be determined. Some key characteristics which help to distinguish between these are outlined by Clark (1997, 1999) and Kleman *et al.* (2006). Where there is insufficient information from the mapped evidence to classify a flow-set confidently, as is the case for many of the flow-sets in this study, the most-likely classification has been determined. The lineations of Fs-4 have attracted most attention in previous work in the area and were thought to indicate the presence of a zone of streaming ice (e.g. Clapperton, 1989; Benn and Clapperton, 2000a). Bearing in mind that one of the main objectives of this study is to investigate this hypothesis, Fs-4 is of great importance and will receive the majority of the attention in this section.

Part of the Kleman *et al.* (2006) inversion model includes the ordering of flow-sets into relative-age stacks. This has been achieved in a number of previous studies (e.g. Boulton and Clark, 1990; Jansson *et al.*, 2002; De Angelis and Kleman, 2005; Stokes *et al.*, 2009), particularly where flow-sets are closely grouped and there are an abundance of well-dated positions. In contrast to these studies, the flow-sets that have been identified in the Strait of Magellan region are largely isolated and fragmentary. As a result, there are no clear overlaps between flow-sets. A combination of this and the lack of well-dated positions throughout the study area means that grouping them into relative-age stacks is problematic. Instead, individual flow-sets will be assigned to time-steps within the ice sheet reconstruction of Section 7.5.

7.2.1 Fs-4: landsystem classification

The most extensive flow-set in the study area is Fs-4 and this is interpreted as an isochronous ice stream flow-set. This is based on the comparison of the mapped geomorphological record with the criteria for palaeo-ice streaming, as outlined by Stokes and Clark (1999) and discussed in detail in Section 3.3.3. Fs-4 displays four out of eight of these criteria, shown in Table 7.2. These are: characteristic shape and dimensions; highly

attenuated bedforms, abrupt lateral margins and presence of deformed till. The evidence for these will be discussed in detail below. Table 7.2 also contains the criteria for both a surging glacier landsystem (Evans and Rea, 1999) and an ice-marginal terrestrial landsystem at the Laurentide Ice Sheet margin (Colgan *et al.*, 2003) because they share a number of characteristics with the palaeo-ice stream landsystem and should be considered as equally plausible explanations.

Table 7.2 – Comparison of mapped evidence from Fs-4 with characteristics of palaeo-ice stream, surging glacier and ice-marginal terrestrial landsystems. Red indicates criteria present in this study area. See Sections 3.3.3 and 3.3.5 for a full discussion of these criteria.

Ice stream landsystem (Stokes and Clark, 1999)	**Surging glacier landsystem** (Evans and Rea, 1999)	**Ice-marginal terrestrial landsystem** (Colgan *et al.*, 2003)
Characteristic shape and dimensions	Thrust-block moraine	Drumlins
Highly convergent patterns	Concertina eskers	Hummocky end moraine
Highly attenuated bedforms	Crevasse-squeeze ridges	Eskers
Boothia-type dispersal train	Highly attenuated bedforms	Small push moraines
Abrupt lateral margin	Hummocky moraine	Deformed sediments
Lateral shear moraine	Complex till stratigraphies	Outwash plain
Deformed till	Thrusting/squeezing	
Trough mouth fan		

7.2.1.1 Characteristic shape and dimensions

The characteristic shape of a terrestrial palaeo-ice stream is described by Stokes and Clark (1999) as converging flow lines in the onset zone feeding into a main channel of streaming ice (see Figure 3.5), before diverging again towards the terminus (Stokes and Clark, 2003). Towards the northern extent of the flow-set the lineations diverge and there is a well defined main trunk of elongate lineations to the east of Laguna Cabeza del Mar (see Figure 6.7). It is not possible to identify converging flow lines up-ice because the area where these might be expected to exist is occupied by the marine embayment of Seno Otway. Kilian *et al.* (2007) obtained echo sounding profiles of the relatively shallow (< 220 m) eastern end of Seno Otway but did not detect subaqueous moraines or other landforms. Stokes and Clark (1999) suggested that palaeo-ice streams are characteristically greater than 150 km long and 20 km wide; Fs-4 is over 60 km long and 20 km wide. This represents the terrestrial record of the ice stream, it seems likely that the full dimensions would have extended further back into Seno Otway and eastwards into the Strait of Magellan. It is therefore speculated that the ice stream could have been over 120 km long and 30 km wide.

7.2.1.2 Highly attenuated bedforms

Fs-4 contains a large number of lineations with high elongation ratios, particularly in the main channel east of Laguna Cabeza del Mar (Figure 7.2). Stokes and Clark (1999) suggested that lineations with elongation ratios > 10:1 may record the flow direction and spatial extent of palaeo-ice streams. Many of the lineations in the central trunk of Fs-4 have elongation ratios of this order, the largest of which is as high as 35:1 (see Table 7.1). Many of the lineations are > 1 km long in the central trunk and the largest examples are up to 3 km long. These streamlined lineations could be classified as highly attenuated drumlins or lineations, rather than MSGL which are typically suggested to be between 8 km and 70 km in length (Clark, 1993).

The spatial variation of lineation lengths and elongation ratios is also thought to be characteristic of palaeo-ice streams, both laterally and longitudinally (Hart, 1999; Ó Cofaigh *et al.*, 2005; Hess and Briner, 2009). Figure 7.2 clearly shows a lateral transition of both lengths and elongation ratios in the area surrounding Laguna Cabeza del Mar, with the longest and most elongate lineations focused within a narrow zone to the east of the lake. The occurrence of more elongate bedforms towards the central axis of flow of palaeo-ice streams, where ice velocities are likely to have been higher, is well documented (Dyke and Morris, 1988; Hart, 1999; Stokes and Clark, 2002a, 2003; Ó Cofaigh *et al.*, 2005). This lateral pattern of bedform elongation was also identified by both Clapperton (1989) and Benn and Clapperton (2000a), who noted that streamlined features tended to increase in elongation towards the central zone of drumlins east of Laguna Cabeza del Mar. The length and width of lineations within Fs-4 is variable, with shorter and longer lineations occurring adjacent to each other. This is similar to MSGL observed beneath the Rutford Ice Stream (King *et al.*, 2009). The orientation of lineations throughout the flow-set exhibit a high degree of parallel concordance, both as an overall group and in relation to lineations in close proximity. There are no obvious examples of cross-cutting lineations within the flow-set which suggests it formed isochronously (Clark, 1999).

7.2.1.3 Abrupt lateral margins

Palaeo-ice streams can be expected to have abrupt lateral margins, created by a sharp zonation between evidence for fast ice flow and non-streamlined terrain (Stokes and Clark, 1999). Fs-4 appears to display such a margin west of Laguna Cabeza del Mar, where there is a clearly defined boundary to the area of drumlins.

7.2.1.4 Deformed sediment

The location of some ice streams has been associated with the presence of a soft sedimentary basin (Anandakrishnan *et al.*, 1998; Bell *et al.*, 1998; Studinger *et al.*, 2001). This has led to the suggestion that evidence for spatially extensive deformable till could be consistent with palaeo-ice stream activity (Stokes and Clark, 1999), although it is also important to note that this association is by no means exclusive. Although no direct evidence for deformed sediment can be identified purely from the mapping in this study, Clapperton (1989) suggested that a potentially deformable bed existed in the region. Southern Patagonia is a region that has undergone repeated glaciation-deglaciation. Thus, each ice advance over low-lying ground would have crossed earlier Quaternary deposits (Clapperton, 1989). The lineations in the area surrounding Laguna Cabeza del Mar may overlie thick sequences of earlier glaciofluvial and glaciolacustrine sediments, evidence for which can be seen in the stratigraphy of a cliff exposure on the eastern side of the lake (see Fig. 9 in Clapperton, 1989). The thickness of these sediments may be as much as 25 m in the hollow that the main zone of lineations lies in (Clapperton, 1989). Benn and Clapperton (2000a) also described evidence for the deformation of sediments on the western side of the Strait of Magellan. The analysis of coastal sections revealed an upper layer of up to 30 m of folded and faulted sediment. This was thought to record a single episode of glacitectonic deformation and was attributed to ice streaming out of the Otway basin (Benn and Clapperton, 2000a).

7.2.1.5 Other landsystems

As discussed in Section 3.3.5 and shown in Table 7.2, there is overlap between the criteria for palaeo-ice streaming and for both a surging glacier landsystem (Evans and Rea, 1999) and an ice-marginal terrestrial landsystem for the southern Laurentide Ice Sheet margin (landsystem B in Colgan *et al.*, 2003). Therefore, it is no surprise that evidence exists within Fs-4 for elements of both of these alternative landsystem classifications. Highly attenuated bedforms are present in both, as is evidence for deformable sediment. In the surging glacier landsystem, the presence of a deformable substrate is included within the characteristic of 'complex till stratigraphies' (Evans and Rea, 1999). Colgan *et al.* (2003) suggested that extensive subglacial deformation occurs in the drumlinised zone of the ice-marginal terrestrial landsystem. No further evidence matching the criteria for glacier surging can be identified from the mapping, although Benn and Clapperton (2000a) described an outer zone of unmodified thrust moraines to the west of the main streamlined zone of Fs-4. The presence of eskers and an extensive outwash plain within the main zone

of lineations are two further features that match criteria for the ice-marginal terrestrial landsystem described by Colgan *et al.*, (2003).

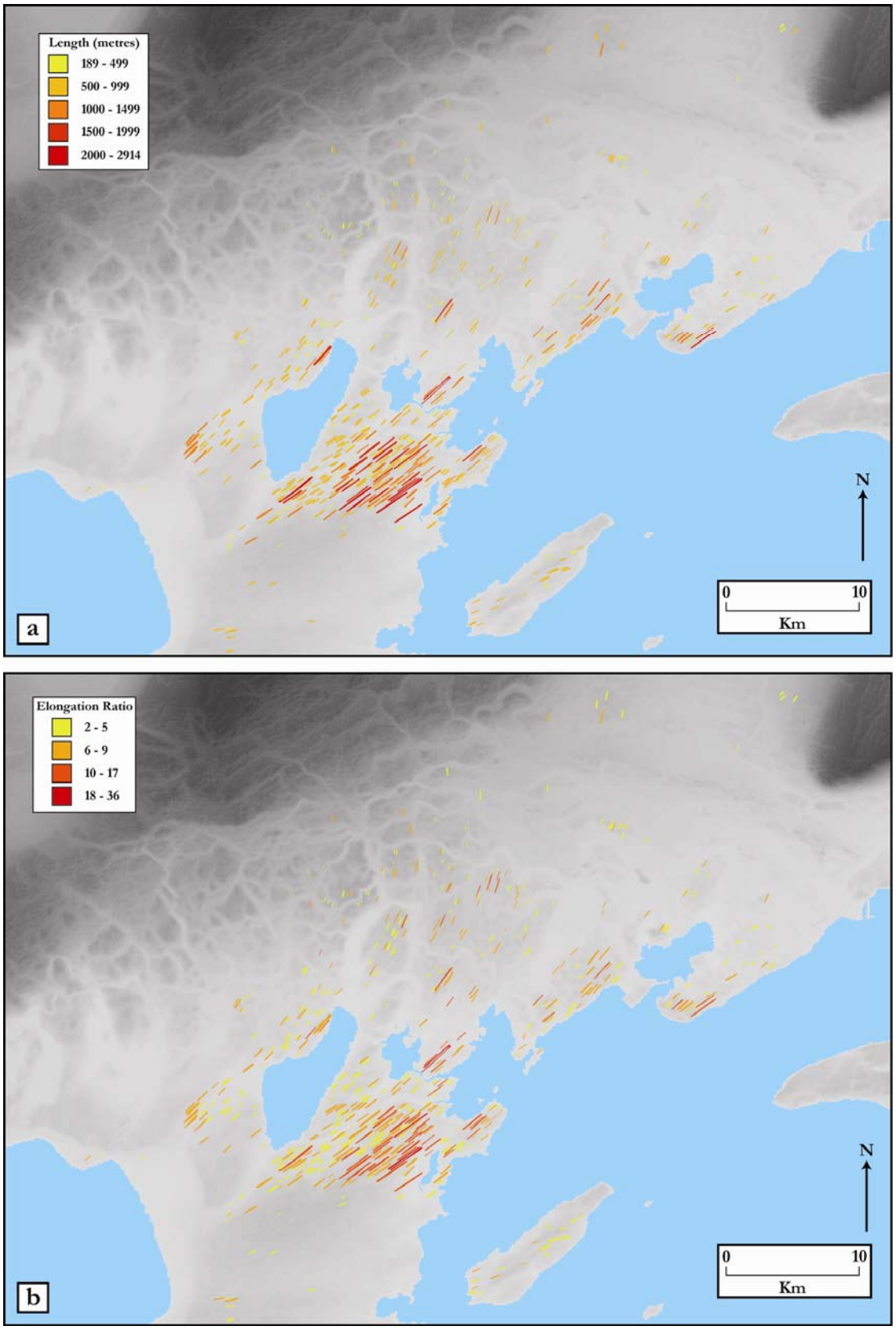

Figure 7.2 – (a) Lineations in Fs-4 coloured by length; (b) Lineations in Fs-4 coloured by elongation ratio.

Despite the mapped evidence matching some of the criteria for both a surging glacier landsystem and an ice-marginal terrestrial landsystem at the southern Laurentide margin, it seems most likely that Fs-4 represents the track of a palaeo-ice stream. This supports Clapperton (1989) and Benn and Clapperton (2000a) who suggested that the pattern of streamlining and the topography in this area were indicative of a longitudinal zone of ice streaming out from the Seno Otway basin. When assessing the characteristics of different landsystems it is clear that some criteria are generic and occur in a number of landsystems. Criteria that are unique to a particular landsystem could be described as diagnostic. Therefore, it is the presence or absence of diagnostic criteria that best allows for the classification of a particular landsystem. An example of generic criteria in this case would be the presence of highly attenuated bedforms. Streamlined lineations with high elongation ratios are a key indicator of fast ice flow, consequently they feature within all three landsystems. Alone this would not be sufficient evidence to allow the classification of a landsystem. However, the clear lateral variation in both length and elongation ratio of lineations within Fs-4 (see Figure 7.2), with the highest values concentrated towards the expected central axis of flow, is unique to palaeo-ice streaming (Dyke and Morris, 1988; Hart, 1999; Stokes and Clark, 2002, 2003; Ó Cofaigh *et al.*, 2005). A second diagnostic characteristic of a palaeo-ice stream is the distinctive shape and dimensions (Figure 3.3). The shape of Fs-4 shows a main trunk of elongated lineations grading into a divergent pattern towards the northern margin of the flow-set. This matches the simplified configuration for a terrestrial ice stream outlined by Clark and Stokes (2003). The lack of a convergent zone up-ice from the main streamlined channel can be explained by its likely coincidence with Seno Otway. The dimensions of the flow-set are also of the order of that expected for ice streams (Stokes and Clark, 1999). Neither alternative landsystem includes such a characteristic shape. Thirdly, the presence of what appears to be an abrupt lateral margin to the main zone of streamlined lineations is unique to palaeo-ice streams because it marks the sharp zonation between streaming and non-streaming ice flow (Stokes and Clark, 1999). Such an abrupt margin might also be expected for a surging glacier, between fast-ice flow and no ice. However, there is clear evidence for the presence of ice outside of this main zone of lineations. The presence of deformed sediment in the study area as suggested by Clapperton (1989) and Benn and Clapperton (2000a) is not a diagnostic characteristic of palaeo-ice streaming because it features in both alternative landsystems. However, when viewed collectively alongside the aforementioned diagnostic criteria it lends support to the interpretation of Fs-4 as a palaeo-ice stream track.

The absence of diagnostic criteria can also aid the classification of a landsystem. Concertina eskers and crevasse-squeeze ridges are unique to the surging glacier landsystem (Evans and Rea, 1999). Neither has been identified in the study area from remote sensing and no mention is made of such features in previous studies that have conducted fieldwork in the region (e.g. Clapperton, 1989; Benn and Clapperton, 2000a). It would be difficult to classify Fs-4 as a surging glacier landsystem without the presence of these key diagnostic characteristics. In addition, the cyclical nature of surging glaciers (Evans and Rea, 1999) suggests that ice reoccupies the same areas again and again. Such activity might be expected to produce a time-transgressive record (Clark, 1999). However, no evidence for readvances or overriding has been found within Fs-4, suggesting that the landform record was produced isochronously (Clark, 1999). The ice-marginal terrestrial landsystem of Colgan *et al.* (2003) contains only generic criteria. This makes it difficult to confidently rule-out this landsystem.

There is a marked similarity between the landform record in the Strait of Magellan and that reported from former ice lobes of the southern Laurentide Ice Sheet margin (e.g. Clark, 1992; Patterson, 1997, 1998; Jennings, 2006; Evans *et al*., 2008). These are thought to be the termini of ice streams (Patterson, 1997, 1998; Jennings, 2006; Evans *et al*., 2008), although they have also been interpreted as surging lobes (Clayton *et al.*, 1985; Colgan and Mickelson, 1997), highlighting the possible confusion when classifying the Strait of Magellan landsystem. The presence of a clearly defined lobate margin and streamlined landforms are key shared characteristics between the landsystems. In addition, Benn and Clapperton (2000a) reported unmodified thrust moraines in the Strait of Magellan region, a further feature of the southern Laurentide lobes (Patterson, 1997; Jennings, 2006; Evans *et al*., 2008). It is possible that some of the moraines mapped in this study are thrust moraines, but fieldwork would be necessary in order to test this. The similarity between the landsystem of Fs-4 and the southern Laurentide lobes lends support to the interpretation of a terrestrial palaeo-ice stream in the Strait of Magellan area. However, the geomorphological signature of terrestrial ice streams is much less well known than that for marine-terminating palaeo-ice streams (Evans *et al*., 2008), and clearly shares many characteristics with surge landscapes (e.g. Evans and Rea, 1999). This raises the possibility of the landsystem being misinterpreted.

When all of the geomorphological evidence is drawn together, the landsystem of Fs-4 seems to fit best with that of a terrestrial palaeo-ice stream, similar to the lobes of the southern Laurentide Ice Sheet margin (Patterson, 1997; Stokes and Clark, 1999). It is

noted that evidence for fast ice flow does not explicitly suggest the existence of an ice stream (Stokes and Clark, 1999), hence the overlap with certain characteristics of surging glaciers (Evans and Rea, 1999). However, as the geomorphological record also matches other aspects of the ice stream template, including size, shape and abrupt lateral margins, then it seems most likely that it is indicative of ice-stream activity (Stokes and Clark, 1999). It is argued that the presence of diagnostic criteria for palaeo-ice streaming and the absence of diagnostic criteria for a surging glacier supports the classification of Fs-4 as a terrestrial palaeo-ice stream track. It is acknowledged that alternative landsystems are possible and further fieldwork is required before these can be discarded.

7.2.2 Classification of other flow-sets

Eight other flow-sets have been identified in the study area, which can be classified according to the categories of Kleman *et al.* (2006). These categories are defined in Section 4.3 of this study. The lack of evidence within these flow-sets means that often there is an equally-plausible alternative classification. Fs-2 could be interpreted as an event flow-set, based on its abundant ice flow traces and apparent lack of aligned eskers (see Figure 7.1 for location of all flow-sets). However, eskers are absent throughout much of the study area. It is therefore difficult to assign a classification based solely on this absence and so Fs-2 could equally be a deglacial flow-set. The location and orientation suggests ice flow within the Magellan lobe. There are no obvious examples of cross-cutting lineations and so it is inferred that the flow-set formed isochronously (Clark, 1999). Based on its lineation record, Fs-5 is interpreted as an isochronous event flow-set, although it could also be a wet-based deglaciation flow-set. Many of the lineations of Fs-5 are orientated approximately 45° to those of Fs-4, indicating that they formed at different times. However, it is also possible that Fs-5 contains the area of ice flow indicators described as ‘drumlinised sediment masses’ by Benn and Clapperton (2000a), which were suggested to have formed coevally with the zone of streamlined lineations of Fs-4. The orientation of Fs-5 suggests ice flow towards the interlobate margin of the Skyring and Otway lobes.

Fs-3, Fs-6, Fs-7 and Fs-8 are all closely associated with ice-marginal meltwater channels aligned both sub-parallel and perpendicular to lineation direction. No eskers have been identified within these flow-sets. Despite this a deglacial classification is favoured. This is mainly based on their location close to the inferred position of a retreating combined Skyring-Otway lobe as indicated by moraine ridges and ice-marginal meltwater channels.

Alternatively these could all be event flow-sets recording ice flow within the lobes. There is no obvious evidence for cross-cutting lineations, suggesting these flow-sets formed isochronously. Fs-3, Fs-6 and Fs-7 are all orientated approximately perpendicular to Fs-4 and the alignments of Seno Skyring, Seno Otway and the Strait of Magellan. This indicates that they could not have formed at the same time as Fs-4. Fs-1 and Fs-9 are both faint flow-sets which contain very little information, making classification difficult. Both are closely associated with small meltwater channels and have no evidence of aligned eskers. Fs-1 is inferred to have formed close to the ice sheet margin based on its location and could represent a deglacial flow-set. Fs-9 is located on higher ground on Isla Riesco and is orientated towards Seno Otway. It could have formed during deglaciation as ice retreated back towards the Seno Otway basin. However, these could both alternatively be event flow-sets.

7.3 Ice margin reconstruction

Ten former ice-margins have been reconstructed in the study area, shown in Figure 7.3. These have been delimited according to a combination of geomorphological evidence, topography and published limits (e.g. Caldenius, 1932; Clapperton *et al.*, 1995; Benn and Clapperton, 2000a, b; Bentley *et al.*, 2005; Kilian *et al.*, 2007). The geomorphological evidence that has been used consists predominantly of moraine ridges and ice-marginal meltwater channels. Margins delimited according to these features are shown as solid lines in Figure 7.3. Inferred margins have been used where there are gaps between solid margin evidence and are represented by dashed lines on Figure 7.3.

The majority of margin 10 has also been classed as an inferred margin. This is because it is based on the well-established local LGM position, or 'Advance B', as agreed upon by many studies (Clapperton *et al.*, 1995; Benn and Clapperton, 2000a, b; Bentley *et al.*, 2005; McCulloch *et al.*, 2005a; Kilian *et al.*, 2007) rather than by evidence mapped in this study. The margin 10 position of the Otway lobe as show in Figure 7.3 (in brown) is thought to be synchronous with the positions of the Skyring and Magellan lobes (e.g. Clapperton *et al.*, 1995; Kilian *et al.*, 2007), but the lack of dates in Seno Otway means that this has never been substantiated. Speculative margins (dash-dot line on Figure 7.3) have been determined at glaciologically-plausible intermediate positions in between positions with more robust evidence and in places are guided by the position of ice-marginal meltwater channels.

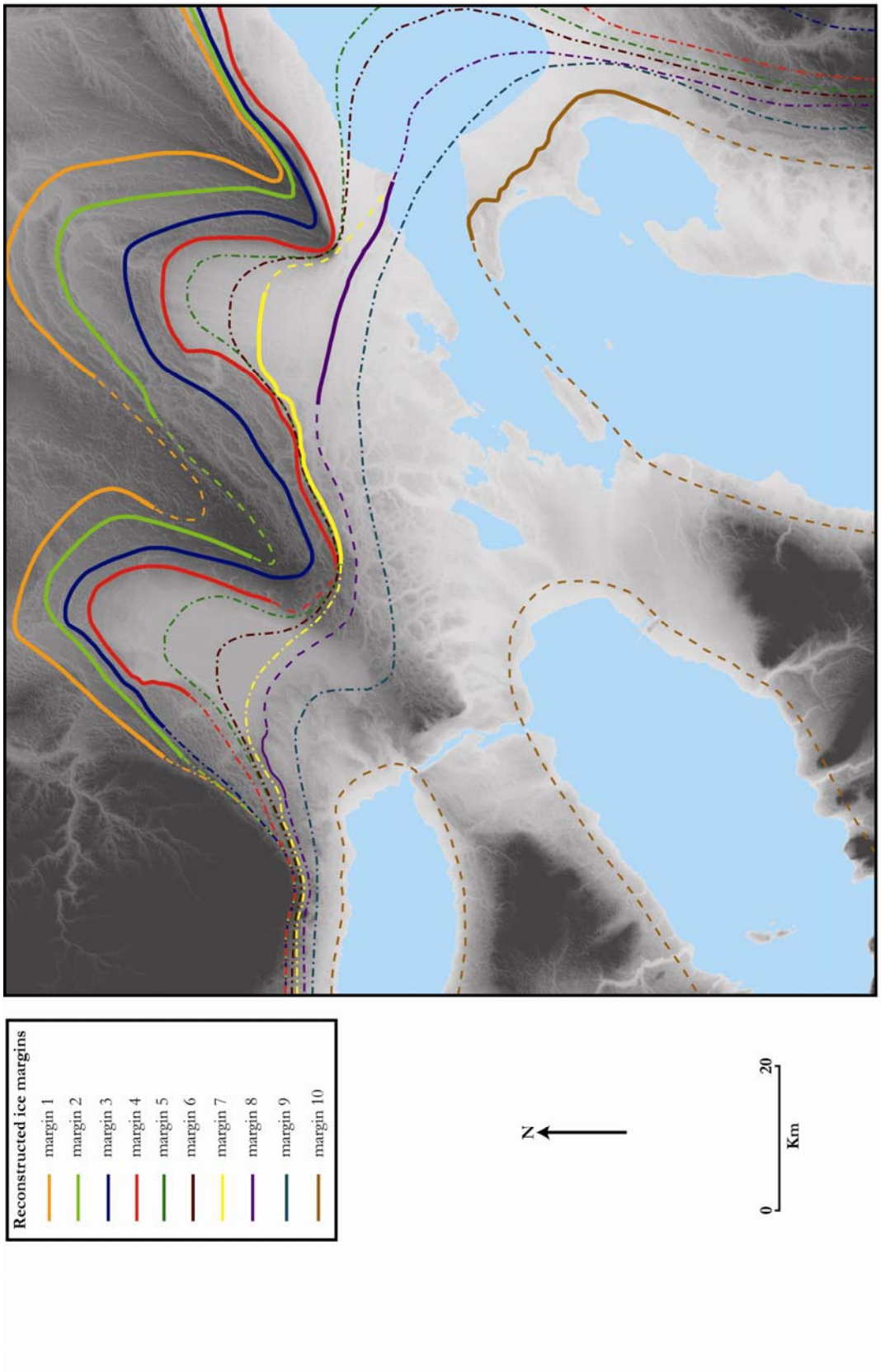

Figure 7.3 – Reconstructed former ice margins, compiled from a combination of geomorphological evidence (thicker lines) and previous work. Where evidence is lacking margins have been inferred (dashed line) or speculated (dash-dot line). Some of the inferred and speculative margins are based on previous work, including Caldenius (1932), Clapperton et al. (1995), Benn and Clapperton (2000a), Bentley et al. (2005) and Kilian et al. (2007).

7.4 Proglacial lake reconstruction

Former lake shorelines have been mapped around Laguna Blanca (see Figure 6.10), indicating the presence of a larger lake at some point. The topography of the region and the position of a number of the reconstructed ice margins shown in Figure 7.3 appear to support this. When the ice margin position and the higher topography blocked off the lower ground contained within both the former Skyring and Otway lobes it is likely that ice-dammed proglacial lakes would have formed. Margins 5 to 9 fit these criteria and, given the availability of sufficient meltwater, ponding would have occurred in front of the ice margin at these positions.

The reconstruction of the proglacial lakes has been achieved by manipulating a DEM of the study area. Following the methods of Jansson (2003) and Stokes and Clark (2004), contemporary drainage routes (slopes) are dammed by the former ice margin. This affect was achieved by clipping the DEM to the shape of the margin. The DEM was then incrementally shaded in every 10 m, ponding water until the point where a spillway is breached. A step-by-step example of this is shown in Figure 7.4.

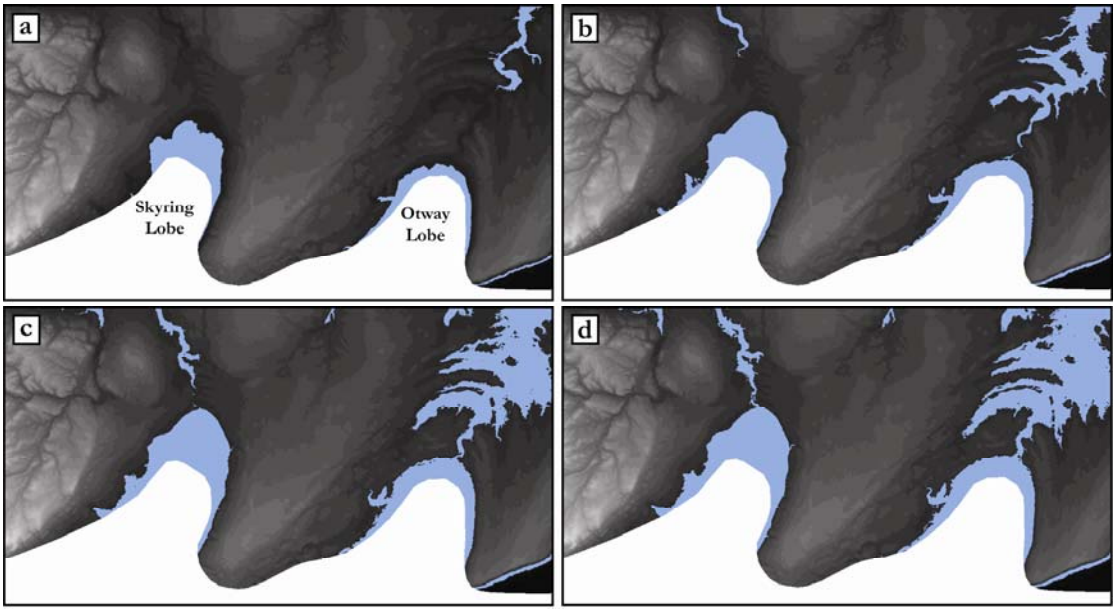

Figure 7.4 – Example of reconstruction of proglacial lakes dammed by the former ice margins. This figure shows the process by which the lakes have been reconstructed at margin 5, by incrementally colouring the topography blue by ten metre increases until a spillway is breached. (a) shows initial filling-up of the lake up to 150 m altitude; (b) shows proglacial Lake Otway at its greatest extent immediately prior to breaching the spillway to the north at 174 m altitude; (c) shows proglacial Lake Skyring at its greatest extent immediately prior to breaching the spillway to the north at 187 m; (d) shows both lakes having breached their spillways.

There are a number of limitations associated with this method of reconstructing proglacial lakes. Stokes and Clark (2004) acknowledged that the use of a 1-km DEM could result in narrow spillways being missed as the lake is filled. This could result in significantly

lowering the lake level or compromising lake existence entirely. The DEM used in this lake reconstruction has a 90 m pixel resolution and it is hoped that this increased resolution will significantly reduce the chance of missing all but the smallest spillways. A further limitation acknowledged by Stokes and Clark (2004) is the assumption that the thickness of the ice margin is always sufficient to prevent drainage over or along the top of the ice margin itself. Similarly to Stokes and Clark (2004), this study assumes that a parabolic ice marginal profile will generally be thick enough to prevent substantial lateral drainage across the ice front. Also, the lake reconstructions do not take isostatic rebound (e.g. Walcott, 1973) into account and assumed the topography at this time was the same as present-day. An additional limitation was encountered when trying to calculate the maximum depth of lakes ponded within the Skyring lobe. The contemporary lake level of Laguna Blanca is at an altitude of 110 m and the DEM has no data below the lake surface. Therefore, any calculated depths for proglacial Lake Skyring are almost certainly underestimated (see Table 7.3).

Figure 7.5 shows the reconstructed lakes at margin 5 to margin 9. Lakes pond against both the Skyring and Otway lobes at margins 5, 6 and 7. Proglacial Lake Otway has a maximum depth of 107 m and covers 229 km^2 at margin 7 (see Table 7.3). Lake Skyring increases in size to 392 km^2 by margin 7. Both lakes breach spillways to the north at each margin (indicated by red arrows on Figure 7.5). By margin 8 ice has retreated back from the topographic high of the large scarp to the east of the Otway lobe. This allows Lake Otway to drain directly towards the Strait of Magellan. Lake Skyring increases to 437 km^2 and continues to drain through the spillway to the north. At margin 9, Lake Skyring reaches a maximum size of 579 km^2 before simultaneously breaching both the northern spillway and a lateral spillway at the south eastern extent of the lake (see Figure 7.5). The reconstructed bathymetries of Lakes Skyring and Otway are shown in Figure 7.6.

Table 7.3 – Calculated areas and maximum depths at the margin for the Skyring and Otway proglacial lakes at each margin position. * indicates depth to current lake level of Laguna Blanca, rather than absolute depth.

	Proglacial Lake Skyring			**Proglacial Lake Otway**		
Margin	Area (km^2)	Maximum depth at margin (m)	Volume (km^3)	Area (km^2)	Maximum depth at margin (m)	Volume (km^3)
5	180	76*	7	80	72	2
6	312	76*	17	157	94	9
7	392	76*	23	229	107	14
8	437	71*	25			
9	579	76*	31			

Figure 7.7 shows how the reconstructed lakes match with mapped geomorphological evidence. The position of the northern spillway of Lake Skyring matches with the large proglacial meltwater channel labelled 'Channel C' in Figure 6.10 (see Figure 7.7a). Similarly, the spillway to the north of Lake Otway matches with a proglacial meltwater channel mapped as 'Channel E' in Figure 6.13. This is shown in Figure 7.7c. Lake Skyring at margin 9 also breaches a lateral spillway at the south eastern edge of the lake. This matches with the large ice-marginal channel labelled 'Channel A' in Figure 6.12a (also shown in Figure 7.7d). Figure 7.7b shows the series of former lake shorelines around Laguna Blanca. These can also be seen in Figures 6.10 and 6.19. When superimposed on top of the maximum northern extent of Lake Skyring, the outermost reconstructed shoreline matches very closely to the mapped shoreline. The inner shorelines, labelled 1 to 3 in Figure 6.19, are interpreted as representing the decreasing level of Lake Skyring as the Skyring lobe retreated. The point should be made here that the *maximum* extent of the lakes at different margins as indicated in Figure 7.5 should be viewed as exactly that, and that it is quite possible that the lakes existed at lower levels. Therefore, shorelines 4 to 1 shown in Figure 6.19 could conceivably represent decreasing lake levels associated with the retreat of the Skyring lobe from margin 5 through to margin 9 (see Figure 7.3).

7.4.1 Proglacial Lake drainage

The size of the Lake Skyring spillways suggests a significant drainage event occurred at some point. Channel A, the spillway which drains from the south eastern edge of Lake Skyring at margin 9, is up to 400 m wide and stretches for over 50 km in an easterly direction towards the Strait of Magellan (see Figure 6.12a). This ice-marginal channel is the largest in an extensive meltwater system that grades into a large outwash plain. The size of this meltwater system indicates a dynamic drainage event towards the Strait of Magellan. Such an event has been postulated in a number of previous studies but has never been expanded upon (Caldenius, 1932; Mercer, 1976; Benn and Clapperton, 2000a). Benn and Clapperton (2000a) suggested that the size and plan form of the channels could have been cut "by a high magnitude drainage event, possibly a jökulhlaup associated with the drainage of a proglacial lake to the west". The matching of the spillway with this meltwater system appears to be strong evidence for the abrupt drainage of proglacial Lake Skyring towards the Strait of Magellan.

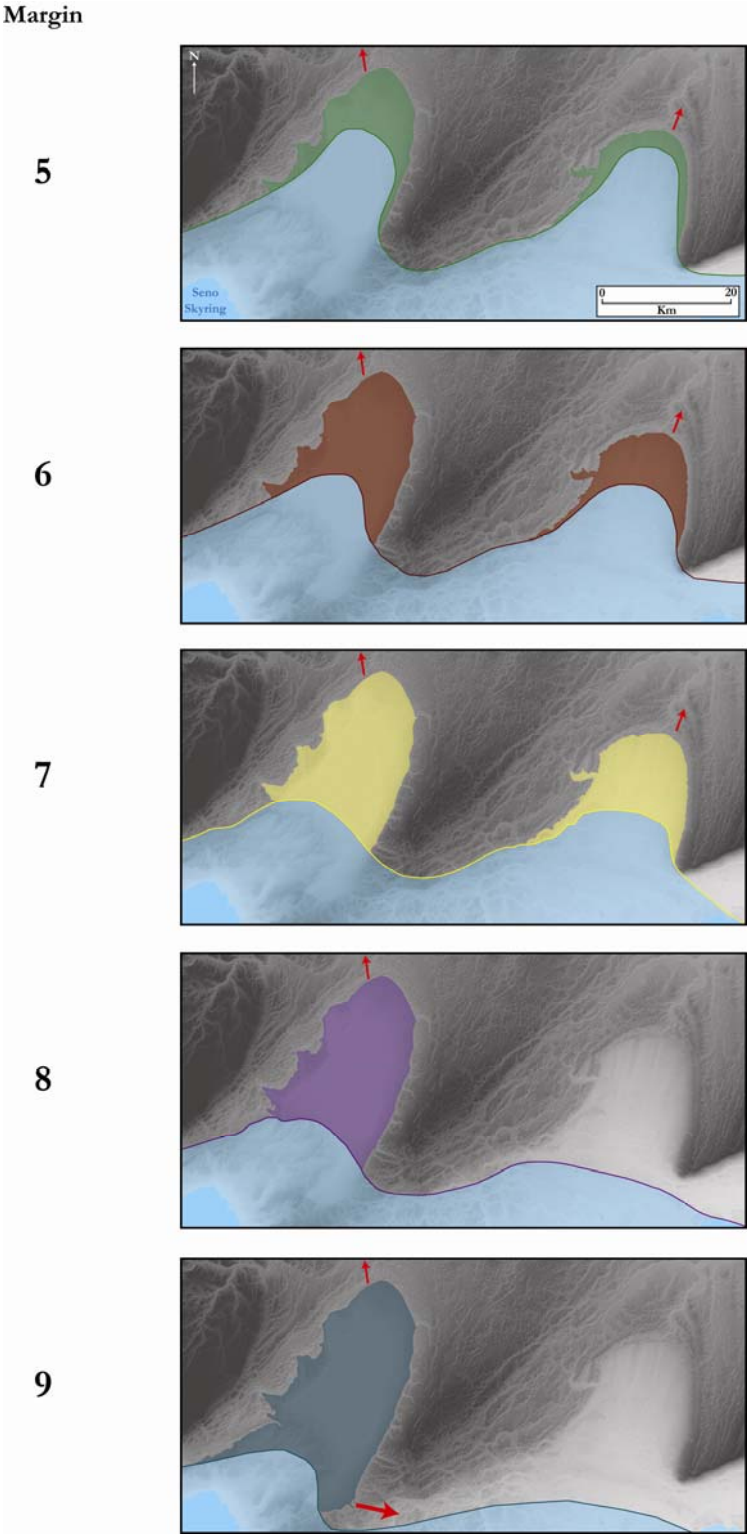

Figure 7.5 – Reconstructed proglacial lakes at their maximum extents immediately prior to breaching a spillway. Red arrows indicate position of spillway breach and direction of drainage. Margin numbers and colours correspond to those in Figure 7.3.

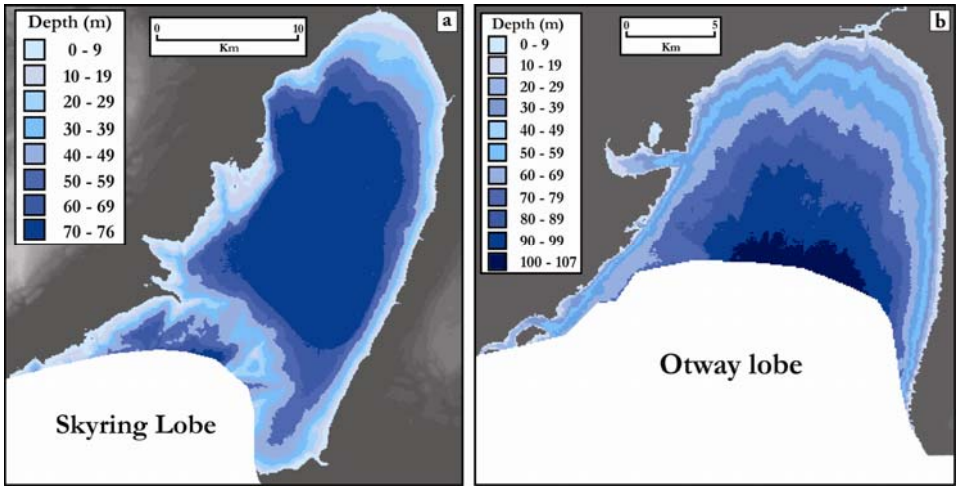

Figure 7.6 – Bathymetries of reconstructed proglacial Lake Skyring at margin 9 (a) and Lake Otway at margin 7 (b).

At margin 9, at the greatest extent of Lake Skyring, the lake contained in the region of 31 km^3 of water (see Table 7.3). The rapid drainage of a water volume of this order could quite conceivably have cut the large channels that have been mapped in this area. The sudden drainage of Lake Skyring at this time is further supported by the lack of lake shorelines around Laguna Blanca lower than shoreline 1 (see Figure 6.19), suggesting that the lake level fell rapidly. The direction of flow of meltwater from this significant drainage event would have partly been guided by the position of the ice margin and partly guided by the natural slope towards the Strait of Magellan (see Figure 6.12c). The orientation of the ice-marginal meltwater channel systems and the outwash plain appear to support this.

The drainage of Lake Skyring and Lake Otway via the northern proglacial spillways seems likely to have been a constant stream flow, rather than sudden drainage events. The size of Channel E (see Figures 6.13 and 7.7a) supports this because it is much smaller (ca. 150 m wide) than the larger spillway of Channel A. The fact that lakes continue to form in both the Skyring and Otway lobes and continue to breach the same spillways at each margin indicates that drainage was probably much more gradual. The close spacing of former shorelines around Laguna Blanca also supports this view. If Lake Skyring constantly drained through abrupt events then the shorelines would be expected to be spaced further apart. The reasoning for this is that the rapid drainage of the lake would lead to a considerable lowering of the lake level and so a bigger difference in altitude between former shorelines.

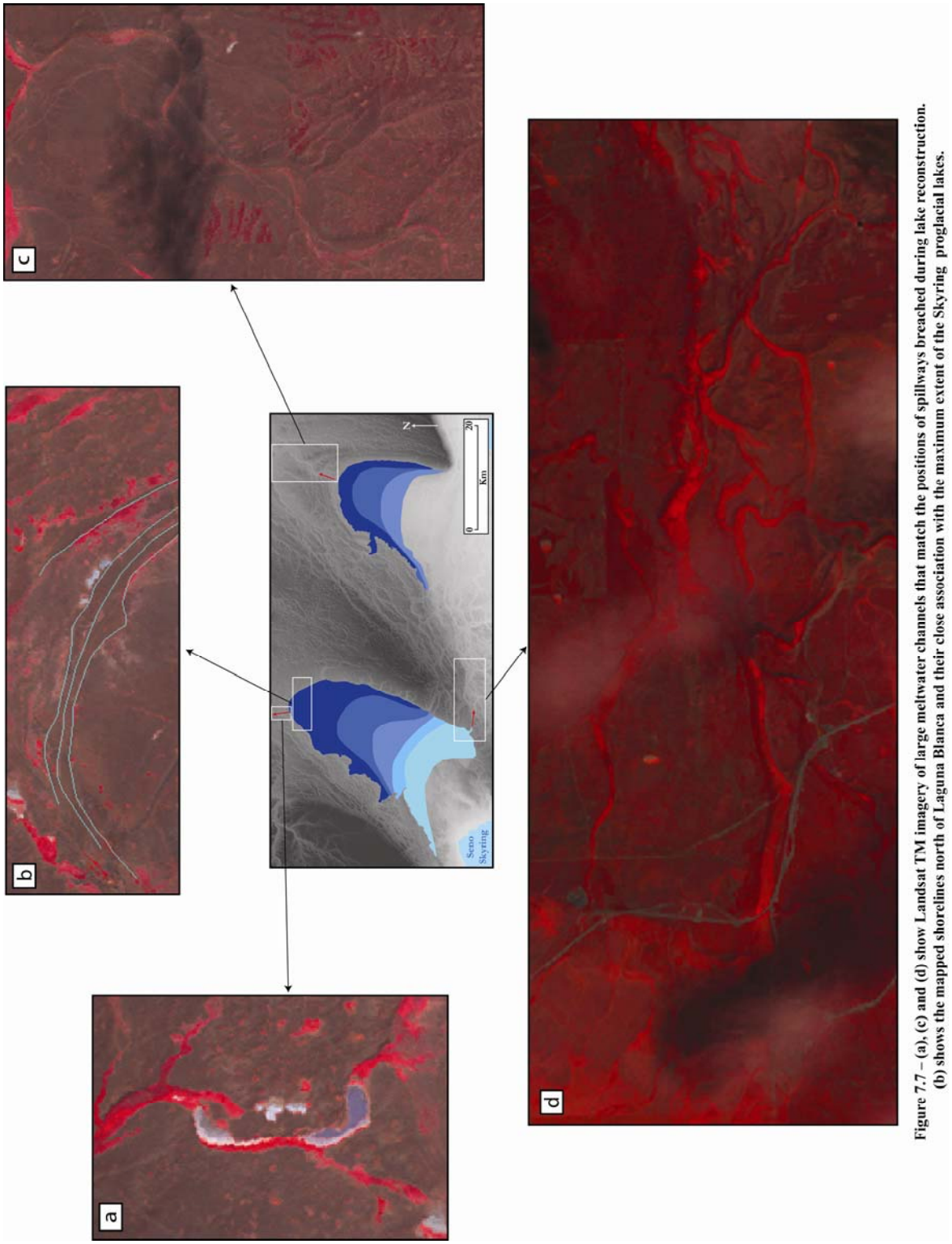

Figure 7.7 – (a), (c) and (d) show Landsat TM imagery of large meltwater channels that match the positions of spillways breached during lake reconstruction. (b) shows the mapped shorelines north of Laguna Blanca and their close association with the maximum extent of the Skyring proglacial lakes.

There appears to be evidence for further abrupt drainage events within the study area. This is inferred from the presence of scarp lines either side of the Fitz Roy Channel (see Figure 6.21). These are interpreted as scarps that may have been formed by meltwater channels running through the modern-day channel, perhaps as water drained from the proglacial lake of Seno Skyring into that of Seno Otway. It is suggested that such a lake could have formed when ice withdrew into the Skyring basin. Mercer (1970) suggested that drainage through the Fitz Roy Channel occurred during glacier retreat from the Advance B (LGM) limit to the Advance D limit and that meltwater drained eastwards towards the Atlantic Ocean. McCulloch *et al.* (2005b) argued that a proglacial lake dammed within the Strait of Magellan drained westwards towards the Pacific Ocean through the Fitz Roy Channel following retreat from the Advance D limits. These features have also been interpreted as moraine ridges in previous work (Glasser and Jansson, 2008). This indicates that further fieldwork is necessary before a more robust interpretation of these features can be made.

Lake drainage events of the type suggested here would have produced a sudden input of freshwater into the oceans, similar to the late-glacial drainage events of the Strait of Magellan (McCulloch *et al.*, 2005b) and LBA (Turner *et al.*, 2005). It has been estimated that up to 1,988 km^3 of lake water was discharged into the Pacific Ocean during the LBA event (Turner *et al.*, 2005), which may have had an impact on sea surface temperature and salinity records (e.g. Lamy *et al.*, 2001, 2004). It is possible, although admittedly unlikely considering the comparative sizes of the lakes (see Table 7.3), that the abrupt drainage of Lake Skyring had an effect on local sea surface temperatures and salinity in the south western Atlantic Ocean.

7.5 Ice sheet reconstruction

This section draws together the classified flow-sets, delimited ice-marginal positions and reconstructed proglacial lakes into a glaciologically and chronologically-plausible reconstruction of this sector of the Patagonian Ice Sheet. Figure 7.8 shows this reconstruction in 10 panels, labelled time-steps 1 to 10 in chronological order from oldest (time-step 1) through to most recent (time-step 10). The pattern of increasingly less-extensive margins matches the trend since the GPG identified by Kaplan *et al.* (2009). The 10 time-steps represent the position of the ice sheet at the 10 ice margins delimited in Figure 7.3. This section will describe each time-step in detail and explain the reasoning for each stage of the reconstruction. It is difficult to determine whether each time-step margin records glacier advance or retreat without further evidence (e.g. sedimentology), and so

these have been speculated. It should be noted that the ice sheet reconstruction is superimposed on top of the present-day topography and so does not take into account isostatic rebound (e.g. Walcott, 1973). In addition, global sea level would have been significantly lower. For example, during the LGM global sea level was over 120 m lower than at present (McCulloch *et al.*, 2005a) and Sugden *et al.* (2009) suggested that sea level was 90 m lower at the time of Advance A.

An attempt has been made to place all the identified flow-sets within the reconstruction. Many of the flow-sets are aligned perpendicular to the main ice lobes and are, therefore, very difficult to explain glaciologically. There is also little overlap between flow-sets and no dating, making it very difficult to order them into relative age stacks (cf. Kleman *et al.*, 2006). As a result, flow-sets have been placed in possible positions within the reconstruction, but many of them could equally have formed at any of the time-steps shown in Figure 7.8 or during a more extensive glaciation.

7.5.1 Time-steps 1 to 4

Time-step 1 represents the oldest and most extensive position of the Skyring, Otway and Magellan lobes in the study area. The delimitation of this margin is based on scattered moraine ridges and lateral meltwater channels. Where evidence is lacking, such as between the lobes, the margin has been inferred based on lateral meltwater channels and the topography. The western margin of the Skyring lobe has also been speculated based on the topography and the position of Seno Skyring. It seems likely that the highest areas of Isla Riesco (up to 675 m) and Península Brunswick (up to 615 m) would have remained ice-free (see panel 1 of Figure 7.8). The ice sheet profiles shown in Figure 7.9 have been calculated using the parabolic formula $h = Ax^{½}$ of Mathews (1974), where h is the height above the terminus, x is the distance up-ice from the terminus and A is a coefficient which varies from glacier to glacier. A has been taken to be 1.0 $m^{½}$ for the purposes of this study because this figure corresponds to values for several ice lobes with low surface gradients in the south western Laurentide Ice Sheet (Mathews, 1974). The assumption has been made that the Skyring and Otway lobes had similarly low surface profiles, as has previously been suggested for glaciers in low-lying areas east of the Andes (Glasser and Jansson, 2005; Kaplan *et al.*, 2009), including the Strait of Magellan (Benn and Clapperton, 2000a). Using this calculation, the Otway lobe would have had a surface elevation of 556 m at a distance of 120 km up ice from the terminus, and the Skyring lobe would have had a surface elevation of 560 m at a distance of 90 km up ice from the terminus. As shown on

Figure 7.9, based on this formula ice would not have overtopped the high areas of Península Brunswick and Isla Riesco at these points. This is supported by Sugden *et al.* (2009), who suggested that Isla Riesco would have been ice free at the time of Advance A, although in their reconstruction Península Brunswick is covered. Ice flow was focused along the Skyring, Otway and Magellan basins before flowing towards the respective lobate margins.

Other than the marginal evidence, no other mapped features within the study area are thought to be associated with this time-step of the ice sheet. The two areas of irregular dissected ridges located north of Laguna Blanca (see Figures 6.15 and 6.16) are outside of this limit. These features are unusual and, to my knowledge, have not been widely reported in the literature, making it difficult to confidently explain their genesis. They are located beyond the evidence for the Skyring lobe, which indicates that they may be older landforms pre-dating the most extensive ice sheet position shown in this reconstruction (time-step 1). This suggests that they could be morainic remnants of an older and more extensive glaciation, which have since been heavily dissected by meltwater, perhaps associated with the ice margin at time-step 1. Fieldwork is necessary in order to better understand the origin and regional palaeoglaciological significance of these features.

A large outwash plain was not identified in front of the maximum position of the Otway lobe, in contrast to the Skyring lobe. This is unusual, as there are likely to have been large quantities of meltwater in this area. There are a number of possible explanations for this. The topography in this area is fairly high (> 170 m altitude) and is steep in places, which could have prevented meltwater from spreading out and depositing an outwash plain. By comparison, the topography of the large outwash plain on Península Juan Mazia is much flatter and lower (< 30 m altitude). The proglacial meltwater channel that has been mapped in front of the Otway lobe (Channel C in Figure 6.10) is very large (> 1 km wide in places), suggesting that it could have channelled large quantities of meltwater away from the ice margin. Indeed, in previous work this channel was mapped as a linear outwash plain (Glasser and Jansson, 2008). A further possibility is that the outer moraines that have been mapped are in fact lake shorelines. The presence of an ice-dammed proglacial lake in a more advanced position than those that have been reconstructed (Figure 7.5), rather than an ice front, provides a further explanation for the absence of a large outwash plain. However, the size of Channel C and the fact that it was previously mapped as a linear outwash plain (Glasser and Jansson, 2008) suggests that it could have drained proglacial meltwater away from an ice margin.

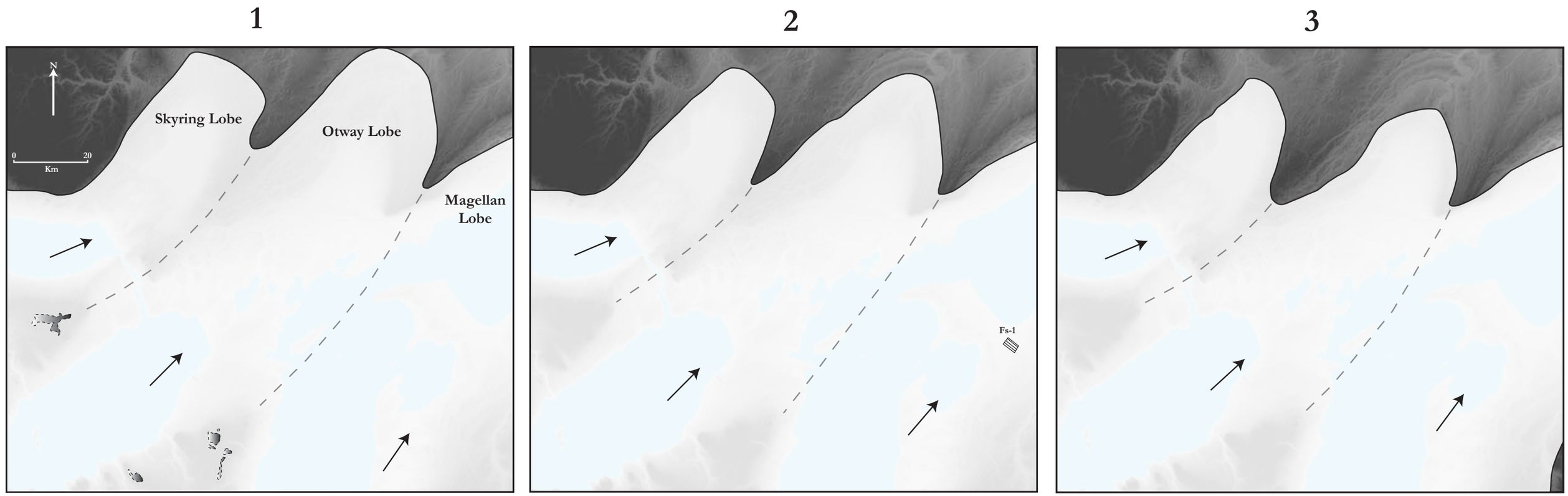

Figure 7.8 - Ice sheet reconstruction, time-step 1 to time-step 10. A full explanation is contained within the text.

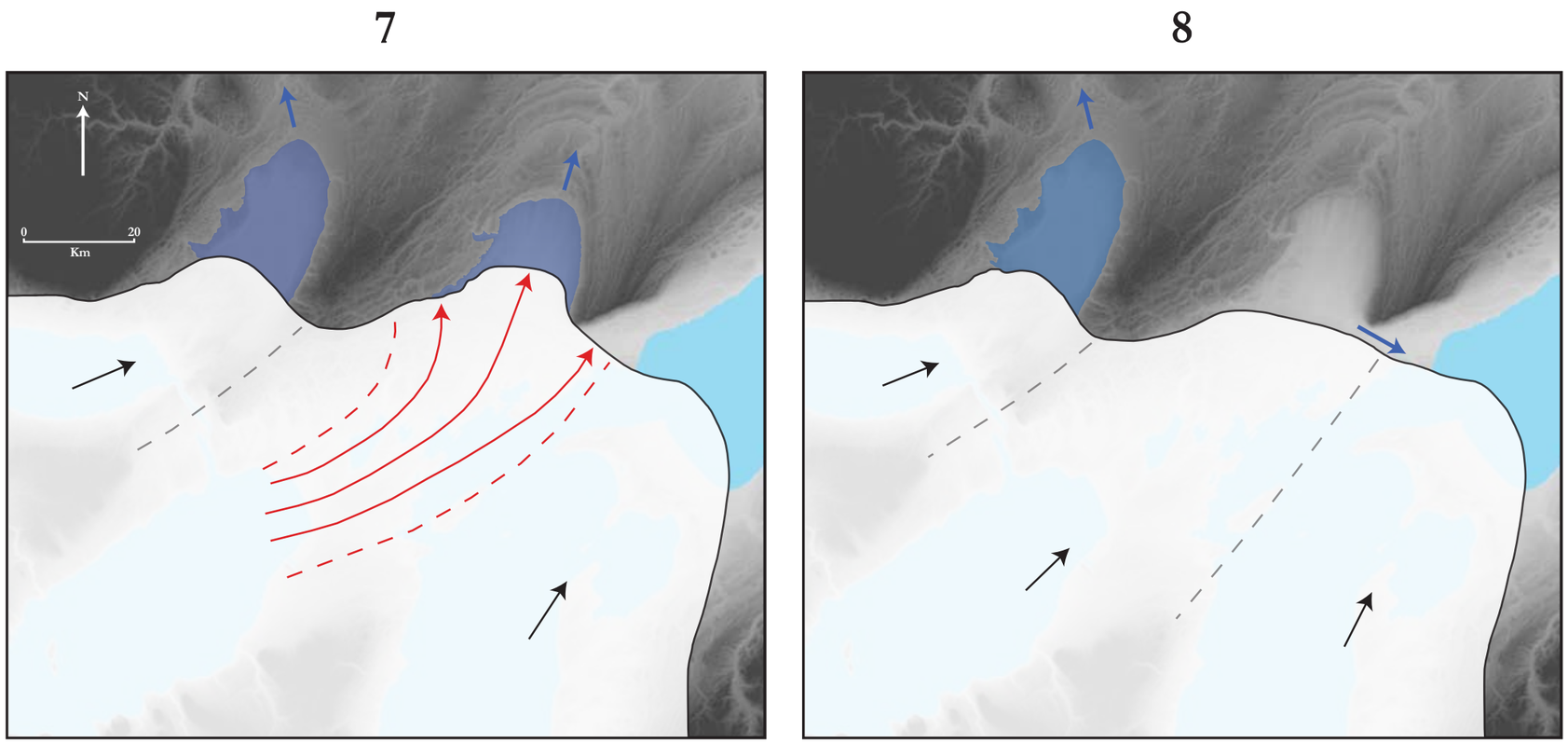

Figure 7.8 (continued)

In addition, Glasser and Jansson (2008) also mapped a large outwash plain to the north of the Otway lobe, beyond the limits of the area mapped in this study. As a result, the interpretation of the outer ridges as moraines is favoured, suggesting that time-step 1 represents the most extensive position of the ice sheet in this reconstruction.

Time-steps 2, 3 and 4 represent successively less extensive positions of the ice sheet. The morainic evidence for the lobe positions is increasingly more continuous from time-step 2 to time-step 4, supporting the view that the margin positions are decreasing in age. The Otway lobe at time-step 3 is defined by a series of nested moraine ridges, indicating that ice occupied a number of closely spaced positions for a sufficient time. The time-step 4 margin for the Otway lobe is at the innermost near-continuous moraine ridge sequence shown in Figure 6.9. This sequence is comprised of three closely spaced arcuate ridges that extend for over 20 km. This suggests that ice occupied three nested positions for a suitable period of time in order for the formation of these moraine ridges. Ice flow was focused along the basins of Seno Skyring, Seno Otway and the Strait of Magellan, as indicated by the arrows in Figure 7.8. The highest areas of Isla Riesco and Península Brunswick are likely to have protruded as nunataks during these time-steps. The speculated south eastern limits of the Magellan lobe in time-steps 3 and 4 are guided by the glacier limits defined in Fig. 2 in Benn and Clapperton (2000a), the presence of lateral meltwater channels along these margins appears to support this position. It is possible that Fs-1 was produced during time-step 2. The flow-set is orientated perpendicular to Fs-4 and the inferred dominant direction of ice flow along the Strait of Magellan, making it very difficult to place within the reconstruction. This is very much a speculated position because Fs-1 could also have formed at time-steps 1, 3 and 4 or during a more extensive glaciation prior to the reconstruction presented here. Extensive lateral meltwater drainage is thought to have occurred along the western margin of the Skyring lobe during these time-steps, producing the meltwater channels and outwash plain to the west and north west of Laguna Blanca (see Figure 6.10). A similar drainage network was in operation between the lobes, particularly at time-step 4 where lateral meltwater channels stretch northwards from the south eastern margin of the Skyring lobe.

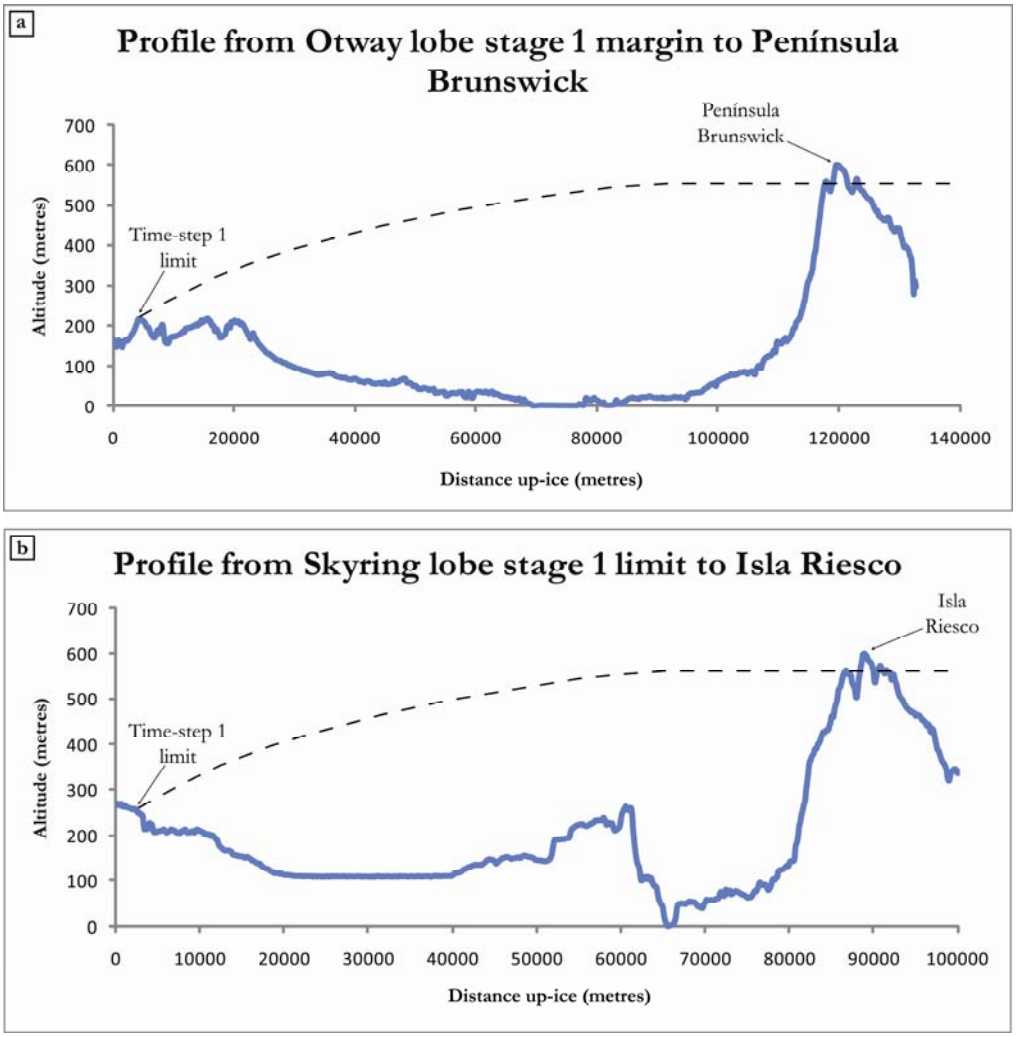

Figure 7.9–Profiles of topography along transects (a) from time-step 1 limit of the Otway lobe to Península Brunswick and; (b) from time-step 1 limit of the Skyring lobe to Isla Riesco. The ice sheet profile has been calculated using the parabolic formula $h = Ax^{½}$ of Mathews (1974), in which h is the elevation of the ice surface above the terminus, x is the distance up-stream from the terminus and A is a coefficient which varies from glacier to glacier. For the purposes of this calculation A is taken to be ≤ 1.0 $m^{½}$ (cf. Mathews, 1974).

7.5.2 Time-steps 5 to 7

As the margin retreated to the position in time-step 5, proglacial lakes formed at both the Skyring and Otway lobes (see Figure 7.8, blue northwards-facing arrows indicate location of spillways). The interaction of the ice sheet with proglacial Lake Otway may have induced calving, resulting in the drawing down of ice and triggering an ice stream, evidence for which is described in Section 7.2.1. A similar process of ice-stream initiation was suggested to have occurred for the Dubawnt Lake palaeo-ice stream on the north western Canadian Shield (Stokes and Clark, 2004). This zone of streaming ice produced the Fs-4 flow-set. The Otway Ice Stream would have drawn ice down through the Otway basin, before diverging towards the terminus as it calved into Lake Otway. Figure 3.3b shows this process in simplified form. No lineations have been mapped beyond this speculated ice limit, suggesting that the ice stream was first active at this time. The

differing orientations of Fs-4 and Fs-5 makes it unlikely that they formed at the same time. It is possible that Fs-5 represents the fragmentary record of an older event that has been largely removed by the fast ice flow that produced Fs-4. This suggests that Fs-5 should be placed prior to time-step 5 in the ice sheet reconstruction. However, the lineations of Fs-5 could be the same as the 'drumlinised sediment masses' of Benn and Clapperton (2000a), which were suggested to have formed at the same time as Fs-4. Fs-8 has been placed at time-step 5, based solely on its similar orientation to Fs-4, but equally it could have formed during any of the other time-steps or prior to time-step 1. These examples demonstrate the difficulty in determining the best position for many of the flow-sets in this reconstruction.

At time-step 6, the ice margin has retreated, increasing the size of both Lake Skyring and Lake Otway. The Otway Ice Stream was still active (delineated in red in Figure 7.8) and may well have experienced increased calving and therefore ice draw-down as the size and depth of Lake Otway increased (see Figures 7.5 and 7.6 and Table 7.3). The eastern margin of the Magellan lobe has retreated further towards the Strait of Magellan. The ice margin at time-step 7 is delimited by discontinuous moraine ridges stretching from the south east corner of the Skyring lobe to the eastern side of the Otway lobe. As the margin retreated both Lake Skyring and Lake Otway continued to be dammed, increasing the maximum possible extent of both lakes (see Figure 7.5 and Table 7.3). Ice continued to stream from the Otway basin and calve into Lake Otway, which was only dammed by a small section of the ice margin hinged on the large scarp to the east (see Figure 7.5). The Magellan lobe had probably retreated almost to the Segunda Angostura by time-step 7.

7.5.3 Time-steps 8 to 10

By time-step 8 the ice margin had withdrawn from the large scarp to the east of the Otway lobe. As a result, proglacial Lake Otway was no longer dammed and drained eastwards along the ice margin towards the Strait of Magellan (indicated by lateral blue arrow on panel 8 in Figure 7.8). The position of the ice margin is delimited by a series of moraine ridges located within the outwash plain to the south of the Otway lobe and by a series of five moraine ridges located south west of Laguna Blanca. It is suggested that the draining of Lake Otway would result in the end of calving, reducing ice draw-down and possibly resulting in the shutdown in activity of the Otway Ice Stream. The ice margin would continue to dam Lake Skyring, which by now had increased to a maximum area of 437 km^2 (see Figure 7.5 and Table 7.3). At time-step 9, Lake Skyring breached the spillway at its south eastern edge and drained along the ice margin towards the Strait of Magellan in an

abrupt event (indicated by lateral blue arrow on panel 9 in Figure 7.8). As suggested by Clapperton (1989) and Benn and Clapperton (2000a), the ice-marginal meltwater channels and outwash plain clearly postdate the formation of the Otway Ice Stream lineations (Fs-4). This confirms that the dynamic drainage event that helped to create the channels must have occurred after the Otway Ice Stream was in operation. Fs-3, Fs-6, Fs-7 and Fs-9 are all orientated approximately perpendicular to the positions of the main ice lobes and Fs-4. This makes them very difficult to explain glaciologically in the context of the reconstruction presented in Figure 7.8. Here, they are placed at time-step 9, based on their classification as wet-based deglaciation flow-sets and their relative proximity to the ice margin at this time. Their orientation makes it highly unlikely that they were coeval with the ice stream activity that produced Fs-4. It is possible that these flow-sets formed at different times to each other and at almost any point during the reconstruction. A further scenario that may explain the orientations of these flow-sets is that they were formed during a more extensive glaciation prior to the reconstruction described in this study. It is possible that they represent the remaining fragments of an earlier glaciation, which had a markedly different flow configuration than that inferred in this reconstruction. This is an idea that would require further investigation.

Time-step 10 is thought to represent the local LGM limit in the Strait of Magellan region, as agreed by a number of studies (Porter *et al.*, 1992; Clapperton *et al.*, 1995; Benn and Clapperton, 2000a, b; Bentley *et al.*, 2005; McCulloch *et al.*, 2005a; Kilian *et al.*, 2007). However, it is also possible that this time-step was a further retreat stage of a more extensive pre-LGM ice sheet. Fs-2 was formed by ice flow within the Magellan lobe towards the north east and was suggested by Bentley *et al.* (2005) to have formed during Advance B. Equally, it could have formed during any of the previous time-steps in this reconstruction when ice advanced within the Magellan lobe in a north east direction. This was acknowledged by Bentley *et al.* (2005), who were not able to exclude the possibility that the lineations belonged to a significantly older advance. Therefore, Fs-2 is only tentatively assigned to time-step 10 in this study.

7.6 Chronological constraints

This section will attempt to briefly speculate on the potential chronology of each time-step of the ice sheet reconstruction in this study within the established wider glacial history of southernmost Patagonia, shown in Table 7.4 (see also Chapter 2). Where available, some time-steps have been assigned dates. A number of these dates are widely agreed on

throughout the literature, whereas other glacial advances are poorly constrained. The lack of an established dating control in this area means that this is only a suggested chronology. There are subtle morphological differences between the preservation and form of some of the groups of moraine ridges, particularly between the outermost evidence for the Otway lobe (time-step 1) and the inner groups of ridges (time-steps 4 and 8), and this has also been used to guide the inferred chronology presented here.

Time-step 1 (Figure 7.8) appears to correspond well with the position of the Cabo Vírgenes Glaciation limit in this region as suggested by Meglioli (1992), Rabassa *et al.* (2000), Coronato *et al.* (2004a) and Kaplan *et al.* (2007), see Figures 2.2a and 2.2b. The Otway lobe at this time-step is delimited by moraine ridges that are more fragmented than those delimiting the inner positions of the lobe (e.g. time-steps 4 and 8), which suggests the outermost evidence represents an older position. Terminal moraines for the Cabo Vírgenes limit are described as surrounding lakes near the heads of Seno Skyring and Seno Otway by Coronato *et al.* (2004a). The time-step 1 limit certainly surrounds Laguna Blanca, although no such lake exists at the margin of the Otway lobe. Coronato *et al.* (2004a) also suggested that a combined ice lobe would have covered the Skyring-Otway-Magellan area. Kaplan *et al.* (2009) identified a trend following the GPG of increasingly less extensive glaciations in southern South America, and the Cabo Vírgenes limit represents the first of these (Rabassa *et al.*, 2000; Coronato *et al.*, 2004a; Kaplan *et al.*, 2007), or post-GPG 1 (Coronato *et al.*, 2004b). The age of this drift was estimated to be between > 0.36 and < 1.07 Ma by Meglioli (1992).

It is suggested that time-step 2, which represents a less extensive position of the ice margin, corresponds to the Punta Delgado Glaciation, the second most extensive advance following the GPG (Rabassa *et al.*, 2000; Coronato *et al.*, 2004a; Kaplan *et al.*, 2007); labelled post-GPG 2 by Coronato *et al.* (2004b). Figure 2.2b shows the Punta Delgado limit for the Otway lobe at a less extensive position than the outer Cabo Vírgenes limit. This is supported by Coronato *et al.* (2004a) and Rabassa (2008) who described it as a second, less extensive advance of the confluent ice lobes. No accurate dating of the Punta Delgado drift exists. Time-step 3 is characterised by lobes of lesser extent, close inside the inferred Punta Delgado limit. This is interpreted as a retreat position of the Punta Delgado Glaciation, rather than a separate glaciation. The reasoning for this is that time-step 4 is delimited by a larger, more substantial suite of arcuate moraine ridges for the Otway lobe and so seems more likely to mark the position of the next glaciation in the sequence, the Primera Angostura Glaciation (Rabassa *et al.*, 2000; Coronato *et al.*, 2004a). However,

time-step 3 could also represent the Primera Angostura limit, due to the close proximity of these margins.

Table 7.4 – Inferred glaciations for each time-step and any available age constraints. Punta Delgado and Primera Angostura age constraints are speculated. Cabo Vírgenes and Segunda Angostura age constraints are from Meglioli (1992) and McCulloch *et al.* (2005a) respectively.

Time-step	Inferred Glaciation	Age Constraints
1	Cabo Vírgenes (maximum)	> 0.36 and < 1.07 Ma BP
2	Punta Delgado (maximum)	> 150 and < 360 ka BP
3	- retreat stage	
4	Primera Angostura (maximum)	ca. 150 ka BP
5	- retreat stage	
6	- retreat stage	
7	- retreat stage (Advance A)	
8	- retreat stage	
9	- retreat stage	
10	Segunda Angostura (maximum; LGM)	> 23.1 and < 25.6 ka BP

The Primera Angostura Glaciation was the next most extensive advance following the Punta Delgado (Rabassa *et al.*, 2000; Coronato *et al.*, 2004a; Kaplan *et al.*, 2007). The maximum extent of this glaciation is interpreted as time-step 4 (see Figure 7.8), based on the clarity of the morainic evidence and the close correspondence of this mapped limit with the 'Gotiglacial' limit of Caldenius (1932). Time-step 3 could also represent the maximum extent of this glaciation, in which case time-step 4 would represent a retreat position. Coronato *et al.* (2004a) suggested that the Skyring lobe separated from the Otway-Magellan lobe during the Primera Angostura. However, the moraines delimiting the margin assigned to the Primera Angostura in this study suggest a confluent Skyring-Otway-Magellan margin, albeit with well-defined lobes (see panel 4 of Figure 7.8).

The Primera Angostura drift is undated, other than a poorly-constrained minimum age of 47 to 45 ^{14}C ka BP, which is likely to be infinite (Kaplan *et al.*, 2007). Rabassa and Clapperton (1990) and Clapperton (1993) suggested that the Primera Angostura Glaciation may be the penultimate glaciation at ca. 140 ka. Based on ^{14}C dating, amino acid racemisation (AAR) and relative weathering data, Kaplan *et al.* (2007) assumed that the Primera Angostura was at least a glacial cycle older than the Segunda Angostura glacial record (representing the local LGM), which was deposited during MIS 2. An age of 150

ka was assigned, indicating that the Primera Angostura Glaciation occurred during MIS 6 (Kaplan *et al.*, 2007). This closely matches the age of ca. 140 ka suggested by Rabassa and Clapperton (1990) and Clapperton (1993). The age for this glaciation coincides with peak glacial-age dust concentrations in the Vostok ice core from Antarctica (Petit *et al.*, 1999). These dust particles have a strong Patagonian signature (Basile *et al.*, 1997), supporting a glacial maximum late in MIS 6 in Patagonia (Kaplan *et al.*, 2005). It is clear that the ages of the Punta Delgado and Primera Angostura Glaciations are not well-constrained, but their relative positions within the glacial history are agreed upon (Clapperton, 1993; Rabassa *et al.*, 2000; Coronato *et al.*, 2004a, b; Kaplan *et al.*, 2007). This study supports the assertions that the Primera Angostura Glaciation was the penultimate glaciation and reached its maximum extent ca. 150 ka. This would allow the age of the Punta Delgado Glaciation to be bracketed somewhere between 360 ka and 150 ka.

Time-steps 5 to 10 are suggested to represent retreat stages during deglaciation of the Primera Angostura Glaciation. Time-steps 5 to 7 are characterised by the formation of proglacial lakes proximal to the Skyring and Otway lobes, which is suggested to have triggered a zone of streaming ice within the Otway lobe. The isochronous appearance of the Otway Ice Stream record and the lack of lake shorelines within the Otway lobe depression both support the idea that this was a rapid and dynamic event. If the Otway Ice Stream had been active during more than one glaciation, then more evidence for cross-cutting would be expected (Clark, 1999). Thus, it is concluded that the Otway Ice Stream was a rapid event that occurred during the Primera Angostura Glaciation.

Time-step 8 closely corresponds to the position of Advance A, as delimited by Clapperton *et al.*, 1995). The group of moraine ridges located south of the Otway lobe that delineate the time-step 8 ice margin appear to be the same moraines described by Clapperton *et al.* (1995) and Benn and Clapperton (2000a) as Advance A moraines. The combined Otway and Magellan basins formed a broad confluent ice front at this time, according to Benn and Clapperton (2000a). This can clearly be seen in panel 8 of Figure 7.8, supporting the view that time-step 8 matches Advance A. Clapperton (1993) attributed Advance A to the penultimate glaciation (Primera Angostura). The clarity of the morainic evidence suggests that ice occupied this position for an extended period of time and could represent a stillstand during deglaciation of the Primera Angostura Glaciation. Alternatively, Porter *et al.* (1992) and Clapperton *et al.* (1995) suggested that Advance A occurred during the

Segunda Angostura Glaciation. As the precise age of Advance A is unknown (McCulloch *et al.*, 2005a) it is difficult to confidently place it within the chronology.

Time-step 9 is suggested to be a further position of a deglaciating ice sheet during the Primera Angostura Glaciation, recording ice retreat back towards the Skyring, Otway and Magellan basins and the higher ground beyond. The lack of morainic evidence (e.g. recessional moraines) between Advance A and Advance B suggests that this retreat was rapid. Time-step 10 is thought to represent the most extensive advance (Advance B) of ice along the Skyring, Otway and Magellan basins during the last glaciation, the Segunda Angostura (Clapperton, 1989; Porter *et al*., 1992; Clapperton, 1993; Clapperton *et al*., 1995; Benn and Clapperton, 2000a, b; Rabassa and Clapperton, 2000; Rabassa *et al*., 2000; Coronato *et al*., 2004a; Bentley *et al*., 2005; McCulloch *et al*., 2005a; Sugden *et al*., 2005; Kaplan *et al*., 2007, 2008b; Glasser *et al*., 2008), although it is possible that it is a further retreat stage of a more extensive glaciation, such as the Primera Angostura.

In summary, the lack of available dating in this area presents a problem when attempting to assess the possible synchrony of the Otway Ice Stream and deglaciation with other regions in southern Patagonia and the northern hemisphere. This study agrees with Kaplan *et al.* (2007), who placed the greatest extent of the Primera Angostura Glaciation at ca. 150 ka, during MIS 6. This corresponds well with the Moreno I and II moraine ages at LBA (140-150 ka; Kaplan *et al.*, 2007). This also coincides with large northern hemisphere ice volume and low Southern Ocean temperatures (see Fig. 6 in Kaplan *et al.*, 2005). This suggests that the major ice advance of the Primera Angostura coincided with not only a major advance in LBA, but also with northern hemisphere ice expansion (Kaplan *et al.*, 2005). According to the chronology suggested here, the Otway Ice Stream and rapid deglaciation were active following this.

7.7 Otway Ice Stream dynamics

It has been interpreted that a zone of streaming ice occurred within the Otway lobe, as previously suggested by Clapperton (1989) and Benn and Clapperton (2000a). This is suggested to have been a terrestrial ice stream, similar to the lobes of the southern Laurentide Ice Sheet margin (Patterson, 1997, 1998; Jennings, 2006; Evans *et al*., 2008). This section will discuss the 'life cycle' of the ice stream (Clark and Stokes, 2003), from the onset of streaming to its shutdown.

The initiation of ice streaming is suggested to have been triggered by calving into a proglacial lake that formed as the Otway ice lobe retreated. The reconstruction of proglacial Lake Otway indicates a lake with a depth of up to 107 m at its maximum extent, at which time it would have been in contact with the ice sheet for a distance of up to 20 km (see Figure 7.6b). Brown *et al.* (1982) suggested that the rate of calving is primarily a function of water depth at the terminus of tidewater glaciers. Warren *et al.* (1995b) found a similar relationship between water depth and calving rate for glaciers calving into freshwater. This was following work at Glaciar Upsala in Patagonia, which calves into Lago Argentino (see Figure 2.1 for location). A contrast between tidewater and freshwater calving rates has also been identified, with rates in tidewater found to be up to an order of magnitude greater than in freshwater (Funk and Röthlisberger, 1989; Warren, 1994; Warren *et al.*, 1995a, b). The depth of reconstructed Lake Otway and the distance that the ice margin is in contact with the lake are both of the same order as for some proglacial lakes in the Thelon Basin on the northwestern Canadian Shield, which were postulated to have triggered the Dubawnt Lake palaeo-ice stream (Stokes and Clark, 2004). Stokes and Clark (2004) argued that a progressively deepening lake in contact with the ice margin would have increased the removal of ice through calving and increased subglacial water pressures proximal to the lake. This would have lead to a reduction in basal shear stress and an increase in ice velocity up-ice from the lake-terminating ice margin (Stokes and Clark, 2004). Increased ice velocity would then have drawn-down ice from inland, lowering the ice sheet profile (Stokes and Clark, 2004). This same process is suggested to be responsible for triggering the Otway Ice Stream.

The precise extent of the up-ice onset zone, where converging slower moving ice is incorporated into the main ice stream channel (Bamber *et al.*, 2000; Hodge and Doppelhammer, 1996) is difficult to identify. This is because this zone may be to the south west of Seno Otway beyond the study area of this project. Alternatively, the onset zone could be located within the present-day extent of Seno Otway, in which case any geomorphic evidence is underwater. However, a bathymetric profile revealed no indications of ice flow direction or morainic evidence of any kind (Kilian *et al.*, 2007).

Other factors may also have influenced the location of the Otway Ice Stream. Clapperton (1989) suggested that a potentially deformable bed existed in this region prior to the formation of the lineations and that the area was pre-disposed to a zone of streaming ice. The sedimentary bed is postulated to have been up to 25 m thick and is suggested to have

induced higher strain rates within the hollow east of Laguna Cabeza del Mar (Clapperton, 1989). The combination of a bed of thick sediments and an abundance of subglacial meltwater channelled into the hollow would have encouraged bed deformation (Clapperton, 1989), one of the main mechanisms suggested for fast ice flow within an ice stream (Boulton and Hindmarsh, 1987; Engelhardt *et al.*, 1990; Boulton *et al.*, 2000; Kamb, 2001; Bennett, 2003). It is likely that the mechanism that facilitated fast flow within the Otway Ice Stream was subglacial bed deformation, basal sliding, or a combination of the two.

The Otway Ice Stream should be placed within the continuum of ice streams identified by Truffer and Echelmeyer (2003) because it shares characteristics with both topographically-controlled ice streams and *pure* ice streams. The Otway basin is a shallow topographic trough and, assuming the convergence of ice occurred within this trough or further up-ice, it is possible that the ice stream was topographically-constrained in this area. The presence of a potentially deformable bed towards the margin is more characteristic of a *pure* ice stream (Stokes and Clark, 1999; Bennett, 2003). If so, reported characteristics of pure ice streams indicate that the Otway Ice Stream may have had thin ice, a low surface slope and a low driving stress ($\leq$ 20 kPa; Bennett, 2003). Benn and Clapperton (2000a) calculated a basal shear stress of 8.8 kPa for part of the Advance B Strait of Magellan glacier (see Section 2.6 for detailed discussion), which was suggested to be similar to values beneath modern fast-flowing outlet glaciers and ice streams. It seems likely that the basal shear stresses towards the margin of the Otway Ice Stream would have been of this order.

Once proglacial Lake Otway had drained at time-step 8, the ice sheet would cease calving. It is possible that this would have reduced ice velocities and the draw-down of ice from the interior, leading to the shutdown of the Otway Ice Stream. However, it is also possible that the ice stream continued to be active after Lake Otway drained. The Dubawnt Lake Ice Stream in Canada was also suggested to have been triggered by calving into a proglacial lake, but following this thermomechanical feedback mechanisms sustained fast ice flow (Stokes and Clark, 2004). Therefore, ice stream shutdown could also have been caused by the lowering of the ice sheet profile (Stokes and Clark, 2004). Rapid ice flow ultimately causes ice thinning, leading to the advection of cold ice closer to the bed and the shutdown of rapid basal motion (Bennett, 2003). Ice thinning would also increase the surface area at lower elevations (Clark and Stokes, 2003), accelerating deglaciation of this sector of the ice sheet. The lack of recessional moraines within the ice stream flow-set suggests that

retreat was rapid following the shutdown of ice stream activity. This suggests that the Otway Ice Stream might be responsible for the rapid deglaciation of the ice sheet in this area.

It is difficult to assess for how long the Otway Ice Stream was active given the lack of dating controls and the uncertainty concerning the method of shutdown. The isochronous appearance of the lineations, as suggested by high parallel conformity and a lack of cross-cutting, indicates that ice streaming occurred in a relatively short time period. It is feasible that the ice stream was active for at least the length of time that Lake Otway was dammed, from time-steps 5 to 7, and possibly longer. However, it is also possible that ice streaming was only triggered when the lake was sufficiently deep enough, in which case it may have been active for less time than this.

The asymmetric cross profiles of many lineations within the Otway Ice Stream were suggested by Clapperton (1989) to reflect the variable response of subglacially deforming sediments, spatially variable water flow through the bed materials and changes in the amount and direction of the basal strain rate as the ice thinned. A further possibility is that meltwater activity has eroded the sides of individual features. Figure 6.4 clearly shows that some lineations have been shaped by meltwater activity following their formation, indicating that it may also be responsible for steepening one side of features. However, it is difficult to envisage why meltwater would preferentially and consistently erode the same south east facing side. It is clear that further fieldwork is required to test these suggestions.

A question that arises in this region concerns the apparent lack of evidence for ice streaming within the Skyring lobe which, it is suggested here, also terminated in a large proglacial lake at this time (see Figure 7.8). A number of reasons can be hypothesised for this. Firstly, only a small section of the ice sheet margin (< 5 km) is in contact with the *deepest* part of the lake (see Figure 7.6a). Compare this to Figure 7.6b, which shows that at margin 7, the deeper parts of Lake Otway are in direct contact with the ice sheet for over 10 km. Another possible reason could be that a deformable bed was not present in this area. Clapperton (1989) suggested that the soft sedimentary conditions found beneath the Otway Ice Stream lineations could well be absent throughout most of South America. However, the absence of a deformable bed is not concrete evidence as ice streams have been found to have operated on hard bedrock (Payne and Baldwin, 1999; Stokes and Clark, 2003; Roberts *et al.*, 2010). A further possibility is that the ice sheet did stream within the Skyring lobe but evidence for this failed to be indentified from remote sensing in this

study, but given the comprehensive geomorphological evidence of Otway streaming this seems unlikely.

7.8 Limitations and further research

This project relies almost entirely on landform mapping from remote sensing and as a result has a number of limitations. Extensive fieldwork in the area would help to reduce these limitations by providing more evidence with which to interpret certain features, such as the irregular dissected ridges and the linear features around the Fitz Roy Channel. This in turn may provide support to a number of the suggestions put forward in this project, or conversely, help to reject them. This section will highlight a number of key areas where fieldwork would improve the scope of this study.

Because mapping has been conducted from satellite imagery and aerial photographs it is conceivable that some landforms have been incorrectly identified and mapped. This is particular clear in a couple of places where the mapping of this study disagrees with others. An example of this is the linear features running sub-parallel to the Fitz Roy Channel (Figure 6.21). In this study, these have been interpreted as scarp lines created by meltwater erosion as a proglacial lake drained eastwards. Glasser and Jansson (2008) interpreted these features as moraine ridges. Fieldwork would aid the classification of these features, which in turn could have implications for this ice sheet reconstruction. A number of suggestions that have been raised by this project could be better clarified through fieldwork. Fs-4 has been interpreted as a palaeo-ice stream, although it was also acknowledged that the geomorphological record bears a resemblance to other landsystems (e.g. surging glacier; Evans and Rea, 1999). Fieldwork could help to validate or falsify this interpretation, particularly if diagnostic criteria for a surging glacier landsystem were found (e.g. crevasse squeeze ridges, concertina eskers; Evans and Rea, 1999). Palaeo-ice streams have converging onset zones (Stokes and Clark, 1999) and the lack of evidence for this was explained by its possible location within Seno Otway or beyond the extent of the study area. A further bathymetric profile of Seno Otway would help the search for this evidence, as would extending the study area to the south west.

The hypothesised ice stream in this area was suggested to have been triggered by calving into a proglacial lake. Although the ice margin position and topography indicate that such a lake could have formed in the Otway lobe, no geomorphological evidence (e.g. former shorelines) could be detected from satellite imagery. It is therefore suggested that fieldwork to look for shorelines and/or evidence for glaciolacustrine sediments in this area

would aid the validity of this reconstruction. Sedimentological analysis of the ice stream lineations may also help to explain their formation and morphology, in particular the asymmetrical profile exhibited by many in the narrow zone east of Laguna Cabeza del Mar (Clapperton, 1989). Further analysis of the sediments beneath the lineations could also help to verify the potential presence of a deformable bed, as suggested by Clapperton (1989).

It is clear that there is a significant lack of dating control within the study area. The acquisition of dated positions is of great importance in order to produce a more accurate chronology of the region and to place the reconstructed ice sheet dynamics within the wider glacial history. Additional dating control would provide a robust test of the inferred chronology suggested in this study. Cosmogenic nuclide and ^{14}C radiocarbon dating are just two of the techniques that could be implemented in order to provide ages for a number of key positions, in particular the moraine ridges and outwash plains in the north of the study area. Cosmogenic nuclide dating of exposed boulders on moraine ridges and gravels in outwash plains has previously been carried out elsewhere in southern Patagonia (e.g. Kaplan *et al.*, 2004, 2005, 2007; Singer *et al.*, 2004a; Hein *et al.*, 2009).

In summary, further research is required in order to test the interpretations of this study. Fieldwork, in particular sedimentological analysis and landform dating, would provide significant support to the geomorphological mapping. This in turn would aid the validity of the reconstruction of ice sheet dynamics and glacial history of the Skyring-Otway-Magellan region presented here.

Chapter 8 - Conclusions

Remote sensing of the Strait of Magellan region reveals a wide variety of glacial geomorphological evidence, documenting the advance and retreat of this sector of the Patagonian Ice Sheet over several glaciations. A combination of Landsat and ASTER satellite imagery, aerial photographs, and SRTM data proves to be an invaluable method by which to accurately map both large-scale regional landform assemblages and individual feature morphologies. Moraine ridge sequences and meltwater channels delimit the extent of the Skyring, Otway and Magellan lobes at a number of major positions, recording a pattern of increasingly less extensive glaciations following the GPG (Kaplan *et al.*, 2009).

The spectacular zone of streamlined lineations located on the western side of the Strait of Magellan is thought to represent a terrestrial palaeo-ice stream, similar to the lobes at the southern margin of the Laurentide Ice Sheet (e.g. Patterson, 1997; Jennings, 2006; Evans *et al*., 2008). The evidence utilised to make this classification includes the highly-attenuated nature of many of the lineations; the characteristic shape and dimensions of the lineation flow-set; an abrupt margin to the main streamlined zone; and the presence of deformed sediment and a potentially deformable bed, as suggested by previous research (Clapperton, 1989; Benn and Clapperton, 2000a). A palaeo-ice stream was hypothesised for this location by Clapperton (1989) and Benn and Clapperton (2000a), and this study argues that there is sufficient geomorphological evidence to support this. This would make the 'Otway Ice Stream' the first palaeo-ice stream to be explicitly described within the former Patagonian Ice Sheet.

Fast ice flow within the Otway Ice Stream is thought to have been triggered by ice calving into one of two large proglacial lakes dammed by the ice margin following retreat from the Primera Angostura Glaciation maximum. This method of initiation was previously argued for the Dubawnt Lake palaeo-ice stream on the northwestern Canadian Shield (Stokes and Clark, 2004). The presence of a potentially-deformable bed at this location (Clapperton, 1989) suggests that the principal mechanism for fast ice flow was through subglacial deformation, basal sliding, or a combination of the two. It is likely that the up-ice section of the Otway Ice Stream was topographically-controlled within the Otway basin. This would appear to place it within the continuum of ice stream types suggested by Truffer and Echelmeyer (2003). The ice stream is likely to have increased the rate of deglaciation of this section of the Primera Angostura ice sheet, as rapid ice velocities lead to thinning of an already-retreating ice mass (Bennett, 2003). This lowering of the ice sheet profile would

have ultimately contributed to the shutdown of ice stream activity, which is suggested to have begun following the draining of proglacial Lake Otway. The isochronous nature of the subglacial record supports the idea that the Otway Ice Stream was a dynamic event of relatively short duration, possibly only active whilst Lake Otway was dammed.

After the shutdown of ice streaming, the ice sheet occupied a stillstand at the 'Advance A' position of Clapperton *et al.* (1995). Deglaciation of the Primera Angostura ice sheet following this stage appears to have been a rapid withdrawal of ice towards the Skyring, Otway and Magellan basins, characterised by meltwater drainage (Clapperton, 1989). During this retreat it is hypothesised that proglacial Lake Skyring drained eastwards along the ice margin towards the Strait of Magellan. The geomorphological evidence, in the form of large meltwater channels and an extensive outwash plain, suggest that this was an abrupt event. This supports the suggestions for such a dynamic drainage event by a number of previous studies (Caldenius, 1932; Mercer, 1976; Benn and Clapperton, 2000a).

This study has drawn together the evidence gleaned through geomorphological mapping and from previous research in order to produce a reconstruction of the glacial history and ice dynamics of this sector of the former Patagonian Ice Sheet. It is suggested that a terrestrial palaeo-ice stream was active in this area, which is thought to be the first of its kind to be described in detail in South America.

References

Alley, R. D. (1989a) 'Water-pressure coupling of sliding and bed deformation: I. Water system', *Journal of Glaciology*, 35: 108-118

Alley, R. D. (1989b) 'Water-pressure coupling of sliding and bed deformation: II. Velocity-depth profiles', *Journal of Glaciology*, 35: 119-129

Alley, R. B., Cuffey, K. M., Evenson, E. B., Strasser, J. C., Lawson, D. E. and Larson, G. J. (1997) 'How glaciers entrain and transport basal sediment: physical constraints', *Quaternary Science Reviews*, 16: 1017-1038

Alley, R. B. and Whillans, I. M. (1984) 'Response of the East Antarctica Ice Sheet to Sea-Level Rise', *Journal of Geophysical Research*, 89 (C4): 6487-6493

Alley, R. B. and Bindschadler R. A. (2001) 'The West Antarctic Ice Sheet and sea-level change', In: Alley, R. B. and Bindschadler, R. A. (Eds.) *The West Antarctic Ice Sheet: Behaviour and Environment, Antarctic Research Series, vol. 77,* American Geophysical Union, Washington, p.11

Anandakrishnan, S. and Alley, R. B. (1997) 'Stagnation of Ice Stream C, West Antarctica by water piracy', *Geophysical Research Letters*, 24: 265-268

Anandakrishnan, S., Blankenship, D. D., Alley, R. B. and Stoffa, P. L. (1998) 'Influence of subglacial geology on the position of a West Antarctic ice stream from seismic observations', *Nature*, 394: 62-65

Anandakrishnan, S., Alley, R. B., Jacobel, R. W. and Conway, H. (2001) 'The flow regime of Ice Stream C and hypotheses concerning its recent stagnation', In: Alley, R. D. and Bindschadler, R. (Eds.) *The West Antarctic Ice Sheet: Behaviour and Environment. Antarctic Research Series vol. 77,* American Geophysical Union, Washington DC, pp. 283-294

Anderson, D. M. and Archer, R. B. (1999) 'Preliminary evidence of early deglaciation in southern Chile', *Palaeogeography, Palaeoclimatology, Palaeoecology*, 146: 295-301

Anderson, J. B. and Oakes Fretwell, L. (2008) 'Geomorphology of the onset area of a paleo-ice stream, Marguerite Bay, Antarctic Peninsula' *Earth Surface Processes and Landforms*, 33: 503-512

Andrews, J. T. and Tedesco, K. (1992) 'Detrital carbonate-rich sediments, northwestern Labrador Sea: implications for ice-sheet dynamics and iceberg rafting (Heinrich) events in the North Atlantic', *Geology*, 20: 1087-1090

Andrews, J. T. and Maclean, B. (2003) 'Hudson Strait ice streams: a review of stratigraphy, chronology and links with North Atlantic Heinrich events', *Boreas*, 32: 4-17

Ashworth, A. C. and Hoganson, J. W. (1993) 'The magnitude and rapidity of the climate change marking the end of the Pleistocene in the mid-latitudes of South America', *Palaeogeography, Palaeoclimatology, Palaeoecology*, 101: 263-270

Bamber, J. L., Vaughan, D. G. and Joughin, I. (2000) 'Widespread Complex Flow in the Interior of the Antarctic Ice Sheet', *Science*, 287: 1248-1250

Bamber, J. L., Alley, R. B. and Joughin, I. (2007) 'Rapid response of modern day ice sheets to external forcing', *Earth and Planetary Science Letters*, 257: 1-13

Bartole, R., DeMuro, S., Morelli, D. and Tosoratti, F. (2008) 'Glacigenic features and Tertiary stratigraphy of the Magellan Strait (Southern Chile)', *Geologica Acta*, 6 (1): 85-100

Basile, I., Grousset, F. E., Revel, M., Petit, J. R., Biscaye, P. E. and Barkov, N. I. (1997) 'Patagonian origin of glacial dust deposited in East Antarctica (Vostok and Dome C) during glacial stages 2, 4, and 6', *Earth and Planetary Science Letters*, 146: 573-589

Bell, R. E. (2008) 'The role of subglacial water in ice-sheet mass balance', *Nature Geoscience*, 1: 297-304

Bell, R. E., Blankenship D. D., Finn, C. A., Morse, D. L., Scambos, T. A., Brozena, J. M. and Hodge, S. M. (1998) 'Influence of subglacial geology on the onset of a West Antarctic ice stream from aerogeophysical observations', *Nature*, 394: 58-62

Bell, R. E., Studinger, M., Shuman, C. A., Fahnestock, M. A. and Joughin, I. (2007) 'Large subglacial lakes in East Antarctica at the onset of fast-flowing ice streams', *Nature*, 445 (22): 904-907

Benn, D. I. and Evans, D. J. A. (1998) *Glaciers and Glaciation*, Hodder Arnold, London

Benn, D. I. and Clapperton, C. M. (2000a) 'Pleistocene glacitectonic landforms and sediments around central Magellan Strait, southernmost Chile: evidence for fast outlet glaciers with cold-based margins', *Quaternary Science Reviews*, 19: 591-612

Benn, D. I. and Clapperton, C. M. (2000b) 'Glacial Sediment-Landform Associations and Paleoclimate during the Last Glaciation, Strait of Magellan, Chile', *Quaternary Research*, 54: 13-23

Benn, D. I. and Evans, D. J. A. (2006) 'Subglacial megafloods: outrageous hypothesis or just outrageous?', In: Knight, P. G. (Ed.) *Glacier Science and Environmental Change*, Blackwell, Oxford

Bennett, K. D., Haberle, S. G. and Lumley, S. H (2000) 'The Last Glacial-Holocene Transition in Southern Chile', *Science*, 290: 325-328

Bennett, M. R. (2003) 'Ice streams as the arteries of an ice sheet: their mechanics, stability and significance', *Earth-Science Reviews*, 61: 309-339

Bentley, C. R. (1987) 'Antarctic Ice Streams: A Review', *Journal of Geophysical Research*, 92 (B9): 8843-8858

Bentley, M. J. and McCulloch, R. D. (2005) 'Impact of neotectonics on the record of glacier and sea level fluctuations, Strait of Magellan, Southern Chile', *Geografiska Annaler*, 87 A (2): 393-402

Bentley, M. J., Sugden, D. E., Hulton, N. R. J. and McCulloch, R. D. (2005) 'The landforms and pattern of deglaciation in the Strait of Magellan and Bahía Inútil, southernmost South America', *Geografiska Annaler*, 87 A (2): 313-333

Binschadler, R. A., Alley, R. B., Anderson, J., Shipp, S., Borns, H., Fastook, J., Jacobs, S., Raymond, C. F. and Shuman, C. A. (1998) 'What is happening to the West Antarctic Ice Sheet?', *EOS (Transactions of the American Geophysical Union)*, 79 (257): 264-265

Blankenship, D. D., Bentley, C. R., Rooney, S. T. and Alley, R. B. (1986) 'Seismic measurements reveal a saturated porous layer beneath an active Antarctic ice stream', *Nature*, 322: 54-57

Blunier, T., Chappellaz, J., Schwander, J., Dällenbach, A., Stauffer, B., Stocker, T. F., Raynaud, D., Jouzel, J., Clausens, H. B., Hammer, C. U. and Johnsen, S. J. (1998) 'Asynchrony of Antarctic and Greenland climate change during the last glacial period', *Nature*, 394: 739-743

Bond, G., Heinrich, H., Broecker, W., Labeyrie, L., McManus, J., Andrews, J., Huon, S., Jantschik, R., Clasen, S., Simet, C., Tedesco, K., Klas, M., Bonani, G. and Ivy, S. (1992) 'Evidence for massive discharges of icebergs into the North Atlantic ocean during the last glacial period', *Nature*, 360: 245-249

Boulton, G. S. and Jones, A. S. (1979) 'Stability of temperate ice sheets resting on beds of deformable sediment', *Journal of Glaciology*, 24: 29-43

Boulton, G. S. and Hindmarsh, R. C. A. (1987) 'Sediment Deformation Beneath Glaciers: Rheology and Geological Consequences', *Journal of Geophysical Research*, 92 (B9): 9059-9082

Boulton, G. S. and Clark, C. D. (1990) 'A highly mobile Laurentide ice sheet revealed by satellite images of glacial lineations', *Nature*, 346: 813-817

Boulton, G. S., Smith, G. D., Jones, A. S. and Newsome, J. (1985) 'Glacial geology and glaciology of the last mid-latitude ice sheets', *Journal of the Geological Society*, 142 (3): 447-474

Boulton, G. S., Dobbie, K. E. and Zatsepin, S. (2001a) 'Sediment deformation beneath glaciers and its coupling to the subglacial hydraulic system', *Quaternary International*, 86: 3-28

Boulton, G. S., Dongelmans, P., Punkari, M. and Broadgate, M. (2001b) 'Palaeoglaciology of an ice sheet through a glacial cycle: the European ice sheet through the Weichselian', *Quaternary Science Reviews*, 20: 591-625

Bradwell, T., Stoker, M. and Krabbendam, M. (2008) 'Megagrooves and streamlined bedrock in NW Scotland: The role of ice streams in landscape evolution', *Geomorphology*, 97: 135-156

Broecker, W. S. (1994) 'Massive ice berg discharges as triggers for global climate change', *Nature*, 365: 143-147

Brown, C. S., Meier, M. F. and Post, A. S. (1982) 'Calving speed of Alaskan tidewater glaciers, with application to Columbia glacier', *U.S. Geological Survey Professional Paper 1258-C*, 13 pp.

Caldenius, C. C. (1932) 'Las Glaciaciones Cuaternarias en la Patagonia y Tierra Del Fuego', *Geografiska Annaler*, 14: 1-164

Canals, M., Urgeles, R. and Calafat, A. M. (2000) 'Deep sea-floor evidence of past ice streams off the Antarctic Peninsula', *Geology*, 28 (1): 31-34

Carter, R. M. and Gammon, P. (2004) 'New Zealand maritime glaciation: millennial-scale southern climate change since 3.9 Ma', *Science*, 304: 1659-1662

Christoffersen, P. and Tulaczyk, S. (2003a) 'Signature of palaeo-ice stream stagnation: till consolidation induced by basal freeze-on', *Boreas*, 32(1): 114-129

Christoffersen, P. and Tulaczyk, S. (2003b) 'Thermodynamics of basal freeze-on: predicting basal and subglacial signatures of stopped ice streams and interstream ridges', *Annals of Glaciology*, 36: 233-243

Christoffersen, P., Piotrowski, J. A. and Larsen, N. K. (2005) 'Basal processes beneath an Arctic glacier and their geomorphic imprint after a surge, Elisebreen, Svalbard', *Quaternary Research*, 64: 125-137

Clapperton, C. M. (1968) 'Channels formed by the superimposition of glacial meltwater streams, with special reference to the East Cheviot Hills, North-East England', *Geografiska Annaler*, 50 A: 207-220

Clapperton, C. M. (1989) 'Asymmetrical drumlins in Patagonia, Chile', *Sedimentary Geology*, 62: 387-398

Clapperton, C. M (1990) 'Quaternary Glaciations in the Southern Hemisphere – An Overview', *Quaternary Science Reviews*, 9: 299-304

Clapperton, C. (1993) *Quaternary Geology and Geomorphology of South America*, Elsevier, London

Clapperton, C. M., Sugden, D. E., Kaufman, D. S. and McCulloch, R. D. (1995) 'The Last Glaciation in Central Magellan Strait, Southernmost Chile', *Quaternary Research*, 44: 133-148

Clark, C. D. (1993) 'Mega-scale glacial lineations and cross-cutting ice-flow landforms', *Earth Surface Processes and Landforms*, 18: 1-29

Clark, C. D. (1994) 'Large-scale ice-moulding: a discussion of genesis and glaciological significance', *Sedimentary Geology*, 91: 253-268

Clark, C. D. (1997) 'Reconstructing the evolutionary dynamics of former ice sheets using multi-temporal evidence, remote sensing and GIS', *Quaternary Science Reviews*, 16: 1067-1092

Clark, C. D. (1999) 'Glaciodynamic context of subglacial bedform generation and preservation', *Annals of Glaciology*, 28: 23-32

Clark, C. D. and Stokes, C. R. (2001) 'Extent and basal characteristics of the M'Clintock Channel Ice Stream', *Quaternary International*, 86: 81-101

Clark, C. D. and Stokes, C. R. (2003) 'Palaeo-ice Stream Landsystem', In: Evans, D. J. A. (Ed.) *Glacial Landsystems*, Hodder Arnold, London

Clark, C. D., Knight, J. K. and Gray, J. T. (2000) 'Geomorphological reconstruction of the Labrador Sector of the Laurentide Ice Sheet', *Quaternary Science Reviews*, 19: 1343-1366

Clark, C. D., Tulaczyk, S. M., Stokes, C. R. and Canals, M. (2003) 'A groove-ploughing theory for the production of mega-scale glacial lineations, and implications for ice-stream mechanics', *Journal of Glaciology*, 49 (165): 240-256

Clark, C. D., Hughes, A. L. C., Greenwood, S. L., Spagnolo, M. and Ng, F. (2009) 'Size and shape characteristics of drumlins, derived from a large sample, and associated scaling laws', *Quaternary Science Reviews*, 28: 677-692

Clark, P. U. (1992) 'Surface form of the southern Laurentide Ice Sheet and its implications to ice-sheet dynamics', *The Geological Society of America Bulletin*, 104 (5): 595-605

Clayton, L., Teller, J. T. and Attig, J. W. (1985) 'Surging of the southwestern part of the Laurentide Ice Sheet', *Boreas*, 14: 235-242

Colgan, P. M. and Mickelson, D. M. (1997) 'Genesis of streamlined landforms and flow history of the Green Bay lobe, Wisconsin, USA', *Sedimentary Geology*, 111: 7-25

Colgan, P. M., Mickelson, D. M. and Cutler, P. M. (2003) 'Ice-marginal Terrestrial Landsystems: Southern Laurentide Ice Sheet Margin', In: Evans, D. J. A. (Ed.) *Glacial Landsystems*, Hodder Arnold, London

Coronato, A., Salemme, M. and Rabassa, J. (1999) 'Palaeoenvironmental conditions during the early peopling of Southernmost South America (Late Glacial - Early Holocene, 14 - 8 ka BP)', *Quaternary International*, 53/54: 77-92

Coronato, A., Meglioli, A. and Rabassa, J. (2004a) 'Glaciations in the Magellan Straits and Tierra del Fuego, southernmost South America', In: Ehlers, J. and Gibbard, P. L. (eds.), *Quaternary Glaciations: Extent and Chronology, Part III: South America, Asia, Africa, Australia and Antarctica*, Elsevier, Amsterdam, *Developments in Quaternary Sciences*, 2: 45-48

Coronato, A., Martínez, O. and Rabassa, J. (2004b) 'Glaciations in Argentine Patagonia, southern South America', In: Ehlers, J. and Gibbard, P. L. (eds.), *Quaternary Glaciations: Extent and Chronology, Part III: South America, Asia, Africa, Australia and Antarctica*, Elsevier, Amsterdam, *Developments in Quaternary Sciences*, 2: 49-67

De Angelis, H. and Kleman, J. (2005) 'Palaeo-ice streams in the northern Keewatin sector of the Laurentide ice sheet', *Annals of Glaciology*, 42: 135-144

De Angelis, H. and Kleman, J. (2007) 'Palaeo-ice streams in the Foxe/Baffin sector of the Laurentide Ice Sheet', *Quaternary Science Reviews*, 26: 1313-1331

De Angelis, H. and Kleman, J.(2008) 'Palaeo-ice stream onsets: examples from the north-eastern Laurentide Ice Sheet', *Earth Surface Processes and Landforms*, 33: 560-572

Denton, G. H. and Hughes, T. J. (1981) 'The Arctic Ice Sheet: An outrageous hypothesis', In: Denton, G. H. and Hughes, T. J. (Eds.) *The Last Great Ice Sheets*, Wiley, New York

Denton, G. H., Heusser, C. J., Lowell, T. V., Moreno, P. I., Andersen, B. G., Heusser, L. E., Schlüchter, C. and Marchant, D. R. (1999) 'Interhemispheric Linkage of Paleoclimate during the Last Glaciation', *Geografiska Annaler*, 81 A (2): 107-153

Douglass, D. C., Singer, B. S., Kaplan, M. R., Ackert, R. P., Mickelson, D. M. and Caffee, M. W. (2005) 'Evidence of early Holocene glacial advances in southern South America from cosmogenic surface-exposure dating', *Geology*, 33 (3): 237-240

Douglass, D. C., Singer, B. S., Kaplan, M. R., Mickelson, D. M. and Caffee, M. W. (2006) 'Cosmogenic nuclide surface exposure dating of boulders on last-glacial and late-glacial moraines, Lago Buenos Aires, Argentina: Interpretive strategies and paleoclimate implications', *Quaternary Geochronology*, 1: 43-58

Dredge, L. A. (2000) 'Carbonate dispersal trains, secondary till plumes, and ice streams in the west Foxe Sector, Laurentide Ice Sheet', *Boreas*, 29: 144-156

Dyke, A. S. (1993) 'Landscapes of cold-centred Late Wisconsian ice caps, Arctic Canada', *Progress in Physical Geography*, 17: 223-247

Dyke, A. S. and Morris, T. F. (1988) 'Drumlin fields, dispersal trains, and ice streams in Arctic Canada', *Canadian Geographer*, 32(1): 86-90

Echelmeyer, K. A., Harrison, W. D., Larsen, C. and Mitchell, J. E. (1994) 'The role of the margins in the dynamics of an active ice stream', *Journal of Glaciology*, 40(136): 527-538

El-Sheimy, N., Valeo, C. and Habib, A. (2005) *Digital Terrain Modeling*, Artech House, Boston

Embleton, C. and King, C. A. M. (1975) *Glacial and Periglacial Geomorphology*, Wiley, New York

Engelhardt, H., Humphrey, N., Kamb, B. and Fahnestock, M. (1990) 'Physical Conditions at the Base of a Fast Moving Antarctic Ice Stream', *Science*, 248: 57-59

Evans, D. J. A. (2003) (Ed.) *Glacial Landsystems*, Hodder Arnold, London

Evans, D. J. A. (2006) 'Glacial landsystems', In: Knight, P. G. (Ed.) *Glacier Science and Environmental Change*, Blackwell, Oxford, Chapter 18

Evans, D. J. A. and Rea, B. R. (1999) 'Geomorphology and sedimentology of surging glaciers: a land-systems approach', Annals of Glaciology, 28: 75-82

Evans, D. J. A. and Ó Cofaigh, C. (2003) 'Depositional evidence for marginal oscillations of the Irish Sea ice stream in southeast Ireland during the last glaciation', *Boreas*, 32 (1): 76-101

Evans, D. J. A. and Rea, B. R. (2003) 'Surging Glacier Landsystem', In: Evans, D. J. A. (Ed.) *Glacial Landsystems*, Hodder Arnold, London

Evans, D. J. A., Clark, C. D. and Rea B. R. (2008) 'Landform and sediment imprints of fast glacier flow in the southwest Laurentide Ice Sheet', *Journal of Quaternary Science*, 23 (3): 249-272

Everest, J., Bradwell, T. and Golledge, N. (2005) 'Subglacial Landforms of the Tweed Palaeo-Ice Stream', *Scottish Geographical Journal*, 121 (2): 163-173

Finlayson, A. G. and Bradwell, T. (2008) 'Morphological characteristics, formation and glaciological significance of Rogen moraine in northern Scotland', *Geomorphology*, 101: 607-617

Fogwill, C. J. and Kubik, P. W. (2005) 'A glacial stage spanning the Antarctic Cold Reversal in Torres Del Paine (51ºS), Chile, based on preliminary cosmogenic exposure ages', *Geografiska Annaler*, 87 A (2): 403-408

Funk, M. and Röthlisberger, H. (1989) 'Forecasting the effects of a planned reservoir which will partially flood the tongue of Unteraargletscher in Switzerland', *Annals of Glaciology*, 13: 76-81

Funk, M., Echelmeyer, K. and Iken, A. (1994) 'Mechanisms of fast flow in Jakobshavn Isbrae, West Greenland: Part II. Modeling of englacial temperatures', *Journal of Glaciology*, 40(136): 569-594

Glasser, N. F. and Sambrook Smith, G. H. (1999) 'Glacial meltwater erosion of the Mid-Cheshire Ridge: implications for ice dynamics during the Late Devensian glaciation of northwest England', *Journal of Quaternary Science*, 14: 703-710

Glasser, N. F. and Jansson, K. N. (2005) 'Fast-flowing outlet glaciers of the Last Glacial Maximum Patagonian Icefield', *Quaternary Research*, 63: 206-211

Glasser, N.F. and Jansson, K.N. (2008) Published Map. In Glasser, N.F. and Jansson, K.N. (2008) 'The Glacial Map of southern South America', *Journal of Maps*, v2008, 175-196

Glasser, N. F., Jansson, K. N., Harrison, S. and Rivera, A. (2005) 'Geomorphological evidence for variations in the North Patagonian Icefield during the Holocene', *Geomorphology*, 71: 263-277

Glasser, N. F., Jansson, K. N., Harrison, S. and Kleman, J. (2008) 'The glacial geomorphology and Pleistocene history of South America between 38ºS and 56ºS', *Quaternary Science Reviews*, 27: 365-390

Golledge, N. R. and Stoker, M. S. (2006) 'A palaeo-ice stream of the British Ice Sheet in eastern Scotland', *Boreas*, 35: 1-13

Golledge, N. R., Finlayson, A., Bradwell, T. and Everest J. D. (2008) 'The Last Glaciation of Shetland, North Atlantic', *Geografiska Annaler*, 90 A (1): 37-53

Greenwood, S. L., Clark, C. D. and Hughes, A. L. C. (2007) 'Formalising an inversion methodology for reconstructing ice-sheet retreat patterns from meltwater channels: application to the British Ice Sheet', *Journal of Quaternary Science*, 22 (6): 637-645

Greenwood, S. L. and Clark, C. D. (2009) 'Reconstructing the last Irish Ice Sheet 1: changing flow geometries and ice flow dynamics deciphered from the glacial landform record', *Quaternary Science Reviews*, 28: 3085-3100

Hajdas, I., Bonani, G., Moreno, P. I. and Ariztegui, D. (2003) 'Precise radiocarbon dating of Late-Glacial cooling in mid-latitude South America', *Quaternary Research*, 59: 70-78

Hambrey, M. J. (1994) *Glacial Environments*, UCL Press, London

Hambrey, M. J. and Dowdeswell, J. A. (1994) 'Flow regime of the Lambert Glacier-Amery Ice Shelf system, Antarctica: structural evidence from Landsat imagery', *Annals of Glaciology*, 20: 401-406

Hart, J. K. (1999) 'Identifying fast ice flow from landform assemblages in the geological record: a discussion', Annals of Glaciology, 28: 59-66

Hein, A. S., Hulton, N. R. J., Dunai, T. J., Schnabel, C., Kaplan, M. R., Naylor, M. and Xu, S. (2009) 'Middle Pleistocene glaciation in Patagonia dated by cosmogenic-nuclide measurements on outwash gravels', *Earth and Planetary Science Letters*, 286: 184-197

Hess, D. P. and Briner, J. P. (2009) 'Geospatial analysis of controls on subglacial bedform morphometry in the New York Drumlin Field – implications for Laurentide Ice Sheet dynamics', *Earth Surface Processes and Landforms*, 34: 1126-1135

Heusser, C. J. (1993) 'Late-Glacial of Southern South America', *Quaternary Science Reviews*, 12: 345-350

Heusser, C. J. (1999) '^{14}C Age of Glaciation in Estrecho de Magallanes-Bahía Inútil, Chile', *Radiocarbon*, 41 (3): 287-293

Heusser, C. J. and Rabassa, J. (1987) 'Cold climatic episode of Younger Dryas age in Tierra del Fuego', *Nature*, 328: 609-611

Heusser, C. J., Heusser, L. E., Lowell, T. V., Moreira, A. M. and Moreira, S. M. (2000) 'Deglacial palaeoclimate at Puerto del Hambre, subantarctic Patagonia, Chile', *Journal of Quaternary Science*, 15 (2): 101-114

Hindmarsh, R. C. A. and Stokes, C. R. (2008) 'Formation mechanisms for ice-stream lateral shear margin moraines', *Earth Surface Processes and Landforms*, 33: 610-626

Hirano, A., Welch, R. and Lang, H. (2003) 'Mapping from ASTER stereo image data: DEM validation and accuracy assessment', *Journal of Photogrammetry and Remote Sensing*, 57: 356-370

Hodell, D. A., Gersonde, R. and Blum, P. (2002) 'Leg 177 synthesis: insights into Southern Ocean paleooceanography on tectonic to millennial timescales', In:

Gersonde, R., Hodell, D. A. and Blum, P. (Eds.) *Proceedings of the Ocean Drilling Program, Scientific Results,* Volume 177: 1-54

Hodge, S. M. and Doppelhammer, S. K. (1996) 'Satellite imagery of the onset of streaming flow of ice streams C and C, West Antarctica', *Journal of Geophysical Research*, 101(C3): 6669-6677

Hodgson, D. A. (1994) 'Episodic ice streams and ice shelves during retreat of the northwesternmost sector of the Late Weichselian Laurentide ice sheet over the central Canadian Arctic Archipelago', *Boreas*, 23(1): 14-28

Holland, D. M., Thomas, R. H., De Young, B., Ribergaard, M. H. and Lyberth, B. (2008) 'Acceleration of Jakobshavn Isbrae triggered by warm subsurface ocean waters', *Nature Geoscience*, 1: 659-664

Hollin, J. T. and Schilling, D. H. (1981) 'Late Wisconsian-Weichselian glaciers and small ice caps', In: Denton, G. H and Hughes, T. J. (Eds.) *The Last Great Ice Sheets*, Wiley, New York: 179-220

Howat, I. M., Joughin, I. and Scambos, T. (2007) 'Rapid changes in ice discharge from Greenland outlet glaciers', *Science*, 315: 1559-1561

Hubbard, B. and Glasser, N. (2005) *Field Techniques in Glaciology and Glacial Geomorphology*, Wiley, Chichester

Hughes, T. J. (1977) 'West Antarctic ice streams', *Review of Geophysics and Space Physics*, 15: 1-46

Hughes, T. (1992) 'Abrupt climate change related to unstable ice-sheet dynamics: towards a new paradigm', *Palaeogeography, Palaeoclimatology, Palaeoecology*, 97: 203-234

Hulton, N., Sugden, D., Payne, A. and Clapperton, C. (1994) 'Glacier Modeling and the Climate of Patagonia during the Last Glacial Maximum', *Quaternary Research*, 42: 1-19

Hulton, N. R. J., Purves, R. S., McCulloch, R. D., Sugden, D. E. and Bentley, M. J. (2002) 'The Last Glacial Maximum and deglaciation in southern South America', *Quaternary Science Reviews*, 21: 233-241

Iken, A., Echelmeyer, K., Harrison, W. and Funk, M. (1993) 'Mechanisms of fast flow in Jakobshavn Isbrae, West Greenland: Part 1. Measurements of temperature and water level in deep boreholes', Journal of Glaciology, 39 (131): 15-25

Iverson, N. R., Hooyer, T. S. and Baker, R. W. (1998) 'Ring-shear studies of till deformation: coulomb-plastic behaviour and distributed strain in glacier beds', *Journal of Glaciology*, 44: 634-642

Jansson, K. N. (2003) 'Early Holocene glacial lakes and ice marginal retreat pattern in Labrador/Ungava, Canada', *Palaeogeography, Palaeoclimatology, Palaeoecology*, 193: 473-501

Jansson, K. N. (2005) 'Map of the glacial geomorphology of north-central Québec-Labrador, Canada', *Journal of Maps*: 46-56

Jansson, K. N., Kleman, J. and Marchant, D. R. (2002) 'The succession of ice-flow patterns in north-central Québec-Labrador, Canada', *Quaternary Science Reviews*, 21: 503-523

Jansson, K. N., Stroeven, A. P. and Kleman, J. (2003) 'Configuration and timing of Ungava Bay ice streams, Labrador-Ungava, Canada', *Boreas*, 32: 256-262

Jennings, C. E. (2006) 'Terrestrial ice stream – a view from the lobe', *Geomorphology*, 75: 100-124

Joughin, I., Gray, L., Bindschadler, R., Price, S., Morse, D., Hulbe, C., Mattar, K. and Werner, C. (1999) 'Tributaries of West Antarctic Ice Streams Revealed by RADARSAT Interferometry', *Science*, 286: 283-286

Joughin, I., Tulaczyk, S., Binschadler, R. and Price, S. F. (2002) 'Changes in west Antarctic ice stream velocities: Observation and analysis', *Journal of Geophysical Research*, 107(B11): 2289

Joughin, I., Abdalati, W. and Fahnestock, M. (2004) 'Large fluctuations in speed on Greenland's Jakobshavn Isbrae glacier', Nature, 432: 608-610

Kamb, B. (1991) 'Rheological Nonlinearity and Flow Instability in the Deforming Bed Mechanism of Ice Stream Motion', *Journal of Geophysical Research*, 96(B10): 16,585-16,595

Kamb, B. (2001) 'Basal zone of the West Antarctic ice streams and its role in lubrication of their rapid motion', In: Alley, R. D. and Binschadler, R. (Eds.) *The West Antarctic Ice Sheet: Behaviour and Environment, Antarctic Research Series, Volume 7*, American Geophysical Union, Washington DC, pp. 157-199

Kaplan, M. R., Ackert, R. P. Jr., Singer, B. S., Douglass, D.C and Kurz, M. D. (2004) 'Cosmogenic nuclide chronology of millennial-scale glacial advances during O-isotope stage 2 in Patagonia', *Geological Society of America Bulletin*, 116 (3/4): 308-321

Kaplan, M. R., Douglass, D. C., Singer, B. S., Ackert, R. P. and Caffee, M. W. (2005) 'Cosmogenic nuclide chronology of pre-last glacial maximum moraines at Lago Buenos Aires, 46ºS, Argentina', *Quaternary Research*, 63: 301-315

Kaplan, M. R., Coronato, A., Hulton, N. R. J., Rabassa, J. O., Kubik, P. W. and Freeman, S. P. H. T. (2007) 'Cosmogenic nuclide measurements in southernmost South America and implications for landscape change', *Geomorphology*, 87: 284-301

Kaplan, M. R., Moreno, P. I. and Rojas, M. (2008a) 'Glacial dynamics in southernmost South America during Marine Isotope Stage 5e to the Younger Dryas chron: a brief review with a focus on cosmogenic nuclide measurements', *Journal of Quaternary Science*, 23 (6-7): 649-658

Kaplan, M. R., Fogwill, C. J., Sugden, D. E., Hulton, N. R. J., Kubik, P. W. and Freeman, S. P. H. T. (2008b) 'Southern Patagonian glacial chronology for the Last Glacial period and implications for Southern Ocean climate', *Quaternary Science Reviews*, 27: 284-294

Kaplan, M. R., Hein, A. S., Hubbard, A. and Lax, S. M. (2009) 'Can glacial erosion limit the extent of glaciation?', *Geomorphology*, 103: 172-179

Kilian, R., Schneider, C., Koch, J., Fesq-Martin, M., Biester, H., Casassa, G., Arévalo, M., Wendt, G., Baeza, O. and Behrmann, J. (2007) 'Palaeoecological constraints on late Glacial and Holocene ice retreat in the southern Andes (53°S)', *Global and Planetary Change*, 59: 49-66

King, E. C., Hindmarsh, R. C. A. and Stokes, C. R. (2009) 'Formation of mega-scale glacial lineations observed beneath a West Antarctic ice stream', *Nature Geoscience*, 2: 585-588

Kleman, J. (1990) 'On the use of glacial striae for reconstruction of paleo-ice sheet flow patterns' *Geografiska Annaler*, 72 A (3-4): 217-236

Kleman, J. and Borgström, I. (1996) 'Reconstruction of palaeo-ice sheets: the use of geomorphological data', *Earth Surface Processes and Landforms*, 21: 893-909

Kleman, J., Borgström, I. and Hättestrand, C. (1994) 'Evidence for a relict glacial landscape in Quebec-Labrador', *Palaeogeography, Palaeoclimatology and Palaeoecology*, 111: 217-228

Kleman, J., Hättestrand, C., Borgström, I. and Stroeven, A. (1997) 'Fennoscandian palaeoglaciology reconstructed using a glacial geological inversion model', *Journal of Glaciology*, 43 (144): 283-299

Kleman, J., Hättestrand, C., Stroeven, A. P., Jansson, K. N., De Angelis, H. and Borgström, I. (2006) 'Reconstruction of palaeo-ice sheets – inversion of their glacial

geomorphological record', In: Knight, P. (Ed.) *Glaciology and Earth's Changing Environment*, Blackwell: 192-198

Knight, J., McCarron, S. G. and Marshall McCabe, A. (1999) 'Landform modification by palaeo-ice streams in east-central Ireland', *Annals of Glaciology*, 28: 161-167

Kohler, J. (2007) 'Lubricating lakes', *Nature*, 445 (22): 830-831

Kuvaas, B. and Kristoffersen, Y. (1991) 'The Crary Fan: A trough-mouth fan on the Weddell Sea continental margin, Antarctica', *Marine Geology*, 97: 345-362

Lamy, F., Hebbeln, D., Röhl, U. and Wefer, G. (2001) 'Holocene rainfall variability in southern Chile: a marine record of latitudinal shifts of the Southern Westerlies', *Earth and Planetary Science Letters*, 185: 369-382

Lamy, F., Kaiser, J., Ninnemann, U., Hebbeln, D., Arz, H. W. and Stoner, J. (2004) 'Antarctic Timing of Surface Water Changes of Chile and Patagonian Ice Sheet Response', *Science*, 304: 1959-1962

Larter, R. D., Graham, A. G. C., Gohl, G., Kuhn, G., Hillenbrand, C., Smith, J. A., Deen, T. J., Livermore, R. A. and Schenke, H. (2009) 'Subglacial bedforms reveal complex basal regime in a zone of palaeo-ice stream convergence, Amundsen Sea embayment, West Antarctica', *Geology*, 37 (5): 411-414

Long, A. J. and Roberts, D. H. (2003) 'Late Weichselian deglacial history of Disko Bugt, West Greenland, and the dynamics of the Jakobshavn Isbrae ice stream', *Boreas*, 32: 208-226

Lovell, H., Stokes, C. R. and Bentley, M. J. (submitted) 'A glacial geomorphological map of the Seno Skyring-Seno Otway-Strait of Magellan region, southernmost Patagonia', *Journal of Maps*

Lowell, T. V., Heusser, C. J., Andersen, B. G., Moreno, P. I., Hauser, A., Heusser, L. E., Schlüchter, C., Marchant, D. R. and Denton, G. H. (1995) 'Interhemispheric Correlation of Late Pleistocene Glacial Events', *Science*, 269: 1541-1549

Lüthi, M., Funk, M., Iken, A., Gogineni, S. and Truffer, M. (2002) 'Mechanisms of fast flow in Jakobshavn Isbrae, West Greenland. Part III. Measurements of ice deformation, temperature and cross-borehole conductivity in boreholes to the bedrock', *Journal of Glaciology*, 48(162): 369-385

MacAyeal, D. R. (1993) 'Binge/purge oscillations of the Laurentide Ice Sheet as a cause of the North Atlantic's Heinrich events', *Palaeooceanography*, 8: 775-784

Maizals, J. (2002) 'Sediments and landforms of modern proglacial terrestrial environments', In: Menzies, J. (Ed.) *Modern and Past Glacial Environments*, Butterworth Heinemann, Oxford, Chapter 9

Malagnino, E. (1995) 'Discovery of the oldest extra-Andean glaciation in the Lago Buenos Aires Basin, Argentina', *Quaternary of South America and Antarctic Peninsula 9*, A. A. Balkema Publishers, Rotterdam: 69-83

Marden, C. J. (1997) 'Late-Glacial fluctuations of South Patagonian Icefield, Torres Del Paine National Park, Southern Chile', *Quaternary International*, 38/39: 61-68

Markgraf, V. (1993) 'Younger Dryas in Southernmost South America – An Update', *Quaternary Science Reviews*, 12: 351-355

Mathews, W. H. (1974) 'Surface profiles of the Laurentide Ice Sheet in its marginal areas', *Journal of Glaciology*, 13 (7): 37-43

McCulloch, R. D. and Bentley, M. J. (1998) 'Late glacial ice advances in the Strait of Magellan, southern Chile', *Quaternary Science Reviews*, 17: 775-787

McCulloch, R. D. and Davies, S. J. (2001) 'Late-glacial and Holocene palaeoenvironmental change in the central Strait of Magellan, southern Patagonia', *Palaeogeography, Palaeoclimatology, Palaeoecology*, 173: 143-173

McCulloch, R. D., Bentley, M. J., Purves, R. S., Hulton, N. R. J., Sugden, D. E. and Clapperton, C. M. (2000) 'Climatic inferences from glacial and palaeoecological

evidence at the last glacial termination, southern South America', *Journal of Quaternary Science*, 15 (4): 409-417

McCulloch, R. D., Fogwill, C. J., Sugden, D. E., Bentley, M. J. and Kubik, P. W. (2005a) 'Chronology of the last glaciation in Central Strait of Magellan and Bahía Inútil, southernmost South America', *Geografiska Annaler*, 87 A (2): 289-312

McCulloch, R. D., Bentley, M. J., Tipping, R. M. and Clapperton, C. M. (2005b) 'Evidence for late-glacial ice dammed lakes in the Central Strait of Magellan and Bahía Inútil, southernmost South America', *Geografiska Annaler*, 87 A (2): 335-362

McIntyre, N. F. (1985) 'The dynamics of outlet glaciers', *Journal of Glaciology*, 31(108): 99-107

Meglioli, A. (1992) *Glacial Geology of southernmost Patagonia and Tierra del Fuego, Argentina and Chile*, Unpublished PhD thesis, Lehigh University, USA

Mercer, J. H. (1969) 'Glaciation in Southern Argentina More than Two Million Years Ago', *Science*, 164 (3881): 823-825

Mercer, J. H. (1970) 'Variations of some Patagonian glaciers since the Late-Glacial', *American Journal of Science*, 269: 1-25

Mercer, J. H. (1976) 'Glacial History of Southernmost South America', *Quaternary Research*, 6: 125-166

Mercer, J. H. (1983) 'Cenozoic Glaciation in the Southern Hemisphere', *Annual Review of Earth and Planetary Sciences*, 11: 99-132

Mercer, J. H. and Sutter, J. F. (1982) 'Late Miocene-earliest Pliocene Glaciation in Southern Argentina: Implications for global Ice-sheet history', *Palaeogeography, Palaeoclimatology, Palaeoecology*, 38: 185-206

Moreno, P. I., Jacobson, G. L. Jr., Lowell, T. V. and Denton, G. H. (2001) 'Interhemispheric climate links revealed by a late-glacial cooling episode in southern Chile', *Nature*, 409: 804-808

Mosola, A. B. and Anderson, J. B. (2006) 'Expansion and rapid retreat of the West Antarctic Ice Sheet in eastern Ross Sea: possible consequence of over-extended ice streams?', *Quaternary Science Reviews*, 25 (17-18): 2177-2196

Nordenskjöld, O. (1899) *Geologie, Geographie and Anthropologie: Scwedischen Expedition nach den Magellansländern, 1895 -1897*, Norsstedt and Söner, Stockholm

Ó Cofaigh, C., Pudsey, C. J., Dowdeswell, J. A. and Morris, P. (2002) 'Evolution of subglacial bedforms along a palaeo-ice stream, Antarctic Peninsula continental shelf', *Geophysical Research Letters*, 29 (8): 1-4

Ó Cofaigh, C., Taylor, J., Dowdeswell, J. A. and Pudsey, J. A. (2003) 'Palaeo-ice streams, trough mouth fans and high-latitude continental slope sedimentation', *Boreas*, 32: 37-55

Ó Cofaigh, C., Dowdeswell, J. A., Allen, C. S., Hiemstra, J. F., Pudsey, C. J., Evans, J. and Evans, D. J. A. (2005) 'Flow dynamics and till genesis associated with a marine-based Antarctic palaeo-ice stream', *Quaternary Science Reviews*, 24: 709-740

Ó Cofaigh, C., Evans, J., Dowdeswell, J. A. and Larter, R. D. (2007) 'Till characteristics, genesis and transport beneath Antarctic palaeo-ice streams', *Journal of Geophysical Research*, 112: 1-16

Ó Cofaigh, C., Dowdeswell, J. A., Evans, J. and Larter, R. D. (2008) 'Geological constraints on Antarctic palaeo-ice-stream retreat', *Earth Surface Processes and Landforms*, 33: 513-525

Ó Cofaigh, C., Dowdeswell, J. A., King, E. C., Anderson, J. B., Clark, C. D., Evans, D. J. A., Evans, J., Hindmarsh, R. C. A., Larter, R. D. and Stokes, C. R. (2010a) 'Comment on Shaw, J., Pugin A. and Young, R. (2008): "A meltwater origin for Antarctic shelf bedforms with special attention to megalineations", Geomorphology 102, 364-375', *Geomorphology*, 117: 195-198

Ó Cofaigh, C., Evans, D. J. A. and Smith, I. R. (2010b) 'Large-scale reorganization and sedimentation of terrestrial ice streams during late Wisconsian Laurentide Ice Sheet deglaciation', *Geological Society of America Bulletin*, 122: 743-756

Oppenheimer, M. (1998) 'Global warming and the stability of the West Antarctic Ice Sheet', *Nature*, 393: 325-332

Ottesen, D., Rise, L., Knies, J., Olsen, L. and Henriksen, S. (2005a) 'The Vestfjorden-Trænadjupet palaeo-ice stream drainage system, mid-Norwegian continental shelf', *Marine Geology*, 218: 175-189

Ottesen, D., Dowdeswell, J. A. and Rise, L. (2005b) 'Submarine landforms and the reconstruction of fast-flowing ice streams within a large Quaternary ice sheet: The 2500-km-long Norwegian-Svalbard margin (57°-80°N)', *Geological Society of America Bulletin*, 117(7/8): 1033-1050

Ottesen, D., Stokes, C. R., Rise, L. and Olsen, L. (2008a) 'Ice-sheet dynamics and ice streaming along the coastal parts of northern Norway', *Quaternary Science Reviews*, 27: 922-940

Ottesen, D., Dowdeswell, J. A., Benn, D. I., Kristensen, L., Christiansen, H. H., Christensen, O., Hansen, Lebesbye, E., Forwick, W. and Vorren, T. O. (2008b) 'Submarine landforms characteristic of glacier surges in two Spitsbergen fjords', Quaternary Science Reviews, 27: 1583-1599

Patterson, C. J. (1997) 'Southern Laurentide ice lobes were created by ice streams: Des Moines Lobe in Minnesota, USA', *Sedimentary Geology*, 111: 249-261

Patterson, C. J. (1998) 'Laurentide glacial landscapes: The role of ice streams', *Geology*, 26 (7): 643-646

Payne, A. J. and Dongelmans, P. W. (1997) 'Self-organisation in the thermomechanical flow of ice sheets', *Journal of Geophysical Research*, 102(B6): 12219-12233

Payne, A. J. and Baldwin, D. J. (1999) 'Thermomechanical modelling of the Scandinavian ice sheet: implications for ice-stream formation', *Annals of Glaciology*, 28: 83-89

Petit, J. R., Jouzel, J., Raynaud, D., Barkov, N. I., Barnola, J. M., Basile, I., Bender, M., Chappellaz, J., Davis M. and Delay, G. (1999) 'Climate and atmospheric history of the past 420,000 years from the Vostok ice core, Antarctica, *Nature*, 399: 429-436

Pfeifer, N. and Mandlburger, G. (2008) 'LiDAR Data Filtering and DTM Generation' In: Shan, J. and Toth, C. K. (Eds.) *Topographic laser ranging and scanning: Principles and Processing*, CRC Press, London, Chapter 11

Porter, S. C., Stuiver, M. and Heusser, C. J. (1984) 'Holocene Sea-Level Changes along the Strait of Magellan and Beagle Channel, Southernmost South America', *Quaternary Research*, 22: 59-67

Porter, S. C., Clapperton, C. M. and Sugden, D. E. (1992) 'Chronology and dynamics of deglaciation along and near the Strait of Magellan, southernmost South America', *Sveriges Geologiska Undersökning*, Ser. Ca 81: 233-239

Prest, V. K., Grant, D. R. and Rampton, V. N. (1968) *The Glacial Map of Canada*, Geological Survey of Canada, Ottawa

Price, R. J. (1960) 'Glacial meltwater channels in the Upper Tweed drainage basin', *Geographical Journal*, 126: 483-489

Punkari, M. (1980) 'The ice lobes of the Scandinavian Ice Sheet during the deglaciation in Finland', *Boreas*, 9: 307-310

Punkari, M. (1982) 'Glacial geomorphology and dynamics in the eastern parts of the Baltic Shield interpreted using Landsat imagery', *Photogrammetric Journal Finland*, 9: 77-93

Punkari, M. (1997) 'Glacial and glaciofluvial deposits in the interlobate areas of the Scandinavian Ice Sheet', *Quaternary Science Reviews*, 16: 741-753

Rabassa, J. (2008) 'Late Cenozoic Glaciations in Patagonia and Tierra del Fuego', In: Van der Meer, J. J. M (Ed.), *Developments in Quaternary Science 11*, Elsevier, Amsterdam: Chapter 8

Rabassa, J. and Clapperton, C. M. (1990) 'Quaternary Glaciations of the Southern Andes', *Quaternary Science Reviews*, 9: 153-174

Rabassa, J. and Coronato, A. (2009) 'Glaciations in Patagonia and Tierra del Fuego during the Ensenadan Stage/Age (Early Pleistocene – earliest Middle Pleistocene', *Quaternary International*, 210: 18-36

Rabassa , J., Coronato, A., Bujalesky, G., Salemme, M., Roig, C., Meglioli, A., Heusser, C., Gordillo, S., Roig, F., Borromei, A. and Quattrocchio, M. (2000) 'Quaternary of Tierra del Fuego, Southernmost South America: an updated review', *Quaternary International*, 68-71: 217-240

Rabassa, J., Coronato, A. M. and Salemme, M. (2005) 'Chronology of the Late Cenozoic Patagonian glaciations and their correlation with biostratigraphic units of the Pampean region (Argentina)', *Journal of South American Earth Sciences*, 20: 81-103

Retzlaff, R. and Bentley, C. R. (1993) 'Timing of stagnation of Ice Stream C, West Antarctica, from short-pulse radar studies of buried surface crevasses', *Journal of Glaciology*, 39: 553-561

Rignot, E. and Thomas, R. H. (2002) 'Mass Balance of Polar Ice Sheets', *Science*, 297: 1502-1506

Rignot, E. and Kanagaratnam, P. (2006) 'Changes in the velocity structure of the Greenland Ice Sheet', *Science*, 311: 986-990

Roberts, D. H. and Long, A. J. (2005) 'Streamlined bedrock terrain and fast ice flow, Jakobshavn Isbrae, West Greenland: implications for ice stream and ice sheet dynamics', *Boreas*, 34: 25-42

Roberts, D. H., Long, A. J., Davies, B. J., Simpson, M. J. R. and Schnabel, C. (2010) 'Ice stream influence on West Greenland Ice Sheet dynamics during the Last Glacial Maximum', *Journal of Quaternary Science*, 25: 850-864

Rose, K. E. (1979) 'Characteristics of ice flow in Marie-Byrd Land, Antarctica', *Journal of Glaciology*, 24: 63-75

Schytt, V. (1956) 'Lateral drainage channels along the northern side of the Moltke glacier, Northwest Greenland', *Geografiska Annaler*, 38: 64-77

Shabtaie, S., Whillans, I. M. and Bentley, C. R. (1987) 'The morphology of ice streams A, B, and C, West Antarctica, and their environs', *Journal of Geophysical Research*, 92(B9): 8865-8883

Shaw, J., Pugin, A. and Young, R. R. (2008) 'A meltwater origin for Antarctic shelf bedforms with special attention to megalineations', *Geomorphology*, 102: 364-375

Shepherd, A. P. and Wingham, D. J. (2007) 'Recent sea-level contributions of the Antarctic and Greenland Ice Sheets', *Science*, 315: 1529-1532

Singer, B. S., Ackert, R. P. Jr. and Guillou, H. (2004a) '$^{40}Ar/^{39}Ar$ and K-Ar chronology of Pleistocene glaciations in Patagonia, *Geological Society of America Bulletin*, 116 (3/4): 434-450

Singer, B. S., Brown, L. L., Rabassa, J. and Guillou, H. (2004b) '$^{40}Ar/^{39}Ar$ ages of Late Pliocene and Early Pleistocene Geomagnetic and Glacial events in Southern Argentina', *AGU Geophysical Monograph Timescales of the Internal Geomagnetic Field*', Dedicated to N. D. Opdyke: 176-190

Sissons, J. B. (1960) 'Some aspects of glacial drainage channels in Britain: Part I', *Scottish Geographical Magazine*, 76: 131-146

Sisson, J. B. (1961) 'Some aspects of glacial drainage channels in Britain: Part II', *Scottish Geographical Magazine*, 77: 15-36

Smith, M. J., Rose, J. and Booth, S. (2006) 'Geomorphological mapping of glacial landforms from remotely sensed data: An evaluation of the principal data sources and an assessment of their quality', *Geomorphology*, 76: 148-165

Spagnolo, M., Clark, C. D., Hughes, A. L. C., Dunlop, P. and Stokes, C. R. (2010) 'The planar shape of drumlins', *Sedimentary Geology*, 232 (3-4): 119-129

Stearns, L. A., Smith, B. E. and Hamilton, G. S. (2008) 'Increased flow speed on a large East Antarctic outlet glacier caused by subglacial floods', *Nature Geoscience*, 1: 827-831

Stokes, C. R. (2002) 'Identification and mapping of palaeo-ice stream geomorphology from satellite imagery: implications for ice stream functioning and ice sheet dynamics', *International Journal of Remote Sensing*, 23 (8): 1557-1563

Stokes, C. R. and Clark, C. D. (1999) 'Geomorphological criteria for identifying Pleistocene ice streams', *Annals of Glaciology*, 28: 67-74

Stokes, C. R. and Clark, C. D. (2001) 'Palaeo-ice streams', *Quaternary Science Reviews*, 20: 1437-1457

Stokes, C. R. and Clark, C. D. (2002a) 'Are long subglacial bedforms indicative of fast ice flow?', *Boreas*, 31: 239-249

Stokes, C. R. and Clark, C. D. (2002b) 'Ice Stream Shear Margin Moraines', *Earth Surface Processes and Landforms*, 27: 547-558

Stokes, C. R. and Clark, C. D. (2003) 'The Dubawnt Lake palaeo-ice stream: evidence for dynamic ice sheet behaviour on the Canadian Shield and insights regarding the controls on ice-stream location and vigour', *Boreas*, 32: 263-279

Stokes, C. R. and Clark, C. D. (2004) 'Evolution of late glacial ice-marginal lakes on the northwestern Canadian Shield and their influence on the location of the Dubawnt Lake palaeo-ice stream', *Palaeogeography, Palaeoclimatology, Palaeoecology*, 215: 155-171

Stokes, C. R., Clark, C. D., Darby, D. A. and Hodgson, D. A. (2005) 'Late Pleistocene ice export events into the Arctic Ocean from the M'Clure Strait Ice Stream, Canadian Arctic Archipelago', *Global and Planetary Change*, 49: 139-162

Stokes, C. R., Clark, C. D. and Winsborrow, M. C. M. (2006) 'Subglacial bedform evidence for a major palaeo-ice stream and its retreat phases in Amundsen Gulf, Canadian Arctic Archipelago' *Journal of Quaternary Science*, 21 (4): 399-412

Stokes, C. R., Clark, C. D., Lian, O. B. and Tulaczyk, S. (2007) 'Ice stream sticky spots: A review of their identification and influence beneath contemporary and palaeo-ice streams', *Earth-Science Reviews*, 81: 217-249

Stokes, C. R., Lian, O. B., Tulaczyk, S. and Clark, C. D. (2008) 'Superimposition of ribbed moraines on a palaeo-ice-stream bed: implications for ice stream dynamics and shutdown', *Earth Surface Processes and Landforms*, 33: 593-609

Stokes, C. R., Clark, C. D. and Storrar, R. (2009) 'Major changes in ice stream dynamics during deglaciation of the north-western margin of the Laurentide Ice Sheet', *Quaternary Science Reviews*, 28: 721-738

Storrar, R. and Stokes, C. R. (2007) 'A Glacial Geomorphological Map of Victoria Island, Canadian Arctic', *Journal of Maps*, 191-210

Studinger, M., Bell, R. E., Blankenship, D. D., Finn, C. A., Arko, R. A., Morse, D. L. and Joughin, I. (2001) 'Subglacial sediments: A regional geological template for ice flow in West Antarctica', *Geophysical Research Letters*, 28 (18): 3493-3496

Sugden, D. E. (1978) 'Glacial erosion by the Laurentide Ice Sheet', *Journal of Glaciology*, 20: 367-391

Sugden, D. E. (1991) 'Subglacial meltwater channel systems and ice sheet overriding, Asgard Range, Antarctica', *Geografiska Annaler*, 73 A: 109-121

Sugden, D. E., Hulton, N. R. J. and Purves, R. S. (2002) 'Modelling the inception of the Patagonian icesheet', *Quaternary International*, 95-96: 55-64

Sugden, D. E., Bentley, M. J., Fogwill, C. J., Hulton, N. R. J., McCulloch, R. D. and Purves, R. S. (2005) 'Late-glacial glacier events in southernmost South America: A blend of 'northern' and 'southern' hemispheric climatic signals?', *Geografiska Annaler*, 87 A (2): 273-288

Sugden, D. E., McCulloch, R. D., Bory, A. J.-M. and Hein, A. S. (2009) 'Influence of Patagonian glaciers on Antarctic dust deposition during the last glacial period', *Nature Geoscience*, 2: 281-285

Swithinbank, C. W. M. (1954) 'Ice streams', *Polar Record*, 7 (48): 185-186

Swithinbank, C. (1988) 'Antarctica', *U.S. Geological Survey Professional Paper*, 1386-B, B1-B138

Tarasov, L. and Peltier, W. R. (2005) 'Arctic freshwater forcing of the Younger Dryas cold reversal', *Nature*, 435: 662-665

Thomas, R. H. (2004) 'Force-perturbation analysis of recent thinning and acceleration of Jakobshavn Isbræ, Greenland', *Journal of Glaciology*, 50(168): 57-66

Truffer, M. and Echelmeyer, K. A. (2003) 'Of isbrae and ice streams', *Annals of Glaciology*, 36: 66-72

Truffer, M. and Fahnestock, M. (2007) 'Rethinking ice sheet time scales', *Science*, 315: 1508-1510

Tulaczyk, S. M., Kamb, B. and Engelhardt, H. F. (2000) 'Basal mechanics of Ice Stream B, West Antarctica. II. Undrained-plastic-bed model', *Journal of Geophysical Research*, 105(B1): 483-494

Tulaczyk, S. M., Scherer, R. P. and Clark, C. D. (2001) 'A ploughing model for the origin of weak tills beneath ice streams: a qualitative treatment', *Quaternary International*, 86: 59-70

Turner, K. J., Fogwill, C. J., McCulloch, R. D. and Sugden, D. E. (2005) 'Deglaciation of the eastern flank of the North Patagonian Icefield and associated continental-scale lake diversions', *Geografiska Annaler*, 87 A (2): 363-374

Vorren, T. O. and Laberg, J. S. (1997) 'Trough Mouth Fans – Palaeoclimate and Ice Sheet Monitors', *Quaternary Science Reviews*, 16: 865-881

Walcott, R. I. (1973) 'Structure of the earth from glacio-isostatic rebound', *Annual Review of Earth and Planetary Sciences*, 1: 15-37

Warren, C. R. (1994) 'Freshwater calving and anomalous glacier oscillations: recent behaviour of Moreno and Ameghino glaciers, Patagonia', *The Holocene*, 4 (4): 422-429

Warren, C. R., Glasser, N. F., Harrison, S., Winchester, V., Kerr, A. R. and Rivera, A. (1995a) 'Characteristics of tide-water calving at Glaciar San Rafael, Chile', *Journal of Glaciology*, 41 (138): 273-289

Warren, C. R., Greene, D. and Glasser, N. F. (1995b) 'Glaciar Upsala, Patagonia: rapid calving retreat in fresh water', *Annals of Glaciology*, 21: 311-316

Warren, W. P. and Ashley, G. M. (1994) 'Origins of the ice-contact stratified ridges (eskers) of Ireland', *Journal of Sedimentary Research*, A64: 433-449

Wenzens, G. (1999) 'Fluctuations of Outlet and Valley Glaciers in the Southern Andes (Argentina) during the Past 13,000 Years', *Quaternary Research*, 51: 238-247

Wenzens, G. (2000) 'Pliocene Piedmont Glaciation in the Río Shehuen Valley, Southwest Patagonia, Argentina', *Arctic, Antarctic and Alpine Research*, 32 (1): 46-54

Wenzens, G. (2006) 'Terminal moraines, outwash plains and lake terraces in the vicinity of Lago Cardiel (49°S, Patagonia, Argentina): evidence for Miocene Andean foreland glaciation', *Arctic, Antarctic and Alpine Research*, 38: 276-291

Whillans, I. M., Bolzan, J. and Shabtaie, S. (1987) 'Velocity of Ice Streams B and C, Antarctica', *Journal of Geophysical Research*, 92 (B9): 8895-8902

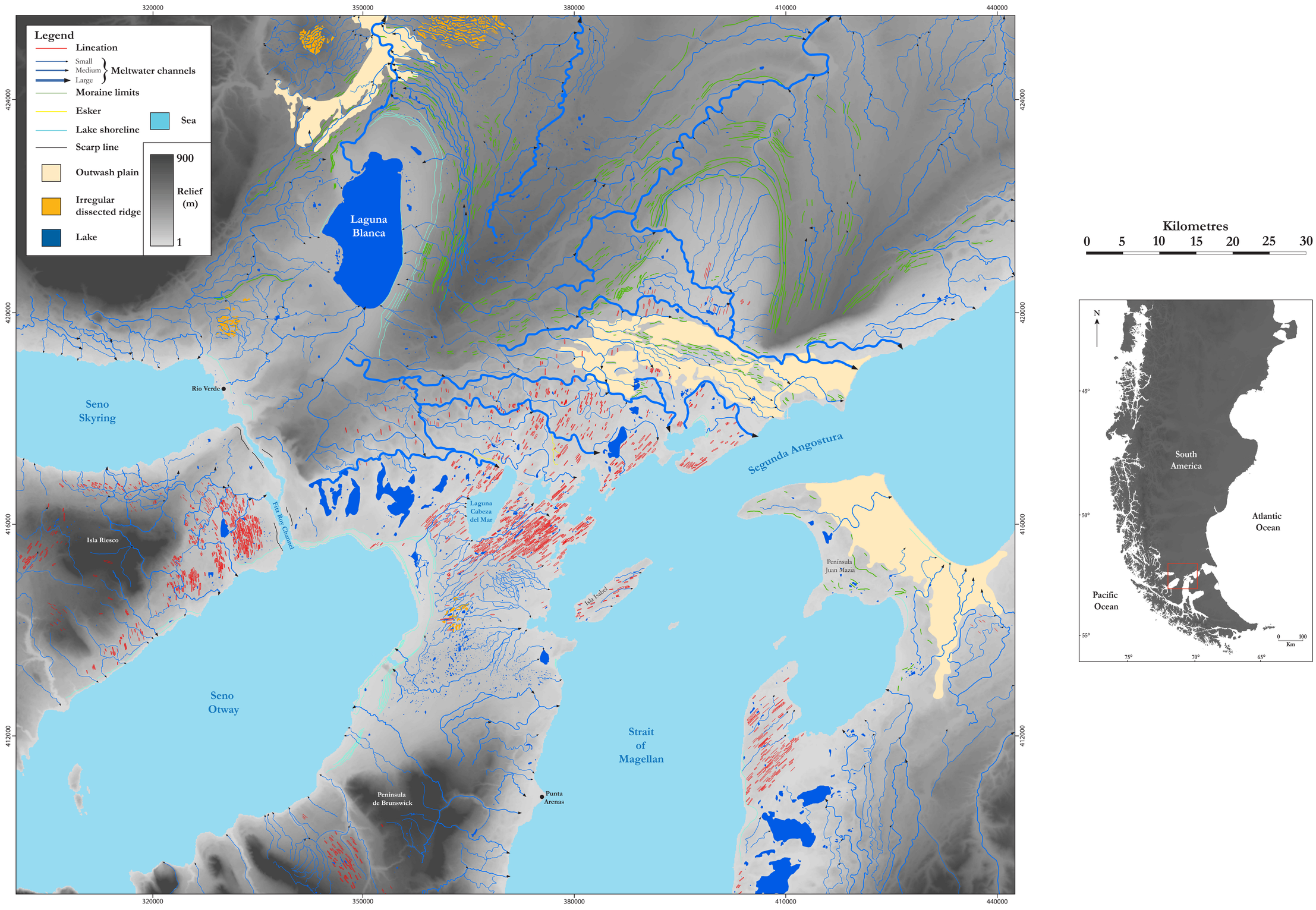

Figure 6.1 - Geomorphological map of the Seno Skyring-Seno Otway-Strait of Magellan region, southernmost Patagonia. Inset shows location. Different thicknesses of meltwater channels represent a hierarchy of channel sizes (approximate widths: small < 50 m; medium = 50 to 150 m; large > 150 m).